Introduction to RADAR systems

Third Edition

Merrill I. Skolnik

McGRAW-HILL INTERNATIONAL EDITIONS
Electrical Engineering Series

chapter

9

The Radar Antenna

9.1 FUNCTIONS OF THE RADAR ANTENNA

The radar antenna is a distinctive and important part of any radar. It serves the following functions:

- Acts as the transducer between propagation in space and guided-wave propagation in the transmission lines.
- Concentrates the radiated energy in the direction of the target (as measured by the antenna gain).
- Collects the echo energy scattered back to the radar from a target (as measured by the antenna effective aperture).
- Measures the angle of arrival of the received echo signal so as to provide the location of a target in azimuth, elevation, or both.
- Acts as a spatial filter to separate (resolve) targets in the angle (spatial) domain, and rejects undesired signals from directions other than the main beam.
- Provides the desired volumetric coverage of the radar.
- Usually establishes the time between radar observations of a target (revisit time).

In addition, the antenna is that part of a radar system that is most often portrayed when a picture of a radar is shown. (More can be learned about the nature of a radar from a picture of its antenna than from pictures of its equipment racks.)

With radar antennas, big is beautiful (within the limits of mechanical and electrical tolerances and the constraints imposed by the physical space available on the vehicle that carries the antenna). The larger the antenna, the better the radar performance, the smaller can be the transmitter, and the less can be the total amount of prime power needed for the radar system. The transmitting antenna gain and the receiving effective aperture are proportional to one another [as given by Eq. (1.8) or Eq. (9.9)] so that a large transmitting gain implies a large effective aperture, and vice versa. As was mentioned in Chap. 1, in radar a common antenna generally has been used for both transmission and reception.

Almost all radar antennas are directive and have some means for steering the beam in angle. Directive antennas mean narrow beams, which result in accurate angular measurements and allow closely spaced targets to be resolved. An important advantage of microwave frequencies for radar is that directive antennas with narrow beamwidths can be achieved with apertures of relatively small physical size.

In this chapter, the radar antenna will be considered as either a transmitting or a receiving antenna, depending on which is more convenient for explaining a particular antenna property. Results obtained for one may be readily applied to the other because of the reciprocity theorem of antenna theory.[1]

Antenna designers have a variety of directive antenna types from which to choose including the reflector antenna in its various forms, phased arrays, endfire antennas, and lenses. They all have seen application in radar at one time or other. These antennas differ in how the radiated beam is formed and the method by which the beam is steered in angle. Steering the antenna beam can be done mechanically (by physically positioning the antenna) or electronically (by using phase shifters with a fixed phased array). The relatively simple *parabolic reflector,* similar to the automobile headlight or the searchlight, in one form or other has been a popular microwave antenna for conventional radars. As will be discussed later in this chapter, a parabolic reflector can be a paraboloid of revolution, a section of a paraboloid, a parabolic cylinder, Cassegrain configuration, parabolic torus, or a mirror scan (also called polarization-twist Cassegrain). There have also been applications of spherical reflectors, but only for special limited purposes.

The mechanically rotating array antenna was the basis for most of the lower frequency air-surveillance radars that saw service early in World War II. They were eventually replaced by parabolic reflector antennas when radar frequencies increased to the microwave region during and just after World War II. In the 1970s the mechanically scanned planar array antenna reappeared, but at microwave frequencies with slotted waveguide radiators or printed-circuit antennas rather than dipoles. The mechanically scanned planar array is found in almost all 3D radar antennas, low sidelobe antennas, and in airborne radars where the antenna is fitted behind a radome in the nose of the aircraft. (A planar aperture allows a larger antenna to be used inside the radome than is practical with a parabolic reflector.) An example of a very low sidelobe rotating planar array used in the AWACS radar is shown later in Fig. 9.49.

Starting in the mid-1960s the electronically steered phased array antenna began to be employed for some of the more demanding military radar applications. It is the most interesting and the most versatile of the various antennas, but it is also more costly and more complex.

9.2 ANTENNA PARAMETERS

Several of the important antenna parameters were introduced in the discussion of the radar equation in Chapters 1 and 2. Here we review and expand on those we have introduced previously and add some other parameters not yet discussed.

Directive Gain *Gain* is a measure of the ability of an antenna to concentrate the transmitted energy in a particular direction. There are two different, but related, definitions of antenna gain. One is the *directive gain,* sometimes called *directivity.* The other is the *power gain,* and is often simply called *gain.* Both gain definitions need to be understood by the radar systems engineer since both are used. The directive gain is descriptive of the nature of the antenna radiation pattern, and is usually the definition of gain that interests the antenna engineer. The power gain is related to the directive gain, but it takes account of loss in the antenna itself. The power gain is more appropriate for use in the radar range equation and is therefore of more interest for the radar engineer.

We will denote the directive gain by G_D. (In other literature it is sometimes denoted by D.) The directive gain of a transmitting antenna may be defined as

$$G_D = \frac{\text{maximum radiation intensity}}{\text{average radiation intensity}} \qquad [9.1]$$

where the radiation intensity is the *power per unit solid angle* radiated in the direction (θ,ϕ), and is denoted $P(\theta,\phi)$. Its units are watts per steradian. A plot of the radiation intensity as a function of the angular coordinates is called a *radiation-intensity pattern.* The power density, or *power per unit area,* when plotted as a function of angle is called the *power pattern.* The power pattern and the radiation-intensity pattern are identical when each is plotted on a relative basis; that is, when the maximum is normalized to a value of unity. When plotted on a relative basis, they are called the *antenna radiation pattern,* or simply *radiation pattern.*

Since the average radiation intensity over the entire solid angle of 4π steradians is equal to the total power radiated by the antenna divided by 4π, the directive gain of Eq. (9.1) can be written as

$$G_D = \frac{4\pi(\text{maximum power radiated per unit solid angle})}{\text{total power radiated by the antenna}} \qquad [9.2]$$

This equation indicates the procedure by which the directive gain may be found from the antenna radiation pattern. The maximum power radiated per unit solid angle is obtained by inspection, and the total power radiated is found by integrating the volume under the radiation pattern. From Eq. (9.2) the directive gain can be expressed as

$$G_D = \frac{4\pi P(\theta,\phi)_{\max}}{\int\int P(\theta,\phi)\, d\theta d\phi} = \frac{4\pi}{B} \qquad [9.3]$$

where B is called the *beam area* and is defined by

$$B = \frac{\int\int P(\theta,\phi)\, d\theta d\theta}{P(\theta,\phi)_{\max}} \qquad [9.4]$$

The beam area B is the solid angle through which all the radiated power would pass if the power per unit solid angle over the entire beam area were equal to $P(\theta,\phi)_{\max}$. It defines, in effect, an equivalent antenna pattern. If θ_B and ϕ_B are the half-power (radian) beamwidths in the two orthogonal planes, the beam area B is approximately equal to $\theta_B\phi_B$. Substituting into Eq. (9.3) gives

$$G_D \approx \frac{4\pi}{\theta_B\phi_B} \qquad \text{[9.5a]}$$

This is only an approximation and should be used with caution. Another approximation, an improvement on the above, is

$$G_D \approx \frac{\pi^2}{\theta_B\phi_B} \qquad \text{[9.5b]}$$

This expression assumes a gaussian beamshape with θ_B and ϕ_B defined as the half-power beamwidths.[2] (This form of the directive gain has been popular with radar meteorologists.) Beamwidths in Eqs. (9.5a and b) are in radians. If the beamwidths are in degrees in Eq. (9.5a), the 4π in the numerator is replaced by 41,253. Equation (9.5a), however, is overly optimistic in that it provides too high a value of directive gain. It applies for a rectangular beam with no sidelobes.

Warren Stutzman,[3] however, recommended that for practical antennas the following "is an excellent approximation for general use:"

$$G \approx \frac{26{,}000}{\theta_B\phi_B} \qquad \text{[9.5c]}$$

where the half-power beamwidths are in degrees. He states that "gain [G] is used here instead of directivity, not because of losses . . . [but] to indicate that the formula is appropriate to real antenna hardware, where gain is the parameter used in performance descriptions." This equation states that a one-degree pencil-beam antenna has a gain of 44 dB. It should not be a substitute for more exact analysis, calculation, or measurement; but it is far better than Eqs. (9.5a and b) when nothing further is known about the antenna other than its beamwidths in the principal planes.

Power Gain The power gain, which we denote by G, is similar to the directive gain except that it takes account of dissipative losses in the antenna. (It does not include loss arising from mismatch of impedances or loss due to polarization mismatch.) It can be defined similarly to the definition of directive gain, Eq. (9.2), if the denominator is the net power accepted by the antenna from the connected transmitter, or

$$G = \frac{4\pi(\text{maximum power radiated per unit solid angle})}{\text{net power accepted by the antenna}} \qquad \text{[9.6a]}$$

An equivalent definition is

$$G = \frac{\text{maximum radiation intensity from subject antenna}}{\text{radiation intensity from a lossless isotropic radiator with the same power input}} \qquad \text{[9.6b]}$$

Whenever there is a choice, the power gain should be used in the radar equation since it includes the dissipative losses introduced by the antenna. The directive gain, which is always greater than the power gain, is more closely related to the antenna beamwidth. The difference between the two antenna gains is usually small for reflector antennas. The power gain and the directive gain are related by the radiation efficiency ρ_r, as follows

$$G = \rho_r G_D \qquad [9.7]$$

The radiation efficiency is also the ratio of the total power radiated by the antenna to the net power accepted by the antenna at its terminals. The distinction between the two definitions of gain often can be ignored in practice, especially when the dissipative loss in the antenna is small.*

The definitions of power gain and directive gain described in the above were given in terms of a transmitting antenna. Because of reciprocity the pattern of a receiving antenna is the same as the pattern of a transmitting antenna, so the receiving antenna can be described by a gain just as can the transmitting antenna. This is why one can talk of a receiving gain even though gain was defined in terms of a transmitting antenna. The effective aperture of a receiving antenna, on the other hand, has no similar attribute in a transmitting antenna.

It should be kept in mind that the accuracy with which the gain of a radar antenna can be measured is usually about ± 0.5 dB.[4] Thus one should not specify or quote antenna gains to an accuracy much better than this unless there is a reason to be more accurate.

Antenna Radiation Pattern In the above, antenna gain meant the maximum value. It is also common to speak of gain as a function of angle. Quite often the ordinate of a radiation pattern is given as the gain as a function of angle, normalized to unity. It is then known as *relative gain.* Unfortunately the term *gain* is used to denote both the maximum value and the gain as a function of angle. Uncertainty as to which usage is meant can usually be resolved from the context.

An example of an antenna radiation pattern for a paraboloidal reflector antenna is shown in Fig. 9.1.[5] This particular pattern might not be representative of a well-designed modern high-gain antenna, but it does illustrate the various features that a simple reflector-antenna radiation pattern might have. The *main beam* is shown at zero degrees. The remainder of the pattern outside the main beam is the *sidelobe* region. As the angle increases from the direction of maximum gain, there is an irregularity in this particular radiation pattern at about 22 dB below the peak. This is called a *vestigial lobe* or "shoulder" on the side of the main beam. It does not appear in all radiation patterns and is not desired since it is indicative of phase errors in the aperture illumination. Normally, when errors in the aperture illumination are small, the first sidelobe appears near where this vestigial lobe is indicated rather than where the first sidelobe is indicated in the figure.

The near-in sidelobes generally decrease in magnitude as the angle increases. The decrease is determined by the shape of the aperture illumination (as described in the next

*In some types of phased array antennas, the losses in the phase shifters and the power dividing networks can be quite high so that the difference between the power gain and the directive gain can be significant. In such cases, the directive gain is what is usually quoted and the losses are accounted for elsewhere.

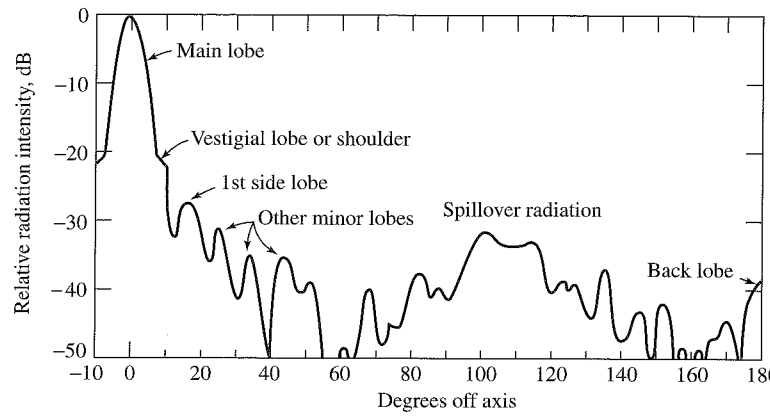

Figure 9.1 Radiation pattern for a particular paraboloid reflector antenna illustrating the main beam and sidelobe radiation. | (After Cutler et al.,[5] Proc. IRE.)

section). Eventually, the sidelobes due to the aperture illumination are masked by sidelobes due to the random errors in the aperture [Sec. (9.12)]. With a conventional reflector antenna, there usually will be spillover radiation from that part of the feed radiation pattern that is not intercepted by the reflector (in the example of Fig. 9.1, this appears from about 100 to 115°). This radiation pattern also has a pronounced lobe in the backward direction (180°) due to diffraction around the edges of the reflector as well as direct leakage through the mesh reflector surface (if the surface is not solid).

The radiation pattern shown in Fig. 9.1 is plotted as a function of one angular coordinate, but the actual pattern is a plot of the radiation intensity $P(\theta,\phi)$ as a function of two angles. The two angle coordinates commonly employed with a ground-based radar antenna are azimuth and elevation, but other appropriate angle coordinates also can be used.

A complete three-dimensional plot of the radiation pattern can be complicated to display and interpret, and is not always necessary. For example, an antenna with a symmetrical pencil-beam pattern can be represented by a single plot in one angle coordinate because of its circular symmetry. The radiation intensity pattern for rectangular or rectangular-like apertures can often be written as the product of the radiation-intensity patterns in the two coordinate planes; for instance,

$$P(\theta,\phi) = P(\theta,0)\, P(0,\phi) \qquad [9.8]$$

Thus when the pattern can be expressed in this manner, the complete radiation pattern in two coordinates can be determined from the two single-coordinate patterns in the θ and in the ϕ planes.

Effective Aperture The effective aperture of a receiving antenna is a measure of the effective area presented to the incident wave by the antenna. As was given previously as Eq. (1.8), the transmitting gain G and receiving effective area A_e of a lossless antenna are related by

$$G = \frac{4\pi A_e}{\lambda^2} = \frac{4\pi \rho_a A}{\lambda^2} \qquad [9.9]$$

where λ = wavelength, ρ_a = antenna aperture efficiency, A = physical area of the antenna, and $A_e = \rho_a A$. The aperture efficiency depends on the nature of the current illumination across the antenna aperture. With a uniform illumination, $\rho_a = 1$. The advantage of high efficiency obtained with a uniform illumination is tempered by the radiation pattern having a relatively high peak-sidelobe level. An aperture illumination that is maximum at the center of the aperture and tapers off in amplitude towards the edges has lower sidelobes but less efficiency than the uniform illumination.

Sidelobe Radiation Sidelobe radiation is radiation from an antenna that is not radiated by the main beam. It is possible in theory to have an antenna radiation pattern with only a single main beam and no sidelobes, but not only is this impractical to achieve, it is not desirable since the main beam would be unusually wide (as mentioned later in Sec. 9.13). In general, the lower the sidelobes, the lower will be the antenna gain and the aperture efficiency, and the greater will be the width of the main beam.

The sidelobe level of an antenna may be described by the value of the peak sidelobe, the rms value of all the sidelobe radiation (usually of the dB values), or some other suitable measure. The peak sidelobe is a good measure of sidelobe behavior for purposes of the radar system engineer. For a line-source aperture with a uniform illumination, the peak sidelobe (which is the first sidelobe) is 13.2 dB down from the maximum value of the main beam, or a value of -13.2 dB. This is usually too high for most radar applications even though its aperture efficiency is unity, that is, 100 percent.

Low antenna sidelobes are desired in a radar so as to avoid detecting large targets when they are illuminated by the antenna sidelobes. Any echoes received from the sidelobes will not be indicated by their true angle. (The angle assigned to an echo from a sidelobe will be the angle at which the main beam points at the time of detection rather than the angle of the sidelobe which illuminates the target.) Low sidelobes are also useful for minimizing the effect of strong jamming and interference and to reduce the large clutter echoes that can enter the antenna sidelobes of a high-prf pulse doppler radar (as was discussed in Sec. 3.9).

The highest sidelobe of an antenna is usually the first sidelobe adjacent to the main beam. A typical parabolic reflector antenna fed from a waveguide horn might have a peak sidelobe of -23 to -28 dB. Peak sidelobes of -40 to -50 dB are possible with specially designed array antennas. Peak sidelobes less than -50 dB are sometimes called *ultralow sidelobes.*

Aperture Efficiency The aperture efficiency is based on the maximum radiation intensity, which usually occurs at the center of the main beam. It is not like the radiation efficiency that is a measure of the energy dissipated as the signal travels through the antenna. A radiation efficiency less than unity means that energy is lost. On the other hand, an aperture efficiency less than unity means that the radiated energy is redistributed in angle rather than be dissipated. For example, consider a line-source antenna aperture-illumination proportional to $\cos^2(\pi z/2)$, where z is the distance from the center of the aperture, $-D/2 \leq z \leq +D/2$, and D is the aperture dimension. In this example the amplitude of the aperture illumination is one-half cycle of the square of the cosine over the aperture. Its radiation pattern has a first sidelobe of -32 dB compared to the -13.2 dB of a uniform

illumination. The gain is reduced by 0.67 and its beamwidth is increased by 1.63 compared to the radiation pattern from a uniformly illuminated antenna. With a scanning antenna, as might be used in a surveillance radar, the reduction in gain is compensated in part by the increased number of pulses received because of the wider beamwidth.

There are other antenna properties that might be more important to the radar systems engineer than the aperture efficiency. Thus the aperture efficiency might be reduced in order to obtain other benefits. These might include low-sidelobe levels, a radar antenna beam which maximizes the radiated energy within a specified angular region,[6,7] shaped beams such as the cosecant-squared pattern, and monopulse antenna patterns optimized for good angle-tracking accuracy. The aperture efficiency might be important to the antenna designer, but to the radar systems engineer it is often something to be traded in order to achieve some more important antenna characteristic.

Polarization The polarization of an electromagnetic wave is defined by the orientation of the electric field. Most radar antennas are *linearly polarized,* with the orientation of the electric field being either horizontal or vertical. Air-surveillance radars generally employ horizontal polarization. Most tracking radars are vertically polarized. *Circular polarization* occurs when the electric field rotates at a rate equal to the RF frequency. It is sometimes used to enhance the detectability of aircraft targets in the midst of rain (Sec. 7.8). There is also *elliptical polarization,* where the electric field also rotates at the RF frequency; but unlike circular polarization, the amplitude of the elliptically polarized electric field varies during the rotation period. Circular and linear polarizations are special cases of elliptical polarization. Although some radar applications seem to prefer a particular polarization (based sometimes on tradition), in many applications there is often not a strong requirement for one polarization over the other. Even the use of circular polarization for rain is not absolutely necessary since orthogonal linear polarizations can be used instead.

9.3 ANTENNA RADIATION PATTERN AND APERTURE ILLUMINATION

The electric-field intensity $E(\phi)$ (units of volts per meter) produced by the electromagnetic radiation emitted from a line-source antenna is a function of the amplitude and phase of the distribution of current across the aperture. The angle ϕ, shown in Fig. 9.2, is with respect to the normal to the center of the antenna aperture. $E(\phi)$ may be found by adding vectorially the individual contributions radiated from the various current elements that constitute the line-source antenna aperture. The mathematical summation at a point in space of all the contributions radiated by the current elements contained within the aperture gives the field intensity in terms of an integral that is difficult to evaluate in the general case.[8] It reduces, however, to a conventional inverse Fourier transform when the distances from the antenna are large enough for the radiation to be considered a plane wave. This occurs in the so-called *far field* of the antenna, when the range $R > D^2/\lambda$, where D is the size of the aperture and λ is the radar wavelength, with D and λ being in the same units. (Although antenna engineers call this region the far field, optical physicists call it the *Fraunhofer region.*) In radar, the target is almost always in the far field.

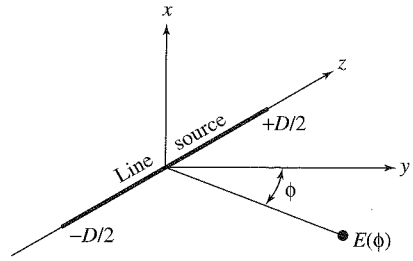

Figure 9.2 Coordinate system for a line source lying along the z axis. Field-intensity pattern $E(\phi)$ lies in the yz plane.

Electric-Field Intensity and the Fourier Transform In Fig. 9.2, the width of the aperture in the z coordinate is D and the angle in the y,z plane as measured from the y axis is ϕ. The aperture is a line source, or linear antenna, in that its dimension in the z-coordinate is much larger than its dimension in the x-coordinate, and the latter (x-coordinate dimension) is small compared to a quarter wavelength. We are interested in the electric-field intensity in the y,z plane. Assuming $D >> \lambda$ and $R > D^2/\lambda$, the variation of the electric field intensity with angle ϕ in the far field is proportional to

$$E(\phi) = \int_{-D/2}^{+D/2} A(z) \exp\left(j2\pi \frac{z}{\lambda} \sin \phi\right) dz \qquad [9.10]$$

where the *aperture illumination* $A(z)$ is the current at a distance z from the center of the radiating line-source antenna. The aperture illumination, also called the *current distribution,* can be a complex quantity including both an amplitude $|A(z)|$ and a phase $\psi(z)$, so that $A(z) = |A(z)| \exp [j\psi(z)]$. The phase of the aperture illumination becomes important if the beam is to be steered in a direction other than broadside or if the antenna is focused (which is rare in radar applications). Here we assume $\psi(z) = 0$.

The electric-field intensity given by Eq. (9.10) applies to a one-dimensional radiating antenna lying along the z axis. If the aperture were two-dimensional and situated in the x,z plane, the aperture illumination, $A(z)$, would be the integral of $A(x,z)$ over the variable x. The electric field in the far field is a function only of the angle ϕ and does not depend on the range R except for the usual $1/R$ factor. The expression of Eq. (9.10) can be extended to two dimensions by considering the aperture illumination to be a function of x as well as z. The plot of the magnitude of the electric-field intensity $|E(\theta,\phi)|$ is called the *electric-field intensity pattern* of the antenna. The plot of the square of the field intensity $|E(\theta,\phi)|^2$ normalized to unity is the *power pattern* or the *radiation pattern.*

The integral describing the electric-field intensity of a radiating source in the far field is an inverse Fourier transform, which most electrical engineers are familiar with since the Fourier transform relates the frequency spectrum and waveform of a temporal signal. The Fourier transform of a time waveform $s(t)$ is the frequency spectrum

$$S(f) = \int_{-\infty}^{+\infty} s(t) \exp(-j2\pi ft)\, dt \qquad [9.11]$$

and the inverse Fourier transform of the spectrum $S(f)$ is the time waveform

$$s(t) = \int_{-\infty}^{+\infty} S(f) \exp(j2\pi ft)\, df \qquad [9.12]$$

This happens to be of the same form as the field-intensity expression of Eq. (9.10). Since the aperture illumination is zero beyond $z = \pm D/2$, the limits of Eq. (9.10) can extend from $-\infty$ to $+\infty$ to make it consistent with the inverse Fourier transform of Eq. (9.12). Thus the mathematical model that relates the time waveform and its spectrum is analogous to the mathematical model that relates the radiated field-intensity and the aperture illumination. The (spatial) antenna pattern $E(\phi)$ is related mathematically to the (temporal) waveform $s(t)$, and the aperture illumination $A(z)$ is related to the spectrum $S(f)$. What is known from signal theory about the role of the spectrum $S(f)$ in determining the nature of the signal $s(t)$ is applicable to how the aperture illumination $A(z)$ affects the radiation in space $E(\phi)$. The converse is also true.

In the above, the antenna was viewed as transmitting. As was stated earlier, the property of antenna reciprocity means that the variation of the radiated field on transmit as a function of angle will be similar to the variation of the received signal as a function of angle when the same antenna is used for both transmit and receive.

In the remainder of this section, the antenna field intensity will be examined for various analytical aperture illuminations. The phase distribution is assumed zero or constant so that only the effects of the amplitude variation across the aperture need be considered. The aperture over which the integral of Eq. (9.10) is taken is defined as the projection of the antenna surface on a plane perpendicular to broadside. In this formulation of antenna radiation based on the inverse Fourier transform of Eq. (9.10) it does not matter whether the illumination is produced by a reflector antenna, a lens, or an array so long as the illumination is that in the plane of the aperture.

One-Dimensional Aperture Illumination Consider in Fig. 9.2 a uniform (constant) aperture illumination extending from $-D/2$ to $+D/2$, and zero outside. This represents the illumination across a line source or the projected illumination in one of the principal planes of a uniformly illuminated rectangular aperture. If the constant value of the amplitude of the aperture illumination is A_0, the variation of the electric-field intensity as a function of angle ϕ is computed from Eq. (9.10) as

$$E(\phi) = A_0 \int_{-D/2}^{+D/2} \exp\left(j2\pi \frac{z}{\lambda} \sin\phi\right) dz = \frac{A_0 D \sin[\pi(D/\lambda)\sin\phi]}{\pi(D/\lambda)\sin\phi} \qquad [9.13]$$

Normalizing to make $E(0) = 1$ results in

$$E(\phi) = \frac{\sin[\pi(D/\lambda)\sin\phi]}{\pi(D/\lambda)\sin\phi} \qquad [9.14]$$

This is of the form $(\sin x)/x$. The square of the above is the antenna radiation pattern or power pattern. It is shown by the solid curve in Fig. 9.3. The first sidelobe adjacent to the main beam is 13.2 dB below the peak value of the main beam. The angular distance between the two nulls defining the main beam is $2\lambda/D$ radians, and the beamwidth as

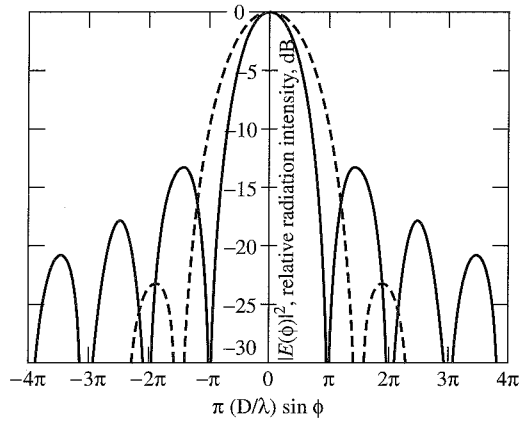

Figure 9.3 Solid curve is the radiation pattern produced by a uniform aperture illumination of a line source of dimension D. The dashed curve is the radiation pattern of an aperture illumination proportional to the cosine function. Both curves are normalized to unity maximum gain.

measured between the half-power points is $0.88\lambda/D$ radians, or $51\lambda/D$ degrees. (Quite often the half-power beamwidth for this uniform illumination is approximated by λ/D radians.) The field-intensity pattern of Eq. (9.14) is positive over the entire main lobe, but changes sign in passing through the first zero, returning to a positive value in passing through the second zero, and so on. The odd-numbered sidelobes are therefore out of phase with the main beam, and the even-numbered ones are in phase.

The normalized field-intensity pattern for an aperture illumination $A(z)$ proportional to one-half cycle of the cosine function, given by cos $(\pi z/D)$, with $|z| \leq D/2$, is from Eq. (9.10)

$$E(\phi) = \frac{\pi}{4}\left[\frac{\sin(\psi + \pi/2)}{\psi + \pi/2} + \frac{\sin(\psi - \pi/2)}{\psi - \pi/2}\right] = \frac{\pi^2 \cos\psi}{\pi^2 - 4\psi^2} \qquad [9.15]$$

where $\psi = \pi(D/\lambda)$ sin ϕ. The square of the above is shown as the dashed curve in Fig. 9.3. In this figure, the peak gains of both patterns (for the uniform and the cosine illuminations) are normalized to unity. In reality, however, the maximum gain of the pattern from the cosine function is 0.9 dB less than that of the maximum gain of the uniform illumination. Notice that the peak sidelobe of the pattern from the cosine function is much lower than the peak sidelobe from the uniform illumination. Its beamwidth, however, is increased and its maximum gain decreased. The greater the taper of the aperture illumination as it approaches the edges of the antenna aperture, the lower will be the sidelobe level, but at the cost of a wider beamwidth and a lower maximum gain.

Table 9.1 lists some on the characteristics of the radiation patterns produced by various one-dimensional (line-source) antenna aperture-illuminations.[8] These aperture illuminations are expressed in analytic form so that the solution of the inverse Fourier transform of Eq. (9.10) can be conveniently determined. They are not necessarily what might be employed by the antenna designer, but they do illustrate how variations in the form of the aperture illumination affect the antenna pattern. More complicated distributions, which cannot be found from available tables of Fourier transforms, may be determined by computer computation. Using the Schwartz inequality, Silver[8] showed that the uniform

Table 9.1 Radiation-pattern characteristics produced by various aperture distributions

	λ = *wavelength;* D = *aperture wideth*		
Type of distribution, $\lvert z\rvert < 1$	**Relative gain**	**Half-power beamwidth, deg**	**Intensity of first sidelobe, dB below maximum intensity**
Uniform; $A(z) = 1$	1	$51\lambda/D$	13.2
Cosine; $A(z) = \cos^n(\pi z/2)$:			
$n = 0$	1	$51\lambda/D$	13.2
$n = 1$	0.810	$69\lambda/D$	23
$n = 2$	0.667	$83\lambda/D$	32
$n = 3$	0.575	$95\lambda/D$	40
$n = 4$	0.515	$111\lambda/D$	48
Parabolic; $A(z) = 1 - (1 - \Delta)z^2$:			
$\Delta = 1.0$	1	$51\lambda/D$	13.2
$\Delta = 0.8$	0.994	$53\lambda/D$	15.8
$\Delta = 0.5$	0.970	$56\lambda/D$	17.1
$\Delta = 0$	0.833	$66\lambda/D$	20.6
Triangular; $A(z) = 1 - \lvert z\rvert$	0.75	$73\lambda/D$	26.4
Circular; $A(z) = \sqrt{1 - z^2}$	0.865	$58.5\lambda/D$	17.6
Cosine-squared plus pedestal;			
$0.33 + 0.66\cos^2(\pi z/2)$	0.88	$63\lambda/D$	25.7
$0.08 + 0.92\cos^2(\pi z/2)$, Hamming	0.74	$76.5\lambda/D$	42.8

aperture illumination produces the maximum gain. When either the $\cos^n$ (cosine raised to the nth power) or the parabolic distributions shown in this table are examined, it is seen that, as has mentioned before, the more tapered the illumination the lower is the peak sidelobe, the wider the beamwidth, and the lower the maximum gain. Note that relative gain in Table 9.1 is the same as the aperture efficiency ρ_a defined previously by Eq. (9.9).

The cosine-squared on a pedestal listed one line from the bottom of the table is a representative illumination for conventional antennas. This is close to the so-called 25-dB Taylor illumination discussed later in Sec. 9.11. The Hamming illumination produces the lowest peak sidelobe for a cosine-squared on a pedestal illumination (in this case the peak lobe is not the one closest to the main beam). The reduction of the spatial sidelobes of an antenna by a tapered aperture illumination is similar to the windowing employed in digital processing to reduce filter sidelobes and to the filter weighting in pulse compression to reduce the time sidelobes of the compressed pulse (Sec. 6.5).

Having the proper aperture illumination is an important requirement for achieving suitable antenna radiation patterns. There is more to consider, as will be discussed in Sec. 9.13, which is on the subject of very low sidelobes.

Two-Dimensional Aperture Illumination To extend the above discussion of radiation from a line source to an aperture with two dimensions, the angles θ,ϕ are defined by the coordinate system shown in Fig. 9.4. The antenna is in the x,y plane. This is the coordinate

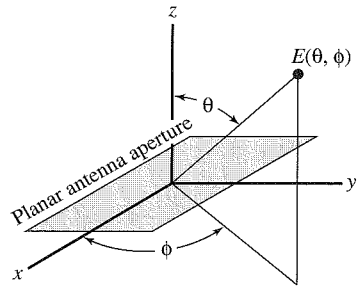

Figure 9.4 Coordinate system for a planar antenna lying in the *xy* plane.

system usually used by antenna theorists, and differs from the azimuth-elevation coordinates preferred by radar engineers. With the coordinate system of Fig. 9.4, the two-dimensional field-intensity pattern from an aperture is given by[8]

$$E(\theta,\phi) = \int\int A(x,y) \exp[j(2\pi/\lambda) \sin\theta\,(x\cos\phi + y\sin\phi)]\,dxdy \qquad [9.16]$$

This integral is not easy to solve analytically, so that numerical techniques are sometimes used. Equation (9.16) is easier to use when the aperture illumination is separable; that is, when $A(x,y) = A_1(x)\,A_2(y)$, where $A_1(x)$ is the projection of the aperture illumination along the x axis and $A_2(y)$ is the projection along the y axis. Silver[9] showed that when aperture illuminations are separable, the field-intensity patterns are also separable. Thus the two-dimensional pattern of Eq. (9.16) can be written as the product of the one-dimensional patterns in the two principal planes, as was indicated earlier by Eq. (9.8). One principal plane occurs when $\phi = 0$, and the other when $\phi = 90°$ in the coordinate system of Fig. 9.4. When the patterns are separable, the pattern in the xz plane is the same as would be produced by a linear antenna with aperture illumination $A_1(x)$, and the pattern in the yz plane is the same as that produced by the linear aperture illumination $A_2(y)$.

Circular Aperture[10–12] Instead of the rectangular coordinates used in Eq. (9.16), polar coordinates are used to describe the aperture illumination $A(r,\theta)$ of a circular aperture. The radial distance from the center of the circular aperture is r, and θ is the angle measured in the plane of the aperture with respect to a reference. When the aperture illumination depends only on the radial distance and is independent of the angle θ, the field intensity is proportional to

$$E(\theta) = 2\pi\int_0^{r_0} A(r)\,J_0[2\pi(r/\lambda)\sin\phi]\,rdr \qquad [9.17]$$

where $A(r)$ is the aperture illumination as a function of the radial distance, r_0 is the radius of the circular aperture, and ϕ is the angle with respect to the normal to the circular aperture. If the aperture illumination is uniform [$A(r) = 1$], this reduces to

$$E(\theta) = 2\pi r_0^2\,J_1(\xi)/\xi \qquad [9.18]$$

where $\xi = 2\pi(r_0/\lambda)\sin\phi$ and $J_1(\xi)$ is the first-order Bessel function. A normalized plot of the square of this equation is shown in Fig. 9.5. The first sidelobe is 17.5 dB below

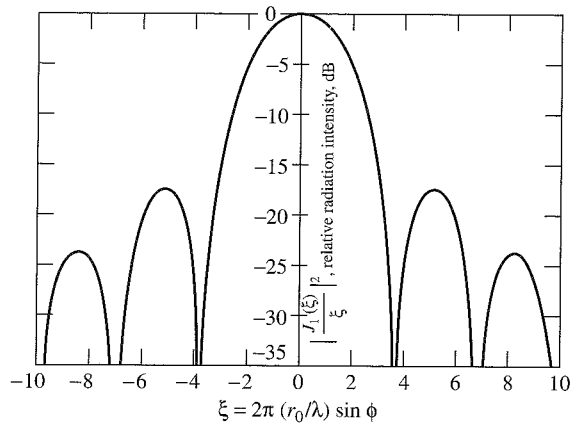

Figure 9.5 Radiation pattern for a uniformly illuminated circular aperture of radius r_0.

the main-beam maximum, and the beamwidth in degrees is $58.5\lambda/D$. Note that this is the same as from a one-dimensional (line source) antenna with a circular aperture-illumination (as was listed in Table 9.1) since the projection of the uniform circular-aperture-illumination on its diameter is a circular one-dimensional illumination.

Tapering of the amplitude illumination in the radial dimension of a circular aperture reduces the peak sidelobe, but at the expense of broader beamwidth and less antenna gain. Consider the family of circularly symmetrical aperture illuminations[8] given by

$$A(r) = [1 - (r/r_0)^2]^p \qquad \textbf{[9.19a]}$$

where $p = 0, 1, 2, \ldots$. This aperture illumination depends only on r and not on θ. The field-intensity pattern is[12]

$$E(\theta) = \pi r_0^2\, 2^p p!\, \frac{J_{p+1}(\xi)}{\xi^{p+1}} \qquad \textbf{[9.19b]}$$

where ξ is defined as it was for Eq. (9.18). When $p = 0$, the illumination is uniform and the radiation pattern reduces to that given by Eq. (9.18). For $p = 1$, the gain is 0.75 of the gain of a uniformly illuminated aperture, the half-power beamwidth is broadened to $72.6\lambda/D$, and the first sidelobe is 24.6 dB below the maximum. The sidelobe level is 30.6 dB down for $p = 2$, and the gain is 0.56 relative to that of the uniform illumination.

Aperture Blocking[13] An obstacle in front of an antenna can alter the effective aperture illumination and distort the radiation pattern. This is called *aperture blocking* or *shadowing*. Examples are the feed and its supports in a reflector antenna; masts on board a ship; and nearby buildings, trees, and other obstructions to a land-based radar. The subreflector, as well as the feed, of a Cassegrain antenna (Sec. 9.4) also blocks the aperture illumination. Aperture blocking lowers the antenna gain, raises the sidelobes, and fills in the nulls. It would not be unusual for a low-sidelobe antenna with −30 to −40 dB peak sidelobe level to be increased to a sidelobe level of from −15 to −20 dB when its beam is obstructed.

The effect of aperture blocking can be approximated by subtracting from the antenna pattern of the undisturbed aperture the antenna pattern produced by the shadow of an obstacle. This procedure is possible because of the linearity of the Fourier transform that relates the aperture illumination and the radiation pattern. An example of the effect of aperture blocking caused by the feed in a paraboloid-reflector antenna is illustrated in Fig. 9.6.[14] This relatively simple method for determining the effect of blocking a portion of the radiated energy is only an approximation.

The reduction of the antenna gain η due to the blockage of a circular obstacle of radius r_b placed in front of a circular aperture of radius r_0 whose aperture illumination is given by Eq. (9.19a) is

$$\eta = \left[1 - \delta^2\{[(1 - \delta^2)^p]p + 1\}\right]^2 \qquad [9.20]$$

where $\delta = r_b/r_0$ and p is defined by Eq. (9.19a). This equation, due to Sciambi,[15] would apply to a circular feed at the focus of a parabolic reflector or to the subaperture of a Cassegrain antenna. (Sciambi included in his paper the aperture illumination of Eq. (9.19a) on a pedestal, but it was omitted here for simplicity.) When $\delta = r_b/r_0$ is small, then $\eta \approx [1 - (p + 1)\delta^2]^2$. Based on this approximation, the new sidelobe level due to aperture blocking can be written as

$$sl_b = \left(\frac{\sqrt{sl} + (p + 1)\delta^2}{1 - (p + 1)\delta^2}\right)^2 \qquad [9.21]$$

where sl is the original sidelobe level relative to the main-beam peak when there is no aperture blockage. The sidelobes sl_b and sl are power ratios less than one. In obtaining the above, the maximum value of the obstacle pattern based on Eq. (9.19b) was taken as $\pi r_b^2/2$ (with $p = 0$ and replacing r_0 with r_b).

As an example, consider a parabolic aperture illumination as in Eq. (9.19a) with $p = 1$ and $\delta = r_b/r_0 = 0.1$ (one-percent of the antenna area is blocked). The reduction in gain due to blockage from Eq. (9.20) is 0.96 (about 0.2 dB), and the peak sidelobe of the antenna from Eq. (9.21) is increased from −24.6 dB to −21.9 dB. When $\delta = 0.2$ (4 percent blockage), the peak sidelobe is increased to −16.4 dB. Thus with antennas having

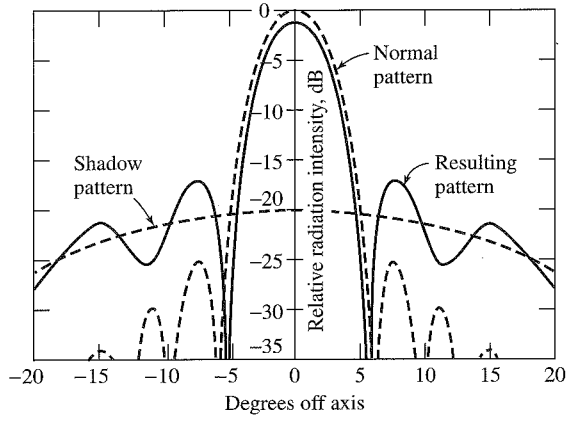

Figure 9.6 Effect of aperture blocking caused by an obstacle (such as a feed) in a parabolic-reflector antenna. (From C. Cutler[5] Proc. IRE.)

conventional sidelobes of −23 to −28 dB, the aperture blockage should not be more than about 1 percent in order to maintain decent sidelobes. With low peak sidelobes of −40 dB, the aperture blockage should be less than 0.05 percent, and with ultralow sidelobe levels (Sec. 9.13), no aperture blockage at all can be tolerated.

9.4 REFLECTOR ANTENNAS

The parabola, sketched in Fig. 9.7, works well as a reflector of electromagnetic energy and has been the basis for many radar antennas. The parabolic surface is illuminated by a source of radiated energy called the *feed,* which is placed at the focus of the parabola. The parabola converts the spherical wave radiated from the feed to a plane wave because (1) any ray radiated from the focus that intersects the parabolic surface is reflected in a direction parallel to the axis of the parabola, and (2) the distance traveled by any ray from the focus to the parabola and by reflection to a plane perpendicular to the parabola's axis is the same for all rays no matter what angle they emanate from the focus. (This description is only an approximation based on geometric optics. In practice a plane wave does not emerge after reflection until the wave travels a sufficient distance to be in the far field of the antenna, but this need not be of concern at present.)

Paraboloid There are several ways in which the parabola is used for antennas. Rotating the parabolic curve shown in Fig. 9.7 about its axis produces a surface which is a parabola of revolution called a *circular parabola;* or, more usually, a *paraboloid.* When properly illuminated by a source at the focus, the paraboloid generates a nearly symmetrical pencil-beam antenna pattern. This has been a popular antenna for tracking radars. (The paraboloid reflector is sometimes called a *dish.*)

Section of a Paraboloid Instead of a circular shape, consider the reflector antenna to have an elliptical shape (as though an elliptical section were cut from the symmetrical paraboloid). This produces an asymmetrical beam shape known as a *fan beam.* It is often used

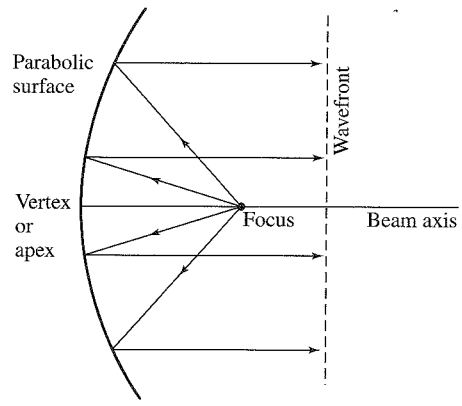

Figure 9.7 Contour of a parabolic-reflector antenna.

for two-dimensional (range and azimuth angle) air-surveillance radars, as shown in the example of Fig. 9.8. Sometimes this type of asymmetrical antenna has a different curvature in the horizontal and vertical planes so as to shape the beams differently in the two planes. This might be the case for an antenna used with an air-surveillance radar where the azimuth beamwidth is required to be narrow, and the vertical beam is shaped to provide a broader coverage, such as the cosecant-squared pattern discussed in Sec. 9.11.

Feeds for Paraboloids The "ideal" feed for a paraboloid reflector would be a source at the focus with a radiation pattern that (1) had no phase variation with angle, (2) produced on the reflector surface the desired aperture amplitude illumination, and (3) had a directivity that allowed all of the feed radiation to be intercepted by the aperture without spillover. The ideal may be approximated but never fully accomplished. The radiation pattern produced by the feed is called the *primary pattern* and that radiated by the aperture is called the *secondary pattern.*

A simple half-wave dipole with a parasitic reflector to direct most of its energy towards the antenna aperture can be used as the feed for a paraboloid, Fig. 9.9a. A dipole, however, is of limited utility as a reflector feed since it is difficult to shape the primary pattern and it is limited in power handling, especially at the higher microwave frequencies. An open-ended waveguide is usually preferred over a dipole for microwave-radar reflector feeds. A circular paraboloid, for example, might be fed by a circular, open-ended waveguide operating in the TE_{11} mode. A rectangular guide operating in the dominant TE_{10} mode, however, does not result in a perfectly symmetrical secondary pattern since its dimensions in the E and H planes are different.

When more directivity is required from the feed than is available from an open-ended waveguide, some form of waveguide horn can be used. A horn can be made to provide the asymmetrical feed illuminations (the primary pattern) for a fan beam generated by a

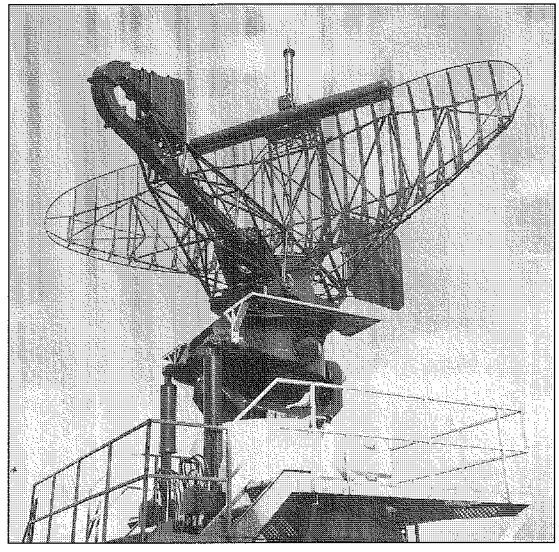

Figure 9.8 Signaal LW08 2D (Jupiter) *L*-band fan-beam air and surface surveillance radar with an elliptical shape fan-beam antenna fed by a horn (on the left). The reflector surface is a mesh, the horizontal antenna mounted on the top is for IFF (identification friend or foe). At the middle right can be seen a fin which is added to the back of the antenna to counterbalance the wind forces on the reflector in the position of the worst yawing moment.
(Courtesy Hollandse Signaalapparten B. V., The Netherlands.)

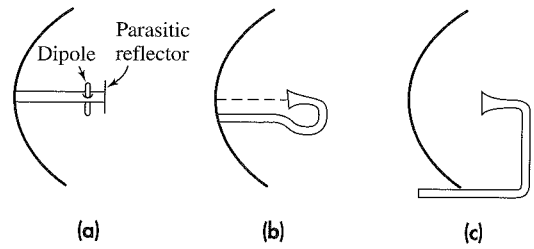

Figure 9.9 Examples of the placement of the feeds in parabolic reflectors. (a) Rear feed using half-wave dipole with parasitic reflector; (b) rear feed using horn; (c) front feed using horn.

section of a paraboloid. Feeds for reflector antennas can come in many varieties in addition to the simple horn and open-ended waveguide.[16]

As an approximate rule of thumb, the intensity of the radiation from the feed toward the edge of the reflector should be about 10 dB down from the maximum radiation. The aperture illumination at the edges of the reflector surface will be even less than this because of the longer path length from the feed to the edge compared to the path length from the feed to the center of the reflector. When the primary feed pattern is 10 dB down toward the edges, the first sidelobe in the secondary pattern usually is in the vicinity of 22 to 25 dB.

The *f/D ratio* of a reflector antenna is the focal length f divided by the aperture diameter D. Most practical reflector antennas have f/D ratios ranging from 0.3 to 0.5. A small ratio means a deep reflector that is difficult to illuminate properly. A large f/D ratio results in a shallow reflector. The shallow reflector is easier to support and to position mechanically, but the feed must be supported farther from the reflector. The farther the feed is from the reflector, the narrower must be the primarily pattern (to avoid spillover loss) and the larger must be the feed. A large f/D is preferred for tracking radars and when the beam must be offset in angle by displacing the feed from the focus.

Calculations of the antenna efficiency based only on the aperture illumination established by the primarily pattern from a feed as well as the spillover indicate theoretical efficiencies of about 80 percent compared to an ideal uniformly illuminated aperture without spillover. In practice, however, phase variations across the aperture, poor polarization characteristics, and antenna mismatch reduce the overall antenna efficiency to the order of 55 to 65 percent for ordinary paraboloidal-reflector antennas.

Feed Support The dipole and the waveguide horn (or open-ended waveguide) can be arranged to feed the paraboloid from the rear as shown in Fig. 9.9a and b. Other types of rear-feed systems have also been used. Figure 9.9c illustrates what is called a front feed using a horn radiator at the focus. It is well suited for supporting horn feeds, but the supports obstruct the aperture.[17] These obstructions due to the feed and its supports reduce the antenna gain, increase the sidelobes, and cause some of the radiated energy to be cross polarized. Analytical expressions and design curves for determining the adverse effects of aperture blockage have been proposed.[18] There is also an impedance mismatch at the feed due to some of the energy reflected by the antenna surface re-entering the feed and its transmission line. Both aperture blockage and mismatch due to reflection can be eliminated by the offset feed.

Offset-Fed Reflector[19,20] As seen in Fig. 9.10, the feed in this arrangement is placed at the focus of the parabola, but the horn is tipped (upwards in the figure) with respect to the parabola's axis. The lower half of the parabolic surface is removed, leaving that portion shown by the solid curve in the figure. The feed is therefore outside the path of the energy reflected from the antenna surface. There is no pattern deterioration due to aperture blocking nor is there any significant amount of radiation intercepted by the feed to produce an impedance mismatch (high VSWR).

Although the offset feed eliminates aperture blockage and mismatch of rear and front feeds, it introduces problems of its own. Its *f/D* ratio (focal length divided by diameter) is greater than that of conventional paraboloids so that the feeds are larger. Furthermore, this type of antenna is generally more difficult to support mechanically. Because of the increased asymmetry of this geometry, when illuminated by a conventional linearly polarized feed, cross-polarized radiation lobes are produced which can reduce radar system performance by indicating false targets. It has been said[19] that when circular polarization is used, the offset-fed reflector does not depolarize the radiated field, but the beam will be squinted relative to the electrical boresight of the antenna. With the increased importance of operating satellite communications with dual orthogonal polarizations, there have been improvements made in the cross-polarization properties of offset-fed reflector antennas.[21,22] Cross-polarized sidelobes of a single-reflector offset-fed antenna can be made comparable to the co-polarized sidelobes, and can be much lower if a dual-reflector antenna is used.

Cassegrain Antenna This is a dual-reflector antenna, Fig. 9.11, with the feed at or near the vertex of the parabola rather than at its focus. The larger (primary) reflector has a parabolic contour and the (secondary) subreflector has a hyperbolic contour. One of the two foci of the hyperbola is the real focal point of the system. The feed is located at this point, which can be at the vertex of the parabola or, more usually, in front of it. The other focus is a virtual focal point and is located at the focus of the primary parabolic surface. Parallel rays coming from a target are reflected by the parabola as a convergent beam and are re-reflected by the hyperbolic subreflector so as to converge at the position of the feed. There exists a family of hyperbolic surfaces that can serve as the subreflector. The larger the subreflector, the nearer it will be to the primary reflector and the shorter will be the axial dimension of the antenna assembly. A large subreflector, however, results in large aperture blocking, which may not be desirable. A small subreflector reduces aperture blocking, but it has to be supported at a greater distance from the primary reflector.

The chief advantage of the Cassegrain configuration is that the feed at or near the apex of the parabola does away with the need for long transmission lines out to a feed at

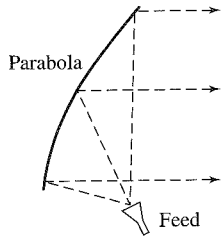

Figure 9.10 Parabolic reflector with offset feed.

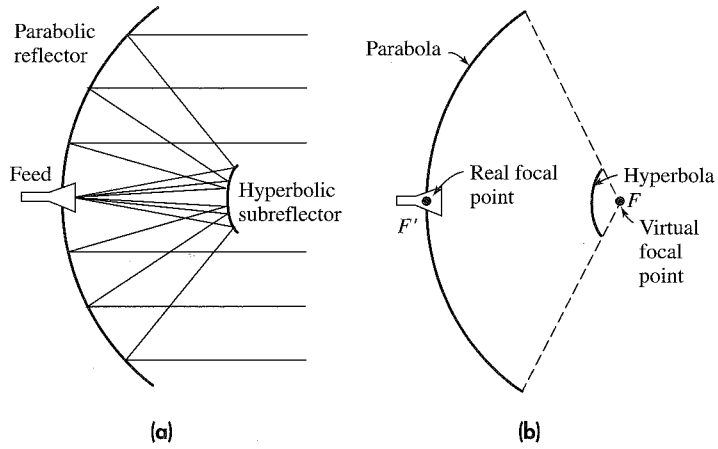

Figure 9.11 (a) Cassegrain antenna showing the hyperbolic subreflector, the feed at the vertex of the main parabolic reflector, and the paths of the rays from the feed; (b) geometry of the Cassegrain antenna.

the normal focus of the parabola. Furthermore, it allows greater flexibility in the size of the feed system. It is popular for monopulse tracking radars since the microwave hardware for generating the sum and difference patterns can be located behind the reflector without increasing aperture blocking. It has also been a good structure for experimental systems that use radar and other electromagnetic systems for different purposes, such as in the MIT Lincoln Laboratory Haystack Hill microwave research system. In that system there were separate RF systems for radar, radiometer, and space communications which operated at various frequencies. Each was constructed in replaceable modules, 8 by 8 by 12 ft in size, which were mounted directly behind the primary reflector.[23]

The antenna noise temperature (Sec. 11.2) of a Cassegrain configuration is usually smaller than that of a conventional front-focus antenna since there are no lossy transmission lines between the receiver and the feed. Also, the sidelobes caused by the spillover of the feed radiation from the subreflector illuminate the cold sky rather than the warm earth. Low antenna noise temperature is important for antennas used for radio astronomy or space communications, but it is generally not an issue in radar since extremely low-noise receivers are not always desirable, especially for military applications.

Aperture Blocking in the Cassegrain Antenna The hyperbolic subreflector of the Cassegrain antenna causes aperture blocking. Aperture blocking can be reduced by decreasing the size of the subreflector. This requires that the feed be made more directive or moved closer to the subreflector in order to minimize the spillover from the subreflector. A more directive feed means a larger feed that partially shadows the primary reflector and contributes to blockage. Thus blockage includes the obstacle presented by the feed as well as the subreflector. Minimum total aperture blocking occurs when the area of the subreflector and the projected area of the feed are equal.[24]

Polarization-Twist Reflector[24] The technique diagrammed in Fig. 9.12 can reduce aperture blocking if the application permits the antenna to operate with only a single polarization. The subreflector consists of a horizontal grating of wires, called a *transreflector.*

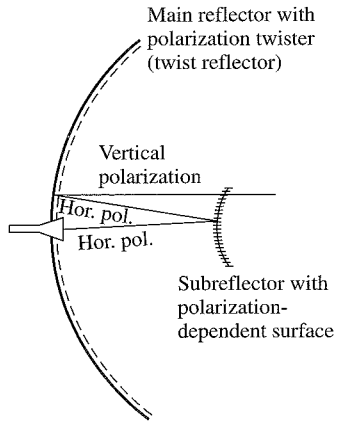

igure 9.12 Polarization-twist :assegrain antenna. Aperture locking by the subreflector is :educed with this design.

It will pass vertically polarized radiation with negligible attenuation but will reflect horizontal polarization radiated by the feed. At the primary reflector the horizontally polarized radiation reflected by the subreflector is rotated 90° by the *twist reflector.* The twist reflector consists of wires oriented 45° to the incident polarization and placed one-quarter wavelength from the reflector's surface. Half the energy incident on the wires oriented at 45° passes through the grating; the other half is reflected. The one-quarter wavelength spacing of the wire grid from the reflector surface results in half-wavelength total travel of the component reflected from the surface. When combined with the component reflected from the wire grid, the resultant polarization is rotated 90°, and is therefore vertically polarized. This vertically polarized component is perpendicular to the horizontal-wire grid of the subreflector and passes through with negligible attenuation. The twist reflector as described above is narrowband, but it can be made to have very wide bandwidths.[25,26]

Gregorian Antenna The Gregorian antenna uses a dual-reflector similar to the Cassegrain except that the subreflector is an ellipsoid with one of its foci at the focus of the primary paraboloidal reflector. The ellipsoid lies beyond the focus of the paraboloid, instead of closer to it as does the subreflector of the Cassegrain. Also in the Gregorian configuration, the concave side of the secondary reflector ellipsoid faces the primary reflector, which differs from the Cassegrain in which the secondary reflector has its convex side facing the feed. The Gregorian has not seen as much application to radar as has the Cassegrain. There are other multireflector antennas; but they also have not had significant radar application.

Parabolic Cylinder Another method for obtaining an asymmetrical antenna pattern is to use a *parabolic cylinder,* shown in Fig. 9.13. This antenna surface is generated by moving the parabolic contour parallel to itself. A line source, such as a linear array, located at the focus of the cylinder is used to illuminate the parabolic-cylinder reflector (the focus is a line rather than a point). The beamshape and beamwidth in the plane containing

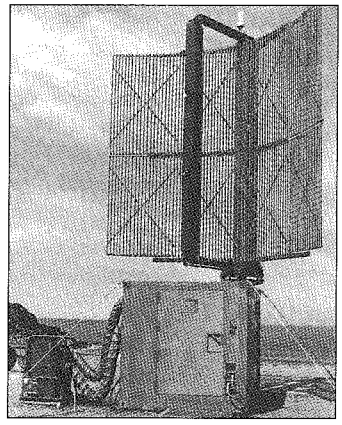

Figure 9.13 Example of a vertically oriented parabolic cylinder reflector antenna with a linear-array feed. This is the antenna used for the U.S. Marine Corps AN/TPS-63 air-surveillance radar.
| (Courtesy Northrop Grumman Corp.)

the linear feed are determined by the illumination of the line-source feed, while the beamwidth in the perpendicular plane is determined by the illumination across the parabolic profile. The reflector is usually made slightly longer than the linear feed to avoid spillover and diffraction effects.

An advantage of the parabolic cylinder is that the large number of individual radiators on its linear-array (line-source) feed provides more control of the aperture illumination than does a single point-source feeding a paraboloid. The aperture illuminations required for low-sidelobe radiation patterns are more readily achieved with a parabolic cylinder than a paraboloid or a section of a paraboloid because of the control that can be applied at each of the radiating elements of the linear-array feed. The line feed, however, shapes the radiated beam in one plane only. Shaping of the beam in the orthogonal plane is determined by the reflector. Precise elevation-beam shaping is the purpose of the parabolic cylinder shown in Fig. 9.13, where the cylindrical antenna is oriented in the vertical so that the elevation radiation pattern can be shaped to minimize the radiation that strikes the ground.

The parabolic cylinder can generate an asymmetrical fan beam with a much larger ratio of the two orthogonal beamwidths than can a section of a paraboloid. Aspect ratios greater than 8:1 are practical with a parabolic cylinder but are difficult to achieve with a section of a paraboloid. Also, there is usually less depolarization on reflection from a parabolic cylinder than from a paraboloid.

9.5 ELECTRONICALLY STEERED PHASED ARRAY ANTENNAS

Background A phased array is a directive antenna made up of a number of individual antennas, or radiating elements. Its radiation pattern is determined by the amplitude and phase of the current at each of its elements. The phased array antenna has the advantage of being able to have its beam electronically steered in angle by changing the phase of the current at each element. The beam of a large fixed phased-array antenna therefore can

be rapidly steered from one direction to another without the need for mechanically positioning a large and heavy antenna. A typical phased array radar for microwave radar might have several thousand individual radiating elements using, for example, ferrite or diode phase shifters that allow the beam to be switched from one direction to another in several microseconds, or less.

Electronically steerable phased arrays are of interest because they can provide:

- Agile, rapid beam-steering.
- Potential for large peak and large average power. Each element can have its own transmitter. The power-aperture product can be large, especially at the lower frequencies.
- Multiple-target tracking. This can be accomplished either by generating multiple, simultaneous, independent beams or by rapidly switching a single beam to view more than one target in sequence.
- A convenient means to employ solid-state transmitters.
- Convenient shape for flush mounting or for blast hardening.
- Control of the aperture illumination because of the many antenna elements available.
- A lower radar cross section, if properly designed.
- Operation with more than one function (a multifunction radar), especially if all functions are best performed at the same frequency.

The chief disadvantages of a phased array radar are that it is complex and can be of high cost. Although an advantage of a phased array is that it can perform multiple functions in a sequential (time-shared) manner, its ability to employ multiple functions requires serious compromises for some applications.

A *linear array* consists of antenna elements arranged in a straight line in one dimension. It was mentioned in the last section that a linear array can be used as the feed for a parabolic cylinder antenna. A *planar array* is a two-dimensional configuration of antenna elements arranged to lie in a plane. In both the linear and planar arrays, the element spacings usually are uniform (equal spacing). The planar array may be thought of as a linear array of linear arrays. Most phased arrays of interest for radar are planar, but in this section we will start with the linear array as the model since it is simpler to analyze. A *broadside array* is one in which the direction of maximum radiation is perpendicular to, or almost perpendicular to, the plane (or line) of the antenna. An *endfire array* has its maximum radiation parallel to the array or at a small angle to the plane of the array.

Radiation Patterns of Phased Arrays Consider, as in Fig. 9.14, a receiving linear array made up of N elements equally spaced a distance d apart. The elements are assumed to be isotropic radiators in that they have uniform response for signals from all directions. Although isotropic radiators are not realizable in practice, they are a convenient concept in array theory. The outputs received from all N elements are summed via lines of equal length to produce a sum output voltage E_a. Element 1 will be taken as the reference with zero phase. From simple geometry, the difference in path length between adjacent elements for signals arriving at an angle θ with respect to the normal to the antenna, is

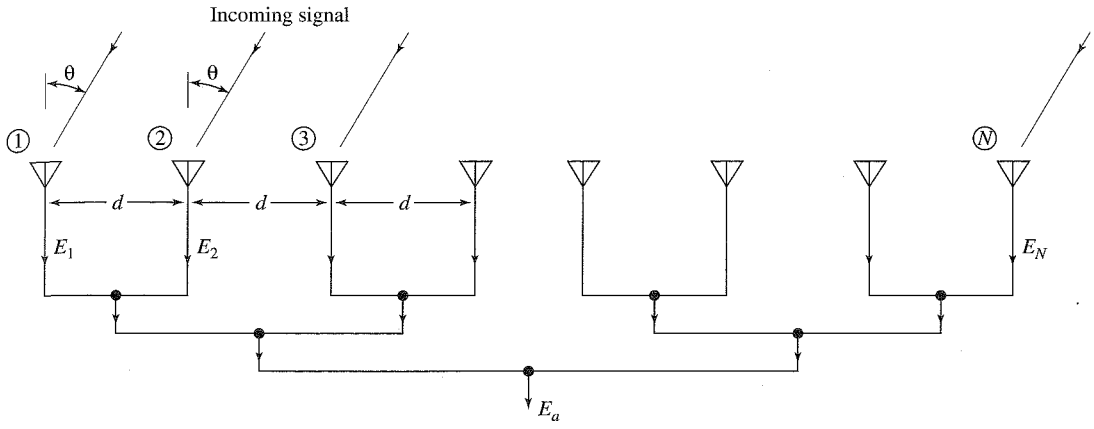

Figure 9.14 N-element receiving, parallel-feed, linear array, with equal lengths of transmission lines between each antenna element and the antenna output (at the bottom on the figure).

$d \sin \theta$. This gives a phase difference between adjacent elements of $\phi = 2\pi(d/\lambda) \sin \theta$, where λ = wavelength of the received signal. It is assumed that there is no further amplitude or phase weighting of the received signals. For convenience, we take the amplitude of the received signal at each element to be unity. The sum of all the voltages from the individual elements, when the phase difference between adjacent elements is ϕ, can be written

$$E_a = \sin \omega t + \sin(\omega t + \phi) + \sin(\omega t + 2\phi) + \cdots + \sin[\omega t + (N-1)\phi] \quad \textbf{[9.22]}$$

where ω is the angular frequency of the signal. The sum can be written[27]

$$E_a = \sin\left[\omega t + (N-1)\frac{\phi}{2}\right] \frac{\sin(N\phi/2)}{\sin(\phi/2)} \quad \textbf{[9.23]}$$

The first factor is a sinewave of frequency ω with a phase shift $(N-1)\phi/2$. (If the phase reference were taken at the center of the array instead at the left-hand side, this phase shift would be zero. In any event this factor is not as important as the second factor.) The second factor is an amplitude of the form $(\sin NX)/(\sin X)$. The magnitude of Eq. (9.23) represents the *field-intensity pattern,* or

$$|E_a(\theta)| = \left| \frac{\sin[N\pi(d/\lambda) \sin \theta]}{\sin[\pi(d/\lambda) \sin \theta]} \right| \quad \textbf{[9.24]}$$

The field-intensity pattern has zeros when the numerator is zero. This occurs when $N\pi(d/\lambda) \sin \theta = 0, \pm\pi, \pm 2\pi, \ldots, \pm n\pi$, where n = integer. The denominator, on the other hand, is zero whenever $\pi(d/\lambda) \sin \theta = 0, \pm\pi, \pm 2\pi, \ldots, \pm n\pi$. When the denominator is zero, it is seen that the numerator is also zero, and the value of $|E_a(\theta)| = 0/0$ is indeterminate. By applying L'Hopital's rule (differentiating numerator and denominator separately) it is found that $|E_a(\theta)|$ is a maximum and is equal to N when $\sin \theta = \pm n\lambda/d$. The maximum at $\theta = 0$ defines the main beam of the field-intensity pattern. The other maxima are

called *grating lobes* and are of the same magnitude as the main beam. They are generally undesirable in that they can cause ambiguities by being mistaken for the response of a target in the main beam. Grating lobes can be avoided if the spacing d between elements is equal to or less than λ. (There is still a grating lobe at $\theta = \pm 90°$ when $d = \lambda$, but practical radiating elements are not isotropic and can have negligible radiation $\pm 90°$.)

Equation (9.24) indicates that $E_a(\theta) = E_a(\pi - \theta)$; which means that an array of isotropic elements has a similar pattern in the rear of the antenna as in the front. The same is true for an array of dipole antennas. To avoid ambiguities between echoes from the front and the rear, the backward radiation can be eliminated by placing a reflecting screen behind the array so that only radiation over the forward half of the array antenna ($-90° \leq \theta \leq +90°$) need by considered. The field-intensity pattern with a back screen will be different from that of Eq. (9.24).

The normalized radiation pattern of an array of isotropic elements, which is sometimes called the *array factor,* is

$$G_a(\theta) = \frac{|E_a|^2}{N^2} = \frac{\sin^2 [N\pi(d/\lambda) \sin \theta]}{N^2 \sin^2 [\pi(d/\lambda) \sin \theta]} \qquad [9.25]$$

If Nd = D, the antenna dimension, and if the sine in the denominator can be replaced by its argument (implying that the angle θ is small), the pattern of the uniformly illuminated array is similar to the pattern of a uniformly illuminated line-source antenna, as was given by Eq. (9.14). The half-power beamwidth of this uniformly illuminated array of N elements when d = $\lambda/2$ is approximately

$$\theta_B = \frac{102}{N} \qquad [9.26]$$

When N is sufficiently large, the first (and largest) sidelobe is 13.2 dB below the main-beam maximum value.

When the radiating elements are not isotropic, the antenna radiation pattern of Eq. (9.24) has to be modified by the radiation pattern $G_e(\theta)$ of an individual directive element, so that

$$G(\theta) = G_e(\theta) \frac{\sin^2 [N\pi(d/\lambda) \sin \theta]}{N^2 \sin^2 [\pi(d/\lambda) \sin \theta]} = G_e(\theta)\, G_a(\theta) \qquad [9.27]$$

This is the product of the *element factor* $G_e(\theta)$ times the *array factor* $G_a(\theta)$, the latter being the pattern of an array composed of isotropic elements. Grating lobes caused by element spacings greater than half-wavelength may be eliminated by using directive elements whose pattern is zero or small in directions of undesired grating lobes. For example, if the element spacing $d = 2\lambda$, grating lobes occur at $\pm 30°$ and $\pm 90°$, in addition to the main beam at $\theta = 0°$. If the individual radiating elements, for example, have a radiation pattern whose null width (defining its main beam) is less than 60°, the grating lobes produced by the array factor will be suppressed. When this occurs, the antenna beam cannot be steered beyond the coverage of the individual elements that make up the array.

Equation (9.27) assumes that the radiation pattern of each element is the same. This is not true in practice, however. The radiation from an element in an array will be affected

by the mutual coupling among elements and the coupling due to the outward-traveling wave. An element in the center of the array sees a different electromagnetic environment from an element at the edge of the array. The radiation patterns of the elements will not be the same and will depend on the mutual coupling. Thus the pattern of an individual element depends on where it is located within an array. In order to obtain a more accurate representation of the radiation pattern of an array antenna, the pattern of each element within the array should be measured (or otherwise determined) in the presence of all others. Because the element pattern is not the same for each element, the radiation pattern of Eq. (9.27) is only an approximation, but one which has been widely employed.

Two-Dimensional Radiation Pattern In a two-dimensional, rectangular planar array whose aperture illumination can be separated into two orthogonal planes such as the horizontal and the vertical planes, the radiation pattern may then be written as the product of the radiation patterns in these two planes (sometimes called *principal planes* of the antenna). If the radiation patterns in the two principal planes are $G_1(\theta_a)$ and $G_2(\theta_e)$, the two-dimensional antenna pattern in this case is

$$G(\theta_a, \theta_e) = G_1(\theta_a)\, G_2(\theta_e) \qquad [9.28]$$

The angles θ_a and θ_e are not necessarily the elevation and azimuth angles normally associated with radar antennas. The normalized radiation pattern of a uniformly illuminated rectangular array of isotropic elements with spacing d is

$$G(\theta_a, \theta_e) = \frac{\sin^2 [N\pi(d/\lambda) \sin \theta_a]}{N^2 \sin^2 [\pi(d/\lambda) \sin \theta_a]} \frac{\sin^2 [M\pi(d/\lambda) \sin \theta_e]}{M^2 \sin^2 [\pi(d/\lambda) \sin \theta_e]} \qquad [9.29]$$

where N = number of (vertical) columns of the array that give rise to the (azimuth) angle θ_a and M = number of (horizontal) rows that generate the (elevation) angle θ_e. The above assumes the spacing between elements in the two directions is the same; but if they are not, the required modification is simple. Since array elements are not isotropic, the two-dimensional element factor should multiply this equation to obtain the antenna pattern.

Beam Steering and Array Feed Networks The beam of a linear array can be steered in angle by changing the relative time delays between the elements. Consider, as in Fig. 9.15a, two elements of a many-element array spaced a distance d apart. The signal from a direction θ_0, relative to the normal to the two elements, arrives at element 2 before it arrives at element 1. If the signal is delayed at element 2 for a time $\Delta T = (d/c) \sin \theta$, it will be in time coincidence (congruent) with the signal at element 1. If they are added together, it is as though the "main beam" of this simple two-element array was pointed in the direction θ_0. Beam steering occurs by changing the time delay. Inserting variable true-time-delays at each element of a many-element phased array, however, can be quite complicated and is generally unattractive with available technology. Instead, it is much simpler to employ a (modulo 2π) phase shift equal to $\phi = 2\pi f_0\, \Delta T = 2\pi(d/\lambda) \sin \theta_0$, where f_0 = frequency. The signals are then in phase rather than coincident in time. This is illustrated by Fig. 9.15b.

In a linear array, the phase shift that needs to be inserted at each of the elements in order to have all the signals with the same phase is $m\phi$, where m, an integer from 0 to

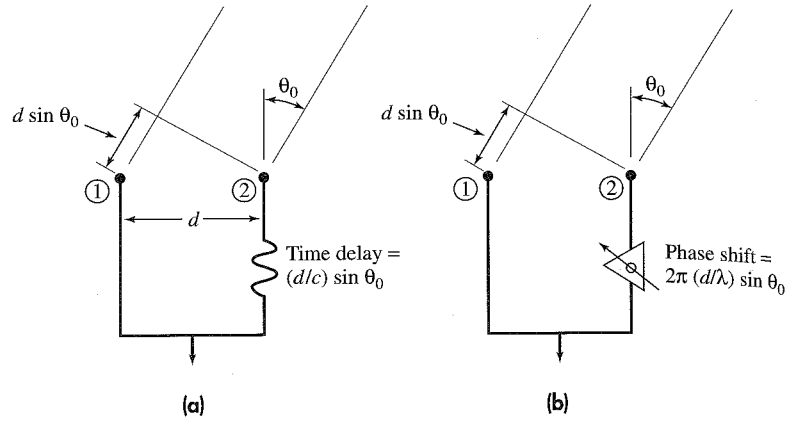

Figure 9.15 Two array elements spaced a distance d apart with a received signal arriving at an angle θ_0 measured with respect to the broadside direction. (a) Beam steering based on true time-delay; (b) beam steering using a phase shifter that is variable over the range from 0 to 2π radians.

$N - 1$, is the number of the element relative to the reference element. This means that the phase difference between elements is ϕ. The normalized radiation pattern of a linear array of isotropic elements is

$$G(\theta) = \frac{\sin^2 [N\pi(d/\lambda)(\sin \theta - \sin \theta_0]}{N^2 \sin^2 [\pi(d/\lambda)(\sin \theta - \sin \theta_0]} \qquad [9.30]$$

The maximum of this pattern occurs when $\sin \theta = \sin \theta_0$; hence, θ_0 is the direction at which the main beam points. As before, the element pattern should multiply this equation to get the antenna radiation pattern. Thus the beam can be steered in an array by changing the phase shift at each element.

Feeding an Array Variable phase shifters may be used at each element of a linear array to steer the beam as illustrated by the simple four-element array of Fig. 16a. This is called a *parallel-fed array.* The difference in phase between elements is $\phi = 2\pi(d/\lambda) \sin \theta_0$. When a series of power splitters, such as hybrid junctions, are used to create a tree-like structure as in the figure, it is sometimes called a *corporate feed,* since it vaguely resembles (when turned upside down) the organization chart of a corporation. Equal lengths of line between the elements and the transmitter/receiver are desired, but that is not always possible. The phase at each element should be the same (other than that introduced by the phase shifter). If the power is equally divided among all the elements and if the loss at each element is L_{ps}, then the entire loss in the parallel feed network is also given by L_{ps}.

A *series-fed* linear array is shown in Fig. 9.16b. Each phase shifter has the same phase, which means that only one steering command (the phase ϕ) need be generated, as compared to the $N - 1$ phase commands needed for the parallel-fed array. This is an advantage since it simplifies the computer that has to generate the phase commands. A serious disadvantage, however, of the series-fed array is its high loss. If the loss of each phase shifter is L_{ps}, then the loss through the array feed network is $(N - 1)L_{ps}$. Since it is not unusual for the loss of a phase shifter to be a significant fraction of a dB and since

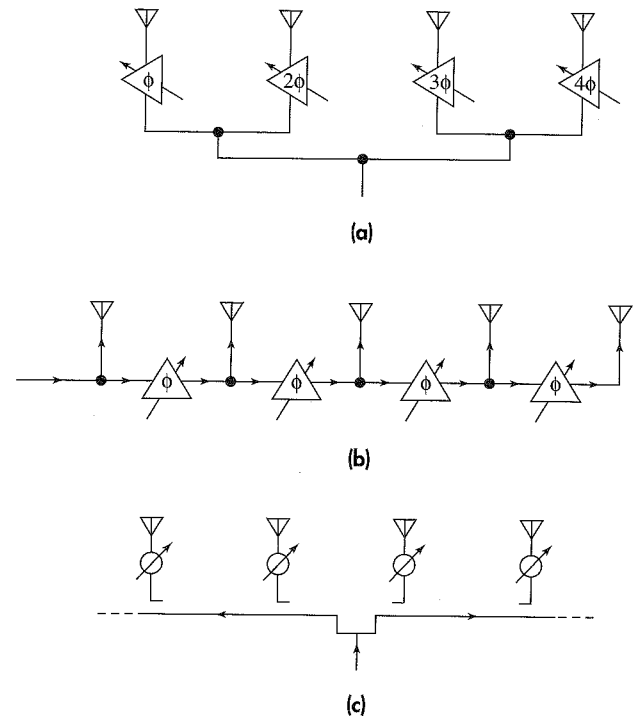

Figure 9.16 Steering of a linear array with variable phase shifters: (a) parallel-fed; (b) series-fed from one end; (c) series-fed from the center.

there might be many tens of elements in a linear array, the loss with a series feed is generally unacceptable.

There are two ways in which a series-fed array can be acceptable. One is when frequency scanning (Sec. 9.7) is used with low-loss waveguides connecting the elements. (The frequency scan array does not employ lossy phase shifters.) The other is when power amplifiers and low-noise receivers are placed between the phase shifter and the radiating element. There is still loss, but it is at low power level on transmit since it occurs before the power amplifier. On receive, the loss due to the phase shifter occurs after signal amplification so that it doesn't seriously affect the receiver overall noise figure.

The series-fed array, even when it is configured to have an acceptable low loss, is sensitive to changes in frequency. It has the properties of a frequency-scan array in that the direction of its beam will change with a change in frequency. Compensation for the shift of the beam position due to a change in frequency can be made in the computer by having it indicate the true beam-pointing direction for any given frequency. Inadvertent beam-steering with frequency can be avoided if the array is fed from the center as indicated in Fig. 9.16c. Although the beam is not shifted in angle, its beamshape will change with frequency.

The phase shifters in a two-dimensional parallel-fed planar array of $M \times N$ elements require $M + N - 2$ separate control signals. A two-dimensional series-fed array, however, requires but two control signals.

Grating Lobes Using an argument similar to the nonscanning array described previously, grating lobes will appear at an angle (or angles) θ_g whenever the denominator of Eq. (9.30) is zero, which means that

$$\pi \frac{d}{\lambda}(\sin \theta_g - \sin \theta_0) = \pm n\pi \qquad [9.31]$$

or

$$|\sin \theta_g - \sin \theta_0| = n\frac{\lambda}{d}$$

From this equation it is found that the element spacing d should be no greater than half wavelength in order to avoid grating lobes. With $d = \lambda/2$, a grating lobe will only appear at $\theta_g = -90°$ when the main beam is steered to $\theta_0 = +90°$. Practical phased arrays, however, cannot scan $\pm 90°$. If the scan were limited to $\pm 60°$, Eq. (9.31) states that the element spacing should not be greater than 0.54λ.

Change of Beamwidth with Steering Angle As the beam of a phased array scans in angle θ_0 from broadside, its beamwidth increases as $1/(\cos \theta_0)$. This may be shown by assuming the sine in the denominator of Eq. (9.30) can be replaced by its argument, so that the radiation pattern is of the form $(\sin^2 u)/u^2$, where $u = N\pi(d/\lambda)(\sin \theta - \sin \theta_0)$. The $(\sin^2 u)/u^2$ antenna pattern is reduced to half its maximum value when $u = \pm 0.443\pi$. Denote by θ_+ the angle corresponding to the half-power point when $\theta > \theta_0$, and denote by θ_- the angle corresponding to the half-power point when $\theta < \theta_0$; that is, θ_+ corresponds to $u = +0.443\pi$ and θ_- to $u = -0.443\pi$. The $\sin \theta - \sin \theta_0$ term in the expression for u can be written[28]

$$\sin \theta - \sin \theta_0 = \sin (\theta - \theta_0) \cos \theta_0 - [1 - \cos (\theta - \theta_0)] \sin \theta_0 \qquad [9.32]$$

The second term on the right-hand side of this equation can be neglected when θ_0 is small (beam is near broadside), so that $\sin \theta - \sin \theta_0 \approx \sin (\theta - \theta_0) \cos \theta_0$. With this approximation, the two angles corresponding to the half-power (3 dB) point of the antenna pattern are

$$\theta_+ - \theta_0 = \sin^{-1} \frac{0.443\lambda}{Nd \cos \theta_0} \approx \frac{0.443\lambda}{Nd \cos \theta_0}$$

$$\theta_- - \theta_0 = \sin^{-1} \frac{-0.443\lambda}{Nd \cos \theta_0} \approx \frac{-0.443\lambda}{Nd \cos \theta_0}$$

The half-power beamwidth is

$$\theta_B = \theta_+ - \theta_- \approx \frac{0.886\lambda}{Nd \cos \theta_0} \qquad [9.33]$$

Thus when the beam is scanned an angle θ_0 from broadside, the beamwidth in the plane of scan increases as $(\cos \theta_0)^{-1}$. This expression, however, is not valid when θ_0 is large, and the array performance can be much worse. In addition to the approximation made in

this derivation not being valid at large angles, mutual coupling effects can increase as the beam is scanned from broadside. At a scan angle of 60° from broadside, the beamwidth of a practical phased array antenna increases by more than the factor of 2 predicted from Eq. (9.33) and the sidelobe levels increase more than expected from simple theory.

Equation (9.33) applies for a uniform line-source distribution, which seldom is used in radar. With a cosine-on-a-pedestal aperture illumination of the form $a_0 + 2a_1 \cos(2\pi n/N)$ for a linear array of N elements with spacing d, the beamwidth is approximately[29]

$$\theta_B \approx \frac{0.886\lambda}{Nd \cos \theta_0}[1 + 0.636(2a_1/a_0)^2] \qquad [9.34]$$

where a_0 and a_1 are constants, and the parameter n in the aperture illumination represents the position of the element. Since the illumination is assumed to be symmetrical about the center element, n takes on values of $0, \pm 1, \pm 2, \ldots, \pm(N-1)/2$. The antenna aperture illuminations cover the span from uniform illumination to a tapered illumination that drops to zero at the ends of the array. (The effect of the array is assumed to extend a distance $d/2$ beyond each end element.) Although the above applies to a linear array, similar results are obtained for a planar aperture; that is, the beamwidth varies approximately inversely as $\cos \theta_0$.

A consequence of the beamwidth increasing with scan angle is that the antenna gain also decreases with scan angle as $\cos \theta_0$.

9.6 PHASE SHIFTERS

The shift in phase of a signal of wavelength λ transiting a line of length l at a velocity v is

$$\phi = 2\pi l/\lambda = 2\pi f l/v = 2\pi f l\sqrt{\mu\epsilon} \qquad [9.35]$$

where the frequency $f = v/\lambda$, μ = permeability and ϵ = permittivity. Usually the velocity of propagation v of electromagnetic waves is taken to be the velocity of light c; but with phase shifters it can be different. Here we have assumed for simplicity that the velocity of propagation corresponds to that in a TEM transmission line such as a coaxial cable, so that $v = 1/\sqrt{\mu\epsilon}$. The velocity of propagation of TE and TM waves propagating in waveguides is a bit more complicated than the above, but it is still proportional to $1/\sqrt{\mu\epsilon}$. Based on the far right-hand side of this equation, the various methods for obtaining a change in the phase shift may be summarized as follows:

- *Frequency f.* This is a relatively simple method for electronically scanning a beam. It was the first practical method for electronic beam steering and was at one time widely employed for many phased array radars. In spite of its simplicity, it is no longer popular since it restricts the use of bandwidth for other than beam-steering purposes and it is only practical for electronically steering the beam in one angular coordinate. Frequency scanning has been superseded by the development of other methods for phase shifting that do not have its limitations.

- *Line length l.* This may be accomplished by electronically switching in or out various lengths of transmission line to achieve the desired phase shift. Diodes are often used as the switches.
- *Permeability* μ. Ferrite, or ferrimagnetic, materials exhibit a change in permeability, and therefore a change in phase, when the applied magnetic field is changed. They have been popular for use at the higher microwave frequencies.
- *Permittivity* ϵ. The permittivity, or dielectric constant, of ferroelectric materials changes with a change in applied voltage. A change in the current of an electrical discharge also results in a change in the electron density which produces a change in permittivity.
- *Velocity v.* Changes in μ and ϵ cause the velocity of propagation to change; but a change in velocity can be had directly by changing the broad dimension of a rectangular waveguide, the so-called "*a*" dimension. By varying the "*a*" dimension of a rectangular waveguide, the proper phase change can be applied across an entire row of radiators of a linear array antenna to scan a beam in one angular coordinate. This form of rapid one-dimensional scanning was used for many years in *X*-band landing radars. It was called a *delta-a scanner* or an *eagle scanner.* The beam could be mechanically scanned over an angle of about 60° at a rate of 10 times per second.

All of the above have been employed or seriously considered as phase shifting devices for phased arrays. There are many other devices that can be used to obtain a phase shift for phased array radars, as has been mentioned in previous editions of this text; but the most popular are those that use ferrites or diodes.

Early electronic phase shifters were analog. Their phase shift could be continuously adjusted. Later they were replaced by digital phase shifting in which the values of phase took on discrete values, generally in binary steps. For example an *N*-bit phase shifter covers 360° of phase change in 2^N steps. Four-bit phase shifters with phase increments of 22.5° are commonly used, but digital phase shifters can have much finer quantization if needed. Although the analog phase shifter permits continuous variation of the phase shift, the relationship between its control current (or voltage) and phase is usually not linear, so that setting an analog phase shifter to a precise value of phase might not be as easily accomplished as obtaining similar or better accuracy with a digital device. Digital phase shifters have come to be the preferred method. Phase shifters have also been known as *phasors.*

Phase shifters for most phased array radar applications should be:

- Able to change phase rapidly (a few microseconds)
- Capable of handling high peak and high average power
- Require control signals that operate with little drive power (generally, one wouldn't want to use more power to drive the phase shifters than the total power that is radiated by the antenna)
- Low loss (a fraction of a dB if it is not used in an active aperture radar)
- Insensitive to changes in temperature
- Of small size (to fit within an element spacing of about a half-wavelength)

- Low weight (especially for airborne or mobile radars)
- Low cost (since the cost of a phase shifter is multiplied by the total number of phase shifters in the system).

There have been many types of phase shifters examined for radar application, and they possess these properties in varying degrees. No one type of phase shifter is sufficiently universal to meet the requirements of all applications.

Diode Phase Shifters[30–34] The semiconductor diode works well as a switching device for radar phase shifters. They are capable of relatively high power and low loss, and they can be switched rapidly from one state to another (low impedance to high impedance, or vice versa). They are not significantly affected by normal changes in temperature; they can be switched with low control power; and they are compact in size. They lend themselves well to microwave integrated circuitry and are capable of being used over the entire range of frequencies of interest to radar, except their loss increases and their power handling decreases at the higher microwave frequencies.

There have been three methods by which diodes have been used: (1) digitally switched lines, (2) hybrid coupled, and (3) loaded-line. Each will be briefly discussed.

Digitally Switched Lines A digital phase shifter can be obtained using a cascade of switched lines of length $\lambda/2$, $\lambda/4$, $\lambda/8$, and so forth. An N-bit phase shifter has N line lengths. Figure 9.17, for example, is a four-bit cascade of digitally switched phase shifters capable of switching in or out lengths of line equal to $\lambda/16$, $\lambda/8$, $\lambda/4$, and $\lambda/2$ to obtain a quantization level of $\lambda/16$, which corresponds to a phase increment of $360/16 = 22.5°$. Each phase bit consists of two lengths of line that provide the differential phase shift, and two single-pole, double-throw switches made up of four diodes. In this diagram, when the upper two switches are open, the lower two are closed, and vice versa. In the "zero" phase state, the phase shift is not zero, but is some residual amount ϕ_0, so that the two states are ϕ_0 and $\phi_0 + \Delta\phi_0$. The difference $\Delta\phi_0$ is the desired phase increment. The residual phase of the zero state has to be calibrated out in the radar system.

Hybrid Coupled The hybrid-coupled phase bit, as shown in Fig. 9.18, uses a 3-dB hybrid junction with balanced reflecting terminations connected to the coupled arms. Two switches (diodes) control the phase change. The 3-dB hybrid junction has the property that a signal at port 1 is divided equally in power between ports 2 and 3, and no signal power appears at port 4. The diodes act to either pass or reflect the incident signals,

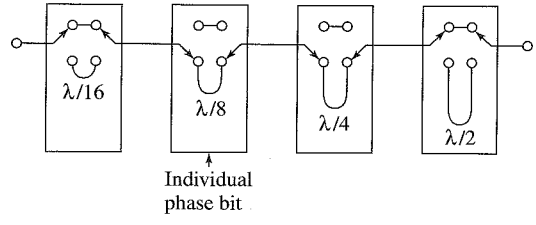

Figure 9.17 Digital phase shifter with four-bit diode-switched line lengths with $\lambda/16$ quantization. Particular arrangement shown gives 135° of phase shift (3/8 wavelength).

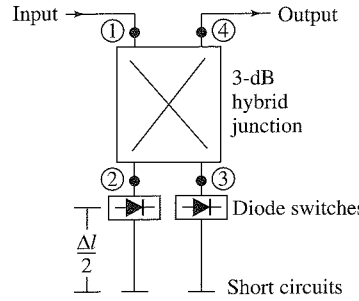

Figure 9.18 Hybrid-coupled phase bit.

depending on the bias applied to the diode. When the diodes allow the signals to pass, they are reflected by short circuits located farther down the transmission lines. The reflected signals combine at port 4, but no reflected signal appears at port 1. If the diode impedances are such as to reflect rather than pass the signals, the total path length traveled is less. The difference Δl is the two-way path length with the diode switches open and closed, and is chosen to correspond to the desired increment of digitized phase shift. An N-bit phase shifter can be obtained by cascading N such hybrid junctions and diode switches, with different lengths of lines for each bit.

Loaded Line This is a little different from the two diode phase shifters mentioned above. As shown in Fig. 9.19, it consists of a transmission line periodically loaded with spaced, switched impedances, or susceptances. Diodes are used to switch between the two states of susceptance. The spacing between diodes is one-quarter wavelength at the operating frequency. Adjacent quarter-wave-spaced loading-susceptances are equal and can take either of two values. If the magnitude of the susceptance is small compared to the characteristic impedance of the line, the quarter-wave spacing will result in cancellation of the reflections from any pair of symmetrical susceptances so that there will be matched transmission for either of the two susceptance conditions. Each pair of diodes spaced a quarter-wave apart produces an increment of the total phase required. Shunt capacitive elements increase the electrical length of the line and shunt inductive elements decrease its length. The number of pairs of shunt susceptances determines the total transmission phase shift. To obtain high power-handling capability, many such sections with small phase increments can be used so there are a large number of diodes available to share the power.

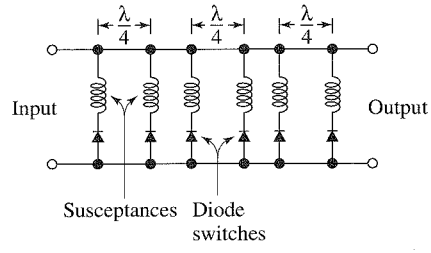

Figure 9.19 Periodically loaded-line phase shifter.

The advantage of the loaded line is its ability to handle larger power than other diode-based phase shifters. If the largest practical phase shift per diode pair is $\lambda/16$ (or 22.5°), 32 diodes would be needed to shift the phase 360°.

Comparison of Diode Phase Shifters The hybrid-coupled phase shifter generally has less loss than the other two, uses the least number of diodes, and can be made to operate over a wide band. The switched-lines phase shifter uses more diodes than the other types and has an undesirable phase-frequency response that can be corrected at the expense of a higher insertion loss. It is often used in solid-state TR modules where the phase shifting is done at low power ahead of the power amplifier on transmit and following the receiver front end on reception. For a four-bit phase shifter with a total phase change of 360°, the loaded line requires 32 diodes, the switched line 16, and the hybrid-coupled shifter needs only 8 diodes. The theoretical peak power capability of the switched-line device is twice that of the hybrid-coupled circuit since voltage doubling is produced by the reflection of the hybrid junction. The switched-line phase shifter has the greatest insertion loss, but its loss does not vary with the amount of phase shift as it does in the other two types of circuits.

Diode phase shifters have been built in practically all types of transmission-line media, including waveguide, coax, and stripline. Microstrip is useful for medium power devices because of its ease of manufacture and circuit reproducibility, as well as its reduced size, weight, and cost of production. Diode chips can be mounted directly on the substrate without the parasitic reactances of the diode package.

A multiple-bit diode phase shifter need not be constructed with just one type of phase shifting device. The loaded-line is often preferred for small phase increments because of its compact size. It is not as suitable for large phase increments because it is difficult to match in both states when large. For example, a four-bit phase shifter might use a loaded-line configuration for the 22.5 and 45° bits, and the hybrid-coupled reflection circuit for the 90 and 180° bits to obtain the minimum insertion loss with suitable bandwidth and power-handling capability.

PIN Diodes The PIN diode has been a popular choice for use in diode phase shifters since it can handle higher power than other diodes; it can be designed to have relatively constant parameters in either or its two states; and it can have switching times from a few microseconds for high-voltage diodes to tens of nanoseconds with low-voltage operation. (Typically, switching times of the order of one or a few microseconds are quite suitable for most radar applications.) As sketched in Fig. 9.20, the PIN diode consists of a thin slice of high-resistivity intrinsic semiconductor material sandwiched between heavily doped low-resistivity P^+ and N^+ regions. The intrinsic region acts as a slightly lossy dielectric at microwave frequencies, and the heavily doped regions are good conductors. When d-c biased in the reverse (nonconducting) state, it resembles a low-loss capacitor since it is essentially an insulator situated between two conductors. Its parallel-plate capacitance is determined by the dielectric of the intrinsic region and is independent of the reverse-bias voltage. The series resistance is determined by the resistivity and geometry of the metallic-like P and N regions. In the forward-bias (conducting) state, when appreciable current is passed, the injection of holes and electrons from the P and N regions,

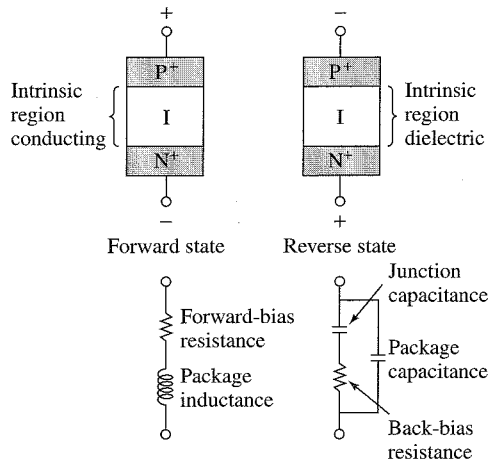

Figure 9.20 PIN diodes and simplified equivalent circuit for forward and reverse states.

respectively, creates an electron-hole plasma in what was formerly the dielectric region. Thus the slightly lossy dielectric is changed to a fairly good conductor with the application of forward bias. The capacitive component of the circuit disappears and the equivalent circuit becomes a small resistance that decreases with increasing forward current. The resistance can vary from thousands of ohms at zero bias to a fraction of an ohm with tens of milliamperes bias current. With forward bias, the diode resembles a resistance of low value.

Varactor Phase Shifters The varactor, or variable capacitance semiconductor, also can be used as the switch in a diode phase shifter. Its capacitance is varied by a change in voltage under reverse bias. It is capable of very rapid switching, of the order of a nanosecond, but its average-power handling is limited to a few tens of milliwatts as compared to about 100 W for a PIN diode.[35] The varactor peak-power rating is about 100 times less than that of the PIN. Instead of being used as a switch as is the PIN diode, the varactor can be employed as an analog (continuously variable) voltage-tuned phase shifter. This property has been used as an added module in a 6-bit digital diode phase shifter to provide a continuously variable phase change of from 0 to 11°.[36]

Monolithic Microwave Integrated Circuit (MMIC) Phase Shifters[37,38] The diode phase shifters that have been discussed thus far have generally been implemented as hybrid microwave integrated circuits (MIC) in that the passive components are deposited on the surface of a low-loss dielectric substrate and the active semiconductor devices are either bonded or soldered to the passive circuit. Phase shifters can also be constructed using monolithic microwave integrated circuit (MMIC) technology in which the entire circuit of passive elements, active devices, and interconnections are incorporated into a single semiconductor substrate. A MMIC phase shifter can be of much smaller size and weight than similar devices in hybrid MIC. They provide better reliability, they are highly reproducible because of the absence of wire bonds, and they can be produced economically

with high-volume production. Because of their small size they can be integrated on a single chip with other circuit functions such as power amplification, low-noise receiver front-end, and switching to form a compact T/R (transmit/receive) module for use in active array antennas. These advantages are accompanied, however, by the loss of flexibility in circuit tuning and troubleshooting that is available in hybrid MIC. This loss of flexibility to adjust (or tweak) the circuits means that more attention has to be paid to the use of computer-aided design to insure that the device, once manufactured, will do its job.

MMIC devices have usually utilized gallium arsenide (GaAs) metal semiconductor field-effect transistors (MESFET) as the switches for digital phase shifting. Although silicon technology has been extensively employed at the lower and middle microwave frequency regions, GaAs is preferred at the higher frequencies where MMIC techniques are employed. MESFETs are capable of rapid switching speeds of less than a fraction of a nanosecond, and they operate with relatively low d-c bias power.

The high-pass/low-pass phase-shifter configuration, Fig. 9.21, has been used with MESFETs as the switching elements for MMIC phase shifters. Its small size results from lumped elements being used, rather than distributed elements. A change in phase is obtained by switching between a high-pass filter and a low-pass filter. The insertion of a high-pass filter produces a phase advance and the insertion of a low-pass filter produces a phase delay.

Phase shifters using monolithic microwave integrated circuits at the higher microwave frequencies have been reported[38] to have wide bandwidth and constant phase shift over the band, insertion losses of 5 to 10 dB, and a maximum dimension of from a few millimeters to about a centimeter. The high loss has only a small effect since it occurs at a low power level before the power amplifier on transmit or after the low-noise amplifier on receive.

Ferrite Phase Shifters A ferrite is a ceramic-like metal-oxide insulator material that possesses magnetic properties while maintaining good dielectric properties.[39–41] Its dielectric constant is in the range from 10 to 20. In contrast to ferromagnetic materials such as iron, ferrites are insulators rather than conductors and have a high resistivity which

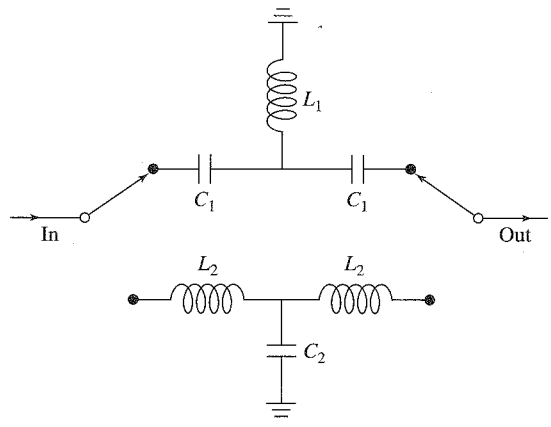

Figure 9.21 High-pass/low-pass phase shifter using T-type networks, shown switched to the high-pass filter.[38]

allows electromagnetic waves to propagate with low loss through the material. The term *ferrimagnetism* was introduced to describe the novel magnetic properties of these materials now known as ferrites.

Ferrite phase shifters are two-port devices that may be either analog or digital with either reciprocal or nonreciprocal characteristics. They are generally used at the higher microwave frequencies since their loss decreases with increasing frequency. Ferrites are generally preferred over diode phase shifters for radars above *S* band (except when the phase shifters are used before the power amplifier on transmit and after the low-noise amplifier on receive). At *S* band, either ferrites or diodes might be used. Below *S* band, the diode phase shifter usually is preferred.

The physics of propagation of electromagnetic energy in ferrite materials is not easy to describe, and will not be attempted here. The basic operation occurs by the interaction of electromagnetic waves with the spinning electrons of the ferrite material to produce a change in the microwave permeability of the ferrite, and therefore a change in phase. The magnetic permeability of a ferrite is anisotropic in that it must be represented by a complex tensor rather than a scalar. For this reason, the value of permeability and the resulting phase shift in a ferrite can depend on the direction of propagation. Some types of ferrite phase shifters, therefore, are *nonreciprocal* in that their phase change depends on the direction of propagation. This is different from the semiconductor phase shifters discussed earlier in this section, which were reciprocal devices. Nonreciprocal phase shifters have to be set differently for receiving than for transmitting.

There have been many different types of ferrite phase shifters developed, but those of most interest for radar include the latching, flux drive, and dual-mode phase shifters. One of the first successful ferrite phase shifters, the Reggia-Spencer shifter, will be described so as to illustrate some of the properties of ferrites, their limitations, and how these limitations were overcome in later types of ferrite devices. In spite of its shortcomings, the Reggia-Spencer device was used in an operational phased array radar at very high power (at the time, in the 1960s, when there was no better device available).

Reggia-Spencer Phase Shifter This device consisted of a rod or bar of ferrimagnetic material suspended at the center of a section of rectangular waveguide. A solenoid was wound around the waveguide to provide a longitudinal magnetic field. A change in phase was obtained by changing the current flowing through the solenoid coil. It was a reciprocal, analog phase shifter that had a high *figure of merit* (defined as the *change of phase per dB of loss*) and was more compact than previous experimental ferrite phase shifters. It had two serious limitations, however. First, the location of the ferrite rod at the center of the waveguide meant it was out of contact with the metal waveguide walls. Thus it was difficult to conduct the dissipated heat away. Second, the time required to switch from one phase state to another was relatively long; hundreds of microseconds rather than the microsecond or two that is characteristic of diode phase shifters. Furthermore, this phase shifter was sensitive to changes in temperature so it usually had to be operated in a temperature-controlled environment. There were also hysteresis effects that had to be accommodated when the phase had to be changed.

The lack of a convenient thermal path to dissipate heat was overcome in one design[42] by having the axially located garnet bar directly cooled by a low-loss liquid dielectric that

was allowed to flow along the surface of the garnet material. (A garnet is a ferrite with a different crystal structure than other ferrites.) The flow was confined by completely encapsulating the garnet in a teflon jacket so that the cooling liquid was in direct contact with the garnet bar. A *C*-band Reggia-Spencer phase shifter with this method of cooling operated over an 8 percent bandwidth at a peak power of 100 kW, average power of 600 W, insertion loss of 0.9 dB, and a VSWR of 1.25. The device was 2.4 by 2.1 by 8.2 inches and weighed 1.5 lb. It required, however, 125 μs to switch its phase, and at a switching rate of 300 Hz it used 16 W of switching power.

The long switching times for the Reggia-Spencer phase shifter were due to (1) the large inductance of the solenoid that provided the magnetic field and (2) the "shorted turn" effect caused by the metallic waveguide around which the solenoid was wrapped generating eddy currents in the metallic waveguide wall. There were things that could be done to reduce the switching time, but the Reggia-Spencer switching times were always much longer than those of other phase shifters.

Latching Ferrite Phase Shifter[40,43] A latching ferrite phase shifter overcomes many of the limitations of the Reggia-Spencer device by taking advantage of the hysteresis loop of a magnetic material so as to latch, or lock, its permeability to one of the two remanent magnetization points on the ferrite material's *B-H* curve. It does not need a continuous holding current to maintain the phase shift; hence, its drive power might be an order of magnitude less than that of the Reggia-Spencer shifter. It is not as temperature sensitive, it has a much faster switching speed, and there is less of a problem caused by hysteresis in the ferrite. It also lends itself to implementation as a digital phase shifter. Figure 9.22a illustrates one bit of a latching ferrite phase shifter mounted in a waveguide. The ferrite is in the form of a rectangular toroid. The contact of the toroid with the walls of the waveguide allows the generated heat to be dissipated. The toroid, however, results in this device being nonreciprocal.

Figure 9.23 is a hysteresis loop, or *B-H* curve, for a magnetic material such as a ferrite. It is plot of the magnetization, or magnetic induction (units of flux density, or webers/m^2) as a function of the applied magnetic field (ampere-turns/m) for a toroidal-shaped section of ferrite. The applied magnetic field is proportional to the current in the drive wire, which can be considered a solenoid of one turn. When a sufficiently large pulse of current is passed through the drive wire threading the center of the toroid, the magnetization is driven to saturation. When the current is then reduced to zero, there exists a remanent magnetization B_r. Similarly, when a large current pulse of opposite polarity is passed through the drive wire, the ferrite becomes saturated with the opposite polarity, and when the current is reduced to zero the remanent magnetization of opposite sign is obtained. Thus a toroidal ferrite may take on two values of magnetization, $\pm B_r$, obtained by pulsing the drive wire with either a positive or a negative current pulse. The difference in the two states of remanent magnetization produces the differential phase shift. Only a short-duration current pulse is needed to set the phase of a latching phase shifter.

The amount of differential phase shift depends on the ferrite material and the length of the toroid. A digital latching phase shifter may be obtained by placing in cascade a number of separate toroids of the proper lengths. The lengths of each toroid are selected to provide a differential phase shift of 180°, 90°, 45°, 22.5°, and so on, depending on the

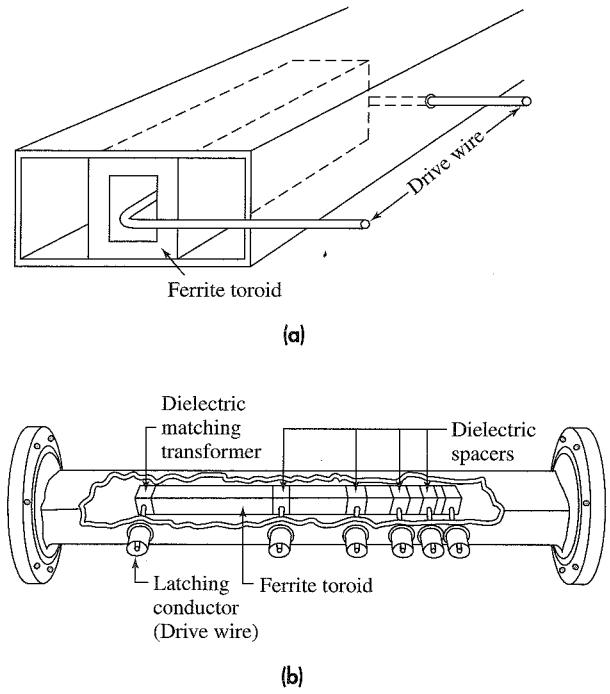

Figure 9.22 (a) Single bit of a latching ferrite phase shifter mounted in waveguide, showing the drive wire through the center of the toroid that establishes the magnetic field to latch the phase shift; (b) sketch of a five-bit latching ferrite phase-shifter.
(From Wicker and Jones,[44] Courtesy IEEE.)

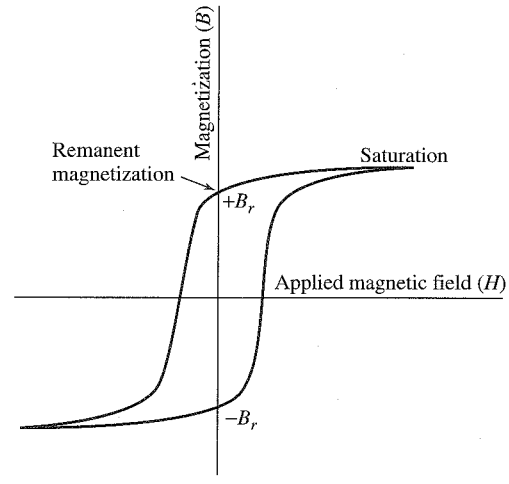

Figure 9.23 Hysteresis loop, or *B-H* curve, of a ferrite toroid.

number of bits required. The sketch in Fig. 9.22b illustrates a five bit latching ferrite phase shifter.[44] A separate drive wire is used for each bit. Impedance matching is provided at the input and output toroids. Filling the center slot of the toroids with a high dielectric-constant material produces a higher value of phase change per dB of loss (higher figure of merit) and lower switching power, but the lower will be the peak power that the device can handle before breakdown. The individual toroids usually are separated by thin dielectric spacers to avoid magnetic interaction. The drive wire is oriented for minimum RF coupling. It is also important that there be the proper mechanical contact between the toroid and the waveguide wall since an air gap can cause the generation of higher-order modes that result in relatively narrow-frequency-band, insertion-loss spikes. These unwanted air gaps have to be eliminated with care since excessive mechanical pressure on the material can cause magnetostriction that changes the magnetic properties of the material, especially if garnets are used. This type of latching phase shifter has also been called a *twin-slab toroidal phase shifter* since the major action is due to the two vertical branches of the toroids. The horizontal branches of the toroid do not contribute to the phase shift, but they are needed is to complete the magnetic circuit.

Introducing the applied magnetic field from within the waveguide via the single-turn drive wire eliminates the shorted-turn effect and avoids the long switching times that were characteristic of the original Reggia-Spencer phase shifter. Switching times of the order of microseconds become practical. Hysteresis was a nuisance to be tolerated in a Reggia-Spencer phase shifter, but the latching ferrite phase shifter takes advantage of the hysteresis loop to produce two discrete values of phase shift without the need for continuous holding power.

Different phase shifts must be used for transmit and receive with a nonreciprocal phase shifter. The nonreciprocal latching phase shifter, therefore, must be reset just after transmission is completed in order to receive the echo signals. The switching speeds of the latching phase shifter, which are of the order of microseconds, permit the rapid switching required. The phase shift for reception is obtained by simply reversing the polarity of the drive pulses that were used to set the phase for transmission. This reverses the direction of magnetization of the ferrite toroid, which is equivalent to reversing the direction of propagation. Although nonreciprocal phase shifters can be employed in many radar applications, they cannot be used in space-fed reflectarrays (Sec. 9.9) since the electromagnetic energy rapidly changes direction during both transmission and reception in such an antenna. Their use is also not practical in high-duty-cycle pulse doppler radars or in very short-range radars.

A nonreciprocal digital latching five-bit ferrite phase shifter was used in the S-band 3D radar known as the RAT 31/S built by Alenia of Rome, Italy.[45] It had the following characteristics: peak power = 7 kW, average power = 70 W, insertion loss <0.9 dB, VSWR < 1.3, bandwidth = 3 percent, switching time ≤ 2.5 μs, temperature tracking of the insertion phase = 0.6°/°C, and temperature range from 0 to 60°C. The rms value of the standard deviation of the insertion loss was 0.03 dB. The deviation of the insertion phase from its anticipated value was compensated in the path between phase shifter and antenna element. The rms value of the deviation of the phase of the smallest bit (nominally 12.25°, but actually an average value of 12.40°) was 1.13°; and that of the largest bit (nominally 180°, but actually an average of 199.8°) was 3.89°.

Twin-Toroid Latching Phase Shifter[46,47] The latching phase shifter described above has been improved by the use of the twin toroid, the geometry of which is sketched in Fig. 9.24a. The two toroids are separated by dielectric which concentrates the RF energy in the center of the waveguide. The active ferrite regions (in which the nonreciprocal interaction with the RF field occurs) are the two vertical ferrite arms that are in contact with the dielectric in the center. The differential phase shift of the twin-toroid ferrite can be made independent of frequency, and it is capable of wide bandwidths. The twin-toroid phase shifter is said[48] to be easier to construct than the single-toroid device. Hord[46] gives the following characteristics for an *X*-band twin-toroid phase shifter: loss = 0.4 dB, switching time = 3 μs, switching energy = 100 μJ, and size = 0.27 by 0.18 by 2.3 inches. Bandwidth can be 10 percent or greater.

A variant of the twin-toroid employs what is called a grooved waveguide, as is illustrated by the cross section view of Fig. 9.24b.[49] Note that there are different gaps between the waveguide ridges. It has been said that this geometry increases the differential phase shift by 20 percent, decreases the insertion loss for 360° differential phase shift by about 10 to 30 percent (thus providing a better figure of merit), and allows better thermal conductivity and an increase in average-power capability.

Flux Drive[50] The toroid ferrite phase shifter can be operated in an analog fashion to obtain digital phase-shift increments by varying the current of the drive pulse to provide different values of remanent magnetization. This is called *flux drive.* It has the further advantage of having reduced temperature sensitivity. A single long section of ferrite toroid is used that is capable of providing the total differential phase shift of 360°. The required digital phase increment is obtained by operating on a minor hysteresis loop, as indicated in Fig. 9.25. If $B_r(1)$, for example, were the remanent magnetization needed to produce a phase change of 180° (relative to the remanent magnetization $-B_r$), the amplitude and width of the driving pulse would be selected so as to rise to the point (1) on the hysteresis curve.

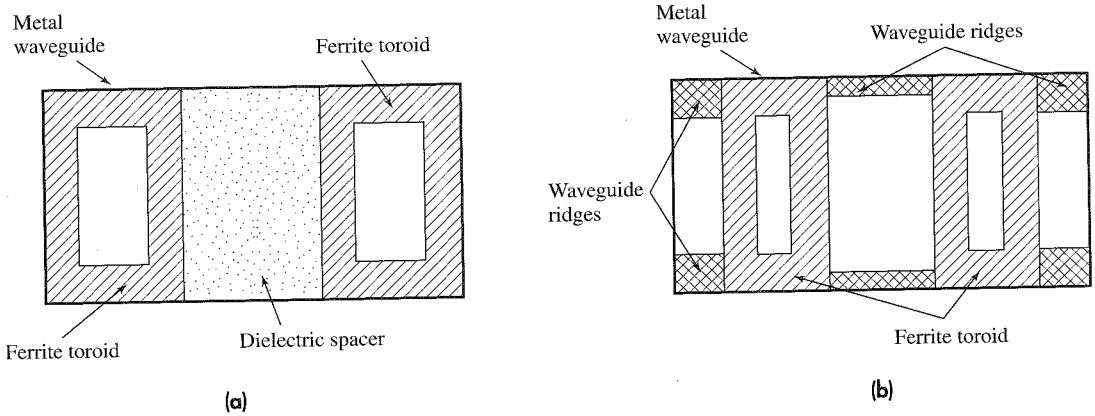

Figure 9.24 (a) Cross section of a twin-toroid ferrite phase shifter. (b) Cross section of a twin-toroid ferrite phase shifter with a grooved waveguide.

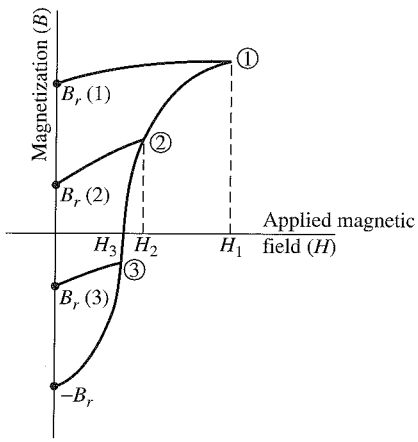

Figure 9.25 Hysteresis loop showing the operation of flux drive, where a single ferrite toroid is excited by discrete current pulses to produce digital phase-shift increments from what is basically an analog device.

When the pulse current decays to zero, the magnetization falls back to the remanent value $B_r(1)$ along the indicated curve. The difference in phase between $B_r(1)$ and $-B_r$ determines the differential phase increment. With a different value of current pulse, a different value of remanent magnetization and a different phase shift are obtained. In this manner, the ferrite toroid is basically an analog device that can provide any phase increment. It acts as a digital phase shifter if the drive currents are digital. The length of the toroid can be made 15 to 20 percent greater than the normal value to allow for some shrinkage of the total available increment of magnetization due to temperature changes. When the drive output impedance is small, the effect of the temperature-caused variations in magnetization will be small.

Dual-Mode Ferrite Phase Shifters[46,51] This is a latching phase shifter that is reciprocal, but without the limitations of the reciprocal Reggia-Spencer phase shifter. It is a variant of the Faraday rotation phase shifter[52] and the mechanical Fox phase shifter[53] (Faraday rotation is the rotation of the polarization, or electric field, when the wave propagates in a ferrite material in the presence of a magnetic field.) An outline of the configuration of a dual-mode ferrite phase shifter is sketched in Fig. 9.26. In the center portion is the ferrite bar that supports the propagation of circularly polarized waves. The bar is metallized to form a ferrite-filled waveguide that is accessible for dissipating the heat generated by the loss in the ferrite. A solenoid (not shown in the figure) is wound around the ferrite rod so as to apply an axial magnetic field that rotates the circular polarization to provide a phase change. A linearly polarized signal that enters the rectangular waveguide at the left-hand port is converted to circular polarization by a nonreciprocal circular polarizer (which is a ferrite quarter-wave plate, or quadrapole-field ferrite polarizer[54]). The applied axial magnetic field rotates the circular polarized wave in the ferrite bar, an action that imparts the desired phase shift. After propagating through the ferrite, the phase-shifted circular polarized wave is converted back to linear polarization by a second nonreciprocal polarizer. In a similar manner, a wave incident from the right is converted to circular polarization of the opposite sense by the nonreciprocal quarter-wave plate, and a

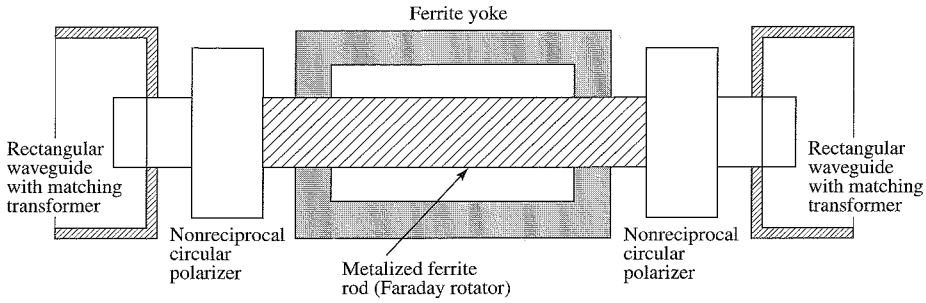

Figure 9.26 Outline of the configuration of a dual-mode ferrite phase shifter. The metalized ferrite rod in the center is based on the Faraday rotator.

phase shift occurs. Since both the sense of polarization and direction of propagation are reversed, the phase shift for a signal traveling from right to left is the same as that of a signal traveling from left to right. The magnetic circuit is completed externally by a temperature-stable ferrite yoke to permit latching of the magnetic field. Flux drive can be used to control the value of the remanent magnetization.

The dual-mode ferrite phase shifter is lightweight and capable of high average power. It also has a good figure of merit. Switching times are from 10 to 100 μs, which is longer than what is achieved with nonreciprocal ferrite phase shifters. Its longer switching times are due to the shorted-turn effect of the thin metallic film covering the ferrite rod. Hord[46] states that an *X*-band dual-mode phase shifter can have an insertion loss = 0.6 dB, switching speed = 100 μs, switching energy = 400 μJ, length = 1.6 in., and diameter = 0.48 in. Whicker and Young[55] indicate that dual-mode phase shifters are capable of 10 percent bandwidth, 1 kW peak and 100 W average power, and with latching (switching) speeds of 20 to 40 μs. Dual-mode phase shifters were used in the AN/TPN-19 *X*-band landing radar, where the phase shifter weight was 3.7 oz and had a phase error of 15°.[56]

Polarization-Insensitive Phase Shifters It has been said[57] that the dual-mode phase shifter can be made to be insensitive to polarization; that is, have the same phase shift for differently polarized electromagnetic waves so that they can be used in phased array antennas that employ more than one polarization. Polarization insensitive phase shifters are of interest when the radar must use dual orthogonal polarizations to avoid the large loss of signal caused by Faraday rotation of the plane of polarization when VHF or UHF radar waves propagate through the ionosphere, when circular polarization is used for detecting targets in the rain, or in any other situation where a choice of more than one polarization is desired.[58]

Rotary-Field Phase Shifter[59] This is similar to the dual-mode phase shifter mentioned above in that it also acts as a Faraday rotator to impart a phase shift. It is a reciprocal

device, but is nonlatching. It is very accurate, being capable of phase errors of one degree or less, which is considerably better than many other types of phase shifters. Such accuracy is required for low sidelobe array antennas. Linear polarization in the input rectangular waveguide is converted to circular. The circular polarized wave propagates in the ferrite rod which completely fills a circular waveguide. A phase shift is obtained in the ferrite by a constant-magnitude magnetic bias that is rotated in space by the application of currents to two orthogonal windings on a ferromagnetic yoke fitted over the ferrite. This is accomplished with a pair of coils wound on a motor-like stator. The quadrapole field generated by the two coils can be smoothly rotated to any desired angle. The accuracy of the differential phase shift is determined by the ratio of the control currents in the two coils. The ferrite rod then acts as a half-wave plate whose orientation determines the amount of phase shift, which is similar to the function of the mechanical rotation of the half-wave plate (or 180° differential phase shift section) used in the original Fox phase shifter.[52] A rotation of the half-wave plate by an angle θ results in a 2θ-radian change in the time phase of the signal. After propagating through the ferrite rod and experiencing a phase change, the circular polarization is converted back to linear.

Boyd[60] states that at X band, a rotary-field phase shifter might have 0.5 dB loss, 10 percent bandwidth, rms phase error less than one degree, and switching time of 50 μs. The control power to the stator windings is less than 0.5 W. These devices are capable of moderate to high power, are less temperature sensitive than other ferrite phase shifters, have a phase shift that varies little with frequency over a wide band, are highly accurate, and their low weight makes them suitable for airborne application.

Other Phase Shifters There have been many other phase shifters developed in the past, including other types of ferrite devices, electromechanical shifters, traveling wave tubes used as phase shifters, plasma devices, and ferroelectric phase shifters in which the dielectric constant of a ferroelectric material is a function of the applied electric field. The ferroelectric phase shifter has been said[61] to have high power capability, low drive power, voltage control of phase, and low production costs; but it has been difficult to obtain suitale ferroelectric materials to satisfy the important requirements of a phase shifter.

9.7 FREQUENCY-SCAN ARRAYS[62–64]

Because of its relative simplicity, the frequency-scan array was at one time the most popular form of phased array and was widely used. Its beam was steered by simply changing the radar frequency. It was especially popular for scanning a beam in one angular coordinate, such as with 3D air-surveillance radars.* A frequency-scan array has, however, significant limitations. The use of frequency for beam steering prevents the frequency domain from being used for other important purposes in radar, such as high range-resolution, electronic counter-countermeasures, and pulse-to-pulse frequency agility.

*A 3D air-surveillance radar is one which mechanically rotates in azimuth and scans one or more pencil beams in elevation or has multiple fixed beams in elevation for the purpose of measuring elevation angle. Other radars, of course, also can obtain three-dimensional data, but they are not usually "3D radars" in the sense of this definition.

Beam Steering by Change of Frequency The frequency-scanned array is almost always series fed as depicted in Fig. 9.27. Although series-fed arrays using phase shifters have high loss (as was mentioned in Sec. 9.5), it is not the case here since only waveguide connects the elements. The loss in propagating through waveguide transmission line is low.

We next derive the relationship between the radar frequency and the beam steering angle. The difference in phase between two adjacent elements in the series-fed array of Fig. 9.27 is

$$\phi = 2\pi fl/v = 2\pi l/\lambda \qquad [9.36]$$

where f = frequency of the electromagnetic signal, l = length of line connecting adjacent elements (generally l is much greater than the distance between elements), v = velocity of propagation, and λ = radar wavelength. [Eq. (9.36) is basically the same as Eq. (9.35)]. For convenience in this simplified analysis, the velocity of propagation is taken to be c, the velocity of light. This applies for coaxial lines and other transmission lines which propagate a TEM mode. Waveguides, which are more often used than TEM lines for the end-fed transmission line, can have a velocity of propagation that varies with frequency (i.e., it is dispersive).

As described in Sec. 9.5, if the beam is to point in a direction θ_0, the phase difference ϕ between elements spaced a distance d apart must be equal to $2\pi(d/\lambda)\sin\theta_0$. In a frequency-scan array, it is advantageous for practical reasons to add an integral number m of 2π radians of relative phase change. Since phase is modulo 2π and m is an integer, $2\pi m = 0$; so that the inclusion of $2\pi m$ has no effect on the phase difference between elements. The addition of the $2\pi m$ radians phase is achieved with the length of line l that connects adjacent array elements. The reason for adding the fixed $2\pi m$ phase shift is that it allows a given scan angle to be obtained with a much smaller frequency change than if a line of length $d = \lambda/2$ were used. This will become evident from Eq. (9.38). Equating the phase difference $\phi + 2\pi m$ between adjacent elements that is required to scan the beam to an angle θ_0, to the phase shift [Eq. (9.36)] introduced by a transmission line of length l, results in

$$2\pi(d/\lambda)\sin\theta_0 + 2\pi m = 2\pi l/\lambda \qquad [9.37a]$$

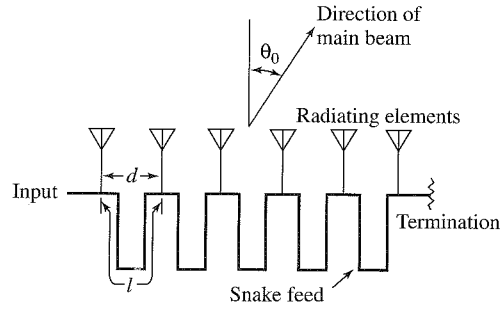

Figure 9.27 Series-fed, frequency-scan linear array.

or

$$\sin \theta_0 = -\frac{m\lambda}{d} + \frac{l}{d} \qquad \textbf{[9.37b]}$$

When $\theta_0 = 0$, the beam points to broadside and the above equation yields $m = l/\lambda_0$, where λ_0 is the wavelength that points the beam to broadside. If the frequency corresponding to beam pointing at broadside is denoted f_0, the direction of beam pointing can be written

$$\sin \theta_0 = \frac{l}{d}\left(1 - \frac{\lambda}{\lambda_0}\right) = \frac{l}{d}\left(1 - \frac{f_0}{f}\right) \qquad \textbf{[9.38]}$$

From the above, the wavelength excursion $\Delta\lambda$ required to scan the beam over an angular region $\pm\theta_s$ is

$$\Delta\lambda = 2\,\lambda_0(d/l)\sin\theta_s \qquad \textbf{[9.39]}$$

This equation shows that the greater the ratio l/d, the smaller will be the wavelength excursion $\Delta\lambda$ required to cover a given angular region $\pm\theta_s$. The ratio l/d is usually called the *wrap-up factor.* (The beam position is symmetrical with wavelength, but it is not symmetrical as a function of frequency.) To scan the beam $\pm 45°$ from the broadside direction requires a fractional wavelength change of 0.28 when the wrap-up factor is 5, and a 0.07 change when the wrap-up factor is 20 (fractional wavelength $= \Delta\lambda/\lambda_0$.)

Equations (9.38) and (9.39) apply for a TEM transmission line where the velocity of propagation is equal to the velocity of light. It is more usual, however, for waveguides to be used as transmission lines in this type of radar. Since the velocity of propagation in a waveguide depends on the frequency, a different and more complicated expression for the beam pointing angle results when waveguides are used instead of TEM lines. The velocity vs. frequency characteristic of waveguides can be used to good advantage to scan an angular region with less frequency change than indicated for a TEM line with the same wrap-up factor.

Grating lobes can occur in a frequency scan array, just as in other array antennas, when the electrical spacing between elements is too large. Equation (9.31) therefore applies. If we assume that a grating lobe can be tolerated at $\theta_g = -90°$ when the main beam is steered to the maximum scan angle $\theta_0 = +\theta_m$, then the following relationship applies

$$|1 + \sin\theta_m| < \lambda/d \qquad \textbf{[9.40]}$$

The onset of a grating lobe can limit the maximum angle the beam can be scanned.

Bandwidth Limitation Equation (9.39) illustrates the need for large frequency tunability of the radar transmitter in order to employ frequency scanning, especially if l/d is small. A large bandwidth might cause a potential problem of interference with other electromagnetic systems. Interference among frequency-scan radars operating in the same band, however, might not be that serious a problem since such a radar dwells at any one frequency for only a short time. Of more significance, however, is the reduction in signal bandwidth that can be used with a frequency scan antenna as the l/d ratio increases. If a wideband signal is used, distortion of the main beam will result.

With a series-feed, such as was indicated by Fig. 9.27, the signal travels a total distance $(N - 1)l$ from one end of the array to the other, where N is the number of elements in the linear array and l is the length of the transmission line between adjacent elements. For example, consider an S-band frequency-scan radar ($\lambda_0 = 10$ cm) with a linear array antenna of 101 elements spaced one-half wavelength apart. The wrap-up factor is assumed to be 10. The width of the antenna is taken to be 5 m, so that the total length of the feed line is 10×5 m $= 50$ m. An impulse incident at the input of a TEM feed line would require 0.167 μs to travel down the 50 m feed line and reach the other end (assuming propagation at the velocity of light). This build-up time, or time to fill the array, has a similar effect on the radar's signal bandwidth as does the transient response time of the more familiar signal filter. Thus the time t_D for the signal to travel from one end of the antenna to the other will limit the bandwidth to $1/t_D$, or 6.7 MHz in this example. If the wrap-up factor were 20 instead of 10, the limitation on the bandwidth would be 3.3 MHz. Thus the greater the wrap-up factor, the less frequency excursion that need be used to provide a given angular coverage, but the more narrowband will be the radar. Another way to see the effect of too wide a bandwidth is to note that if the signal has a wide frequency spectrum, the beam will be smeared in angle. Frequency scanning, therefore, is generally not compatible with high-resolution radar that might require large bandwidths.

Various Forms of Frequency-Scanned Radars There have been several methods by which frequency scanning has been employed, mostly as 3D air-surveillance radars that scan in one angular coordinate (elevation). Each of the following has been used in radar systems.

Single Scanning-Pencil-Beam The original 3D frequency-scan radars used a single pencil-beam antenna to scan in elevation as they mechanically rotated 360° in azimuth, Fig. 9.28a. The antenna beam dwells at a particular frequency at one elevation beam position before moving on to the next position and a different frequency. If the pencil beam is narrow (order of 1 or 2°), and if long range and large elevation-angle coverage are required, the revisit times with a single scanning beam will likely be excessively long (perhaps more than a minute). For example, if a pencil-beam antenna had azimuth and elevation beamwidths of 1.5°, elevation coverage 30°, range coverage to 200 nmi, and 10 pulses integrated from each target, then the time to cover 360° in azimuth is 66.7 s. This is far too long. Thus a single narrow-beamwidth scanning-beam radar operating as described is not suitable as a long-range radar because of its long revisit time. This applies to any type of electronically steered single-beam phased array, not just frequency scan.

The scan time can be reduced by increasing the pulse repetition frequency (decreasing the time between pulses) as a function of elevation angle. A low prf would be used at low elevation angles to obtain the desired maximum unambiguous range. As the elevation angle increases, the maximum range decreases since aircraft do not fly above a certain altitude. The prf can be increased correspondingly at the higher elevation angles to decrease the total time it takes for the antenna to cover 360°.

The number of pulses per dwell can be reduced to decrease the total scan time. Fewer pulses mean a larger transmitter peak power and perhaps longer pulse widths to make up for the smaller energy available from the fewer number of echo pulses received from a target. The limit occurs when there is only one pulse per dwell, which has serious

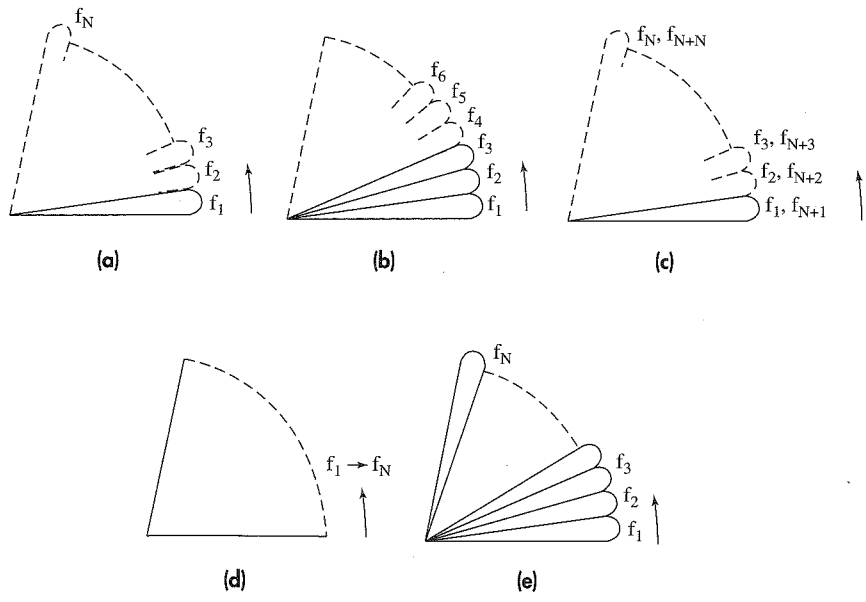

Figure 9.28 Several beam configurations for frequency-scan phased arrays that scan in a single angle coordinate, usually elevation. (a) Single-beam scanning; (b) multiple-beam scanning; (c) multiple-frequency frequency-scanning (radiating on more than one frequency at each beam position); (d) within-pulse scanning, transmit; and (e) within-pulse scanning, receive.

consequences for target detection. A single pulse per beam position can result in a large loss of two-way antenna gain if the target is near the half-power position of the antenna pattern when the pulse is transmitted. Another problem when using only one or a few pulses for target detection is that good doppler processing as required to eliminate clutter in an MTI radar cannot be achieved. Large MTI improvement factors (Sec. 3.7) require a large number of pulses to be processed (a longer time on target). Thus 3D long-range radars that employ one or a few pulses per beam position generally have poor, or no, clutter rejection.

Multiple-Beam Scanning One method to reduce the time for the antenna to cover its surveillance volume is to simultaneously, or almost simultaneously, transmit more than one beam (at more than one frequency), Fig. 9.28b. In the example of this figure, three pulses might be radiated at frequencies f_1, f_2, and f_3, respectively, so as to cover three contiguous elevation beam positions. The next set of three pulses is transmitted at frequencies f_4, f_5, and f_6. In this example there are three pulses radiated nearly simultaneously, but the number of frequencies radiated as one burst typically might vary from 3 to 9. The time required to scan 360° in azimuth is reduced in proportion to the number of simultaneous beams (frequencies) radiated.

A disadvantage of this approach is that there must be a separate receiver and signal processor for each of the n beams radiated simultaneously. In a military radar that must use sidelobe cancelers to reduce the effects of jamming, a separate set of sidelobe cancelers is required for each beam. When there are a large number of simultaneous beams, the cost of the radar can increase significantly.

Even though multiple contiguous beams are formed, one might not be able to perform an accurate elevation-angle measurement by comparing the amplitudes received in

adjacent beams. The reason is that amplitude-comparison angle measurement requires that the cross section of the target seen in the two adjacent beams to be the same. In a frequency-scan antenna, adjacent beams are at different frequencies. If the radar cross section of a target is a sensitive function of frequency, there can be a change in amplitude of the received echo signal due to changes in radar cross section that can result in an error when measuring angle by comparison of the amplitudes in adjacent beams.

Multiple-Frequency Frequency-Scan (or Multiple Mode) In the frequency-scan radars described so far, each elevation beam corresponds to a fixed frequency. This is not good for a military radar since measurement of the frequency by a hostile intercept receiver can provide the elevation angle of the radar beam. Effective hostile jamming can be achieved in some types of frequency scan radars by concentrating the jammer's power over a narrow range of frequencies (angles) rather than force the jammer to cover the entire frequency range of the radar transmitter. Furthermore, the rigid relationship between frequency and elevation angle does not allow a target to be observed at two or more frequencies, something that is desired in order to decorrelate the target cross section for improved detection performance.

It is possible, however, for a frequency-scan array to radiate more than one frequency at the same elevation angle, Fig. 9.28c, assuming that the antenna and the rest of the radar are sufficiently broad band.[64] This can be seen from an examination of Eq. (9.37b). The factor m in this equation is an integer. As the frequency is increased, a beam will scan from the endfire direction (in the direction of the input) through broadside and to the endfire direction in the other direction (pointing to the termination of the array series feed). When the frequency is increased further, another beam will eventually form, corresponding to a higher value of m. The range of frequencies corresponding to one value of m has sometimes been called a *scan band.*

Only one beam at a time will be radiated if the grating lobe relation of Eq. (9.40) is satisfied. It can be shown that if an array radiates at a particular angle corresponding to a value m_1 in Eq. (9.37b) when the frequency is f_1, then for some other value of m, say m_2, a beam will be radiated at the same angle when the frequency is $f_2 = (m_2/m_1)f_1$. As an example, consider an array with spacing $d = 0.6\lambda_0$ and $l/d = 15$, which corresponds to $m_1 = l/\lambda_0 = 9$. From Eq. (9.37b), the array will scan over a region $\pm 30°$ as the frequency changes from $0.968f_0$ to $1.035f_0$, where f_0 is the frequency corresponding to the broadside position of the beam ($\theta_0 = 0$). As the frequency is increased further, the factor $m_2 = 10$ applies and the same angular region is scanned as the frequency varies from $1.075f_0$ to 1. $149f_0$. For $m_3 = 11$, the corresponding frequency range is $1.183f_0$ to $1.264f_0$. The beams corresponding to different values of m are related to grating lobes discussed previously.

In addition to allowing better target detection and better electronic counter-countermeasures, the ability to operate similar frequency-scan radars in different parts of the frequency band can help in reducing mutual interference among nearby radars.

Within-Pulse Scanning In the frequency-scan systems discussed above, the antenna beam dwells at each angular resolution cell (beamwidth) for one or more pulse-repetition intervals before moving to the next resolution cell. Another method that has been used for

frequency scanning arrays is to radiate a single frequency modulated pulse that covers a frequency range wide enough to scan the beam over the entire elevation coverage, as in Fig. 9.28d. During each pulse, the antenna beam rapidly scans through all elevation angles. This is sometimes called *within-pulse scanning*. The transmitted waveform is similar to that of a linear FM pulse-compression radar, but it serves a different purpose. The frequency of an echo signal reflected from a target will be a function of its elevation angle. The receiver employs a bank of filters, each tuned to a different carrier frequency which in turn depends on the target's elevation angle, Fig. 9.28e. The number of filters depends on the antenna beamwidth and the total angular coverage. The bandwidth Δf_B of each filter is determined by the frequency change required to scan the antenna one beamwidth, which is then

$$\Delta f_B = \frac{df}{d\theta_0}\,\theta_B \approx \frac{df}{d\theta_0}\,\frac{\lambda}{D} \qquad [9.41]$$

where θ_B = beamwidth = λ/D, and D = aperture dimension. Rearranging Eq. (9.38), differentiating and substituting into the above gives

$$\Delta f_B = \frac{f}{f_0}\,\frac{\cos\theta_0}{(l/d)(D/c)} = \frac{f\cos\theta_0}{f_0 t_D} \qquad [9.42]$$

where t_D is the time for the signal to propagate through the transmission line of length $(l/d)\,D$. Thus in the vicinity of broadside ($\theta_0 = 0$), the received signal has a bandwidth $\Delta f_B \approx 1/t_D$, over which the signal is linearly frequency modulated. This bandwidth can be used for achieving a modest amount of pulse compression on receive. Normally, pulse compression cannot be used with frequency scan; but with within-pulse frequency scan, pulse compression processing can reduce the pulse to a width no smaller than the time t_D it takes for the signal to travel from one end of the array to the other. Another way to look at this is that the finite beamwidth of the scanning antenna causes the target to be illuminated with a changing frequency, which can be compressed on receive.

Back-to-Back 2D/3D Antennas A 3D frequency-scan radar has the advantage of being able to obtain a measurement of the elevation angle (target height). A 2D radar does not obtain elevation angle, but since it has a longer time on target and more received pulses than does a 3D radar it has better MTI processing. In a military radar, a 2D radar can take advantage of the wide frequency range of a 3D frequency-scan transmitter to operate with greater flexibility in the choice of frequency so as to reduce the effectiveness of electronic jamming. The advantages of both 2D and 3D radars can be had by employing a 2D (fan beam) antenna back-to-back with a 3D (scanning pencil beam) antenna on the same rotating antenna mount. The agile-frequency transmitter can be switched between the two antennas to obtain the type of performance desired. A separate transmitter can be used for each antenna so as to achieve simultaneous, rather than time-shared, operation of the two.

Phase-Frequency Planar Array Frequency scanning has been employed in the past for obtaining beam steering in one angle coordinate, with phase shifters to steer in the orthogonal angular coordinate. This is called a *phase-frequency* array in contrast to a

phase-phase array which uses phase shifters to steer in both angle coordinates. In an $N \times N$ planar array a phase-frequency array needs only N phase shifters in addition to the fixed frequency-scan transmission lines, while a phase-phase array needs N^2 phase shifters. The phase-frequency array may be considered as a number of frequency-scan arrays placed side by side. The phase-frequency array was used in the early days of phased arrays when phase shifters might be said to have been primitive. As phase shifter technology improved, the all-phase-shifter array became more popular.

Frequency-Scanned Reflector Antennas[65,66] A very different form of frequency-scanned antenna, compared to those described above, is one that employs a frequency-sensitive grating as the reflector surface. Those familiar with optics might recall the *diffraction grating* which has had an important history as an optical device. The optical diffraction grating is a planar or curved surface obtained by ruling many closely spaced parallel grooves on an optical surface (such as a polished metal mirror). It has the property that a beam incident on the grating will reflect at an angle that depends on the frequency. A similar property can be obtained at microwave frequencies with a periodic array of thin conducting elements etched on a dielectric substrate placed over a surface. When a beam is incident on such a surface, the angle at which it is reflected will depend on the frequency of the incident beam, Fig. 9.29. The dielectric substrate over which the periodic array is etched can be designed to convert most of the incident energy to the diffracted direction governed by its frequency rather than have it reflect in the specular direction given by Snell's law. The shape of the reflecting surface is not parabolic as is common for reflector antennas, but is determined by the properties of the grating and the need to suppress the direct wave whose reflection would be given by Snell's law. As seen in Fig. 9.29, the feed is offset from the normal to the reflector surface in order to achieve the frequency scanning properties. In one experimental demonstration, a 10 percent change in frequency resulted in a beam scan of 10°. The power reflected in the direction of the angle given by Snell's law (equal to the incident angle) was suppressed approximately 20 dB below the power in the frequency-scanned beam.

Frequency Scan in Two Coordinates In principle, an array can be made to frequency scan a beam in two angular coordinates (a TV raster type of scan) by employing an array of slightly dispersive arrays fed from a single highly dispersive array. It has been said that a 90 by 20° sector can be scanned using a 30 percent frequency change.[67] Two-coordinate frequency scan is almost never used, however, since it requires a very large tunable frequency range of operation and it results in a very narrow signal bandwidth.

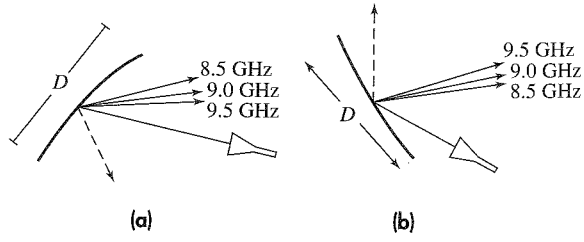

Figure 9.29 Geometries of a frequency-scanned reflector antenna employing a diffraction grating. In (a) the feed is positioned between the specular reflected beam and the diffracted beam; in (b) the specular and diffracted beams are reflected on the same side of the feed.
(From Johansson et al.,[65] Copyright 1989 IEEE.)

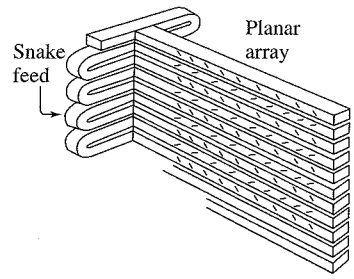

Figure 9.30 Sketch of a frequency-scan array showing, on the left, a folded waveguide delay line (snake feed) feeding a set of waveguides with radiating slots cut in their narrow wall.

Transmission Lines for Frequency Scan A popular form of transmission line for series-feeding a frequency-scan array has been the *snake feed,* shown at the left in Fig. 9.30. It has also been known as a *serpentine* or *sinuous feed.* Waveguide wrapped in the form of a helix has also been used, especially as the line feed for a parabolic cylinder reflector.

9.8 RADIATORS FOR PHASED ARRAYS

Types of Radiators Many different types of radiating elements (antennas) have been used in phased array radars, but the most popular have been various types of dipoles, slots cut into a wall of a waveguide, notch radiators, patch radiators, and open-ended waveguides, Fig. 9.31.[68,69] The pattern of a radiating element differs when located in the midst of a phased array than when it is all by itself in free space.[70] The *radiation impedance* (impedance which accounts for the power radiated) also can change; for example, the radiation impedance of a dipole in free space is 73 ohms; but in an infinite array with half-wavelength element-spacing and a back screen of quarter-wave separation, it is 153 ohms when the beam is directed broadside.[71] These changes are due to the effects of mutual coupling among neighboring elements. Furthermore, the impedance and antenna pattern

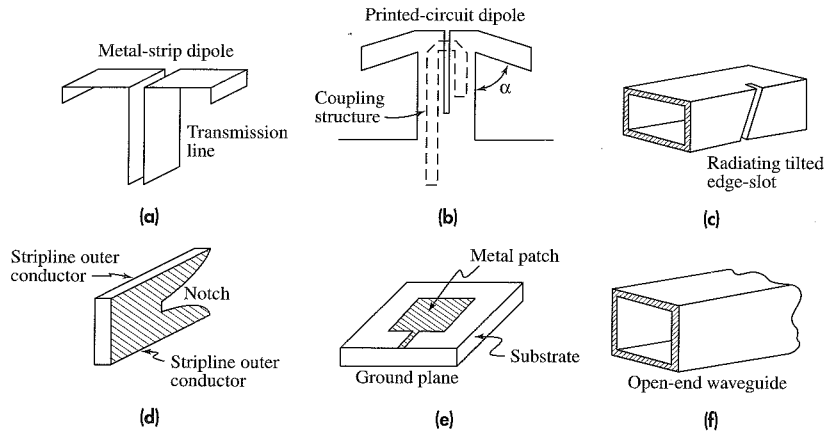

Figure 9.31 Sketches of single radiating elements for phased array antennas. (a) Metal-strip dipole with transmission line; (b) outline of printed-circuit dipole (solid lines) showing the coupling structure (dashed lines); (c) slot cut in the narrow wall of a waveguide; the tilt determines the amount of energy coupled from the slot; (d) notch radiator in stripline, radiation is to the right in this figure; (e) rectangular patch radiator; and (f) open-end waveguide.

of a radiator in an array can vary with scan angle. Array antennas are of finite size so that the properties of an individual radiator will depend on where it is located within the array. An element at or near the edge experiences an environment different from an element near the center of the array. When trying to determine experimentally how a radiator will perform when located within a large array (prior to building the entire array), the element might be located at the center of an $n \times n$ array of identical elements. It has been said[72] that when using dipoles above a ground plane, an element in the middle of a 7×7 test array may be taken as typical of an element in a large array. With an array of open-ended waveguides the test array should be 9×9. Sometimes the test array might even be as large 11×11.

The well-known *dipole radiator* is a widely used antenna that might be described as "T" shaped. It consists of two collinear metallic rods, tubes, or strips arranged in-line, and is fed at its center from a two-wire transmission line. Figure 9.31a is a sketch of a dipole made of metal strip. Figure 9.31b illustrates a printed-circuit dipole.[73] Generally the dipole is a half-wavelength in dimension. Dipoles are more likely to be used at lower, rather than higher, radar frequencies. In addition to the conventional dipole, the dipole can have its arms bent back (like an arrowhead) so as to obtain wider angle coverage. The thick dipole can reduce mutual coupling between elements and provide a wider bandwidth. Crossed dipoles (two dipoles orthogonal to one another) can provide dual orthogonal linear polarizations or circular polarization. Printed-circuit dipoles are simple to fabricate, especially at the higher frequencies.[73] A dipole with a *director* (a passive rod placed in front of it) might be used to reduce mutual coupling. Dipoles are used with a reflecting ground screen, or its equivalent, to confine the radiation to the forward direction. The distance between dipole and reflecting screen might be in the vicinity of quarter-wavelength. The reflecting ground screen further modifies the properties of the dipole compared to its radiation in free space.

Slots cut into the walls of waveguides, Fig. 9.31c, are similar in many respects to dipoles. The waveguide in which the slots are cut serves as a low-loss line-feed for the array. At the higher microwave frequencies, slots are generally easier to construct than dipoles and can be accurately manufactured using numerically controlled milling machines. Edge-slots in the narrow wall of a waveguide are usually preferred over slots in the broad wall since the waveguide "sticks" (as they sometimes are called) may be stacked sufficiently close to avoid grating lobes in the orthogonal plane. The waveguide-slot array is more suited for scanning in one angular coördinate, which is why it has been popular for 3D radars. (The sketch in Fig. 9.30 was an example.) The power coupled out of the guide by a narrow-wall slot is a function of the angle at which the slot is cut. No power is coupled when the narrow-wall slot is perpendicular to the edges of the guide. The greater the tilt from the perpendicular, the greater will be the coupling. Thus in a phased array with a tapered aperture illumination (like a cosine on a pedestal), the tilt of the slotted radiators near the center will be greater than the tilt of the radiators near the outer ends of the array. When half-wave-spaced slots are fed in a series fashion with the energy propagating down the waveguide, the field inside the guide changes phase by 180° from element to element. The phases of every other slot must be reversed to cause the radiated energy to be in phase. This phase reversal can be accomplished by alternating the tilt of adjacent radiating elements. In a series-fed dipole array, the phase is reversed by rotating every other dipole 180°.

A *flared notch* antenna in stripline is indicated in Fig. 9.31d. These might be envisioned as starting with a dipole, tilting its two arms into a V shape, and then curving the arms of the V and smoothing the normally abrupt transition at the input. Such antennas might have a bandwidth of from 2 to 1 to 6 to 1.[74]

A *patch antenna*[75] consists of a thin metallic film bonded to a grounded dielectric substrate, Fig. 9.31e. Its shape is usually rectangular or circular, and it can be excited with microstrip. It has the advantage of being low profile, lightweight, and is easy and economical to manufacture. It can be mechanically robust and is readily employed with solid-state modules. Patch antennas, however, usually are not as broad band as other radiating elements.

Open-ended waveguides, Fig. 9.31f, are an extension of the waveguide sections in which the phase shifters are located. Their performance can be calculated or measured in a simple phased array waveguide simulator.[76] The waveguide may be loaded with dielectric to reduce its physical size in order to fit the element within the available space. If wide-angle scan is not required, the open-ended waveguides may be flared to form a horn radiator with greater directivity. An array of open-ended waveguides might be covered with a thin sheet of dielectric to better match the array to free space, as well as act as a radome to protect the array from the weather. A dielectric sheet across the face of the array, however, can result in coupling effects that modify the expected performance of the antenna.[77]

Other radiators that have been used with phased arrays include polyrods, Yagis, log-periodic antennas, spirals, and helices. Almost any type of radiator can be considered for application in a phased array; but the dipole, or its equivalent, probably has been the most popular.

Mutual Coupling The analysis of the phased array used in this chapter, as well in many other books and publications on antennas, is based on a relatively simple model, as was used in Sec. 9.5. It simply combines in space the radiation from the individual antenna elements, taking account of their relative amplitude and phase. Maxwell's equations are not involved, which is why it should not be surprising that the simple theory is not adequate for predicting the performance of actual phased arrays. In particular, the simple theory does not account for interaction among the radiating elements. The current at a particular element depends on the amplitude and phase of the currents in many of its neighboring elements, as well as the original current applied by the antenna feed network. The effect of one element on the other is expressed by the term *mutual coupling.* When the antenna is scanned from broadside, mutual coupling can cause a change in antenna gain, shape of the antenna pattern, shape of the individual element patterns, sidelobe levels, and the radiation impedance.

A major effect of mutual coupling is the change in the impedance seen at the element due to the presence of nearby elements. This is important for properly matching the element as the beam is scanned. The purpose of matching is to avoid high voltage standing-wave ratios (VSWR) that can result at certain scan angles.

Much of the classical theory of mutual coupling[78–80] has been based on modeling the antenna as an infinite array so that all elements within the array see the same environment. This has been a widely applied model for predicting phased array antenna behavior even though an infinite array is not realistic, and it can led to questionable results at times. In most practical arrays a large fraction of the elements can be considered *edge elements,* or elements

near the edges. For example, it was mentioned previously that an element must be placed in the center of a 9 by 9 or an 11 by 11 array to accurately determine the effect of the neighboring elements on its performance. With half-wave spacing this means that significant coupling will occur between a radiating element and all elements that are within $2\frac{1}{2}$ wavelengths (if the 11 by 11 array represents an infinite array). In a square array of 60 by 60 elements, approximately 30 percent are edge elements. With such a large fraction being edge elements, one has to use caution when applying the results of infinite array theory.

The energy applied to a radiating element can appear in the main beam, the sidelobes, or be returned to the transmitter. The infinite array theory generally *assumes* that as the antenna scans off broadside, the reduction in radiated power due to the reduction in gain of the radiating element (the element factor) causes energy to be returned to the transmitter rather than be radiated elsewhere in space. The energy that returns to the transmitter results in an increase in the VSWR seen at each element. When the beam is steered, therefore, to a null of the element factor, some theorists assume that all the power is returned to the transmitter, which can be catastrophic. The situation has been called *blindness*[81] or *lost beams.*[82] This is a well-accepted concept by some antenna theorists, but there remain unanswered questions about its applicability to real antennas. When the beam is steered to the null of the element factor, the main beam will be distorted or even disappear, but one can argue that most, if not all, of the energy of the main beam radiates into space in other directions (producing a weird radiation pattern) rather than return to the transmitter.

Experimentally, the VSWR has been observed to increase at some of the many elements of a phased array when the beam is scanned; but there seems to be little experimental evidence for all or a large part of the transmitter power being returned from the array when the main beam is scanned to the direction of an element factor null. One might be skeptical about theories based on the infinite array model that assert that *all* the power returns to the source at certain beam-steering angles. If the power is not returned to the transmitter it seems plausible to assert that it is radiated into space. One should not expect a neat main-beam pattern or low sidelobes when this happens. An example of an experimental measurement in which the power was found to radiate in space rather than be returned to the transmitter when the beam is scanned is described next.

Forward-Wave Interaction in an Array Before leaving the subject of mutual coupling, an experimental measurement will be mentioned from the early 1960s which illustrates that further understanding of this subject is still required. Donald King and Harry Peters[83] reported measurements of small phased arrays using relatively high-gain closely spaced polyrod elements. Polyrods have seldom been used in phased arrays in the United States, but they illustrate the effects of mutual coupling that involve forward-traveling waves as well as diffraction effects and blockage. Measurements were made of a five-element array with polyrod radiators 6λ in length, spaced 3/4 wavelength apart. This is a rather close spacing for such high-gain endfire antenna elements, so it should not be expected that conventional array theory will apply. The E-plane pattern of a single 6λ polyrod in free space is shown in Fig. 9.32a. Its gain was 15.7 dB. The pattern of the center element of the five-element array is shown in Fig. 9.32b when the other four elements were terminated in a matched load. The pattern in the array is seen to be quite different from that in free space. It is broadened and becomes more rectangular in shape. The pattern of one

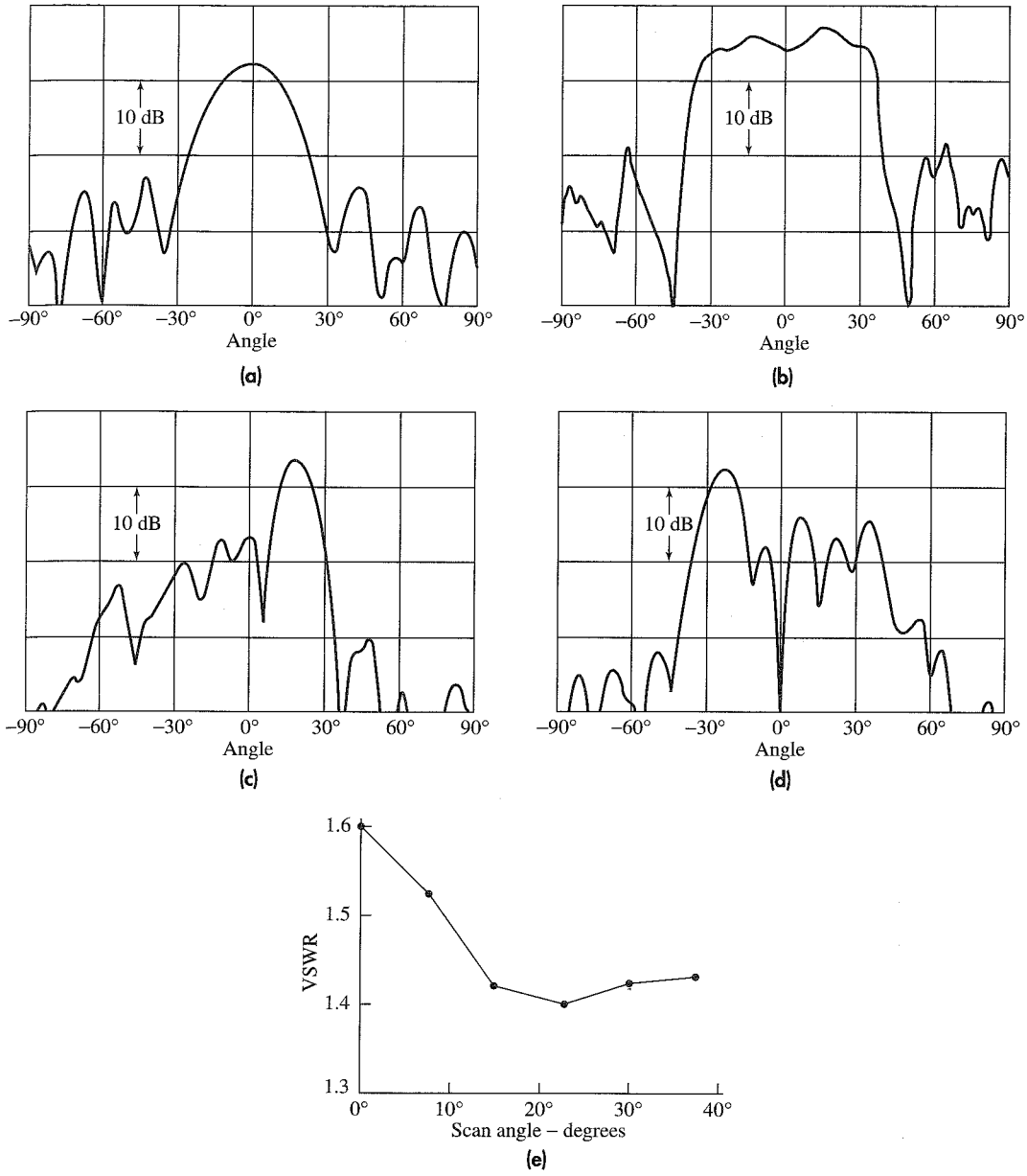

Fig. 9.32 Illustration of forward-wave mutual coupling in a five-element array with polyrod elements each six wavelengths long and spaced 3/4 wavelength apart. (a) measured *E*-plane radiation pattern of a single isolated polyrod element; (b) Measured *E*-plane radiation pattern of the center element with each of the other four elements terminated in a matched load; (c) pattern with the beam scanned to 15°; (d) pattern with the beam scanned to 37.5° (the main beam is not seen at its scan angle of 37.5°, but is "lost"); and (e) VSWR of the feed line of the center element as a function of the scan angle. Note there is no significant change in VSWR even for a scan angle of 37.5°.

[(From King and Peters,[83] Courtesy Microwave J.)

of the end elements was not given, but it would be different and would not be symmetrical in angle. Figures 9.32c and d show the beam scanned to 15 and 37.5°, respectively. The VSWR as a function of scan angle is given in Fig. 9.32e. (VSWR, or voltage standing-wave ratio, is a measure of how much signal is reflected by the antenna element back towards the transmitter.) Similar results were obtained when the element spacing was 1.5λ.

There are several interesting observations from these measurements. The VSWR did not increase as the beam was scanned from broadside, as would be expected from simple theory. The VSWR actually decreased, which is opposite to what is normally believed should happen when the beam of an array is scanned from broadside. There was no significant change in VSWR when the antenna was scanned to 37.5°. The antenna radiation pattern deteriorated considerably at this wide scanning angle and there was no main beam (the beam was "lost"), but there was energy radiated in other directions in space rather than reflected back to the transmitter, contrary to what is usually assumed in studies of mutual coupling. Thus there can be serious mutual coupling that affects the nature of the radiated pattern *without* energy being reflected back to increase the VSWR. Arrays of endfire elements such as polyrods, Yagis, log periodics, and axial-mode helices can experience similar mutual coupling due to forward-wave interaction, blockage, and diffraction rather than only the effects that appear at the terminals of the antenna elements. It might be expected that some of this behavior could also occur in an array of dipoles.

Closely spaced endfire elements have been used in radar antennas, but not often. The reason for mentioning this is that it gives evidence that what happens in the external near-region of the array and the interaction of the elements on the radiating aperture might be as important to understanding what is happening in an array as is the more familiar backward coupling that affects the circuit impedance, or VSWR, of the antenna. Further evidence of the importance of what takes place in front of the antenna is the effect of a dielectric slab or a periodic structure of baffles in front of the array, or even an array of open-ended waveguides, all of which can cause surface waves to travel across the array and contribute to mutual coupling effects.

Mutual Coupling and the Radar Systems Engineer The existing theoretical analyses of mutual coupling for finite (realistic) phased arrays do not seem complete since they do not account sufficiently for the forward-wave coupling among the elements. In spite of this deficiency, there is sufficient theoretical basis to allow the phased array antenna engineer to approach the design of real systems. As is common with many antenna design problems, the experimental skill and ingenuity of antenna engineers in dealing with real-world design have allowed phased array radars to be successfully built in spite of the shortcomings of existing theory.

9.9 ARCHITECTURES FOR PHASED ARRAYS

The term "architecture" is often used in the discussion of phased array radars but it has not been officially defined and there does not seem to be universal agreement as to what it encompasses. Here we use the term to include the various ways that phased array radars can be configured or structured.

An extremely important part of any practical phased array system architecture is the means by which the power from the transmitter is efficiently divided and distributed to the radiating elements, and the reciprocal problem of combining the signals received at the elements and providing them to the receiver and signal processor. The structure that performs this function is called the *array feed.* Two major methods for this purpose are *constrained feeds* (a network of transmission lines, or power dividers) and *space feeds* (which resemble feeds for reflectors or lens antennas). The constrained feed is sometimes called a *corporate feed.* Analog multiple-beam-forming arrays, active-aperture arrays, and digital beam-forming also require special consideration of the array feed method. Array feeds should not introduce significant loss nor should they be of excessive weight and size. Since the array feed is not always one of the more "glamorous" or visible parts of an array, it is not always appreciated that any loss it introduces is equivalent to a loss in antenna power gain and has to be compensated by an increase in transmitter power or other, usually undesirable, means.

Constrained Feed Simple illustrations of a parallel-fed and a series-fed constrained feed for one-dimensional linear arrays were shown in Fig. 9.16. The constrained feed is basically a $1 \times N$ power divider, where N = total number of elements in the array. Figure 9.33 is an example of a constrained feed for an array in two dimensions. This particular example is a combination of a single parallel feed and a number of series feeds. In one dimension, the parallel feed is shown and in the other dimension series feeds are shown. Each element has its own phase shifter. The required phase shift to steer the beam in two dimensions can be determined for each element by the beam-steering computer and then distributed to each phase shifter. Alternatively, a small computation chip can be placed at each element to compute the phase required at that particular element, based on being told the azimuth and elevation angles to which the beam is to be steered. Feeds consisting of waveguide or coaxial transmission lines can handle high power with low loss and can be constructed with excellent precision. They can, on the other hand, be bulky and expensive. At the higher microwave frequencies (L band and above), strip lines which can be precisely fabricated with computer-aided manufacturing techniques are sometimes used.

The power distribution to the columns of the two-dimensional array of Fig. 9.33 is shown with a single parallel feed. The power in each column is distributed with a series

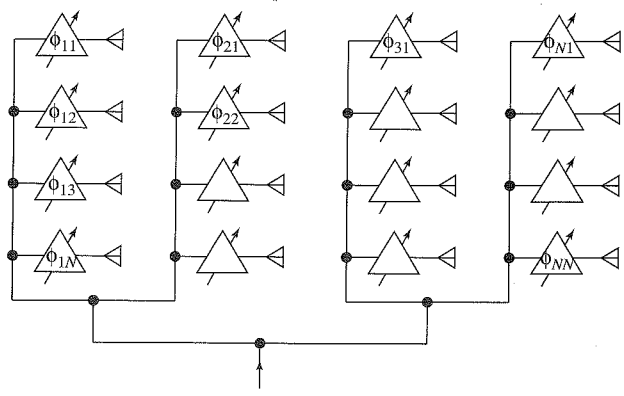

Figure 9.33 Planar array for scanning in two angular coordinates.

feed to the vertical elements. This is called a *parallel-series* feed. It the columns were fed with a parallel feed, it would be a *parallel-parallel* feed. There can also be a *series-series* feed. Series feeds may sometimes be easier to implement, especially in an active-aperture array where the transmitters and receivers are located between the feed and the radiators; but they have narrower bandwidth than the parallel feed.

Losses in constrained feeds are due to attenuation in the transmission lines as well as reflections from the junctions. Mailloux[84] states that the total length l of transmission line from an antenna element to the single array input is at least

$$l = (N^{1/2} - 1)d \qquad \textbf{[9.43a]}$$

This expression applies to a square array with total number of elements N and element spacing d. (The total length l can be longer than given by this equation, depending on the specific architecture.) The longer the length of line between antenna element and input, the greater will be the loss due to transmission line attenuation. Mailloux also states that the total number of power dividers (which also introduce loss) in series with each element is

$$\text{Total number of power dividers} = \log_2 N = 3.32 \log_{10} N \qquad \textbf{[9.43b]}$$

When the power splitters in a parallel-feed are four-port hybrid junctions, or the equivalent, the feed is said to be *matched.* Theoretically, there are no spurious signals generated by internal reflections in a matched feed. It is not always convenient or practical to use four-port hybrid junctions. Three-port tee junctions are sometimes used instead, for economic reasons, to provide the power splitting. Such a network cannot be perfectly matched in theory, and internal reflections can occur which can appear as spurious sidelobes in the radiation pattern.

Brick and Tile Assemblies Brief mention should be made of two types of array architectures, one called *brick* and the other *tile.* They will not be described in sufficient detail to fully understand, but further information is available in the literature.[85,86] These terms relate to the manner in which the array is contructed in relatively larger sections to make assembly easier. They are used with a corporate feed. The array is often grouped into subarrays of rows, columns, or areas, with each subarray fed separately. In the brick construction, the array is assembled with circuits on boards that are mounted *perpendicular* to the array face. In tile construction, which has also been called *monolithic array construction,* the array is assembled with one or more layers *parallel* to the array face. The array face contains the radiating elements and semiconductor active subarrays. The phase shifter drivers might be mounted on a layer just below the radiating face, and another layer with the RF power dividers mounted below that. Brick construction utilizes greater depth than does tile construction, so it allows more room for circuits, better thermal dissipation, and more convenient maintenance. It is also compatible with dipole and flared-notch radiators which can have greater bandwidth than the flat microstrip patch-radiators of the tile type of construction. Tile construction has the advantage of being thin so that it can be made to conform to aircraft or missile surfaces. It can be folded and stowed for erection in space, and it can be compatible with robotic or other automatic means of fabrication. Generally, the brick and tile structures have been of more interest at the higher frequencies (X band and above) than at lower frequencies.

Monopulse Beams When multiple beams are needed for monopulse angle measurement with a constrained-feed phased array, the output of each receiving element can be split into three separate outputs that connect to three separate beam-forming networks. One output is used with a beam-forming system to provide the sum beam and the other two outputs are used with separate beam formers to generate the two angle beams. The two angle beams can have different aperture illuminations (weightings) than the sum beam so as to produce desirable difference patterns with low sidelobes and a good error-signal slope.

Space Feeds A space feed is similar to the feed of a reflector antenna. It enjoys the advantage of the relative simplicity that characterizes feeds for reflectors. There are two types of space feeds depending on whether the array is analogous to a lens or to a reflector.

Lens Arrays Although the lens array is considered first in this discussion, much of what is said about it is applicable to the reflectarray as well. The lens array, Fig. 9. 34a, is fed just as would a lens antenna. It is shown in Fig. 9.34a as a one-dimensional representation, but the space-fed array is almost always two-dimensional. The primary feed might be a single horn, a collection of horns, or a monopulse cluster of horns. (The space-fed array is described as a transmitting antenna, but an analogous description can be given as a receiving antenna.) An array of antenna elements collects the energy radiated by the feed and passes it through phase shifters which provide a phase correction to convert the incident spherical wave to a plane wave. The phase shifters also apply the phase shifts required to steer the plane wave to some angle off of broadside. The antenna elements on the opposite side of the lens array then radiate the beam into space. The feed illuminating the space-fed array provides a natural amplitude taper to produce lower sidelobes than would a uniform illumination. The feed may be placed off-axis to avoid reflections from the lens returning to the feed and producing a large VSWR.

Reflectarrays A space-fed reflectarray with an offset feed is diagrammed in Fig. 9.34b. The energy from the feed enters the antenna elements, passes through the phase shifters,

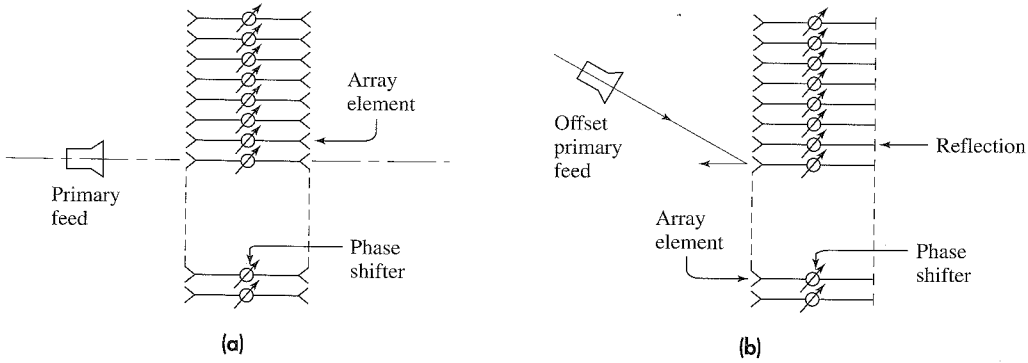

Figure 9.34 Space-fed arrays. (a) Lens array; (b) reflectarray.

is reflected, and passes back through the phase shifters to be radiated as a plane wave in the desired direction. Because the energy passes through each phase shifter twice, a phase shifter need only be capable of half the phase shift needed for a lens array or a conventional array. The phase shifters, however, must be reciprocal. This can be a limitation since some ferrite phase shifters with excellent properties for use in phased arrays are nonreciprocal and therefore cannot be used in a reflectarray.

Comparison Spillover radiation from the feed of a space-fed array can result in higher sidelobes at angles far from broadside than would be obtained with a constrained feed, unless some means are taken to minimize the spillover. Both sets of antenna elements at the front and back of the lens array require matching. This increases the matching problem of the array and can result in lower antenna efficiency. It is relatively straightforward, however, for the space-fed array to generate a cluster of beams, as for monopulse angle tracking, by use of multiple feed horns similar to those used for monopulse tracking with a reflector antenna. Compared to the constrained feed, space-fed arrays have the advantage of lower loss.

The lens array allows more freedom than the reflectarray in designing the feed assembly since there is no aperture blocking. The presence of a back surface in the reflectarray, however, not only allows better mechanical support and heat removal than in a lens array, but it also makes it easier to provide the needed control signals to the phase shifters. Space-fed arrays are generally cheaper than conventional arrays because of the omission of transmission-line feed networks. The space-fed array with a single transmitter and receiver is usually cheaper than an active-aperture array (to be described later) whose transmitters (and receivers) are distributed along the aperture.

A space-fed array may be cheaper than an array with a constrained feed or an active-aperture array, but it might not have the ability to control the aperture illumination sufficiently well to obtain ultralow sidelobes; and it is not capable of the very large powers possible with a conventional array where a transmitter can be placed at each of the many elements of the array.

Parallel-Plate Feeds A folded pillbox antenna, a parallel-plate horn, or other similar microwave devices can be used to provide the power distribution to the antenna elements. These are called *reactive* feed systems. They are basically used with a linear array and can be considered as another form of space-fed array, but only for one dimension. They would have to be stacked to feed a planar array, and would thus be a heavy feed system.

Further information on the many methods for feeding a phased array can be found in Patton.[87]

Subarrays It is sometimes convenient to divide the array into subarrays. These can simplify the manufacture and assembly of the array, provide broader signal-bandwidth, and allow multiple transmitters to be used to obtain greater power. Each subarray could have its own transmitter and receiver, but it is not necessary to do so to utilize subarrays. It is also possible to give identical phase steering commands to similar elements in each subarray to allow simplification of the beam-steering unit (which generates the beam steering commands). Because of the discrete nature of the subarrays, the phase distribution

across the aperture has the character of a stair-step, with one step over each subaperture.[88] This can result in what are called *quantization lobes.* Such lobes can be reduced by either overlapping the subapertures or inserting a small amount of randomization[89] to the phases of the subapertures. The term subarray also has, at times in the past, been applied to the array feed networks of a constrained feed system that produce sum and difference patterns for monopulse angle measurement.[90]

Subarrays can achieve wide signal-bandwidth by employing a variable time-delay element at each subarray.[91] Although time-delay elements allow wideband operation, they have not been economically feasible to use at each radiating element of a large phased array. A compromise is to utilize them at each subarray.

The original U.S. Navy Aegis (AN/SPY-1) phased array radar system for ship air defense employed 32 transmitting and 68 receiving subarrays of different sizes.[92] Each of the 32 transmit subarrays had its own CFA (crossed-field amplifier) power amplifier.

Triangular Element Spacing[93,94] For the most part, it has been assumed here that the radiating elements of a phased array are laid out in a square grid. A triangular, rather than a square, arrangement of elements, however, permits a savings in the total amount of elements needed in an array when the spacings are determined to avoid grating lobes (spurious beams comparable to the main beam that appear in the radiation pattern when the element spacings are too large). The reduction in the number of elements depends on the solid angle over which the main beam is scanned. For example, if the beam is to be scanned anywhere within a cone defined by a half-angle of 45°, the number of elements required with equilateral triangular spacing is 13.4 percent less than with square spacing. (The altitude of the equilateral triangle in this case is equal to the element spacing of a square grid.) The smaller the angular region to be covered, the less is the saving. Triangular spacings are more likely to produce higher sidelobes in some directions because of the phase quantization of digital phase shifters.[95] For most applications, however, these quantization lobes do not significantly limit system performance.

Active-Aperture Phased Arrays There are several different ways to configure a phased array radar system. One traditional method is to use a high-power phase shifter at each antenna element, with a single high-power transmitter and a single receiver for the entire radar. This has sometimes been called a *passive aperture,* or passive array, in contrast to what is known as an *active aperture,* or active array. They are illustrated in Fig. 9.35a and b respectively. An active aperture has a transmitter (low or modest power) at each antenna element. There is also included at each element an individual receiver, phase shifter, duplexer, and control, as well as the RF power source. Thus an active-aperture phased array implies there is a miniature radar system at each of the array elements. The construction of the electronics at each element of an active-aperture array radar can be highly integrated as a module or with MMIC (monolithic microwave integrated circuitry) construction. The active-aperture module, Fig. 9.35c, is called the T/R (transmit/receive) module or transceiver module.

The passive aperture has had the advantage of usually being cheaper than an active aperture, but cost has not been the only criterion used in selecting a particular array architecture. There are factors in favor of the passive approach and factors in favor of the

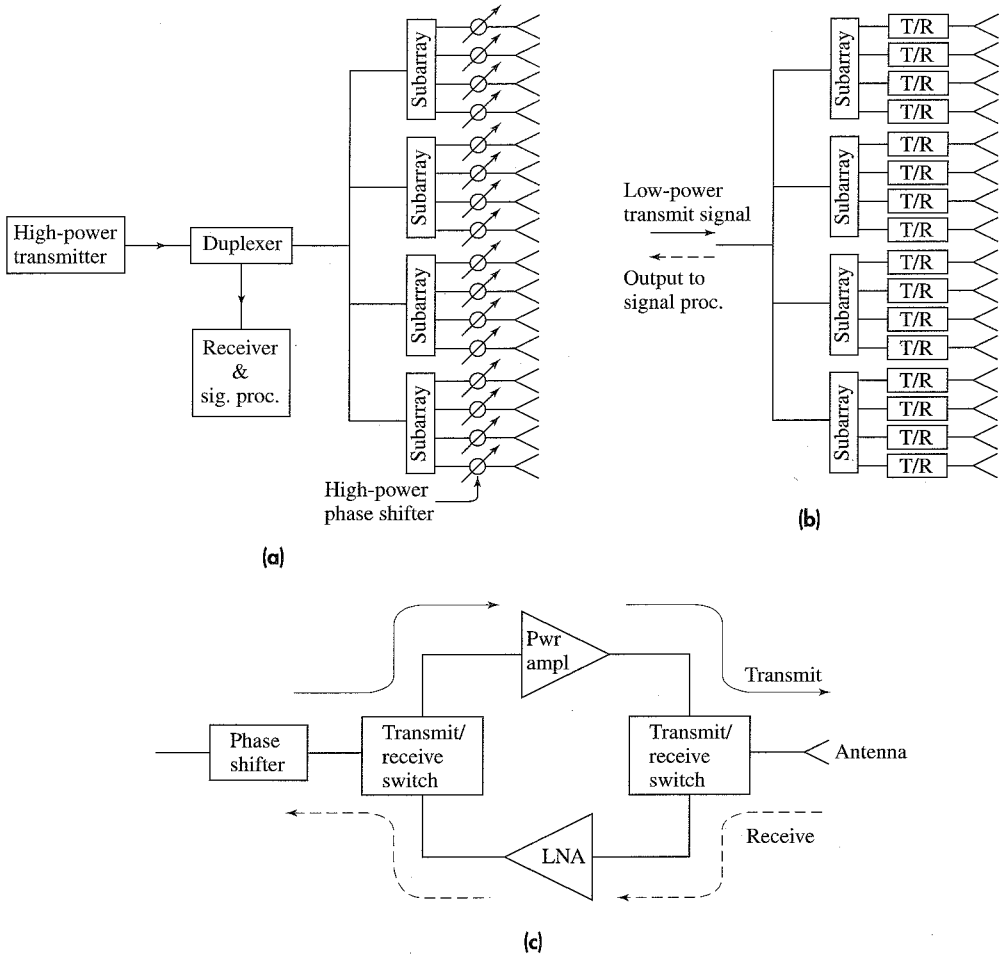

Figure 9.35 Comparison of the passive- and active-aperture array configurations, both shown with subarrays. (a) Passive-aperture phased array with a single high-power transmitter on the left and high-power phase shifters at each element. (b) Active-aperture array with T/R (transmit/receive) modules at each element. Sometimes there might be a booster amplifier on transmit at each subarray (that is bypassed on receive) and/or a time-delay element for increasing the signal bandwidth. (c) T/R module configuration, with a power amplifier on transmit and a low-noise amplifier (LNA) on receive.

active approach, and the choice as to which to use will depend on how the pros and cons balance for any particular application.

There are some generalities that can be cited regarding the relative costs of the two types of arrays. In the past it has been observed that it has often been cheaper to achieve a required total average power by employing a single high-power transmitter rather than obtain the same power by combining the outputs from a number of low-power sources. It has also been observed that high-power vacuum-tube transmitters usually have been

more efficient than the solid-state transmitters employed in active-aperture arrays at the higher microwave frequencies. These advantages of a single transmitter might be balanced by the fact that in an active aperture the power from the individual, low-power sources is combined in space so there is no loss in distributing the power as there is in a passive aperture that uses a constrained feed. If the passive array is space-fed, the loss is less than would be experienced by an array with a constrained feed. In a passive aperture the phase shifters must be capable of handling higher power than the phase shifters in the active aperture. The phase shifter loss in a passive aperture is often some fraction of a dB, which is low. The phase shifter loss in an active aperture, however, can be much larger than the phase shifter loss in a passive array since it occurs at low power levels and can be made up by increasing the gain of the power amplifiers that are located between the phase shifter and the antenna element. Thus there is little effect of phase shifter loss on the performance of an active aperture. Similarly on receive, the loss introduced by the phase shifter in the passive aperture can degrade the receiver noise figure. Loss in the phase shifters of an active aperture on receive is less important since the phase shifters are preceded by a low-noise amplifier that determines the noise figure.

There are various corporate-fed beamformer architectures that can be used with active-aperture arrays, depending on (1) whether the amplitude taper is applied in the beamformer network or in the T/R modules, (2) the degree of reliability (mean time between failures) required, and (3) whether the array is narrow or wide band.[96]

It has also been claimed[97] that the distributed architecture of the active aperture can smooth the effect of pulse-to-pulse amplitude and phase variations introduced by the RF power source, and therefore increase the MTI improvement factor and obtain better detection of moving targets in clutter. Since the amplitude and phase variations tend to be random among the many modules of the active aperture, the fluctuations combine in a noise-like fashion to smooth the effect. This assumes that a single large power supply is not used to power the T/R modules.

The proponents of the active-aperture array architecture state that one of its chief attributes is that the total transmitter power will be less than that of a passive aperture (that employs a constrained feed) since it avoids the losses of the high-power phase shifters and feed system. This might make the cost of the active aperture radar less than a passive aperture, if the cost of the active aperture T/R modules is not too large. The proponents of the passive aperture, on the other hand, will argue that the high cost of T/R modules, especially at the higher microwave frequencies (such as *X* band), as well as the lower efficiency of solid-state transmitters, will offset the higher losses of the passive aperture to make the active aperture more expensive. They would also argue that the cost advantage is even more in favor of the passive aperture if a space-fed array is used.

Although one can debate whether the active aperture or the passive aperture is better, the choice—just like many other choices that have to be made in engineering—depends on the particular application and the particular constraints imposed. It is not always obvious without full analysis which approach results in a more cost-effective phased array radar.

Examples of Active-Aperture Phased Array Radars The first "modern" phased array radar was the AN/FPS-85 satellite surveillance radar, which became operational at

Eglin Air-Force Base, Florida, in 1969.[98,99] In some respects, it can be said to have been the first active aperture phased array, in that it employed 5184 individual transmitter units, one at each of the radiating elements. It operated at UHF (centered at 442 MHz). Separate receiving and transmitting arrays were used since it was cheaper to employ two arrays rather than one array with duplexers. The receiving aperture was larger than the transmitting aperture and employed 19,500 receiving elements. Only 4660 of the elements in the receiving array were active (had receivers connected to them), the rest were inactive and were terminated. The receiving elements were arranged in a thinned, space-taper manner to reduce the number of receivers required while maintaining a suitable sidelobe level. The transmitters used a highly reliable tetrode as the final amplifier stage to produce a peak power output of 10 kW at each element. The total peak radiated power was 32 MW and the beamwidth was 1.4°. This radar was considered a success. It has been upgraded, but for a long time it continued to use a vacuum tube as the final stage at each transmitting element since it was cheaper to do so than convert to solid state. The radar has performed well its role in detecting, tracking, identifying, and cataloging earth-orbiting objects.

The first all solid-state active aperture phased array was the AN/FPS-115, more commonly known as Pave Paws.[100] It operated at UHF and was designed to detect subma-

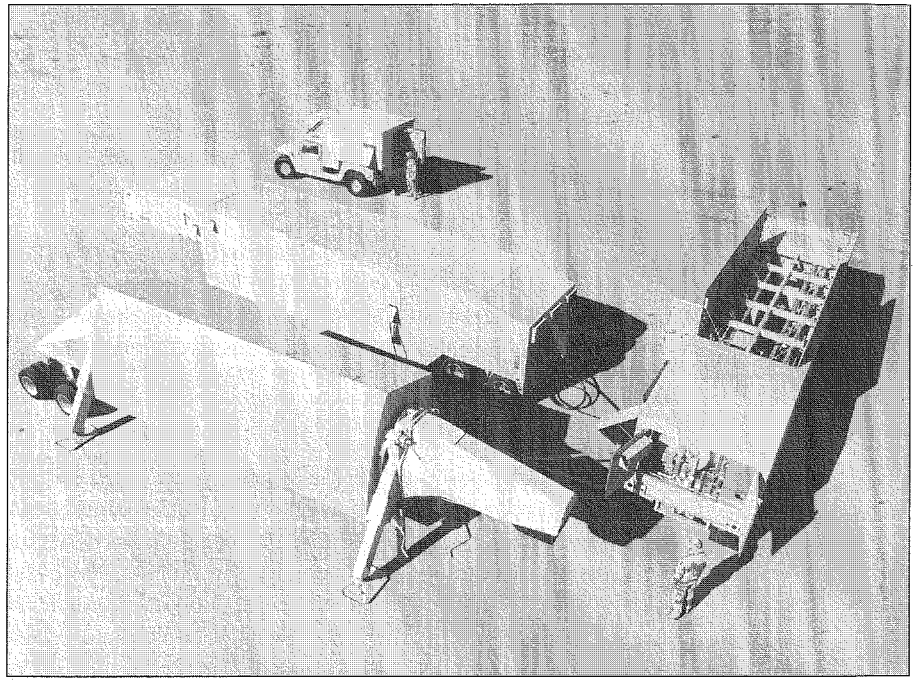

Figure 9.36 (a) The U.S. Army's THAAD *X*-band Ground-Based Radar (GBR) active-aperture radar for tactical ballistic defense. The 25,000-element array antenna equipment is shown at the lower left. Just behind it is the electronics equipment unit that houses signal and data processing, uninterruptable power supplies, receiver/exciter, and waveform generator. To the right is the cooling unit. At the upper left-center is the operator control unit. Not shown is the 1.1-MW diesel generator prime power unit.
| (Courtesy, Raytheon, Inc.)

rine-launched ballistic missiles fired at the United States. It had a secondary mission to perform space surveillance. Pave Paws employed 1792 active elements arranged in a circular aperture 22.1 m (72.5 ft) in diameter, plus 885 dummy elements. The peak power per T/R module was 335 W, which produced a total peak power of 600 kW and an average power of 150 kW per face. A Pave Paws radar consisted of two faces to cover 240° in azimuth. There were 56 subarrays, each containing 32 modules feeding 32 radiating elements. Its range was said to be 3000 nmi for a 10 m^2 target. There were four operational Pave Paws radars in the United States. One of these, located in Georgia, was expected to be increased in capability by 10 dB (by employing more elements) and replace the AN/FPS-85. A larger version of Pave Paws has also replaced the parabolic torus reflector antennas in the Ballistic Missile Early Warning System (BMEWS).

The THAAD (Theater High Altitude Area Defense) radar, Fig. 9.36a, is an active aperture radar designed for ballistic missile defense.[101] It has also been known as the Ground based Radar, or GBR. Radars for ballistic missile defense have to perform target detection, acquisition, track, identification (recognition), discrimination (of reentry vehicles from decoys and chaff), and assessment of target kill as well as in-flight communication to the defensive missile. The THAAD GBR is an *X*-band radar with 25,344

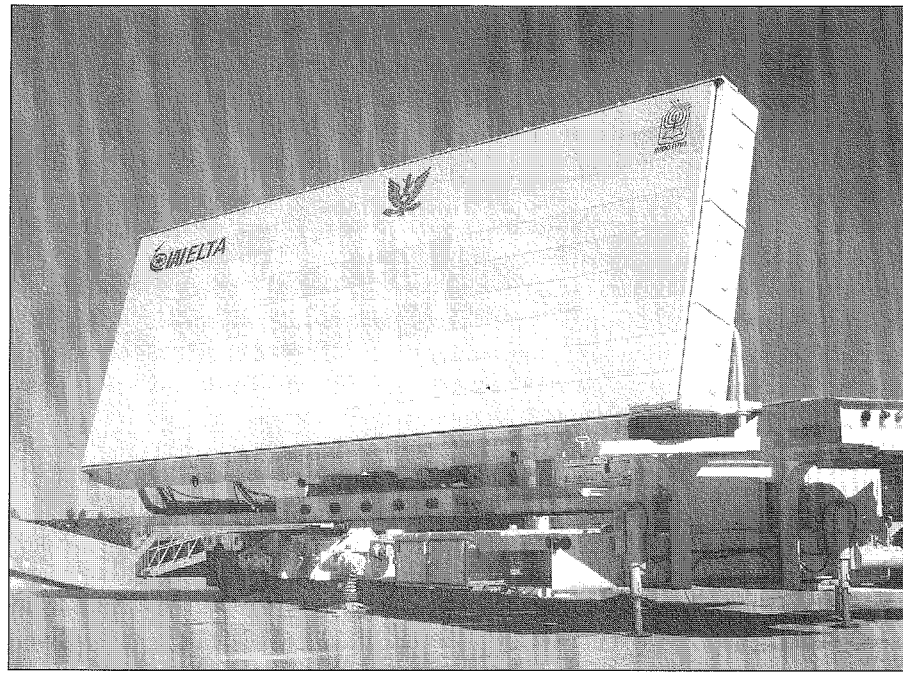

(b) EL/M-2080 *L*-band active aperture radar for the Israeli Arrow Tactical Ballistic Missile Defense System.
(Courtesy IAI/ELTA Electronics Industries, Ltd.)

radiating elements, each with its own gallium arsenide T/R module. In order to be able to operate with a wide-bandwidth signal, the aperture is divided into 72 subapertures, each containing 352 active elements. There is a time-delay steering element at each subarray to permit the use of wideband waveforms without distortion. The array aperture is 9.2 m^2 (almost 100 ft^2), which is quite a large aperture for an *X*-band phased array. Because there are so many of them, the T/R modules are a very important part of this radar (or any active-aperture array) and are the largest cost element of the array. It was said that "every $100 saved in the T/R module cost corresponds to $2.5M for the complete array." The entire array weighed over 46,000 pounds.

A different solid-state active-aperture phased array radar for theater ballistic missile defense is the Israeli *L*-band EL/M-2080 shown in Fig. 9.36b. It performs search, acquisition, and fire control as part of the stand-alone Arrow weapon system.[102] It is said to have detection ranges of hundreds of kilometers and can simultaneously track and engage many tens of missiles.

The active-aperture phased array has also been considered for airborne (fighter/attack) radar and for ship self-defense radar. In the airborne application the number of modules (and radiating elements) might be from 1000 to 2000, and for shipboard air defense there might be from 4000 to 8000 modules. A serious limitation of any fixed electronically steered phased array radar mounted in the nose of a fighter aircraft is its limited angle coverage. Although a phased array is usually said to be able to steer $\pm 60°$ coverage in angle, the main-beam gain decreases, the beam broadens, and the sidelobes rise significantly even before the beam approaches 60° from boresight. A fighter aircraft, however, requires its antenna beam to steer to even greater angles than 60°. This is practical to do with a mechanically steered antenna, but not with an electronically steered phased array. In the AN/APG-77 radar for the F-22 fighter aircraft, provision was made as a growth feature to allow installation of a "side array" on each side of the aircraft to allow coverage at angles beyond that available with a fixed electronically steered phased array antenna.[103] The addition of the side arrays, of course, increases the cost of an already expensive active-aperture radar.

Example of a Russian Phased Array Radar Architecture The Russians have generally employed a different approach from the United States to the design of their phased array air-defense radar systems. The U.S. Army's C-band Patriot and the U.S. Navy's *S*-band Aegis systems use multifunction phased array radars that perform the various radar functions required for air defense with a single system operating within a single frequency band. As discussed later in Sec. 9.14, this represents a compromise since the optimum frequencies for search and for track of aircraft are different. The Russians, on the other hand, use separate radars for each function, and the radars operate at frequencies more suitable for their particular function. Since Russia is a vast country requiring many air-defense systems, they emphasized a low-cost approach to radar design.

The Russian air-defense system S300V (NATO designation SA-12), used a 10,000-element *X*-band lens-array radar for multiple-target tracking and weapon guidance. The NATO designation of this *X*-band radar is *Grill Pan.* (The information in this subsection is taken from a paper by David Barton.[104]) The low cost and low RF loss experienced by this system was due, in part, to the separation of the surveillance and tracking functions

rather than to their being combined in one multifunction array. The space-fed lens array utilized multimode monopulse horn-feeds, so it did not experience the larger loss that a constrained-feed system might have. Faraday rotation dual-mode ferrite phase shifters were used which operated with circular polarization. Rather than convert the normal linear polarization to circular for operation in the phase shifter, and back again to linear (which is normally done with the dual-mode ferrite phase shifter), the two polarization transformations characteristic of U.S. dual-mode ferrite phase shifters were omitted by having the radar transmit and receive circular polarization. The array received the orthogonal circular polarization; that is, it received left-hand circular if right-hand circular was transmitted. (The polarization of the echo from an aircraft when illuminated by one sense of circular polarization contains both right and left circular polarizations in roughly equal amounts.) The ferrite phase shifters were nonreciprocal, but the phase shifters did not have to be reset after transmission in order to receive since the same phase settings were applicable when the received signal was of a circular polarization orthogonal to that transmitted. Since the polarization on receive was different from that on transmit, the receiver was partially isolated from the transmitter. The isolation due to the orthogonal polarizations, plus the use of a rugged cyclotron-wave electrostatic amplifier as the receiver front-end, eliminated the need for a duplexer or solid-state receiver protector, further reducing the loss. (The electrostatic amplifier had a 3-dB noise figure and could withstand average leakage power of several hundred watts and much higher peak power.)

The Russian ferrite phase shifters had two sections in series to provide 720° of phase shift (instead of the more usual 360°). Each section had its own control coil. One coil was for setting the phase required to steer in elevation and the other for the phase to steer in azimuth. All the row coils were in series with each other to provide azimuth steering and all the column coils were in series to provide elevation steering. The 10,000 element array (100×100) required only 100 row drivers and 100 column drivers. There were no driver or logic circuits, data busses, or d-c power busses needed in the aperture for determining the combined phase shift for steering in two angles. The total two-way RF loss from transmitter to receiver, excluding propagation loss, was about 3 dB for the Grill Pan. This compares to the 7 to 12 dB losses found in comparable Western systems.

The lack of individual control of each phase shifter, however, can cause the phase errors at the elements to be correlated over entire rows or columns of elements. Loss of a driver can result in the loss of an entire row or column of elements. The simplicity and low cost of this method for setting phase shifters make it more difficult to achieve low sidelobes.[105]

In addition to lower system cost and more optimum frequency usage, another advantage in using multiple radars in an air-defense system rather than a single multifunction phased array is that the individual radars can employ long-dwell medium-prf and high-prf pulse doppler waveforms that are needed to detect moving aircraft and missile targets in heavy clutter.

The *X*-band Grill Pan described above was the target tracking and guidance radar for the SA-12 air-defense system. Air surveillance was performed with the *S*-band Bill Board radar, which is a scanning beam 3D radar using a phase-scanned planar array with slotted waveguide radiators. The array could be stowed for transport in the short time of one minute. The SA-12 also employed a separate sector-search radar for detection of tactical

ballistic missiles. The Russian SA-10, a similar air-defense radar system, also deployed on a tower a horizon search radar called Clam Shell for detection of low-altitude targets.

According to Barton, this approach to air defense seems to reflect "the Russian military's insistence on high performance against targets of low cross section in environments containing rain, chaff, and other sources of clutter, an almost insoluble problem when the multifunction approach is adopted."

Simultaneous Multiple Beams (Analog) As has been noted, the phased array can form a number of multiple simultaneous beams. This is important for monopulse angle tracking; but in this subsection multiple beams are considered to be more than what is normally needed for tracking. In principle, an N-element array can generate N independent beams. Multiple beams allow parallel operation and a higher data rate than with a single beam. The multiple beams may be fixed in space, steered independently, or steered as a group. They can be generated on transmit as well as on receive. When multiple beams are generated on receive, the transmit beam can have a wide radiation pattern that encompasses the coverage of the multiple receive beams. In the past, multiple beams were generated by analog components, but it is now advantageous to employ digital methods for beam-forming. Digital beam-forming is not appropriate for transmit, but this is not necessarily a limitation since the transmitting antenna is relatively simple and employs a broad radiation-pattern (omnidirectional in some cases).

The simple linear array that generates a single beam can be converted to a multiple-beam array by attaching additional fixed phase shifts to the output of each element. Each beam to be formed requires one additional phase shift per element, as in Fig. 9.37. For

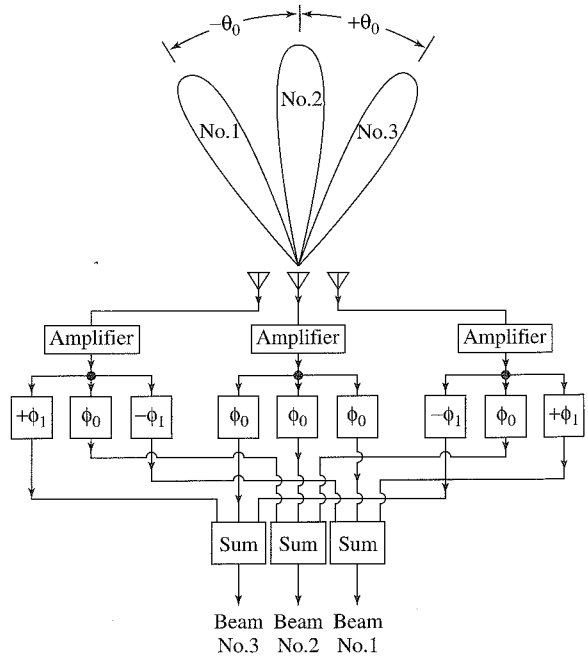

Figure 9.37 Simultaneous beam formation on receive (three beams shown). ϕ_0 = constant phase; $|\phi_1 - \phi_0| = |\Delta\phi| = |2\pi(d/\lambda) \sin \theta_0|$.

simplicity, the array in this figure is shown with but three elements, each with three sets of phase shifters. One set produces a beam broadside to the array ($\theta = 0$). Another set of three phase shifts generates a beam in the direction $\theta = +\theta_0$. The angle the beam points is determined by the relationship $\theta_0 = \sin^{-1}(\Delta\phi\ \lambda/2\pi d)$, where $\Delta\phi$ is the phase difference inserted between adjacent elements. Similarly, there is a set of phase shifters to produce a beam in the $-\theta_0$ direction. The receiving beam-forming networks may be at RF or at IF. At IF, tapped delay lines have been a convenient method to obtain the necessary phase shifts.

Butler Beam-Forming Array, or Butler Matrix[106] This is an analog RF beam-forming network, an example of which is shown in Fig. 9.38. It consists of 3-dB directional couplers (or hybrid junctions) and fixed phase shifts to form N contiguous beams with an N-element linear array. The number N is an integer expressed as some power of 2, that is, $N = 2^p$. The 3-dB directional coupler is a four-port junction. A signal fed into one port will divide its power equally between two other ports and no power will appear at the fourth port. In the process, a 90° phase difference is introduced between the phases of the two equally divided signals. Likewise, a signal inserted at the fourth port will divide its power equally between the same two ports with a 90° relative phase difference, and no power will appear at the first port. The relative phase difference in this case is of opposite sign compared to the phase difference resulting from a signal introduced at the first port.

The example of a *Butler matrix* depicted in Fig. 9.38 is an eight-element array that produces eight independent beams. It utilizes 12 directional couplers and eight fixed phase

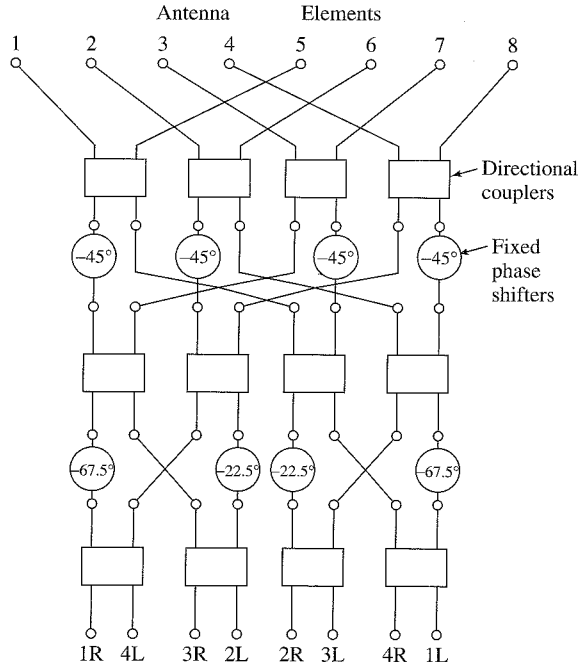

Figure 9.38 Eight-element Butler beam-forming matrix.

shifts. A Butler matrix has 2^p inputs and 2^p outputs. The number of directional couplers or hybrid junctions required for an N-element array is equal to $(N/2) \log_2 N$, and the number of fixed phase shifts is $(N/2) \log_2 (N - 1)$.

The Butler matrix is theoretically lossless in that no power is intentionally dissipated in terminations. There will always be, however, a finite insertion loss due to the inherent losses in the directional couplers, phase shifts, and transmission lines that make up the network. In a theoretically lossless, passive antenna radiating multiple beams, the radiation pattern and the crossover level of adjacent beams cannot be specified independently. With uniform illumination, as in the Butler matrix, the crossover level is 3.9 dB ($2/\pi$ in voltage) below the peak value of the beam. Crossover is independent of the beam position, element spacing, and frequency. The pattern is of the form $(\sin u)/u$, with -13.2 dB peak sidelobe.

The low crossover level of a Butler matrix is one of its disadvantages. If a lossless network could be achieved with a cosine illumination so as to reduce the peak sidelobe compared to that obtained with uniform illumination, the crossover level would be even worse (at a value of -9.5 dB); but the peak sidelobe would be -23 dB instead of -13.2 dB obtained with a uniform aperture illumination. By combining the output beams of the networks with additional circuitry, the Butler matrix can be modified to obtain an aperture illumination with lower sidelobes. The beamwidth will be widened, the gain lowered, and the network will no longer be theoretically lossless.

The flow diagram of the well-known fast Fourier transform (FFT) is similar to the circuit diagram of the Butler matrix.[107] The Butler matrix, however, was known before the FFT. Some of those familiar with the Butler matrix were surprised when they learned they were unknowingly using what would become an important procedure for the mathematical calculation of the Fourier transform. The FFT uses $(N/2) \log_2 N$ computations for an N-point transform, the same as the number of junctions needed for a Butler matrix.

The antenna equivalent of the conventional Fourier transform is called the *Blass beamforming network.* It requires N^2 couplers for N inputs and N outputs, just as the conventional Fourier transform requires N^2 computations for an N-point transform.

There have been other analog beam-forming methods considered for generating multiple beams with a phased array, as discussed in Sec. 8.7 of the second edition of this text. Most of them, as well as those mentioned above, are more suited for generating beams in one angular coordinate than in two coordinates.

Pattern Limitations in (Analog) Multiple-Beam Antennas In the above discussion of the Butler matrix it was said that it was not possible to arbitrarily select the crossover level of adjacent beams. The crossover of 3.9 dB down from the peak of the beam is determined by the theoretical lossless nature of the Butler matrix beamformer. This crossover level, however, is a characteristic of any passive, lossless antenna that forms multiple independent beams when the aperture illumination is uniform, as was indicated by Warren White.[108] He showed that a passive lossless beam-forming antenna requires that the individual beam patterns be orthogonal in space, which means that

$$\int_0^{2\pi} d\theta \int_{-\pi/2}^{+\pi/2} E_j(\theta,\phi)\, E_k^*(\theta,\phi) \cos\phi \, d\phi = 0 \qquad [9.44]$$

where θ = the longitude angle on the unit sphere, ϕ = the latitude angle, $E_j(\theta,\phi)$ = the radiation pattern associated with the jth input terminal, and $E_k^*(\theta,\phi)$ = the complex conjugate of $E_k(\theta,\phi)$. Independent orthogonal beams mean that when two or more beam input ports are simultaneously excited, the resulting radiation is a linear superposition of the radiations that would be obtained when the ports are excited separately. In addition, when a signal is applied to one port it should have no output at the other ports. An antenna which is lossless and passive means that the radiated power is the same as the input power.

As has been mentioned, the $(\sin u)/u$ pattern produced by a uniform illumination is an example of a pattern with orthogonal properties and produces a crossover of 3.9 dB between adjacent beams. With a cosine-squared illumination, however, White stated that the crossover with a lossless passive multibeam antenna is 15.4 dB down, and for a Hamming distribution it is 18.4 dB down. These are unacceptably high values. They apply to one-dimensional antennas. For two-dimensional antennas with pencil beams, the crossover in dB is double.

White suggested that these poor values of beam crossover can be avoided by use of active elements (amplifiers) inserted between the antenna radiating elements and the resistive beam-forming network. The sensitivity of the receiving antenna is established by the active circuits (low-noise amplifiers) at each element. Any losses that follow the amplifier do not affect the overall receiving system sensitivity. This method for generating efficient multiple-beam array antennas is similar to what is done in a digital beam-forming array, as will be described later in this section.

Systems Considerations for Multiple Beam-Forming Arrays A surveillance radar with a broad-beamwidth transmitting antenna (beamwidth θ_T) and with N fixed, narrow receiving beams (each of beamwidth θ_R) that cover the same angular region (so that $N\theta_R = \theta_T$) can have performance equivalent to a conventional radar that uses a single rotating transmit-receive beam of width θ_R. Equivalent performance means, in this case, that the two different types of radars will be able to detect the same size targets at the same range and have the same revisit time, which, in the case of a mechanically rotating antenna, is the antenna scan time, or the time to rotate 360° in azimuth. This requires that the signal integration time for the radar with fixed multiple beams also be the same as the time for the rotating antenna to make one revolution. The transmitting antenna gain of the multiple-beam radar is $1/N$th that of the scanning single-beam system. However, the observation time available to each of the fixed beams of the multiple-beam system is increased by $\theta_T/\theta_R = N$. If the signal is integrated without loss over this time, the reduction in transmitting antenna gain in the multiple-beam system is just compensated by the increased signal energy obtained because of its much longer integration time. The assumption of no integration loss is correct for perfect pre-detection (coherent) integration. When post-detection integration is used, however, there will be a theoretical integration loss so that the two radar systems will not be of exactly equivalent performance.

In a radar with fixed multiple receiving beams and a single broad transmitting beam, the two-way sidelobes are not as low as with a single-beam scanning radar. In some applications where low two-way sidelobes are important, it may be desirable to decrease the antenna sidelobes of the multiple receiving beams more than normal.

Multiple beam-forming array radars that use analog beam-forming are usually more expensive and require more equipment than a conventional scanning surveillance radar. They also do not seem to offer significant advantages in performance or capabilities over a conventional scanning radar. For these reasons they have seldom been considered for operational radar system applications. The production of multiple beams using digital beam-forming, to be discussed next, can also be expensive, but the use of digital technology offers advantages not readily available otherwise. Digital beam-forming, therefore, is of much more interest for multiple-beam radar applications than are analog beam-forming methods.

Digital Beam-Forming (DBF)[109–113] Almost all modern phased array radars utilize some sort of digital phase shifting to form a beam; but the term *digital beam-forming* (DBF) usually means something different—the formation of multiple receive beams by digitizing the outputs of the receiving array elements and forming beams by means of a digital processor. Although a single beam can be formed in this manner, digital beam-forming has more often been considered when multiple, simultaneous, directive beams are wanted. When digital beam-forming is employed to generate multiple receiving beams, the accompanying transmitting antenna has a broad beamwidth covering the same total angular region as the multiple receiving beams. The outputs from the multiple beams can be processed in parallel by the radar.

The basic configuration of a digital beam-forming receiving array might be as shown in Fig. 9.39. At each antenna element there is a receiver whose analog signal is digitized by the A/D converter. The A/D converter is a critical component since it can place a limit

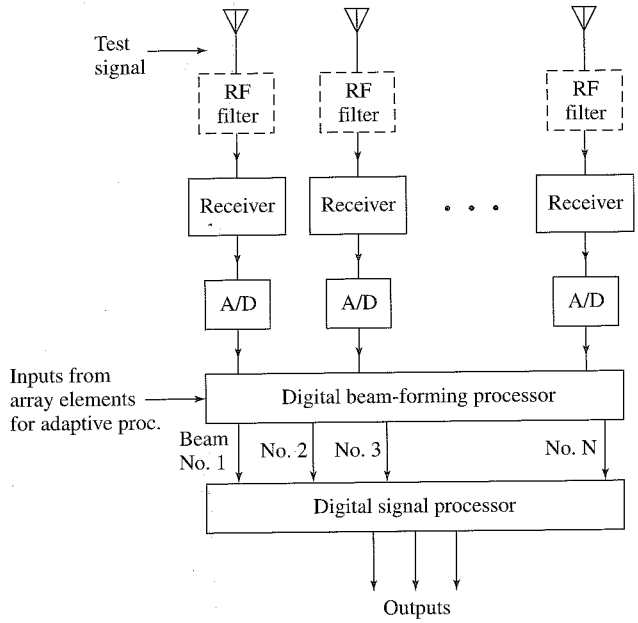

Figure 9.39 Basic configuration of a digital beam-forming receiving array.

on the system bandwidth and dynamic range. The lower the frequency at which the A/D converter operates, the greater can be its dynamic range and bandwidth. For this reason the input to the receiver is usually heterodyned (downconverted) to a lower frequency, filtered, and amplified to a power level suitable for the A/D converter. The receivers must be closely matched to one another so that the relative amplitude and phase of the signals at each element are preserved. If other than a uniform aperture illumination is desired (for example, to reduce the antenna sidelobes), amplitude weights can be applied to the digital output of each element and the weighted signals combined in the processor to produce the antenna beam. If a linear phase weight is applied to the digitized signal at each element, the antenna beam can be made to appear as if steered to a different angular direction. In this manner the digital processor can produce a multitude of receiving beams, each pointing in a different direction. An antenna beam, of course, is not actually formed in space by the processor. The pattern is evident as the variation of the output response of the digital signal processor as a function of angle.

Since the signal-to-noise ratio is established at the digital output of each receiver, there is no loss in signal-to-noise ratio when manipulating the digital outputs to form multiple beams. There can be any number of closely spaced antenna beams formed without degradation in SNR. Digital beam-forming, therefore, does not suffer the limitations inherent in analog beam forming, which are the low crossover of adjacent beams and the loss that occurs when trying to obtain lower peak sidelobes than the -13.2 dB of a uniform illumination.

The operation of the beam former is to take the outputs from each element, apply a complex weight (an amplitude and/or phase) to each, and then sum them to provide the output signal. The form of this output is similar to a digital Fourier transform (or inverse digital Fourier transform). When the phase weights are expressed in terms of the beam pointing angle θ_0, the relative response of the weighted outputs of the N-array elements as a function of the angle θ is represented as

$$g(\theta,\theta_0) = \sum_{n=1}^{N} a_n s_n \exp\left[j2\pi n(d/\lambda)\,(\sin\theta - \sin\theta_0)\right] \qquad \textbf{[9.45]}$$

where a_n = weight (amplitude for sidelobe control), s_n = output of the nth element, d = element spacing, λ = wavelength, and θ_0 = direction of the maximum beam response. In this manner, $M \leq N$ multiple beams can be formed. For each of the M beams there is a temporal sequence of digital numbers (data) that represent the temporal signals received at each beam position.

The computation of the Fourier transform in real time by the signal processor when there are many elements in the array can require a large number of operations per second. The computation requirements can be significantly decreased if the fast Fourier transform (FFT) is used. The FFT requires that the number of elements be some integer power of 2 (i.e., $N = 2^p$ and p = integer). There is less control of the beam patterns, however, with the FFT than if the conventional digital Fourier transform is used. The patterns of each FFT beam (in sin θ space) are the same, the peak sidelobes will be high, and the crossover of adjacent beams is predetermined (by the orthogonality constraint) and may be lower than desired. Thus with the FFT one trades control of the radiation pattern for ease of computation.

Two-Dimensional Beam-Forming The above description of digital beam-forming assumed a linear array forming beams in one angular dimension. With a two-dimensional rectangular array of $M \times N$ elements, beam-forming in two angular dimensions can be accomplished with the two-dimensional FFT. An N-point FFT is taken on each of the M rows to obtain $N \times M$ outputs. This is followed by an M-point FFT on each of the N columns to provide $M \times N$ beam outputs.[112]

Baseband versus IF Digitizing In any radar the digitizing of the received signal can be done either in the IF stage of the receiver or at baseband (zero IF) with I (in-phase) and Q (quadrature) channels. The I and Q channels at baseband are obtained in a similar manner to that described in Chapter 3 for an MTI radar (Fig. 3.29). It will be recalled that the received signal is divided into two baseband channels. The two channels are identical except that the phase of the reference oscillator in one differs from the reference phase in the other by 90°. The bandwidth of the signals in each of the two baseband channels is half that of the signal bandwidth; but two A/D converters are necessary, one in each channel. The smaller bandwidth of each A/D can sometimes be of advantage as opposed to requiring digitizing with the full signal bandwidth in the IF stage. To obtain good performance, the phase difference between the I and the Q channels should not deviate significantly from 90°. This requires careful design or some form of feedback control to maintain the precise phase relationship between the two channels. The signals in the two channels must also be well matched in amplitude.

Digitizing of the received signal may also be done directly in the IF of the receiver. There is only one channel and one A/D converter, so that the problem of balancing the phases and amplitudes of the I and Q channels is not present. The A/D converter has to be capable of greater bandwidth (sampling rate) than with a baseband I,Q arrangement. P. Barton[109] states that the minimum sampling rate of an A/D converter in the IF has to be 5.4 times the signal (half-power) bandwidth. (The sampling rate has to be greater than the theoretical Nyquist rate of 2 × bandwidth because of the need to avoid distortion of the signal spectrum caused by the folding of the spectrum around zero frequency.) This compares with a minimum sampling rate of 1.4 times the signal bandwidth required for each of the two A/D converters of the equivalent baseband implementation.

A/D Converters The sampling rate and the dynamic range of an A/D converter can set limits on what might be achieved in a digital processor. In practical A/D converters the greater the sampling rate (bandwidth), the smaller will be the number of bits into which the A/D converter can digitize a signal. In addition, as the bandwidth or number of bits increase, the size and cost of the converter can also increase. The limitations of A/D converters are practical ones, but their capabilities have been continually improved over the years. Section 3.5 gives values of the performance of A/D converters, but it is always risky to state in a text such as this what the state of the art of such devices might be. The prudent engineer, of course, should always consult current manufacturers catalogs for up-to-date information.

Other Characteristics of Digital Beam-Forming In addition to the attractive aspects of digital beam-forming (DBF) array radars mentioned previously in this subsection, the following are further favorable attributes of such radars.

Self-calibration and error correction—Errors in the phase and amplitude that occur in the analog portion of the receivers of a DBF can be compensated with relative ease in the digital portion. This may be obtained by injecting a precise RF signal at the front-ends of each receiver, or by placing an external RF source at a known position in the near or far field of the antenna, or by use of the echo signal from a well-defined scatterer of the transmitter signal.[110] This precise RF signal is used as the standard to adjust the phase and amplitude at each element.

Low antenna sidelobes—The ability to digitally self-calibrate the array allows the potential for achieving low or even ultralow receiving antenna sidelobes after digital processing. The effect of mutual coupling can also be compensated. It has been said:[114] "Mathematically, the compensation consists of a matrix multiplication performed on the received signal vector. This, in effect, restores the signals as received by the isolated elements in the absence of coupling. An attractive feature is that this matrix is fixed and thus is valid for all desired pattern shapes and scan directions. Although it may be difficult to realize in analog form, it can be readily implemented in a digital beam-forming antenna system."

Adaptive nulling—The flexibility of a DBF array allows nulls to be placed in the antenna radiation pattern in the direction of noise sources (jammers) so as to reduce the noise that enters the receiver. The placement of nulls in a receiving antenna pattern to cancel unwanted noise sources that enter via the antenna sidelobes is a well known technique, and can be done with much simpler systems than a DBF array.[115] Sidelobe cancellation, for example, can be readily achieved with a mechanically scanned reflector antenna and a relatively small number of auxiliary elements. But when one has a DBF array radar, it can be implemented to cancel noise sources that appear in the antenna sidelobes in a manner different from the conventional sidelobe canceler or a fully adaptive array, and with advantages not found in radars that do not have multiple beams. Nulls are achieved in "beamspace" by using one or more formed beams properly attenuated to adaptively cancel noise sources rather than using one or more omnidirectional elements.[116,117,110] If there are J noise sources to be nulled, the angular location of each source is found in a conventional manner and J directive beams are then formed to adaptively cancel each source. Use of beamspace allows cancellation without disturbance to the main beam or the main-beam sidelobes, except in the immediate vicinity of the noise sources. The use of beamspace for sidelobe cancellation has not normally been used in the past with conventional radar because of the complexity in forming multiple independent beams by other methods. In a DBF array, however, this is not a consideration since the forming of multiple independent beams is what such a system normally does anyway.

Adaptive nulling of clutter as a function of range—Nulls can be formed adaptively in those directions where there are large clutter echoes as well as in those directions in which there are noise sources. Unlike noise, however, clutter might be limited in range (for example, a large mountain or a patch of chaff). In such cases, range-dependent antenna pattern nulls can be formed only around those individual range cells containing localized clutter or chaff.

Correction for failed elements[111]—The complete failure of a sufficient number of antenna elements can seriously degrade the performance of a low sidelobe array antenna. It has been said[118] that it is possible to compensate, however, for the loss of antenna elements in a digital beam-forming receive array by using simple linear operations with the

outputs of a small group of good elements within the array. By properly utilizing the signals received at P elements of the array when P signals are received from different incident directions, it is possible to reconstruct the signal that would have appeared at the failed elements, if all of the array antenna elements have the same radiation pattern and some other restrictions apply. The technique has been said to work when the incident signal directions are not precisely known or even when they are only known to be within a broad angular sector.

Flexible data rates—As has been mentioned, the digital beam-forming array which looks everywhere can have a data rate that varies with the operational situation. This is unlike a conventional rotating radar whose data rate is fixed by the antenna rotation rate. At long ranges, a high data rate is not as important for an air-defense surveillance radar as it is at short ranges where weapons are engaged. Thus a lower data rata can be employed at long range which means that the integration times can be increased and improved target detection can be obtained without an increase in transmitter power. The flexibility of a DBF array to provide unrestricted data rates is important to a military weapon-control radar that should operate with high data rates during an engagement or when the target is seen to maneuver.

Simultaneous multiple functions—In an ubiquitous radar (one which looks everywhere all the time with fixed multiple receive beams) that uses digital beam-forming, it is possible to perform multiple functions simultaneously rather than sequentially. A conventional phased array such as Patriot or Aegis, on the other hand, has to time-share its various functions. Sometimes such radars run out of time to perform all the various functions required of them, so that some functions with lower priority have to be neglected in favor of more important ones. In an air-defense system, for example, priority will go to targets actually being engaged by missiles or to the searching for low-altitude pop-up targets, rather than to long-range surveillance. The ubiquitous radar with DBF, however, can perform its various functions simultaneously so long as it doesn't run out of computer capability.

Improved noncooperative target recognition—The ability to see everywhere all the time with whatever data rate is required is of benefit for those methods of noncooperative target recognition that depend on an observation time longer than normally needed for detection. The imaging of a ship or an aircraft by use of inverse synthetic aperture radar, for example, requires that the aspect of the target change sufficiently so that recognizable doppler-frequency shifts from different parts of the target can be isolated (resolved). Time is needed to allow for the target aspect to change, and time is something available with a DBF array. Recognition of helicopter targets based on the transient "flash" of the rotating blades when they are briefly oriented perpendicular to the radar line of site requires that the radar dwell long enough on the target to detect this phenomena.[119] The fixed beams of DBF provide this flexibility in target observation time.

Lower probability of intercept—It is relatively easy for an intercept receiver to detect the radiated signals of conventional radars at long ranges. To reduce a radar's detectability to a hostile intercept receiver, its peak power should be made as low as possible. The radiated energy should be spread over a wide angular region, over a long time interval, and over a wide frequency band. The ubiquitous DBF array offers the ability to spread the radiated energy over a wide angular region, something not possible with a scanning directive transmitting beam.

A beam-forming array that produces many multiple beams has capabilities not readily obtained with a conventional radar that employs a mechanically scanning antenna. Digital beam-forming offers advantages over analog beam-forming in generating multiple beams in that the same digital outputs from each array element are reused to readily generate multiple beams as well as perform other types of spatial and temporal processing. Digital processing has increased the feasibility and capability of the ubiquitous radar.

Examples of Digital Beam-Forming Arrays Digital beam-forming has been employed in both HF over-the-horizon radar and in 3D air-surveillance radar. Neither of these applications employ the full benefits of digital beam-forming arrays as described above, so they are not indicative of what might be done with this radar concept.

The U.S. Navy's Relocatable Over-the-Horizon Radar (ROTHR), AN/TPS-71, is designed to detect aircraft and ships at ranges from 500 to 2000 nmi.[120] It employs a receiving linear-array antenna 2.7 km in length with a total of 372 monopole antenna elements. At each antenna element there is a receiver that converts the signal to an IF frequency. The digital outputs of these 372 antenna elements are used to form 16 contiguous receiving beams that can be placed anywhere within the radar's angular coverage. Both spatial processing (beam forming) and temporal processing (doppler filtering and matched filtering) are performed with the same digital data from each receiving antenna element.

The *SMART 3D radar,* developed by Signaal of the Netherlands, is a 3D air-surveillance radar with an azimuth-rotating antenna which generates a number of simultaneous multiple-beams in elevation to provide a measurement of elevation angle using digital beam-forming. The original version of this radar was at *S* band, a later version was at *L* band. The *L* band radar formed 16 beams and the *S*-band version 14 beams.

9.10 MECHANICALLY STEERED PLANAR ARRAY ANTENNAS

Mechanically steered planar arrays offer important advantages not available with conventional reflector antennas in some radar applications. They have been employed at the lower radar frequencies (VHF) for air-surveillance applications, at microwave frequencies for 3D radars which need to obtain a measurement of target elevation angle, in airborne radars that operate from the nose of the aircraft, in missiles, civil marine radars, and in low-sidelobe antennas such as used for AWACS. The large number of elements in an array aperture allows better control of the aperture illumination and therefore, better control of the antenna radiation pattern.

Mechanically Rotating Arrays for Air Surveillance The first radar antennas developed by the United States in the 1930s, such as the Army's 100-MHz SCR-270 and the Navy's 200 MHz CXAM were mechanically steered phased arrays. At these low radar frequencies, it was natural to use planar arrays of dipoles since they were consistent with the communications antenna technology of that time. Also, they were well suited for the VHF frequencies at which the early radars operated. As radar frequencies increased, the parabolic

reflector was introduced since it was simpler than a planar array when there had to be a large number of dipoles. The German World War II Wurtzberg radar that operated at 550 MHz employed a parabola. The first U.S. microwave air-defense radar, the S-band SCR-584, also used a parabolic reflector. The parabolic reflector was well-known in optics, and it was not difficult to translate its technology and theory from optics to microwave frequencies.

The early air-surveillance radars were 2D in that they measured azimuth angle and range, but not elevation angle (or height). When pencil-beam 3D radars (such as the AN/SPS-39) first appeared in the 1950s to obtain elevation angle, they originally used a parabolic cylinder antenna with a line feed. These were followed by planar arrays (as in the AN/SPS-48) consisting of rows of slotted waveguides to obtain multiple beams in elevation. These original 3D systems utilized frequency-scanned phased arrays to electronically steer one or more beams in one angular coordinate (elevation). The other angle coordinate was obtained by mechanically rotating the entire antenna 360° in azimuth.

Almost all modern 3D air-surveillance radars employ a planar array antenna of some type that is mechanically steered in azimuth and which uses some form of electronic steering or beam-forming in elevation. Mechanical rotation is satisfactory for the air-surveillance application since it is not necessary to have rapid beam switching among many targets as it is in the weapons control application. The mechanically rotated planar array not only provides a convenient means for obtaining electronic steering in elevation, but the availability of many elements in the antenna also provides more flexibility in achieving the desired radiation pattern.

Mechanically Steered Slotted Planar Arrays[121–123] This type of planar array antenna is widely used for radars mounted in the nose of an aircraft. An example is shown in Fig. 9.40. Such antennas are common for military radars used in fighter and attack aircraft, airborne weather radar, and for missiles. An important advantage of this type of antenna for application in the nose radome of an aircraft is that it can be made relatively thin. This allows a larger diameter antenna to be mechanically scanned within an aircraft's nose radome than is possible with a relatively thick parabolic antenna and a feed that projects a distance from the reflector surface.

Microwave planar array antennas generally employ radiators that are slots cut into waveguide, a simple example of which was shown in Fig. 9.31c. They may be edge slots cut into the narrow wall or slots cut into the broad wall. The use of slots cut into the narrow wall allows the rows of an array to be spaced closer than if they were cut into the broad wall. The slot is the so-called *Babinet equivalent* of the dipole. Its pattern resembles that of a dipole, except that a vertical slot radiates horizontal polarization and a vertical dipole radiates vertical polarization. The waveguide feed structure lies directly behind the radiating slots of the array antenna.

There are two basic methods for structuring a series-fed mechanically scanned slotted waveguide radiator. One is called the standing wave, or resonant, configuration. The other is the traveling wave, or nonresonant, configuration. The spacings between elements in a resonant array is half a guide wavelength. (The guide wavelength is the wavelength measured in the waveguide rather than in free space.) The beam is broadside to the aperture, but the half-wavelength spacing between elements means that impedance mismatches

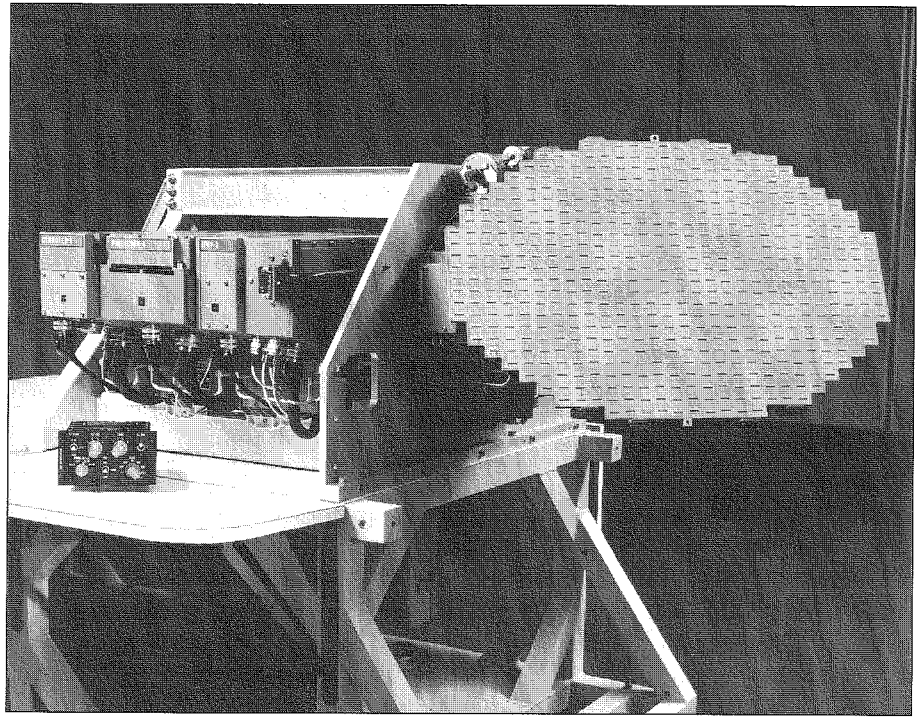

Figure 9.40 Mechanically steered planar array antenna for the AN/APG-68 airborne radar found on the F-16 aircraft.
(Courtesy Northrop Grumman Corp.)

at the elements can accumulate and cause a high VSWR (large mismatch). This results in restricting the number of elements in a linear array to less than 20,[124] which might be too low for most radar applications. Resonant arrays also have narrow bandwidths. The nonresonant array usually has an element spacing greater than half a guide wavelength and so does not experience the high VSWR or the narrow bandwidth of the resonant array. The waveguide of the nonresonant array, however, has to be terminated with a matched load to absorb the fraction of the input power that is not coupled to the other elements. The amount of power lost because of the matched load is about 5 to 10 percent of the power at midband.[121] Thus the array efficiency will be less than unity. (If the array is not well matched, a portion of the signal can be reflected from the termination and radiate as a high sidelobe in some spurious direction.) The direction of the peak of the beam radiated by a series-fed nonresonant array varies with frequency; similar to a frequency-scan array, but much less dramatic. With a wavelength λ, the beam is directed at an angle θ given by

$$\sin \theta = \lambda/\lambda_g - \lambda/2d \qquad \textbf{[9.46]}$$

where λ_g = guide wavelength, and d = element spacing. Yee and Voges[123] state that in most nonresonant slot arrays, $2d$ is selected to be greater than λ_g so that the angle of the

beam will move toward the load-end of the array as the frequency is increased. The frequency dependence of the beam direction might need to be taken into account in some applications.

The mechanically scanned planar array can be designed to provide monopulse beams in two angular coordinates.

Endfire Arrays In the above we have considered the array that radiates its main beam perpendicular (broadside) to the aperture. It is also possible to radiate a beam parallel to the aperture. These are known as *endfire array antennas.* If we consider the dipole as the radiating element, it must be oriented so that its element pattern allows radiation in the endfire direction, and the spacing between elements and the phase shift at each element allow propagation in the endfire direction. For example, the spacing between elements in an equal-amplitude linear endfire array fed from one end might be a quarter-wavelength, with phase shifts of $\pi/2$ radians between elements, to give an antenna pattern with most of its energy oriented in one endfire direction. In this example, the phase is retarded progressively by the same amount as that experienced by the traveling wave from one element to the next. (A phase retardation of 0.6π radians actually produces a higher directivity for this endfire antenna, according to the Hansen-Woodyard criterion, as mentioned by Kraus.[125])

The Yagi-Uda antenna, which originated in Japan, is a simple and inexpensive example of an endfire array. It consists of a single driven dipole plus several spaced parallel rods that form an endfire array, Fig. 9.41. Each rod may be thought of as a short-circuited dipole. The rod located behind (to the left of) the driven dipole acts to reflect the energy to the forward direction. One or more spaced rods in front of the driven dipole direct the energy forward. The rods are known as either *reflectors* or *directors.* The reflector might have a length of about a half-wavelength and be spaced a quarter-wavelength behind the driven dipole. The directors are slightly smaller (by about 10 percent) with spacings about a third of a wavelength.

Endfire antennas can be arrayed and have been used in radars, especially at VHF and UHF. An example is the antenna for the E2C Airborne Early Warning radar (that was shown in Fig. 3.45a). An advantage of the endfire antenna for this application is that a narrower beamwidth can be obtained in the vertical dimension without the need for a large vertical aperture. The beamwidth of an endfire antenna in the dimension orthogonal to its

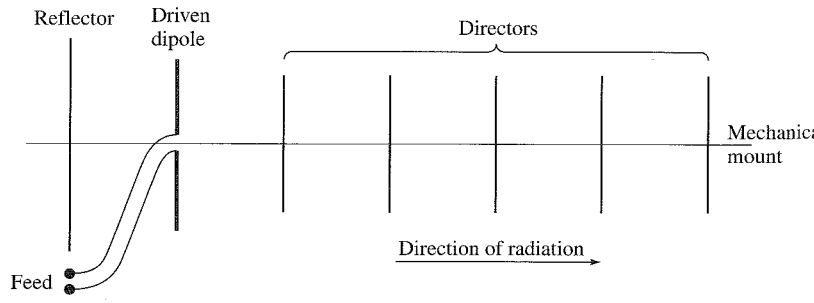

Figure 9.41 Sketch of a Yagi-Uda endfire antenna. (The mechanical mount is insulated from the dipoles.) For radar application they have been used in a linear array configuration; one example is that of the E2C AEW radar shown in Fig. 3.45a.

longitudinal axis is proportional to the square root of the antenna length, as compared to a conventional broadside antenna where the beamwidth is directly proportional to the antenna size.

Rotating Electronically Steered Phased Arrays At times it has been suggested[126,127] that a single face of an electronically steered phased array be mechanically rotated in azimuth but electronically steered in azimuth and elevation. Whether the single rotating phased array is an attractive alternative to a four-faced fixed phased array depends on the particular application and the assumptions that are made. Caution should be exercised, however, when considering this approach since in some cases it is conceivable that a rotating single phased array face might provide the worst attributes of both the phased array and the mechanically rotated antenna rather than the best of both. The mechanically trainable phased array, described next, is different and has some important operational advantages.

Trainable Phased Arrays A trainable phased array is one which is electronically steered in both azimuth and elevation over a wide angular sector, but which is mounted so as to be mechanically positioned to cover a desired sector. (Once in position it remains fixed rather than continuously rotated.) It is a convenient method for using an array for missile-range instrumentation. An example is the transportable *C*-band AN/MPS-39 MOTR (multiple object tracking instrumentation radar) developed by Lockheed-Martin at Moorestown, N. J. (shown in Fig. 4.1b). The 12-ft-diameter space-fed lens array with 8359 elements is mounted on a precision elevation-over-azimuth tracking pedestal so as to achieve coverage of a 60° cone anywhere within the full hemisphere. Its beamwidth is one degree and its measured antenna gain is just under 46 dB. In missile range applications, many targets might have to be tracked simultaneously; including the firing aircraft, the target missile or drone, surface-to-air missiles, air-to-air missiles, and other aircraft that might be on the range (range safety). The MOTR can simultaneously track up to 10 targets with an absolute angle accuracy of 0.2 mils rms and a range accuracy of 1 yd rms. Prior to such radars, a separate air-surveillance radar and more than one mechanical tracking radars had to be used.

The trainable phased array is also of advantage for ship air-defense when the agility of a phased array is needed. Traditionally, when a phased array is used on board a naval ship (for example, the *S*-band Aegis system or the U.S. Navy's original *S*-band AN/SPS-33 phased array radar system), there are four planar array faces mounted around the ship to provide 360 degrees of all-around coverage. Although the designer might want to configure the phased array so that all four apertures can operate simultaneously, the need to reduce the cost of such radars has sometimes resulted in having only one or two transmitters and receivers time-shared among the four array apertures. This might result in acceptable performance, but it is less than what could be obtained if the four faces were able to simultaneously operate all the time.

An alternative method for configuring an air-defense phased array radar system when four complete phased array faces are too costly (or even when they are not), is to employ two trainable arrays instead. An example used by the Russian navy on Cruisers is the trainable array radar shown in Fig. 9.42 which is known by its NATO nomenclature as the Top Dome SAN-6, or by its Russian/Soviet name of RIF. In a Russian Navy Cruiser,

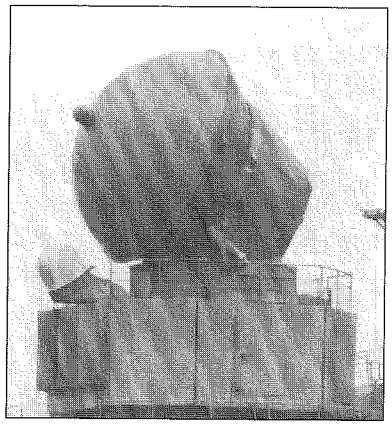

Figure 9.42 Soviet/Russian electronically scanned trainable phased array pulse doppler radar whose Russian name is RIF. Its NATO designation is Top Dome and is part of the SAN-6 shipboard surface-to-air missile system. It is said to employ row-and-column beam steering. The antenna assembly includes a hemispherical radome. In addition to the main phased array there is a wide-angle phased array for acquisition of the surface-to-air missiles just after launch.

one Top Dome radar is located fore and a second one is located aft. (A truism is that if something is important to have on a naval ship—such as a gun, missile system, or radar—there ought to be at least two of them to insure that one is available when needed.) The two trainable array radars can cover attacks simultaneously within any two 90° sectors. An important advantage with this configuration is that one or more attacks from within a single 90° sector can be engaged by both radars simultaneously. A four-face phased array, on the other hand, can bring only one array face to bear to defend against such an attack.

Two trainable phased arrays cannot engage a multiple simultaneous attack from more than two 90° sectors. The likelihood of this being a serious concern is small. The ability to mount a simultaneous attack from three different directions over 360° in azimuth is certainly possible, but having all targets appear simultaneously at the target ship from different directions is very difficult to do. If they are not simultaneous, the ship's air-surveillance radar with 360° of azimuth coverage can be expected to detect and recognize such attacks and the two trainable arrays can be scheduled to engage them without overlap. Also, it is seldom that a major naval ship that carries an expensive phased array radar for air defense operates by itself; so if there is a large multiple attack, one ship does not have to handle the total attack all by itself. Thus employing trainable phased arrays offers advantages not found with the traditional four-faced phased array system.

9.11 RADIATION-PATTERN SYNTHESIS[128]

A radar antenna radiation-pattern is required to have a specified beamwidth along with acceptably low sidelobe radiation. In some cases, the antenna radiation pattern must provide a desired contour, or shape, over a specified angular region. An example is the cosecant-squared elevation pattern of an air-surveillance radar. The aperture illumination for the squinted beams of an amplitude-comparison monopulse tracking radar, on the other hand, must have a suitable sum pattern with low sidelobes, as well as a suitable difference

pattern with low sidelobes and a large slope at beam crossover. This section reviews some of the methods available to the radar antenna designer to achieve the radiation patterns necessary to produce the desired radar performance.

As was mentioned previously in Sec. 9.3, the radiation pattern is determined by the distribution of current across the aperture. We have called the distribution of current the aperture illumination. Equation (9.10) gave the (electric field strength) radiation pattern $E(\phi)$ of a linear one-dimensional antenna in one angle-coordinate ϕ as the inverse Fourier transform of the aperture illumination $A(z)$. Similarly the radiation pattern of a two-dimensional planar antenna is given as a two-dimensional inverse Fourier transform of its aperture illumination. We shall first consider the problem of obtaining a desired main-beam pattern with acceptable low sidelobes and then the problem of obtaining shaped radiation patterns.

Obtaining a desired antenna pattern is slightly different for a continuous aperture (such as a reflector) than a phased array that consists of many individual elements. One can sometimes approximate the continuous (reflector) aperture illumination with a discrete (array) aperture illumination, and vice versa. The discussion of antenna patterns in this section is done chiefly for a linear one-dimensional aperture or for rectangular apertures where the illumination is separable; that is, $A(x,z) = A(x)A(z)$. When the illumination for an array is considered, the array is assumed to have uniformly spaced isotropic elements with element spacing generally taken to be half-wavelength. The radiating elements of a real array are not isotropic but have some element pattern $E_e(\theta)$. If the desired array antenna pattern is $E_d(\theta)$, the pattern to be found is $E_d(\theta)/E_e(\theta)$ when using a technique based on the assumption that the elements are isotropic.

Patterns with a Desired Beamwidth and Low Sidelobes Obtaining a pencil-beam or a fan-beam radiation pattern is not usually a synthesis problem. Instead, the patterns obtained from various aperture illuminations are calculated and a suitable one is selected. Table 9.1 in Sec. 9.3 lists a number of antenna patterns for several types of aperture illuminations that can be expressed in analytical form. These were considered in the past since their analytical form permitted the corresponding radiation patterns to be readily calculated. With modern computers, however, using aperture illuminations just because they are readily integrated is no longer necessary. Thus these aperture illuminations are not now generally used. The table is useful in that it illustrates how the maximum gain, beamwidth, and maximum sidelobe level vary with change in shape of the aperture illumination. The more tapered the aperture illumination (that is, the more rapidly its amplitude falls off as a function of the distance from the center of the aperture) the lower will be the sidelobe level, but the lower will be the antenna gain and the wider will be the beamwidth. In practice, other aperture illuminations, such as Taylor illuminations, are usually used rather than those given in Table 9.1.

Taylor Aperture Illumination For a specified maximum sidelobe level, the antenna pattern which has all of its sidelobes equal produces the narrowest beamwidth (where the beamwidth is measured by the angular distance between the first nulls that define the main beam). This is known as a Dolph-Chebyshev pattern since it was first shown by C. L. Dolph, a mathematician working at the U.S. Naval Research Laboratory during World

War II, who based it on equating the Chebyshev polynomial to the polynomial describing the pattern of an array antenna.[129] In spite of its desirable properties, the Dolph-Chebyshev pattern is seldom used for radar antennas since it is unrealizable with arrays containing other than a small number of elements. As the antenna size increases, the currents required at the ends of the aperture become nonmonotonic and large compared with the currents along the rest of the aperture. More of a restriction is the fact that these large currents are required to occupy a very narrow spatial region at the ends of the aperture, too narrow to be obtained with an actual antenna. This inability to achieve the theoretical aperture illumination sets an upper limit to the size of an antenna that can have a Dolph-Chebyshev pattern and therefore sets a lower limit to the width of the main beam that can be achieved.

A realizable approximation to the Dolph-Chebyshev aperture illumination was devised by T. T. Taylor.[130] The Taylor aperture illumination, as it is known, has been widely used for radar antennas. It produces a pattern with equal-amplitude sidelobes of a specified value, but only in the near vicinity of the main beam. Unlike the equal-sidelobe level of the Dolph-Chebyshev pattern, the sidelobes of the theoretical Taylor pattern are of uniform amplitude only within an angular region ϕ defined by

$$|(D/\lambda) \sin \phi| < \bar{n}$$

where $\bar{n}$ = integer, D = antenna dimension, and λ = wavelength. With a linear aperture, the sidelobes decrease as $1/\sin \theta$ with increasing angle θ outside this region (similar to the fall-off of a pattern with a uniform illumination). Hence $\bar{n}$ divides the sidelobes into a uniform region, which straddles the main beam, and a decreasing sidelobe region. The number of equal sidelobes on each side of the main beam is equal to $\bar{n} - 1$. The integer $\bar{n}$ is usually a small number. (Sometimes it is difficult to observe either on a calculated or an actual antenna pattern a region of equal sidelobes in the vicinity of the main beam, yet they are a part of the theoretical Taylor pattern.) The beamwidth of a Taylor pattern will be broader than that of a Dolph-Chebyshev. If the Taylor design sidelobe level is -25 dB, a value of $\bar{n} = 5$ gives a beamwidth almost 8 percent greater than the theoretical Dolph-Chebyshev. With $\bar{n} = 8$, the beamwidth is 5.5 percent greater.

The Taylor pattern is specified by (1) the peak design sidelobe level and (2) the value of $\bar{n}$. The integer $\bar{n}$ can take on only a small range of values for a given design sidelobe level. Taylor states that $\bar{n}$ must be at least 3 for a design sidelobe of -25 dB and at least 6 for a design sidelobe of -40 dB. The larger the value of $\bar{n}$ the sharper will be the beam. On the other hand, it cannot be too large since the same realizability difficulties will arise as with the Dolph-Chebyshev. A suitable criterion for obtaining a realizable Taylor pattern is to choose an illumination that decreases monotonically from the center out to the ends of the aperture and has a zero derivative at the ends of the aperture. The illumination need not be zero amplitude at the ends but can have a finite value (a pedestal). Taylor showed that a distribution with a pedestal, or nonzero value at the edges, is more effective in producing low sidelobes.

A rough guide to the selection of the parameter $\bar{n}$ has been given by Hansen.[131] For example, when the aperture illumination is monotonic, he states that the value of $\bar{n}$ equals 5 for a peak sidelobe of -25 dB, 9 for a peak sidelobe of -35 dB, and 11 for a peak sidelobe of -40 dB. The aperture efficiencies for these three examples are,

respectively, 0.91, 0.82, and 0.77. (Hansen later added that the maximum value of $\bar{n}$ for a monotonic illumination is 17 for a peak sidelobe of -50 dB and 23 for a peak sidelobe of -60 dB.[132]) Thus care must be exercised in the selection of the sidelobe level and the value of $\bar{n}$ for a Taylor pattern. Although the Taylor pattern was developed as a realizable approximation to the Dolph-Chebyshev, in practice it seldom resembles the theoretical equal-sidelobe pattern.

Taylor aperture illuminations can also be obtained for a circular aperture.[133] Figure 9.43 illustrates the nature of the Taylor circular aperture illumination and their corresponding radiation patterns. (This is from an Institute for Defense Analyses report[134] that was not widely circulated, but some of the information appears in the *IEEE AP-S Transactions.*[135]) Shown in Fig. 9.43a are four circular-aperture antenna patterns with the same half-power beamwidth, $70\lambda/D$, but with different values of the Taylor $\bar{n}$ parameter varying from 3 to 15. As $\bar{n}$ increases, the peak sidelobe decreases. From these patterns it would appear that one would want to select a large value of $\bar{n}$. There is a problem with this, however, as can be seen from their corresponding aperture illuminations in Fig. 9.43b. One might be able to realize the required aperture illumination for $\bar{n} = 3$, and might even be able to roughly approximate the illumination for $\bar{n} = 7$. But at the higher values of $\bar{n} = 10$ and 15, it is not likely that one can achieve the necessary aperture illuminations at the edge of the aperture.

There have been several other methods for selecting the aperture illumination for a conventional antenna pattern, as can be found in many of the texts[74,136] on antennas; but the Taylor seems to have been the most popular for radar applications.

Bayliss Illumination[137,138] Difference patterns are used in monopulse tracking radars along with the sum pattern, as was mentioned in Chap. 4. It has been said before in this text that the sum pattern which produces maximum gain is of the form $(\sin u)/u$, and is obtained with a uniform aperture illumination. The symbol $u = \pi(D/\lambda)\sin\theta$, where D = aperture dimension and λ = wavelength. If one forms a difference pattern by starting with a uniform aperture illumination and subtracting one half of the aperture from the other half (that is, $A(x) = -1$ for $-D/2 < x < 0$, and $+1$ for $0 < x < +D/2$), then the difference pattern is proportional to $(1 - \cos u)/u$. The peak sidelobe is 10.6 dB below the peak of the beam, which is relatively high. The optimum illumination for a difference pattern (one that produces maximum slope, or minimum error) is linear-odd over the aperture. That is, the aperture illumination is a straight line that passes through zero at the center of the aperture and has a maximum (say, for example, $+1$) at one edge and a minimum (-1) at the other edge. Its peak sidelobe of -8.3 dB is even worse than that of the uniform-illumination difference pattern. When a single aperture illumination is used to obtain both the sum and difference patterns, an aperture illumination has to be found which represents a suitable compromise for the gain of the sum pattern, the peak sidelobes of both patterns, and the slope of the difference pattern. A better approach, when permitted, is to use an antenna which can support independent sum and difference patterns.

When the difference pattern of a monopulse antenna can be selected independently of the sum pattern, as in a phased array, the criterion is to obtain the maximum angle accuracy commensurate with a desired sidelobe level. The Bayliss illumination has been popular for this purpose. It is based on the same principles as the Taylor illuminations. As with the Taylor, the Bayliss illumination[137] depends on the peak sidelobe level and the

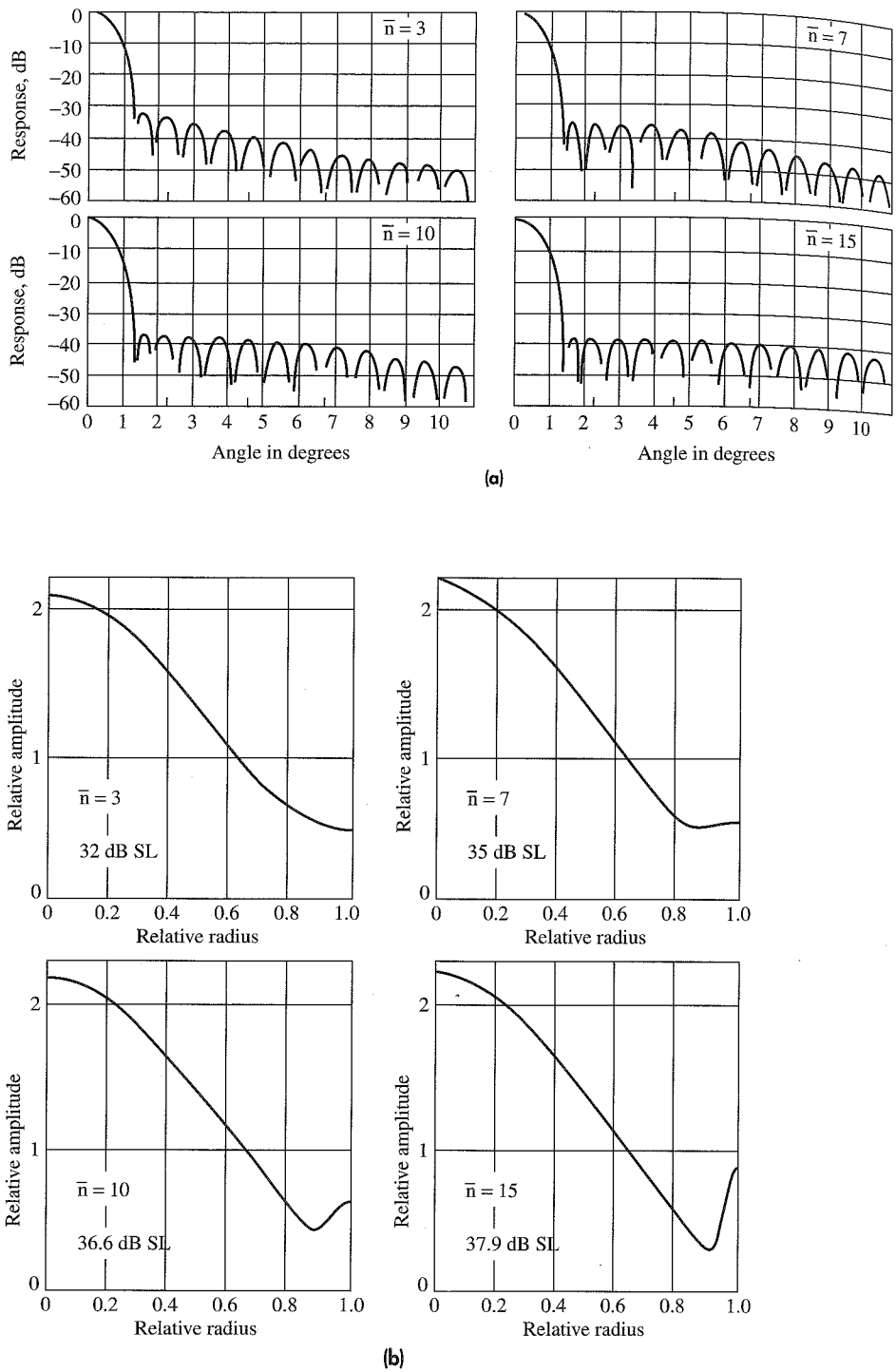

Figure 9.43
(a) Taylor circular aperture radiation patterns each having a beamwidth in degrees of $70\lambda/D$, but with different values of $\bar{n}$. (b) The corresponding aperture illuminations for the patterns of (a). (From W. White[134] Courtesy Institute for Defense Analyses.)

number $(\bar{n}-1)$ of equal sidelobes. Similar restrictions apply on the selection of these two parameters as with the Taylor illuminations.

The Bayliss difference pattern has also been applied to circular apertures, and can be found in any one of several antenna books, including those authored by Mailloux,[74] Hansen,[69] and by Elliott.[136]

Shaped Antenna Patterns In the above, we have considered aperture illuminations for obtaining suitable radiation patterns when a pencil beam or a simple fan beam was required. Sometimes it is necessary to form shaped antenna patterns where the patterns are wide compared to the minimum beamwidth (approximately λ/D radians) that can be obtained with an aperture of dimension D. An important example is the cosecant-squared beam discussed in Sec. 2.11. Other examples are a "square-top" pattern and an elevation pattern with a sharp cutoff at the horizon to minimize surface reflections.[139] In this subsection, we briefly describe two methods for synthesizing such patterns.[128] The methods for finding the aperture illumination to achieve some desired pattern are similar to the methods for finding the filter frequency response function to produce a desired time waveform.

Fourier Synthesis Since the antenna pattern is, in theory, given by the inverse Fourier transform of the aperture illumination [as in Eq. (9.10)], the aperture illumination required to achieve a desired antenna pattern can be found by taking the Fourier transform of the desired pattern, which is

$$A(z) = \frac{1}{\lambda}\int_{-\infty}^{+\infty} E(\phi)\exp\left(-j2\pi\frac{z}{\lambda}\sin\phi\right) d(\sin\phi) \qquad \textbf{[9.47]}$$

where the symbols are the same as described for Eq. (9.10). The limits of the integration actually are finite since $|\sin\phi| \leq 1$. The Fourier transform is such that when the angular region is finite the Fourier transform of $A(z)$ is infinite. Since we have only a finite aperture, the actual radiation pattern will only be approximate, and can be shown to be[140]

$$E_a(\phi) = \frac{D}{\lambda}\int_{-\infty}^{+\infty} E(\xi)\frac{\sin[\pi(D/\lambda)(\sin\phi-\sin\xi)}{\pi(D/\lambda)(\sin\phi-\sin\xi)}\, d(\sin\xi) \qquad \textbf{[9.48]}$$

where $E_a(\phi)$ is the Fourier-integral pattern which approximates the desired pattern $E(\phi)$ when $A(z)$ is restricted to a finite aperture of dimension D. The angle ξ is the variable of integration. The approximation to the antenna pattern obtained on the basis of the Fourier integral for continuous apertures (or the Fourier-series method for discrete array antennas) has the property that the mean-square deviation between the desired pattern $E(\phi)$ and the approximate pattern $E_a(\phi)$ is a minimum. The larger the aperture, the better will be the approximation.

The Fourier series may be used to approximate the pattern of a discrete array, just as the Fourier integral may be used to approximate the pattern of a continuous aperture. The Fourier series method is restricted in practice to arrays with element spacing in the vicinity of a half-wavelength. Spacings larger than a wavelength produce undesired grating lobes. Spacings much smaller than a half-wavelength result in so-called "supergain" radiation patterns (beamwidths much smaller than λ/D radians) that are not realizable since they are a consequence of an overly simplified model of radiation.

Woodward-Levinson Method This is the spatial-domain analogy to the well-known sampling theorem for temporal signals. The classical sampling theorem for time waveforms states: A band-limited signal $s(t)$ with no frequency components greater than B Hz is determined by its amplitude at a series of points spaced $1/2B$ apart in time. The analogous sampling process applied to an antenna is that the radiation pattern $E(\phi)$ from an antenna with a finite aperture D is determined by a series of amplitudes spaced in angle λ/D apart. Figure 9.44a shows a pattern $E(\phi)$ and the sampled points λ/D radians apart. The sampled values $E_s(n\lambda/D)$, which determine the antenna pattern are shown in *b*. An antenna pattern $E_a(\phi)$ can be constructed from the sample values $E_s(n\lambda/D)$ using a pattern of the form $(\sin u)/u$ about each of the sample values, where $u = \pi(D/\lambda) \sin \phi$. The $(\sin u)/u$ pattern is called the composing function. The antenna pattern is given by

$$E_a(\phi) = \sum_{n=-(N-1)/2}^{(N-1)/2} E_s(n\lambda/D) \frac{\sin [\pi(D/\lambda)(\sin \phi - n\lambda/D)]}{\pi(D/\lambda)(\sin \phi - n\lambda/D)} \qquad [9.49]$$

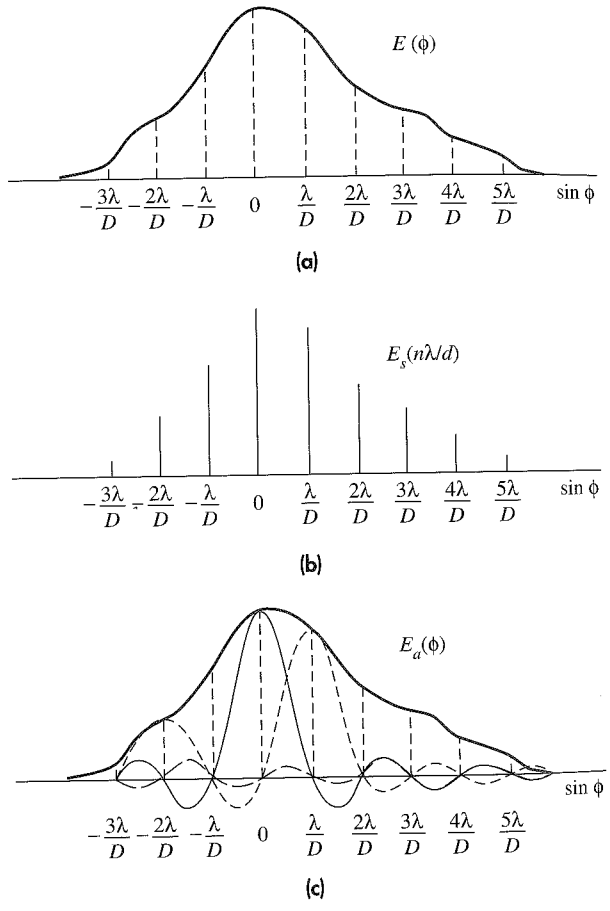

Figure 9.44 (a) Radiation pattern $E(\phi)$ with sampled values λ/D radians apart in angle, where λ = wavelength and D = aperture dimension; (b) sampled values $E_s(n\lambda/D)$, which specify the antenna pattern of (a); (c) reconstructed pattern $E_a(\phi)$ using $(\sin u)/u$ composing function to approximate the desired radiation pattern $E(\phi)$.

where N is the total number of samples, assumed to be odd. Thus the antenna pattern is constructed from a sum of individual (sin u)/u patterns spaced λ/D radians apart, each weighted in amplitude according to the sample values $E_s(n\lambda/D)$, as illustrated in Fig. 9.44c. The aperture illumination corresponding to the radiation pattern of Eq. (9.49) is

$$A(z) = \frac{1}{D} \sum_{n=-(N-1)/2}^{(N-2)/2} E_a(n\lambda/D) \exp(-j2\pi nz/D) \qquad [9.50]$$

The difference between the Woodward-Levinson method and the Fourier-integral synthesis method is that the former gives an antenna pattern which exactly fits the desired pattern at a finite number of points and the latter gives a radiation pattern whose mean-square deviation from the desired pattern is a minimum.

Cosecant-Squared Antenna Pattern This is an antenna with its beam shape proportional to the cosecant-squared of the angle in one plane (usually in elevation) and with a conventional narrow beam in the orthogonal plane. The original reason for using an antenna pattern whose elevation pattern was proportional to $\csc^2 \theta_e$ was to obtain an echo signal that did not vary with range so long as the target flew at a constant altitude and the earth could be assumed to be flat (Sec. 2.11). Many air-surveillance radars have been designed with such an elevation pattern. An even more important reason for using a cosecant-squared elevation pattern is that it allows the radar to provide coverage of targets at high altitudes and shorter ranges much more efficiently than would a conventional fan-beam antenna pattern. In most modern air-surveillance radars, the coverage is modified even further to allow for the curvature of the earth and to provide more radiation at high elevation angles and short range than would be obtained with a cosecant-squared pattern.[141] This additional coverage at high angles is necessary to compensate for the reduction in gain at short ranges caused by the use of sensitivity time control (STC). With STC the receiver gain is reduced at short ranges to attenuate the large clutter echoes that might appear. The cosecant-squared pattern, or a slight variation, has also been important for airborne surface-surveillance radars that must provide relatively uniform coverage of the surface.

The methods available for designing shaped beams, such as the Woodward-Levinson or the Fourier integral, can be applied to obtain the aperture illumination required for a cosecant-squared pattern or its variations. The cosecant-squared pattern may be approximated with a reflector antenna by modifying the shape of the reflecting surface. For example, the upper half of a parabolic reflector can be a parabola that reflects energy from the feed at its focus in a direction parallel to the axis of the parabola axis—as in any other parabolic reflector. The lower half, however, is distorted (tilted slightly forward) to direct a portion of the radiated energy in the upward direction. This is a very simple method, which can be adequate for some applications.

A cosecant-squared antenna pattern may also be obtained by (1) feeding a parabolic surface with two or more horns, (2) a linear array, (3) a parabolic cylinder fed by a linear array or a line source, or (4) a point-source feeding a reflector surface with double curvature. An example is the antenna for the U.S. Air Force's AN/TPN-19 S-band Airport Surveillance Radar which employed an offset paraboloid reflector fed from 12 feedhorns in a vertical line-feed with the uppermost feedhorn located at the focal point of the paraboloid.

Loss in Gain The gain of a cosecant-squared antenna will be less than the gain of a conventional antenna from which it was derived. A very approximate estimate of the reduction in gain for such an antenna is given as

$$\frac{G_{\csc}}{G} = \frac{\theta_0}{\theta_0 + \sin^2 \theta_0 (\cot \theta_0 - \cot \theta_m)} \approx \frac{1}{2 - \theta_0 \cot \theta_m} \quad [9.51]$$

where G = the gain of a rectangular antenna pattern of width θ_0 that radiates uniformly from $\theta = 0$ to $\theta = \theta_0$, and $G_{\csc}$ = gain of the cosecant-squared antenna. The radiation decreases proportional to $\csc^2 \theta$ from θ_0 to θ_m, the maximum angle at which the cosecant-squared pattern is applied. (There is no radiation beyond θ_m.) The approximate expression on the right of Eq. (9.51) applies for small θ_0 and large θ_m. (In addition, the assumption that the beamwidth θ_0 is that of a rectangular-shaped beam can also affect the accuracy of this expression.) For example, if $\theta_0 = 6°$ and $\theta_m = 20°$, the gain of the cosecant-squared antenna is decreased by 2.2 dB compared with a rectangular beam 6° in width. A modified cosecant-squared pattern to allow for the coverage of the earth and to account for the action of the STC will have even lower gain.

Theoretical and Actual Antenna Patterns The discussion of theoretical antenna patterns in this section was based on the Fourier transform relationship between the antenna pattern and the aperture illumination. It has been widely accepted and widely used, but it has limitations. The Fourier transform relationship applies fairly well to the main beam of the antenna and to the region near the main beam. It is less accurate the farther one goes in angle from broadside, and it does not faithfully account for energy radiated near or beyond ±90°.

In a reflector antenna the spillover radiation from the feed, blockage by the feed or feed supports, the radiation diffracted by the reflector, and any leakage through a mesh reflector surface are not accounted for by the Fourier transform. The far-field pattern of any antenna also is affected by nearby structures or other obstructions that can block or diffract the energy radiated by the antenna. The blockage of an antenna by a mast on a ship, for example, might result in a −40 dB peak sidelobe being increased to as high as −15 to −20 dB or greater. Errors in the phase and amplitude across an antenna aperture due to either mechanical or electrical inaccuracies will increase the far-out sidelobe levels over what is predicted from the classical Fourier transform relationship. This is a subject that will be described next.

9.12 EFFECT OF ERRORS ON RADIATION PATTERNS

Experimentally measured patterns of actual antennas often deviate from the theoretically calculated pattern, especially in the region of the far-out sidelobes. Generally, the fault does not lie with the theory, but in the fact that it is not possible to reproduce precisely the necessary aperture illumination specified by synthesis theory. There are small, but ever-present, errors in the fabrication of the antenna and in how it is fed. These contribute unavoidable perturbations in the aperture illumination and result in a pattern different in detail from the one expected.

Errors in the aperture illumination may be either *systematic* or *random.* The former are predictable (usually), but the latter are not and can only be described in statistical terms. Examples of systematic errors include (1) aperture blocking by the feed and its supports in a reflector antenna, (2) mutual coupling among the elements of an array, (3) quantization lobes due to the discrete value of the phase in a digital phase shifter, (4) spurious lobes due to mismatch in a constrained feed for an array, and (5) periodicities introduced in an antenna during the manufacturing process. Random errors include (1) errors in the machining or manufacture of the antenna due to the finite precision of construction techniques, (2) the precision with which a phase shifter can be set to its required phase, (3) errors incurred in adjusting an array, (4) random distortions of the antenna surface, and (5) mechanical and electrical (phase) variations caused by temperature gradients or wind (and in some cases gravity) across the antenna. Although random errors throughout the antenna may be relatively small, their effect on the sidelobes (which are also small) may be relatively large compared to the small levels of the sidelobes. Systematic errors do not differ much from one antenna to another in any particular design constructed by similar methods. Random errors, on the other hand, can differ from one antenna to the next even though they may be of the same design and are constructed similarly. The effect of random errors, therefore, must be discussed in terms of statistical averages found over many similar antennas.

When no specific guidance is available, the antenna designer often assumes that the antenna should radiate a wavefront that differs in phase from the desired wavefront by no more than $\pm\lambda/16$, where λ = wavelength. Because of the two-way propagation from a reflector surface, the mechanical accuracy of a reflector antenna surface must be held within $\pm\lambda/32$. As we shall see, it is possible to obtain more precise criteria for antenna errors, especially when low or ultralow sidelobes are desired. Most of the discussion of errors in this section will concern random errors rather than systematic errors. (If the systematic errors are known, their effect on the antenna pattern can be ascertained by taking the Fourier transform of the actual aperture illumination, including the effects of systematic errors.) The discussion of the effects of random errors in reflectors is separated from the effects of errors in phased arrays.

Random Errors in Reflector Antennas The classical work on the effects of random errors on antenna patterns was due to the pioneering efforts of John Ruze.[142] For small phase errors he showed that the gain G of a circular aperture with mean-square phase-error $\overline{\delta^2}$ is approximately

$$G = G_0 \exp\left[-\overline{\delta^2}\right] = \rho_a(\pi D/\lambda)^2 \exp\left[-(4\pi\epsilon/\lambda)^2\right] \qquad \textbf{[9.52]}$$

where G_0 is the gain of the antenna without errors; the phase error δ, in radians, is with respect to the mean phase plane; ρ_a is the aperture efficiency; D is the diameter of the circular antenna; and ϵ is the rms error of the reflector surface in the same units as the wavelength λ. In the above, the expression $4\pi A_e/\lambda^2$ (discussed early in this chapter) was substituted for the gain G_0. For a given reflector size D, the gain increases as the square of the frequency when the errors are small, until the exponential term becomes significant. Differentiating Eq. (9.52), setting it equal to zero, and solving for wavelength gives the wavelength at which the maximum gain is obtained for an rms error ϵ, which is

$$\lambda_m = 4\pi\epsilon \qquad \textbf{[9.53]}$$

At this wavelength, the gain will be 4.3 dB below what it would have been in the absence of errors. The maximum gain of an antenna due to phase errors is then

$$G_{\max} = \frac{\rho_a}{43}\left(\frac{D}{\epsilon}\right)^2 \qquad [9.54]$$

For wavelengths shorter than λ_m, the gain drops off rapidly with decreasing wavelength (increasing frequency).

The gain of a reflector antenna is limited by the mechanical tolerance to which its surface can be constructed and maintained when in operation. The most precise antennas, under benign, controlled conditions, seem to be limited in practice to a precision of about one part in 20,000. From Eq. (9.54) the diameter of such an antenna is about 1600 wavelengths for maximum gain. Its beamwidth would be 0.04° and it would have a gain of about 68 dB. Special purpose nonradar antennas have been constructed with slightly better tolerances, but these generally have some means for measuring the antenna surface and correcting the surface automatically with feedback control while the antenna is operating. Such antennas are operated in controlled environments that may not be suitable for operational radar applications. In practice, therefore, radar antennas are seldom larger in dimension than approximately 300 wavelengths, which corresponds to a beamwidth of about 0.2°.

The construction tolerance of a reflector antenna is often described by its "peak" error, rather than its rms error. The ratio of the peak to the rms error is found in practice to be about 3:1. This truncation of errors occurs since large errors are usually corrected during manufacture.

With small phase errors the exponential factor in the gain expression of Eq. (9.52) can be approximated by

$$G \approx G_0\left(1 - \overline{\delta^2}\right) \qquad [9.55]$$

If the loss in antenna gain is to be less than 1 dB, this simple expression says that the rms phase variation about the mean phase surface should be less than 0.45 radian, or 26°. This is equivalent to an rms distance error of $\lambda/14$. For shallow reflector antennas, however, the two-way propagation path requires that the rms deviation of the surface from its true value be one half this value, or $\lambda/28$, for a 1 dB reduction of gain.

Ruze showed that under certain conditions the radiation pattern of a reflector antenna which is distorted by a large number of gaussian-shaped "bumps" can be expressed as

$$G(\theta,\phi) = G_0(\theta,\phi)e^{-\overline{\delta^2}} + (2\pi C/\lambda)^2 e^{-\overline{\delta^2}} \sum_{n=1}^{\infty} \frac{\left(\overline{\delta^2}\right)^n}{n!n} e^{-(\pi Cu/\lambda)^2/n} \qquad [9.56a]$$

where C is the correlation distance of the error (the size of the region on the aperture where the errors cannot be considered independent) and u in this case is sin θ. The coordinate system for this equation is the classical coordinates of antenna theory, as was shown in Fig. 9.4, with the antenna lying in the x,y plane. The error current in one region of the antenna (the correlation distance) is assumed independent of error currents in other regions. The size of the correlation distance affects both the magnitude and the direction of the spurious radiation that results from the presence of errors. For small error, when only the first term of the series ($n = 1$) need be considered, Eq. (9.56a) becomes

$$G(\theta,\phi) = G_0(\theta,\phi)e^{-\overline{\delta^2}} + (2\pi C/\lambda)^2\overline{\delta^2}e^{-(\pi Cu/\lambda)^2} \qquad \textbf{[9.56b]}$$

The first term of the above equation [as well as Eq. (9.56a)] represents the no-error pattern reduced by a factor dependent on the mean-square phase error. The second term represents the average value of the sidelobes that are generated by the phase errors (not the average of the peaks, but the *average*). Near the main beam the sidelobes are determined mainly by the inverse Fourier transform of the aperture illumination [Eq. (9.10)], but eventually these drop below the error sidelobes and at angles far from the main beam the errors determine the sidelobe level. When the error sidelobes are dominant, the average sidelobe level is independent of angle.

Other observations about errors in reflector antennas are:

1. Ruze's original analysis[143] showed that the error sidelobes are proportional to the mean-square error and to the square of the correlation distance measured in wavelengths.
2. If errors are unavoidable, they should be kept small in extent; that is, for the same mechanical tolerance, the antenna with the smaller correlation distance will give lower sidelobes than an antenna with a larger correlation distance. An error stretching most of the length of the antenna is likely to have a worse effect than a localized bump or dent of much greater amplitude. Thus small disturbances such as screws and rivets on the reflector surface will have relatively little effect on the antenna radiation pattern.
3. An increase in frequency increases both the phase errors and the correlation distance (measured in wavelengths). Therefore the gain of a constant-area antenna does not increase as rapidly as the square of the frequency when errors are a factor.

Since the radiation pattern in the far-out sidelobe region is more likely to depend on the accuracy with which the antenna is constructed rather than the particular aperture illumination selected, the mechanical engineer, the skilled machinist, and technician are very important in realizing in practice a satisfactory antenna pattern.

Errors in Arrays In the above analysis of reflector-antenna errors, only the effect of the phase errors were considered. In an array antenna, however, other factors may enter to cause degradation of the radiation pattern. These include errors in the amplitude and phase of the current at each element of the array, missing or inoperative elements, rotation or translation of the element from its correct position, errors in the phase provided by the phase shifter, effects of a quantized phase shift, and variations in the individual element patterns because of mutual coupling. These errors can result in a decrease in antenna gain, increase in sidelobe level, generation of spurious sidelobes, and a shift in the location of the main beam.

It is not possible to predict the pattern of an antenna unless the actual errors experienced by that particular antenna are known. The average, or expected, value of a radiation pattern of an *ensemble* of antennas of the same type can be computed based on the rms values of the random errors. The statistical description of the radiation pattern cannot be applied to any particular antenna of the ensemble, but applies to the entire collection of similar antennas whose errors are described by the same statistics. Usually the average pattern is computed, but other statistical descriptions can be obtained if desired.

Average Radiation Pattern Due to Errors The ensemble-average radiation intensity pattern of a uniform array of M by N isotropic elements arranged on a rectangular grid with equal spacing between elements is given by[144]

$$\overline{|f(\theta,\phi)|^2} = P_e^2 e^{-\overline{\delta^2}} |f_0(\theta,\phi)|^2 + \left[\left(1 + \overline{\Delta^2}\right)P_e - P_e^2 e^{-\overline{\delta^2}}\right] \sum_{m=1}^{M} \sum_{n=1}^{N} i_{mn}^2 \qquad [9.57]$$

where

P_e = probability of an element being operative (or the fraction of elements that remain operating)

δ = phase error, radians (described by a gaussian probability density function)

$|f_0(\theta,\phi)|^2$ = no-error pattern

Δ = relative amplitude error (as a fraction of i_{mn})

i_{mn} = no-error current at the mnth element

Similar to the error pattern of a reflector antenna discussed earlier [Eq. (9.56)], the first term is the no-error pattern reduced by a factor which depends on the phase errors and the fraction of operative elements. The second term represents a statistical average sidelobe level due to the phase and amplitude errors and the fraction of elements that are operating. It also depends on the aperture illumination as given by the currents i_{mn}. This second term is independent of angle, and can be thought of as a statistical omnidirectional pattern which we shall call the error sidelobes. This second term causes the far-out sidelobes of the radiation pattern to be higher in the presence of errors as compared to the no-error pattern; but the shape of the main beam and the near-in sidelobes are not significantly affected by these errors, other then by the exponential term which is usually small. [Sometimes the rms error in amplitude is expressed in dB. When in dB it is not the mean square value which is in dB, but the value of $[1 - (\overline{\Delta^2})^{1/2}]^2$. For example, an rms amplitude error of 0.1 is equivalent to an error of 0.9 dB.]

If $P_e = 1$ (no missing elements) and if the errors are small, the normalized radiation intensity obtained by dividing Eq. (9.57) by the maximum radiation intensity at the center of the main beam, $|f_0(0,0)|^2$, is

$$\overline{|f(\theta,\phi)|^2} \approx |f_{0n}(\theta,\phi)|^2 + \left(\overline{\Delta^2} + \overline{\delta^2}\right) \frac{\sum_m \sum_n i_{mn}^2}{\left(\sum_m \sum_n i_{mn}\right)^2} \qquad [9.58]$$

The second term indicates that the larger the number of elements, the smaller will be the error-sidelobe level. The main-beam intensity, being coherent, increases as the square of the number of elements, while the error sidelobes, being noncoherent, increase only directly with the number of elements. The gain of a broadside array of isotropic elements is

$$G_0 = \frac{\left(\sum_m \sum_n i_{mn}\right)^2}{\sum_m \sum_n i_{mn}^2} \qquad [9.59]$$

When i_{mn} = constant, $G_0 = MN$, which states that the gain of an array of isotropic elements with uniform illumination is equal to the total number of elements. The normalized pattern of Eq. (9.58) then can be expressed as

$$\overline{|f_n(\theta,\phi)|^2} \approx |f_{0n}(\theta,\phi)|^2 + \frac{\overline{\Delta^2} + \overline{\delta^2}}{G_0} \qquad [9.60]$$

The average error-sidelobes is given by the second term. The greater the antenna gain, the less will be the effect of errors on the sidelobes. [Sometimes the denominator of the second term of the above equation is given as πG_0, where π is the gain of the so-called "ideal" element factor.]

The component parts of the normalized ensemble-average pattern as given by Eq. (9.60) are sketched in Fig. 9.45. The ordinate is in dB. The horizontal line shown G_0 (in dB) below the peak of the main beam is the radiation that would be produced by an isotropic antenna with the same power output as the directive antenna. The horizontal line shown $G_0/(\overline{\Delta^2} + \overline{\delta^2})$ (in dB) below the peak is the average value of the error sidelobes, which is independent of angle. The error sidelobes have little effect near the main beam, but they are the dominant factor affecting the far-out portion of the radiation pattern. The measured sidelobes of any actual array antenna, of course, would not be constant as shown in this figure. Instead they would have the usual shape expected of sidelobe radiation, but their ensemble-average value would be constant with angle.

Gain Reduction By substituting the radiation intensity of Eq. (9.57) into the definition of gain (or directivity) of Eq. (9.3), it can be shown that

$$G/G_0 = \frac{P_e}{(1 + \overline{\Delta^2}) \exp(\overline{\delta^2})} \approx \frac{P_e}{1 + \overline{\Delta^2} + \overline{\delta^2}} \qquad [9.61]$$

This states that the relative reduction in gain is independent of the number of elements and depends only on the fraction of elements that are operative and the mean-square value

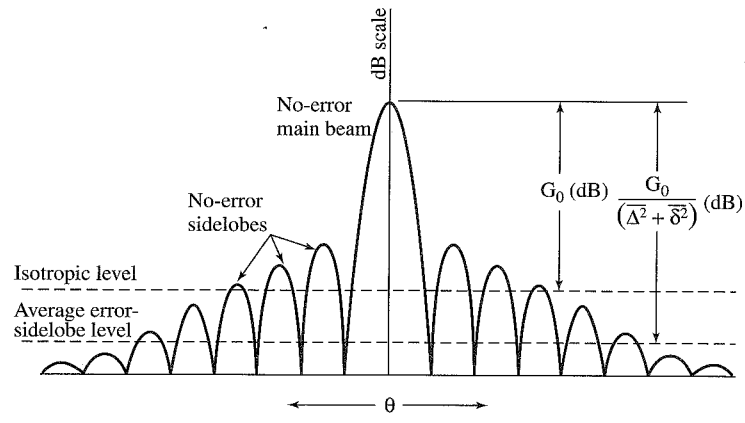

Figure 9.45 Qualitative sketch of the no-error radiation pattern and the average error-sidelobe level, as indicated by Eq. (9.60).

of the relative-amplitude and phase errors. When $P_e = 1$ and $\Delta = 0$, this expression, which applies for small phase errors, is similar to that of Eq. (9.55) for the reflector antenna.

Pointing Error Random phase and amplitude errors in the aperture illumination can give rise to an error in the pointing of the main beam.[145,146] If the aperture illumination is uniform across an M by M square array, the statistical rms beam pointing error in radians is

$$\delta\theta_0 = \frac{\sqrt{3}\sigma}{2\pi(d/\lambda)M^2} \qquad [9.62]$$

where σ = rms value of the normalized error current assuming Rayleigh distributed errors, d = element spacing, λ = wavelength, and M = number of elements along one dimension of a square array. According to this expression, the effect of errors on the beam-pointing accuracy generally is small.

Error-Sidelobe Statistics In the above we have considered the average value of the error sidelobes. The radar system engineer, however, is often more concerned about the peak sidelobe level rather than the average. The actual peak value cannot be predicted, but it can be described on a statistical basis. Usually one wants to determine (or specify) the probability that a sidelobe will not exceed a particular desired value. The approach outlined here is taken from James K. Hsiao.[147,148] He described three methods for finding the effect of errors on the peak sidelobe. These assume that the statistics of the radiation pattern with errors can be described by the Rice probability density function, something we have used in Sec. 2.5 when discussing the statistical detection of a signal in noise. Although all three methods are similar, we shall consider here only the second that he describes in his paper.

From the Rice cumulative probability of sidelobe level, Hsiao obtains a set of curves, shown in Fig. 9.46, for various values of the cumulative probability P that range from 0.90 to 0.98. This figure relates the peak sidelobe level (abscissa) and the amplitude and phase errors of the array (ordinate). The abscissa is actually the ratio of the design sidelobe level to the desired sidelobe level in dB. (The design sidelobe level is always less

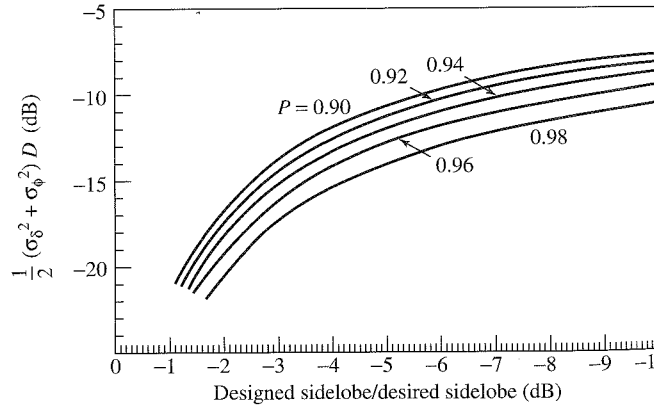

Figure 9.46 Curves for determining the rms amplitude error σ_δ and the rms phase error σ_ϕ as a function of the ratio of the *design* sidelobe level to the *desired* sidelobe level (abscissa) for various values of the cumulative probability P that the sidelobes will be less than the design sidelobe level.

The parameter $D = \sum i_{nm}^2/$(desired sidelobe level), where i_{mn} is the amplitude of the current at the mnth element.

(Due to James Hsiao, taken from refs. 147 and 148.)

than the desired sidelobe level.) The ordinate in Fig. 9.46 includes a factor D, as well as the phase and amplitude rms errors. Hsiao defines D as

$$D = \sum_n \sum_m i_{nm}^2/(\text{desired sidelobe level}) \qquad \textbf{[9.63a]}$$

where i_{nm} is the amplitude of the current at the nmth element, as determined by the desired aperture illumination. It is assumed that the illumination function i_{nm} is normalized such that $\sum_n \sum_m i_{nm} = 1$. Following Hsiao, we consider the example of a 100-element linear array designed with a Chebyshev aperture illumination to provide equal sidelobes -40 dB below the maximum value of the main beam. (As said before in this chapter, the Chebyshev pattern with such low sidelobes is likely to be unrealizable. It is used here to illustrate the procedure.) The design sidelobe level is then -40 dB. In this example we wish to keep the peak sidelobe of the array to a value no greater than -37 dB (the desired sidelobe) with a probability of 0.90. The ratio of the design sidelobe level to the desired sidelobe level (the abscissa of Fig. 9.46) is -3 dB. With an abscissa of -3 dB and a probability $P = 0.90$, we find the ordinate of Fig. 9. 46 to be -14 dB. The aperture illumination for the 40 dB sidelobe Chebyshev pattern results in $\sum_n i_n^2 = -19$ dB. The value of D is then $-19 + 37$ dB $= 18$ dB and the sum of the mean square amplitude and phase errors is -29 dB. If the phase and relative amplitude errors are made equal, then the rms phase tolerance is 1.44° and the rms (relative) amplitude tolerance is 0.025, or 0.22 dB. Such tolerances are quite demanding and not easy to achieve. A plot is shown in Fig. 9.47 of the no-error -40 dB Chebyshev pattern along with a pattern where there are errors that give sidelobes with a cumulative probability of 90 percent that they will not exceed -37 dB.

If the design sidelobe level were -45 dB instead of -40 dB, and the desired sidelobe level were still -37 dB, one would find that the tolerance would be 2.6° for phase and 0.045 for amplitude. These are also quite demanding, but not as much as with the higher value of design sidelobe.

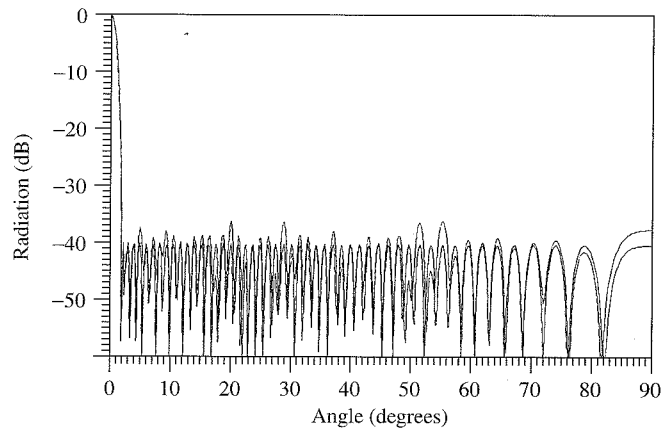

Figure 9.47 The design no-error Chebyshev pattern for a 100-element linear array with a -40 dB design sidelobe is shown along with the resulting desired pattern due to errors when $P = 0.9$, desired sidelobe level $= -37$ dB, rms amplitude error $\sigma_\delta = 0.025$, and rms phase error $\sigma_\phi = 1.44°$.
[(Due to James Hsiao, taken from refs. 147 and 148.)

These are relatively tight tolerances. They result from not only requiring a low sidelobe level, but also because there are only a relatively few antenna elements (100 in this example of a linear array). The tolerances for a large planar array would be easier to achieve. As an illustration, Hsiao shows that a planar array with a directive gain of 40 dB, desired sidelobe of −40 dB, design sidelobe of −43 dB, and a probability of 0.9 that the sidelobes will not exceed the desired value results in an rms phase tolerance of 6.6° and an rms amplitude tolerance of 0.12. If the design sidelobe were reduced to −48 dB, the rms phase tolerance becomes 12.3° and the rms amplitude becomes 0.21.

When using a lower design sidelobe to ease the error tolerances, a price has to be paid. The lower design sidelobes result in an increase in the antenna half-power beamwidth and an even larger increase in the width between the first nulls of the antenna pattern. Alternatively, a larger aperture is required if the beamwidth is to remain constant.

A slightly different approach to determining the error tolerances required for keeping the sidelobes below a specified value was given by Cheston and Frank.[149]

Effect of Digital Phase Shifter Quantization[150,151] Phase shifters, whether analog or digital, will usually have a phase shift that is not exactly what one thinks has been set. There will always be some error, and its effects on the antenna pattern can be determined by the equations given in the above subsection. The deliberate quantization of phase that results with the use of digital phase shifters, however, introduces a different type of "error" in the desired aperture illumination, and produces pattern degradation similar to that produced by a random error.

Reduction in Gain The gain of an array antenna due to phase errors can be obtained from Eq. (9.61) by setting $P_e = 1$, $\Delta^2 = 0$, and assuming $\overline{\delta^2}$ is small, which results in

$$G = G_0\left(1 - \overline{\delta^2}\right) = G_0\left(1 - \frac{\pi^2}{3 \times 2^{2B}}\right) \qquad \text{[9.63b]}$$

The right-hand portion is obtained by assuming that the phase error of a digital phase shifter of B bits is described by a uniform probability density function (Sec. 2.4) that extends over an interval $\pm\pi/2^B$. From Eq. (9.63b) a three-bit phase shifter causes a reduction in gain of 0.23 dB and a four-bit phase shifter has a gain reduction of 0.06 dB. Thus, on the basis of the loss in antenna gain caused by digital phase quantization, a three- or four-bit phase shifter should be satisfactory for most purposes.

Increase in Sidelobes In addition to a reduction in main-beam gain, the quantization of the phase in digital phase shifters can result in an increase in the rms sidelobe level. With the assumptions that (1) the energy lost by the reduction in main-beam gain shows up as an increase in the rms sidelobe level, (2) the element gain is the same for the main beam and the sidelobes (within the region of space scanned by the array, (3) an allowance of one dB for the reduction in gain due to the aperture illumination, and (4) one dB for scanning degradation; then the sidelobe level due to phase quantization is

$$\text{rms sidelobe level} \approx \frac{5}{2^{2B}N} \qquad \text{[9.64]}$$

where N = total number of elements in the array. If an array has 4000 elements, a three-bit phase shifter would give rms sidelobes of 47 dB below the main beam, and a four-bit phase shifter gives −53 dB sidelobes. Thus three or four bits should be sufficient for most large arrays, except when very low sidelobes are desired.

Peak Quantization Sidelobe The above assumed a random distribution of phase error across the aperture for the purpose of computing the rms sidelobe level. The actual phase distribution with digital phase shifters, however, is likely to be periodic which gives rise to spurious quantization lobes, similar to grating lobes but with smaller amplitude. Peak sidelobes sometimes are of more concern to the radar system engineer than are the rms sidelobes. The peak quantization lobe relative to the main beam when the phase error has a triangular repetitive distribution is

$$\text{peak quantization lobe} = 1/2^{2B} \qquad [9.65]$$

This applies when the main beam points close to broadside and there are many radiator elements within the period of quantized phase error. The position θ_q of the quantization lobe in this case is

$$\sin \theta_q \approx (1 - 2^B)\, \theta_0 \qquad [9.66]$$

where θ_0 is the angle to which the main beam is steered.

Equation (9.65) is an optimistic estimate for the peak lobe. The greatest phase quantization lobe is said to occur when the element spacing is exactly one half the phase quantization period or an exact multiple thereof. With an element spacing of one-half wavelength, the quantization lobe will appear at $\sin \theta_q \approx \sin \theta_0 - 1$, and will have a value of

$$\text{peak quantization lobe} \approx \frac{\pi^2}{4} \frac{1}{2^{2B}} \frac{\cos \theta_q}{\cos \theta_0} \qquad [9.67]$$

The peak sidelobes due to the phase quantization of the digital phase shifter can be significant. Attempts should be made to reduce them if their presence is objectionable. One method for reducing the peak sidelobe is to randomize the phase quantization. A constant phase shift can be inserted in the path to each element, with a value that differs from element to element by amounts that are unrelated to the bit size. The added phase shift is then subtracted in the phase command sent to the phase shifter. (With a space-fed array, such as the lens array or the reflectarray, decorrelation is inherent in the array geometry.)

Beam-Pointing Error The maximum pointing error $\Delta\theta_0$ due to quantization, according to C. J. Miller[151] is

$$\Delta\theta_0 = \theta_B \frac{\pi}{4} \frac{1}{2^B} \qquad [9.68]$$

where θ_B is the beamwidth. A four-bit phase shifter, for example, allows an angle error of $\Delta\theta_0/\theta_B = 0.05$. Small steering increments are possible with quantized phase shifters. A linear array of 100 elements, for instance, can be steered in increments of about 0.01 beamwidth with three-bit phase shifters.[149]

9.13 LOW-SIDELOBE ANTENNAS

The highest sidelobe of an antenna pattern is usually, but not always, the first sidelobe adjacent to the main beam. A conventional reflector antenna might have a maximum sidelobe of about 23 to 28 dB below the peak of the main beam. Sidelobes much lower than −35 to −40 dB with conventional reflector antennas are difficult to obtain by normal methods. There are some radar applications, however, that require much lower sidelobes. An example is the airborne high-prf pulse doppler radar, such as AWACS that was discussed in Sec. 3.9. A high-prf radar sees many multiple-time-around clutter echoes that enter the radar receiver through the antenna sidelobes. Such sidelobe clutter can be large enough to limit the performance of an airborne doppler radar. It was the need for a low-sidelobe antenna for AWACS that led Westinghouse (now Northrop Grumman) radar antenna engineers to be the first to successfully demonstrate in the mid-1960s sidelobes almost three orders of magnitude lower than was the practice with conventional antennas. A low-sidelobe antenna is also helpful in combating hostile noise jamming that enters the receiver via the sidelobes. It also aids in combating antiradiation missiles (ARM) that home on the radar's radiation, and in making more difficult the task of a hostile intercept receiver. Low sidelobes, however, come with a price. Such antennas need to be more precise, are more complex, their beamwidth is widened, and they have to operate in a clear environment.

Table 9.2 lists typical performance of low-sidelobe antennas as given by Evans and Schrank.[152] (In their paper, the authors state that "it is probably possible to do 5 dB better with tuning of phase and amplitude during the test." I have taken the liberty to add this 5 dB to the numbers that originally appeared in their paper.) The phased arrays in this table are not scanned in angle.

There has been no generally accepted definition of what are low sidelobes. Schrank[153] proposed that low sidelobes be defined as from −30 to −40 dB and that ultralow sidelobes be below −40 dB. These values probably should be lower. One might consider antennas with sidelobes of the order of −40 dB to be low, and antennas with −50 dB or lower to be ultralow sidelobe antennas.

The peak sidelobe is not always a good measure of the difficulty involved in obtaining low sidelobe levels. The larger the antenna gain, the easier it is (relatively) to obtain low sidelobes. A better measure of the difficulty for an antenna engineer to achieve low sidelobes is how far the peak sidelobe level is below the isotropic value, which we take

Table 9.2 Performance of Low-Sidelobe Antennas

Type of Antenna	Peak Sidelobe	RMS Sidelobe	Bandwidth
Slotted waveguide	−50 dB	−60 dB	10%
Corporate-fed array	−45 dB	−55 dB	60%
Reflector	−45 dB	−55 dB	60%

| Adapted from Evans and Schrank, Ref. No. 152, *Microwave Journal.*

here to be the level which is $1/G_0$ down from the peak, where G_0 = antenna gain. Low or ultralow sidelobe antennas might have peak sidelobes from 10 to 20 dB below isotropic. Thus if an antenna has a gain of 30 dB, its sidelobes might be made as low as -40 to -50 dB. From the second term of Eq. (9.60) it can be seen that the mean square error $\overline{\Delta^2} + \overline{\delta^2}$ must be small compared to the desired peak sidelobe level times the antenna gain G_0. Thus the larger the gain the larger can be the errors for a given sidelobe level relative to the main beam.

To achieve low sidelobes, an antenna must (1) employ an aperture illumination that will theoretically provide the required sidelobe level and be practical to implement, (2) be constructed and maintained with high precision, and (3) have no blocking of the aperture by nearby structures. Both array antennas and reflector antennas can be made to have low sidelobes, but it is easier to do with an array than with a reflector.

Low-Sidelobe Aperture Illuminations The Taylor aperture illumination, discussed in Sec. 9.11, has often been used for obtaining low sidelobe antenna patterns. It will be recalled that the Taylor illumination is characterized by a parameter $\bar{n}$, such that the first $\bar{n} - 1$ sidelobes closest to the main beam are equal. Beyond the $\bar{n}$th sidelobe, the sidelobe level decreases. For a circular aperture, the Taylor far-out sidelobes fall off as $(\sin \theta)^{-3/2}$. As was mentioned in Sec. 9.11, the parameter $\bar{n}$ must be chosen so that the aperture illumination is realizable.

Figure 9.48, from a report by Warren White,[154] is an example of how the normalized beamwidth β of a Taylor pattern varies with the peak sidelobe level and the parameter $\bar{n}$

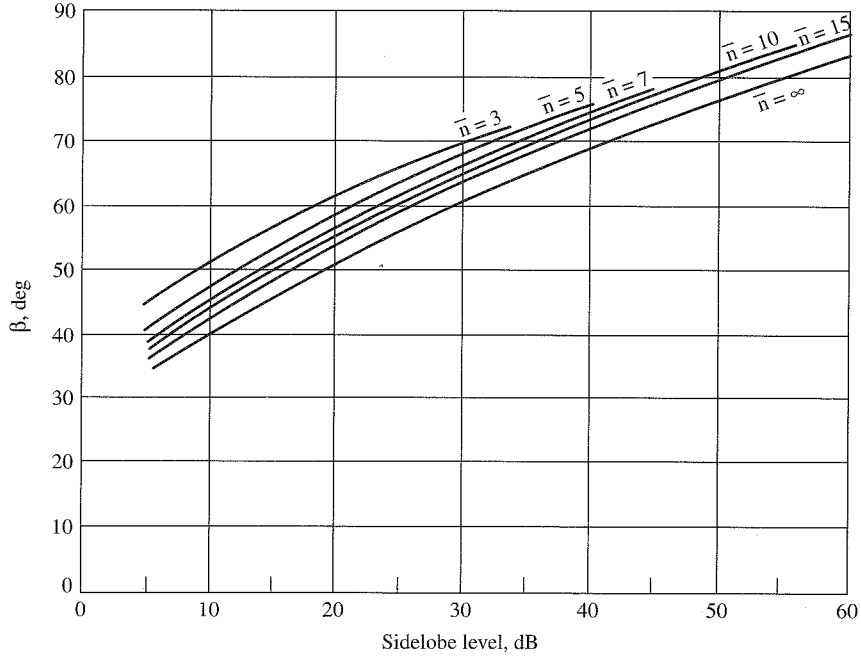

Figure 9.48 Normalized beamwidth β versus the sidelobe level and the value of $\bar{n}$, where the half-power beamwidth $\theta_B = \beta\lambda/D$. (From White.[154] Courtesy Institute for Defense Analyses.)

for a continuous circular aperture. The half-power beamwidth is $\theta_B = \beta\,(\lambda/D)$. The curve for $\bar{n} = \infty$ applies for the Chebyshev illumination, which is not realizable. Comparing a pattern with $\bar{n} = 5$ and a -25 dB sidelobe level with a pattern having $\bar{n} = 15$ and a -60 dB sidelobe level, the half-power beamwidth increases by a factor of almost 1.4 when lowering the sidelobes level from -25 dB to the level of -60 dB. The null width of the Taylor distribution increases even faster; over the same range of sidelobe levels, the null width increases by a factor of about 1.9. Thus one of the costs of low sidelobes is that the beamwidth increases as the sidelobe level is decreased. The gain also decreases with decreasing sidelobes. If the same beamwidth is to be maintained as the sidelobes are lowered, the antenna aperture must be increased in size.

Previously, Fig. 9.43 in Sec. 9.11 illustrated that the Taylor aperture illuminations are not always realizable because of the difficulty in obtaining the required shape of the currents at the edges of the aperture. The value of $\bar{n}$ must be chosen appropriately in order to achieve a pattern that is practical. A suitable criterion for selecting a realizable Taylor illumination is that it have a monotonically decreasing illumination, the slope at the edge of the aperture should be zero, and it should not turn positive. Ludwig[155] states that for a circular aperture the value of $\bar{n}$ should be no greater than 7 for -40-dB sidelobes, 11 for -50-dB sidelobes, and 16 for -60-dB sidelobes. The value of $\bar{n}$ should also not be too small. It should be at least 3 for -30-dB sidelobes and 4 for -40-dB sidelobes.[156] [Note these values of $\bar{n}$ for a circular Taylor aperture-illumination differ slightly from those given in Sec. 9.11 for a line-source Taylor illumination.]

Achieving the Low-Sidelobe Pattern In the above we indicated it is necessary to obtain an aperture illumination that can be implemented. In addition, the desired illumination must be maintained. The phase and amplitude tolerance on the aperture illumination must be determined, as in the previous section. As was indicated with the discussion of Fig. 9.47 in the previous section, the required error tolerances can be quite demanding. Schrank[153] points out that for a low-sidelobe array antenna, one must control the systematic errors and the mutual coupling in addition to the random errors. Mutual coupling can be compensated by appropriate computer-aided design. Systematic errors must be controlled by careful fabrication and serious attention to tolerances. Systematic errors generally affect the near-in sidelobes and can generate spurious lobes. Random errors, as we have seen, affect the far-out sidelobes. According to Schrank, it is the random errors that ultimately limit the ability to obtain low sidelobes.

Blocking or Masking of the Aperture The low-sidelobe antenna must be located in a clear environment in order to maintain the low sidelobes. Any obstruction in front of the antenna can alter the radiation pattern and result in an increase in sidelobes. Obstructions can include nearby buildings and trees. The need to operate in a clear environment is why the AWACS antenna (Fig. 3.45b) is located well above the fuselage of the aircraft that carries it. It is difficult to avoid the blockage caused by the tail, but the antenna is high enough to minimize the effects of the aircraft structure and the engines. The antenna is mounted in a rotodome that rotates in synchronism with the antenna, so that the antenna always sees the same radome environment.

A classic example of the effect of aperture blocking on antenna sidelobes is that caused by the masts and other superstructure on a ship.[157] No matter how low the sidelobes of an antenna might be in free space, when a mast is situated so as to block a portion of its radiation, the sidelobes can increase considerably. Blockage of a shipboard radar antenna can be avoided by mounting the antenna at the top of the mast. This is something that can be accommodated during the design of a new ship, but it is difficult to mount a heavy antenna at the top of a mast on an old ship which very likely has used up all of its margin for topside weight and moment.

There are two factors that cause the sidelobes of an antenna to increase when blockage occurs. One is that a part of the beam has been masked, which is equivalent to having a part of the aperture illumination excised. In other words the effective aperture illumination has been modified. The other effect is that the obstruction can scatter the radiated energy in new directions, so that target echoes or clutter echoes might appear as false targets in an erroneous direction. The radar thinks the scattered echo is in the direction at which the main beam points at the time, when the energy is from some other direction because it was scattered by the mast. Shaping of the mast or covering it with absorbing material can reduce the scattering that produces false echoes, but it does not reduce the distortion of the pattern caused by excising part of the radiated energy.

It is usually difficult to avoid degradation to the sidelobes and the main beam by blockage of a mast. Masts are often of steel, but masts made of dielectric will also cause similar blockage effects. The mast is often modeled as a cylinder for purposes of calculating its scattering effects, but actual shipboard masts are much more complex than simple cylinders. One method to avoid aperture blocking is to employ a four-face phased array antenna distributed around the ship so that none of its faces look into a mast. Even this is not perfect, however, since the ship's superstructure or deck might intercept part of the beam when the ship encounters large pitch or roll angles because of sea conditions.[158,159]

Effect of a Radome on Sidelobes The phase and amplitude of a signal can change when propagating through a radome, and can limit how low the antenna sidelobes can be. The periodicity of a metal space-frame geodesic dome precludes its use with very low sidelobe antennas. A air-inflated "bag" of thin dielectric material will allow lower sidelobes than can the space-frame geodesic dome. An airborne radar antenna located in the nose of an aircraft behind an aerodynamically shaped radome also can inhibit achieving low sidelobes. The radar designer does not have much control over this type of airborne radome since its first priority is to maintain structural integrity and conform to aerodynamical requirements. In addition, the radome must be able to withstand bird strikes, rain erosion, and lightning strikes. For lighting protection the antenna might be enclosed in a cage of metal rods. A radome can cause phase and amplitude changes in the radiated wave that result in loss and distortion. Energy that is scattered by the inner surface of the radome can result in a sidelobe that is known as the *radome flash.* In some cases[160] the peak value of the radome flash was found to be of the order of 40 dB below the main beam. Thus it can be more difficult to achieve low sidelobes with an antenna inside a radome. The effect the radome can have on an antenna pattern must be determined and corrected if low sidelobes are to be achieved. It should be kept in mind that the effects of a radome mounted

above the fuselage can be successfully handled, as it was with the impressive low-sidelobe antenna and radome employed on AWACS.

No-Sidelobe Array In the quest for a low-sidelobe antenna, it might be asked what would an antenna be like if there were no sidelobes whatsoever. Such an antenna pattern can be produced by a linear array with half-wave spacing and with element currents given by the coefficients of the binomial expansion. This no-sidelobe pattern is attributed to J. S. Stone who obtained patents for it in the late 1920s. Leon Ricardi[161] gives its beamwidth as $0.975/(N-1)^{1/2}$ rad and its directive gain as $1.77N^{1/2}$, where N is the number of elements. Although this antenna has no sidelobes it has a very fat main beam (the radiated energy has to go somewhere), the ratio of the current at the center of the array aperture to the current at the edge element is quite large for values of N that may be of interest, and its gain increases only as the square root of the aperture size. The currents at the elements of a nine-element binominal array, for example, are proportional to 1, 8, 28, 56, 70, 56, 28, 8, 1. The ratio of the current at the center to that at the edge is 70 to 1. For many reasons, the antenna with absolutely no sidelobes produces poor patterns and is not something that a radar engineer should aspire to use as a design goal.

It has been said that the gaussian antenna radiation pattern can be used to approximate the pattern of a no-sidelobe binomial illumination when the number of elements in the binomial array is greater than five and if the standard deviation of the gaussian pattern is made equal to $(L\lambda/8)^{1/2}$, where L is the antenna dimension.[162]

Examples of Low-Sidelobe Antennas The first low-sidelobe antenna was for the AN/APY-1 S-band radar that was the basis for the AWACS (E3A) airborne warning and control system.[152] As was mentioned, an antenna with exceptionally low sidelobes was needed for such an application in order to limit the large clutter echoes that might enter the receiver via the antenna sidelobes. The antenna, Fig. 9.49, consisted of 30 slotted waveguides, called *sticks*. These were fed from one end (series fed). The antenna was 24 ft (7.3 m) in width and 5 ft (1.5 m) in height, and was enclosed in a rotodome that was mechanically rotated in azimuth at 6 rpm. It is a rugged antenna, as is needed to maintain the mechanical tolerances.

Slotted Array The series-fed slotted array, of which the AWACS end-fed array was an example, is well suited as a low-sidelobe antenna since the slots provide a convenient means for achieving the necessary aperture illumination. The slots can be milled with precision computer-controlled machines, the structure can be made mechanically sturdy, and there is no blockage of the aperture as would be the case with a conventional reflector antenna. To achieve the desired low sidelobes, the mutual coupling between the slots in each stick and the coupling between sticks must be properly taken into account. The slots may be in the broadwall or the sidewall of the waveguide slots. (The AWACS antenna used sidewall slots.) Sidewall slots must be tilted at an angle in order to achieve coupling of energy from the waveguide. The tilt of the slots causes cross-polarized radiation, which must be surpressed in some system applications. Periodic errors due to the introduction of the necessary phase reversals in adjacent slot radiators (in order to provide the necessary phase in a traveling-wave waveguide array) must also be surpressed.

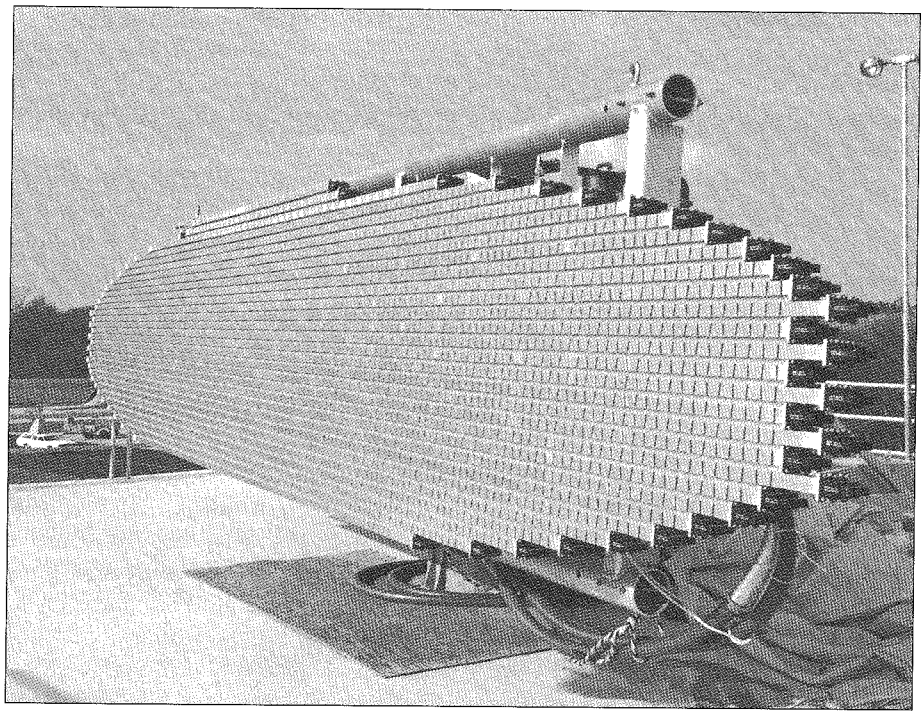

Figure 9.49 Slotted-array low-sidelobe antenna for the AWACS, AN/APY-1 radar. (Courtesy Northrop Grumman Corp.)

The end-fed, or any series-fed, slotted array is usually not of wide bandwidth since the direction of the radiated beam will squint (change angle) when the frequency is changed. With a narrowband signal this is not a serious problem since the direction the beam points relative to the antenna is known and can be compensated accordingly when extracting the angle measurement. When a wideband signal, however, is radiated by such an antenna, the beam will broaden, or smear. If a wide signal bandwidth is required in a low-sidelobe antenna, the corporate-fed array can be used.

Corporate-Fed Planar Array Operation over a wide bandwidth can be obtained with a corporate-fed array if equal path lengths are used connecting the antenna input to each element of the array. With equal path-lengths, changes in frequency do not cause changes in phase between the radiating elements, as they do in a series-fed array. The feed network of the corporate-fed array is not as simple as that of a series-fed array. There are couplers and branch lines in each path to the radiating elements, and they must be exceptionally precise in order to achieve the precision aperture illuminations required for low sidelobes. The use of dielectrics in such a feed system should be kept to a minimum since they can produce a phase change with a change in frequency. Strip transmission lines, with the strips supported by a minimum of dielectric, can be employed if their power handling is satisfactory. The precise tolerances and complexity of the corporate-fed array

can result in greater cost and complexity than the series-fed slotted array, but this is the price that has to be paid to have low sidelobes with wide bandwidth. Because of its greater complexity, Table 9.2 indicates that the corporate-fed array is more likely to have higher sidelobes than the slotted array.

Electronically Steered Low-Sidelobe Arrays It is more difficult to achieve low sidelobes when the array must be electronically steered. (The wide vertical beamwidth of the AWACS antenna can be steered electronically over a limited range of elevation angles, but this is different from an antenna that scans over wide angles in both azimuth and elevation.) Phase shifters introduce error and if they are digital, they must contain a large number of bits in order to suppress spurious sidelobes. The phase shifters might have to have six to eight bits rather than the three to four bits acceptable for antennas with conventional sidelobe levels. The effects of mutual coupling are more difficult to correct since mutual coupling will change when the antenna beam is electronically scanned. Arrays made up of subarrays also can produce periodic errors that can result in high sidelobes. Subarrays, especially large ones, can be a problem when low sidelobes are desired.

The additional cost of low-sidelobe phased arrays has been examined by W. Patton.[163] Based on analyzing three different arrays, each with 40 dB directive gain, but with sidelobes differing by steps of 6 dB, he concluded that the cost of building a phased array increased about 2.3 percent for each dB the sidelobe level is reduced when the size of the array is held constant and about 3.2 percent for each dB of sidelobe reduction when the antenna beamwidth is held constant.

FASR, an Electronically Steered, Low-Sidelobe Array Radar[164] This was one of the first low-sidelobe electronically steerable phased arrays. FASR (Fixed Array Surveillance Radar) was an experimental UHF radar developed by the Naval Research Laboratory to demonstrate how low-sidelobe antennas can be obtained in a shipboard environment by placing four fixed phased-array faces around a ship so as to avoid blockage by masts or superstructure. A single array antenna was 32 by 12.5 ft with 297 dipole radiators arranged in 27 columns and 11 rows. Although not small in physical size, the array contained a small number of elements and was not of high gain. Thus it was more difficult to achieve low sidelobes (tighter tolerances were required) than in an antenna with higher gain (and thus more elements). FASR was designed for -40 dB sidelobes and used six-bit digital diode phase-shifters. The 5 by 12° beam scanned 120° in azimuth and 90° in elevation. Monopulse sum and difference beams were generated. The desired sidelobes of -40 dB were achieved at broadside, but they increased slightly when the beam was scanned. The difference pattern also achieved -40 dB sidelobes with respect to the sum pattern.

Parabolic Reflector[165] There are many advantages of a parabolic reflector for radar applications; however, it is more difficult to achieve low sidelobes with a reflector. Among the things that need to be done to obtain low sidelobes are:

1. A solid rather than a mesh reflector surface should be used to avoid leakage in the back direction.

2. The feed system should illuminate the edges of the reflector with low energy, not only to obtain a highly tapered illumination, but also to minimize the sidelobe energy caused by spillover.
3. Spillover radiation from the edges of the reflector can be attenuated by the appropriate placement of absorbing materials or shields.
4. The feed system might have to consist of more than one horn or radiator in order to properly control the aperture illumination.
5. There can be no aperture blockage by the feed system, which leads to the use of an offset reflector.
6. The mechanical tolerances of the reflector surface have to be better than that of an array by a factor of two because of the two-way path on reflection from the surface.

Scudder[166] described the design of an *S*-band 3D air-surveillance radar using an offset reflector 20 ft wide by 12 ft high with a bandwidth of 600 MHz. The azimuth beamwidth was 1.4°. Seven corrugated feed horns were positioned to provide seven overlapping beams in elevation from 0° to 20°. More than one feed horn was used to form each elevation beam. Absorbers were placed at both the top and bottom edges of the reflector to suppress spillover radiation. Based on measurements of a one-tenth scale model operating at K_a band, the peak near-in sidelobes were -40 dB and decreased rapidly to less than -50 dB, with the wide-angle sidelobes below -60 dB.

Another example is that described by Williams et al.[167] Their elliptical shaped reflector had a major axis of 45 wavelengths and a minor axis of 15 wavelengths producing an azimuth beamwidth of 1.7° and an elevation beamwidth of 5°. It was feed from an offset array of four conical horns. The aperture illumination was designed to produce a peak sidelobe of -50 dB. The price paid for this low sidelobe design was that the beamwidth was broadened by a factor of 1.47 compared to the beamwidth that would have been produced by a uniformly illuminated circular aperture. An *X*-band model produced a peak sidelobe of -43 dB, which was attributed by the authors to spillover radiation from the feed support struts.

An offset-fed parabolic cylinder has some advantage over other reflector antennas for producing low sidelobes because the line source feed (which may be a linear array or a pill box) allows much better control of the aperture illumination than when a conventional parabolic reflector is used with one or several horn feeds.[168] If a corporate-fed linear array is used with equal lengths of lines to the radiators, the antenna can have much broader bandwidth than a series-fed array.

Measurement of Low-Sidelobe Radiation Patterns A good pattern range is needed to accurately measure the radiation pattern of a low-sidelobe antenna, especially if the depth of the nulls are of interest.[169] The pattern range must be sufficiently large so that the curvature of the wavefront due to the finite distance does not affect measurement accuracy. The rule of thumb used by antenna engineers for conventional antennas is that the distance between the antenna and the pattern-measuring source should be at least $2D^2/\lambda$, where D is the antenna dimension and λ is the wavelength. This is adequate for sidelobes

down to about −30 dB; but not for lower sidelobe levels. Hacker and Schrank[170] state, however, that the distance of $2D^2/\lambda$ can be satisfactory for the accurate measurement of the wide-angle (far-out) sidelobes, but it does not accurately measure the first one or two near-in sidelobes. If, on the other hand, the entire antenna pattern is to be determined to an accuracy of better than 0.5 dB, the pattern range must be $8D^2/\lambda$ when the pattern is a modified Taylor with first sidelobe of −50 dB. Using the Taylor $\bar{n}$ linear aperture illuminations, Hansen added to this by determining that that if an error of 1 dB or less is required when measuring a −40 dB sidelobe, the measurement distance should be $6D^2/\lambda$.[131] For a −60 dB sidelobe design, the distance should be $12D^2/\lambda$.

System Implications of Low Sidelobes Low antenna sidelobes are important for achieving the desired performance of pulse doppler radars in the face of heavy clutter. They can also be useful for reducing the effects of sidelobe jamming and making the job of hostile intercept receivers and antiradiation missiles more difficult. Low sidelobes, however, do not come without cost—both monetary and performance.

Compared to the conventional parabolic reflector, low-sidelobe antennas are more expensive, less rugged, more likely to be heavier, require better mechanical and electrical tolerances, and are harder to maintain. As has been mentioned, the lower the sidelobes the less the antenna gain and the wider will be the main beam. If a larger antenna cannot be used to maintain the beamwidth, the wider beam means poorer angular resolution and accuracy, greater susceptibility to main-beam jamming, and larger clutter echoes received in the main beam. In an airborne doppler radar that is concerned with detecting low velocity ground-moving vehicles with doppler frequencies near that of the main-beam clutter, a narrow antenna beamwidth with conventional sidelobe levels may be more important than a low sidelobe antenna with an increased beamwidth.

To avoid negating the benefits of low sidelobes, the antenna must be operated in a clear environment without obstructions or nearby objects that block or scatter the radiated energy. When a low-sidelobe antenna must be operated within a radome, special considerations need to be given to the design of the radome in order that the sidelobes are not degraded. Usually the radome will rotate along with the antenna (a rotodome) in order to maintain the same radome environment seen by the antenna as it rotates.

As with most things, low-sidelobe antennas have both good and bad effects. They are not universally applicable and should be used only when their desirable features outweigh their disadvantages.

9.14 COST OF PHASED ARRAY RADARS

A phased array radar generally costs more than a conventional radar that employs a mechanically scanned antenna but it also can provide unique capabilities not available with other antennas. It has been used chiefly in military applications where the unique features of a phased array may sometimes compensate for its higher cost. It has seldom been employed for civilian radar applications since there are few applications where its greater expense can be justified when competitive market forces make price an important

consideration. There has been much interest in reducing the costs of phased arrays to make them more competitive for both military and civilian applications.

Factors Affecting the Cost of a Phased Array Radar Tang and Brown[171] state that the cost problem of a phased array is attributable to the following:

- The large number of discrete components in a conventional phased array that have to be individually fabricated, assembled, tested, and installed.
- The production yield of components, especially solid-state amplifiers that use monolithic high-power chips.
- The labor involved.
- The limited production quantity of any particular radar system which does not justify large capital investments for a dedicated production line with special production tooling that could reduce manufacturing costs.

These four categories are only a part of the problem. Cost depends on the particular radar architecture, the degree to which multifunction operation is used, computer software for operating the radar, and the radar frequency. Each of these will be briefly reviewed.

Effect of Radar Architecture on Cost Section 9.9 discussed the various architectures for phased array radars, and some mention was made of the effect of the architecture on radar cost. It is difficult to be quantitatively accurate regarding predictions of radar cost, but some generalizations can be made. For example, a space-fed array using a single high-power vacuum tube transmitter has been less expensive than a corporate-fed array or an active aperture solid-state phased array. Also, the row-column control of phase shifters is usually cheaper than when each phase shifter is controlled individually.

There was a brief description in Sec. 9.9 of how Russian (Soviet) air-defense phased array systems achieved lower cost. Cory[105] summarized these as:

- Minimizing the total number of phase shifter modules.
- Simplifying the radar architecture (such as by using a space-fed array).
- Designing simple and inexpensive components.
- Minimizing the size and complexity of the control system.
- Simplifying the feed design.

In addition the Russians used several low-cost radars, each performing a single air-defense function rather than the more complex multifunction phased array that has been the more usual practice in the U.S.

Multifunction Radar and Cost Because of its flexibility and rapid beam steering, an electronically steered phased array antenna can be used to perform multiple radar functions including search, track, weapon control, missile guidance, target recognition, and perhaps others. The ability to perform multiple functions with one phased array radar has been a major selling point of those who market radar systems that employ phased arrays. One

should be cautious, however, since a single multifunction phased array radar might not be the best approach for all radar applications. This is especially true for air defense.

The basic problem with a multifunction electronically steered phased array radar for air defense is that compromises must be accepted when a single radar is used for both surveillance and weapon control. It is well known among radar system engineers that the lower microwave frequencies are more suited than the higher frequencies for long-range air-surveillance radars. The frequency of choice is usually *L* band (1.215–1.4 GHz). On the other hand, the higher microwave frequencies are more desirable for weapon control, with *X* band the usual choice (8.5–10 GHz). When a single phased array radar is required to perform both surveillance and weapon control, a compromise choice of a single frequency has to be made, generally somewhere between *L* and *X* bands. The U.S. Navy's Aegis air-defense system is at *S* band and the U.S. Army's Patriot air-defense system is at *C* band, yet they basically have the same mission (except one is on ships and the other is land mobile). When the beamwidths must be the same no matter what the frequency (which implies that the antenna gain is independent of frequency) the antenna aperture will be smaller at the higher frequencies. Thus performing the surveillance function at S band results in less range performance (for a given average transmitter power) than if it were at *L* band. Air surveillance at higher frequencies (such as *C* band) result in even less range performance. Also, the higher the frequency the less will be the available doppler space (to detect moving targets in clutter) because of blind speeds. When weapon control radars operate at *C* band or *S* band, the antenna beamwidths will be wider than they would be at *X* band, resulting in poorer angle accuracy and less ability to deal with multipath effects from surface reflections. Thus, even if cost were of no concern whatsoever, one usually has to accept lesser performance in both surveillance and weapon control when a multifunction radar is employed for air defense at a single frequency band.

It is not always necessarily true that an air-defense radar system with multiple radars at different frequencies has to be more expensive than a single-frequency multifunction system which has the same performance. Both Barton[104] and Cory[105] have written about the benefits of the Russian design approach to air-defense radar systems that employ several simple cost-effective phased array radars to perform the various functions of surveillance, weapon control, and low-altitude detection.

In some radar system applications the optimum frequencies for surveillance and for track might be the same, so that multifunction radars do not have the same limitations that are experienced with their use for air defense. Space surveillance for the detection and tracking of satellites is one example where both the surveillance and the tracking functions can be performed at the same frequency. (UHF is a good choice, as in the AN/FPS-85 and Pave Paws.) Thus no significant compromises in performance need be made when using a single multifunction radar for the space surveillance functions of detection and tracking.

Multifunction radars that use mechanically scanned planar array antennas have been well suited for military combat aircraft and, in the past, have been the norm. A modern radar for a fighter/attack aircraft has to perform a number of functions, maybe from 6 to 9, for air-to-air purposes and a similar number of different functions for air-to-ground purposes. There have been no significant limitations (other than having sufficient time) in using the same airborne radar to perform all the many functions at *X* band. The multifunction

electronically steered phased array can also be used for airborne fighter/attack radar application, but a single phased array face in the nose of a fighter/attack aircraft (usually limited to less than $\pm 60°$ in angle) cannot provide as large an angular coverage as can a mechanically steered planar array antenna. (Large angular coverage is especially important for the dog-fight role.) Two or more phased arrays might be used for increased coverage, but they result in increased system size and weight. Mechanical antennas thus can be competitive, and in some ways superior, to electronically steered phased arrays for military airborne applications since they can do what is required of an airborne radar antenna at less cost and less weight than an electronically steered phased array.

Offensive bomber aircraft, such as the B-1B, have also employed the multifunction electronically steered phased array to perform the many radar functions unique to the bomber. Such radars have been more expensive than conventional mechanically scanned radars for the same purpose.

Computer Software and Cost The computer can be a significant part of the cost of a versatile multifunction phased array radar. It has not been the computer hardware but the software that can be a sizable fraction of the total radar development cost. In early long-range multifunction phased array radar systems, software cost was about 30 to 40 percent of the total. Over time, computer software has become better and easier to obtain, but it is still a significant factor in achieving a successful phased array radar system. The design of the computer software for phased arrays must enter the radar system development process at an early stage, with sufficient time and funds allowed for it to be successfully completed. Without sophisticated computer control, a phased array can do very little.

Effect of Frequency on Phased Array Radar Cost In general, the lower the frequency of an air-surveillance radar that uses a phased array antenna, the lower the cost. The rationalization is as follows. A passive phased array is assumed, one with a single receiver and a single high-power transmitter, that requires a specified power-aperture product. (That is, the average transmitter power times the antenna area is a constant, Sec. 2.13.) The cost of an antenna element and a phase shifter is more or less independent of frequency, but the cost of an array is proportional to the number of elements. In this comparison it is further assumed that the antenna must have the same gain (same elevation and azimuth beamwidths) at whatever frequency is selected for its operation. Thus a 9000-MHz (*X*-band) phased array radar would have the same number of elements as a 450-MHz (UHF) radar. With the above assumptions, the array antennas at the two different frequencies would cost approximately the same. The aperture of the 450 MHz radar, however, is 20 times larger in linear dimension and 400 times larger in area than that of the *X*-band radar. Since the power-aperture product in this example is assumed to be the same at both frequencies for equal performance, the transmitter power for the *X*-band radar must be 400 times that of the UHF radar, with the result that the cost of the *X*-band radar will be many times greater than that of the radar at UHF. The effect of a higher frequency on cost is probably even greater for active-aperture phased array radars that employ a T/R module at each element containing its own solid-state transmitter, receiver, phase shifter, and duplexer. The cost of a T/R module is likely to be greater at the higher frequencies rather than be relatively independent of frequency as in the passive array. The above

argument assumed a surveillance radar where $P_{av}A$ is constant. In a tracking radar, generally the product $P_{av}A^2$ is a constant with frequency. This makes it even more likely that an equivalent radar at a lower frequency will cost significantly less than one at a higher frequency.

The above has been a very simplistic argument with some very gross assumptions. There may be other requirements the radar must meet which require that a phased array radar operate at higher frequencies in spite of higher cost (such as if it has to fit into the nose of an aircraft). Nevertheless, it is often true that the lower the frequency the more affordable will be the phased array radar.

Reducing Phased Array Cost This subsection summarizes some of the guidelines for lowering the cost of phased array radars.[172]

1. *Operating at as low a frequency as the application will permit.*
2. *Emphasizing low-loss design.* This might seem obvious or trivial, but it has not always been given sufficient attention.
3. *Time sharing a four-faced phased array with a single transmitter.* This is done as a cost-saving measure, but it can affect the overall performance of the system.
4. *Employing the active aperture architecture only when it is appropriate.* The losses in the active aperture array are less than the losses in a passive array with a constrained feed. It is not always obvious, however, that the total system cost of an active aperture radar will be lower or its performance better than other phased-array architectures.
5. *Single transmitter.* It has usually been true that the greater the RF average power from a single device, the lower will be its cost per watt.
6. *Space-fed arrays.* Lower loss and less complexity of the space-fed array can result in lower cost.
7. *Attention to computer issues.* The cost of the computer software for a phased array and the time required to generate it can be significant.
8. *Trainable arrays.* If an application requires 360° of coverage, one might not want to have the expense of four identical phased array radar systems to provide the total coverage. As mentioned in no. 3 above, one or two transmitters might be time-shared among the four apertures of an array radar system. The combination of two trainable arrays and a conventional 2D air-surveillance radar could be less expensive that a full four-face phased array.
9. *Avoiding a multifunction array.* There can be, in some applications, other less costly approaches that can perform more effectively the same mission.

It was mentioned that phased array radars have the advantage of being more readily hardened to withstand nuclear blast effects than a mechanically steered radar. Hardening only adds to the already large costs of phased arrays. In the U.S. development of intercontinental ballistic missile defense systems in the 1960s and early 1970s, the high cost of a fully hardened system was a factor in leading to the ABM (antiballistic missile) treaty between the U.S. and the Soviet Union.

It might be mentioned that the life-cycle costs of military systems, which were not considered in the above, include the cost of development, procurement, installation, training, operating, and maintenance. A further consideration is that the development cost of a radar usually is a small fraction of the total life-cycle costs of the system.

9.15 OTHER TOPICS CONCERNING PHASED ARRAYS

Bandwidth of a Phased Array Antenna Two different kinds of bandwidths need to be considered for phased arrays. One is the instantaneous, or signal, bandwidth, which is an indication of the maximum bandwidth of a signal that the array can handle without distortion. Usually, it is difficult to obtain an array signal bandwidth of more than a few percent. The other is the operating, or tunable, bandwidth over which a narrowband signal can be received (or transmitted) without distortion.

Signal Bandwidth Figure 9.15a showed a two element array receiving a signal that arrives at an angle θ_0 relative to broadside. The signal appears at element 2 before it appears at element 1. If a delay line of the proper length is inserted at element 2, the two signals will coincide and add without loss. There is no theoretical limitation to the signal bandwidth in this case when delay lines are used to bring signals from the various elements of the array into time coincidence. As has been said in the original discussion of Fig. 9.15, time delays inserted at each of the many elements of a large array have not been not practical. Instead, the delay line is replaced with a phase shifter that is limited in phase to the range 0 to 2π radians. Signals can be phase coherent so long as they overlap in time. But the signals do not overlap with 0 to 2π phase shifters during the transient build-up time. Thus phase shifters produce coherent addition only for narrowband (long time duration) signals.

The limitation on bandwidth when phase shifters are used in an array is dependent on the rise time, or build-up time, of the signal as it transits across the array. The transient response of the incident signal as it builds up across the array has the same effect on signal bandwidth as the transient response, or build-up time, of a conventional filter. The build-up time of a linear array of dimension D when a signal is incident on the array at an angle θ_0, is $(D \sin \theta_0)/c$, where c is the velocity of propagation. If, for example, the angle of arrival $\theta_0 = 45°$, and $D = 30$ ft, the transient build-up time is about 22 ns. The signal bandwidth is thus limited to the reciprocal of the transient build-up time, or about 45 MHz. There is zero build-up time for a signal that arrives from the broadside direction ($\theta_0 = 0$); hence, there is no theoretical bandwidth limitation. (This assumes that the signals from all the antenna elements are summed with equal-length transmission lines.)

Another aspect of signal bandwidth has to do with the change of phase with a change in frequency. The phase shift ϕ required to steer a beam to a given direction is assumed to be independent of frequency. If the value of ϕ is chosen so as to point the beam to a direction θ_0 when the frequency is f_1, the beam will point to a new direction when the frequency is f_2. If it is assumed that the signal's frequency spectral width must not cause the beam to scan more than $\pm$ one-fourth beamwidth, Cheston and Frank[173] show that

$$\text{signal relative-bandwidth in percent} = \text{broadside beamwidth in degrees} \quad \textbf{[9.69]}$$

where the signal relative-bandwidth in percent is 100 times the absolute bandwidth divided by the RF carrier frequency, or $(B/f_0) \times 100$. This expression is based on the array having an equal-path-length feed and the beam is scanned to an angle of 60°.

Although it has been impractical to employ delay lines at each element of an array, they have sometimes been used at the subarrays to increase bandwidth. Phase shifters are used at each element in addition to the delay lines at each subaperture. This reduces the complexity of an array compared to one with delay lines at every element, but it also has less bandwidth than a true time-delay array. Subarrays with delay lines increase the bandwidth of a linear array in proportion to the number of subarrays, compared to the bandwidth of an array that does not have subarrays.[174] The sidelobes will increase, however, with the use of subarrays, which may not be desirable for some applications.

Operating, or Tunable, Bandwidth Although the build-up time of an array limits the signal bandwidth that it can handle without distortion, it is possible to operate an array over a very wide band of frequencies by retuning; that is, by re-setting the phase shifters to new values when the frequency (of a narrowband signal) is changed. Such an array can radiate different narrowband signals one at a time at different frequencies by readjusting the phase shifters with each new frequency. The operating bandwidth of the array can be quite large and might be limited only by the onset of grating lobes. This assumes that the antenna elements and other components of the array are wideband.

It has been reported[175] that an array containing 4096 open-ended waveguide radiators with a triangular arrangement of elements was capable of operating over a 30 percent frequency band and over a scan volume of more than 120° in both azimuth and elevation. A wide-angle impedance matching dielectric sheet was placed in front of the array. (The frequency at which this array operated was not given.)

Computer Control of an Array Although a radar with a conventional mechanically scanned antenna can operate without computer control, the multifunction electronically scanned phased array must be controlled by a computer if it is to achieve its full potential. An important task of a computer is to generate the phase shifter commands for each element of the array to steer the beam in the desired direction. But this is only a small part of what an array computer must accomplish. A much more demanding task is to effectively manage the various radar functions required of the array. The computer hardware for the multifunction operation of an array usually is not as much a concern as is the computer software needed to generate and schedule the various waveforms, data rates, and processing without degradation of performance.

The demands on the computer that controls the phased array radar vary with the application. Generally, the various radar tasks that have to be performed by a phased array under computer control must be done sequentially rather than simultaneously. In a phased array radar for air defense, for example, it is the job of the computer to allow the radar to track a large number of targets as well as search a large volume of space within a specified time for the detection of targets. The tracking data rate depends on whether or not the target is considered hostile and is being engaged. The revisit time during search, for example, might need to be one or two seconds when looking for pop-up, low-altitude targets that first appear over the horizon at short ranges (perhaps 8 to 20 nmi). With long-range

targets (150 to 200 nmi), the revisit time can be greater (perhaps 10 s) since there is more time for an air-defense system to react to a long-range threat than to a short-range threat. (A sea-skimming missile flying at Mach 3 at very low altitude might first appear above the radar horizon at a range of 10 nmi from the radar. If the detection decision is made almost instantaneously, then there is then less than 20 s available to destroy the missile before it reaches its objective.) If the radar is to detect tactical ballistic missiles at long ranges, the search patterns and data rates will be different from those used for aircraft targets. Thus the computer must program different search procedures depending on the range and type of target expected.

Once a target is detected, the data is used to update an existing track or initiate a new track. When the radar is performing its search function, the scanning must be interrupted periodically in order to radiate one or more pulses in the direction of known targets already held in track. Since the target is in track, the radar will know the approximate time the echo is supposed to arrive back at the radar. At that time, the phased array beam can be pointed to the direction of the target so as to receive the echo signal. Search and track are therefore accomplished in an interleaved manner. The computer has to be programmed to be able to accomplish this efficiently; that is, to search the required volume with the required revisit times and to track a large number of targets without serious degradation.

In spite of best efforts, there will likely be radar functions that become overloaded when the number of targets is large. This occurs because the various functions of a conventional phased array are performed sequentially in time. Everything cannot be done at once, so priorities must be assigned to the various functions to be performed. Those with less importance are performed at a lower data rate—or maybe, not at all. Among the highest priority functions are those involved with the engagement of threatening hostile attacks. This includes tracking of the attacker and providing guidance information to the intercepting missile. Time critical functions, such as short-range horizon-search for low altitude threats are also of high priority. Next in priority might be the tracking of confirmed hostile threats. Of lower priority is the tracking of known friendly targets. Low priority is also given to above-horizon search for targets at long range. These are only a few of the many tasks or functions that a phased array radar has to perform as part of an air-defense system.[176,177]

As the number of targets increases or as the demands of the air-defense increase, the computer can become increasingly overloaded and it will be more difficult for the phased array radar to perform all of its tasks with equal effectiveness. The problem has sometimes been described as there not being enough microseconds in a second to do all that is required of the phased array radar. One author[178] described the problem as not being able "to get round the sky quickly enough." Among the many factors that can cause the phased array to be overloaded and result in compromised performance are (1) a relatively large number of angular resolution cells that the radar must examine, (2) the need for the radar to detect small moving targets in large clutter, which requires that it dwell in each direction long enough to obtain good doppler filtering to suppress the clutter, and (3) a relatively long time to acquire targets and to initiate tracks.

The overloading of the functions performed by a conventional phased array radar is less of a problem with a radar that uses digital beam forming to look everywhere all the time since the various functions can be performed simultaneously (in parallel) rather than sequentially (in series), as was discussed in Sec. 9.9.

Radant Phased Array[179,180] Radant, originally developed by Thomson-CSF of France, is a different method for employing diodes or microelectromechanical switches (MEMS) to produce agile beam steering. Instead of using diode phase shifters in the conventional manner, Radant employs strips of metalized diodes arranged in columns to produce phase shift in one angular dimension by changing the voltage applied to each strip of diodes. The principle of the Radant diode lens for scanning in one angular coordinate is illustrated in Fig. 9.50. The vertical strips of diodes that produce the phase shifts are illuminated from the back by a plane wave as might be generated by a simple planar array. A parabolic reflector or a lens also might be used to illuminate the Radant, as might space feeding (but not offset space feed).

Radant can be thought of as a lens whose index of refraction (or dielectric constant) can be varied by appropriately biasing each string of diodes.[181] Biasing the PIN diodes can provide the desired change in susceptance to change the "index of refraction" of the lens consisting of many diodes. A number of planes of diodes are used to obtain the total phase shift. In a Radant array antenna with the geometry of Fig. 9.50, there might be 20 planes of diodes having a total thickness of 4 inches at X band.

As described, beam steering occurs in only one plane. Figure 9.51 illustrates two-dimensional steering. In this arrangement the first lens steers the beam in the horizontal direction. The plane of polarization is then rotated 90°, and a second lens oriented 90° to lens no. 1 steers the beam in the vertical. Control of two-dimensional beam steering is done with row and column commands so that with a $N \times M$ element array there need be only $N + M$ commands rather than $N \times M$. An advantage claimed for the Radant antenna is that it can be of lower cost than other array configurations.[182]

A Radant lens electronically steered phased array radar, called the RBE2, was developed by Thomson-CSF for the French Rafale multirole combat aircraft built by Dassult Aviation.[183]

Ferroelectric Phased Arrays A change in phase can be had by a change in the dielectric constant (permittivity) of the material in which the electromagnetic signal propagates. Materials whose dielectric constant varies with the d-c voltage applied across it are known

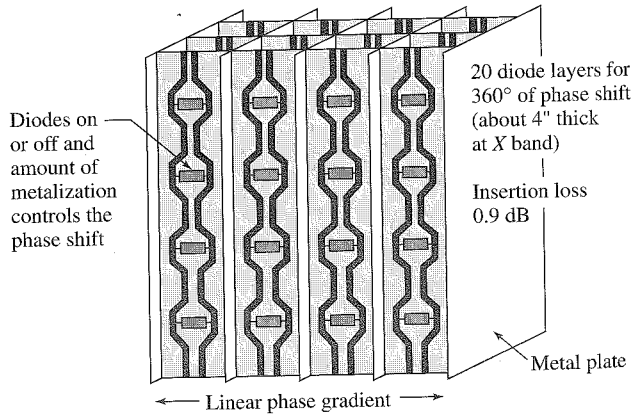

Figure 9.50 Principle of the Radant antenna for scanning in one angle coordinate, horizontal in this case.
(Courtesy of Jaganmohan Rao, Naval Research Laboratory Radar Division.)

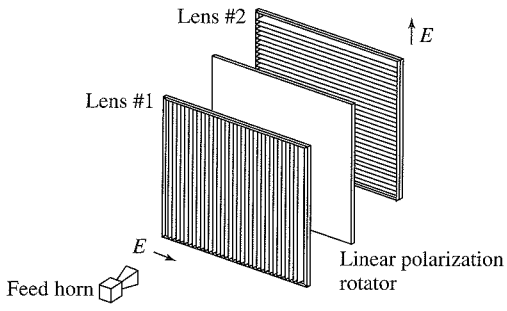

Figure 9.51 Method of obtaining a two-coordinate beam steering Radant antenna. (Courtesy of Jaganmohan Rao, Naval Research Laboatory Radar Division.)

as *ferroelectrics*. Ferroelectric phase shifters have been investigated in the past, but they were difficult to match because of their large dielectric constant and they have higher losses than might be desired. With time, ferroelectric materials have improved and they have shown more promise.

An interesting approach to a ferroelectric phased array based on a lens array with bulk phase shifting is that of Jay Rao and colleagues.[184] Figure 9.52 is a very simplified sketch of the operation of a ferroelectric lens array that steers in one plane. It is made up of ferroelectric slabs sandwiched between conducting plates that apply the d-c voltage that determines the dielectric constant and the phase shift. Changing the voltage on the conducting plates changes the direction of the beam. Beam steering in two orthogonal planes is obtained by rotating the plane of polarization 90° and using a second lens array oriented 90° to the first lens, as was illustrated in Fig. 9.51 for the Radant lens. Similarly the ferroelectric array can be illuminated with a conventional non-steerable planar array or by a horn feed, just as for Radant. The material used was a bulk oxide-ceramic composite of barium strontium titanate oxide (BSTO) with a typical dielectric constant between 90 and 120.

Theory and experimental measurements indicate that a ferroelectric array at *X* band can operate over the frequency range from 8 to 12 GHz with a voltage standing-wave

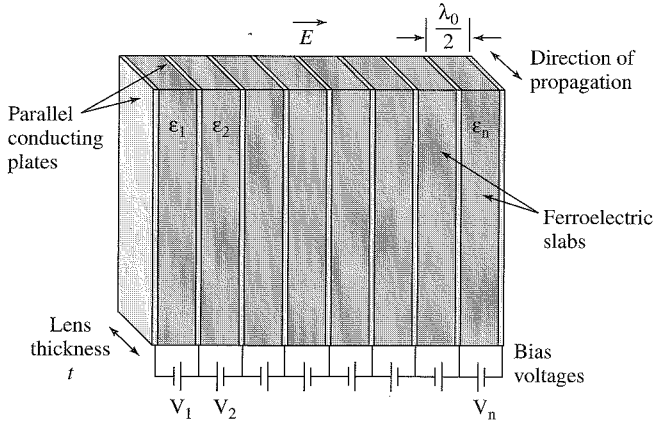

Figure 9.52 Basic configuration of a ferroelectric lens array for steering in the horizontal plane with horizontal polarization.[184] (Provided by J. Rao and D. Patel of the Naval Research Laboratory Radar Division.)

ratio less than two, and with a loss between one and two dB.[184] The advantage of this form of phased array compared to other phased arrays is its potential for low cost. It uses row and column steering that requires far fewer phase-shift control signals than an array which requires control signals for each element of the array. It is said to have smaller lens thickness, higher power capability, simpler beam steering controls, and use less power to control the phase shift than a Radant lens array. The use of row-column bulk phase steering instead of individual phase shifters at each element can make it more difficult, however, to achieve low sidelobe levels.

Conformal Array Antennas A long-sought, but difficult to achieve, desire of radar system engineers is to be able to place array elements anywhere on a surface of a relatively arbitrary shape and obtain a directive beam with good sidelobes, good efficiency, and which can be conveniently scanned electronically. An array on a nonplanar surface is called a *conformal array.* Such an array, if practical, might be configured to conform to the nose, wing, or fuselage of an aircraft or missile. Most of the work on conformal arrays has been for relatively simple shapes such as the cylinder, hemisphere, cone, or truncated cone.[185] It has been difficult to achieve a practical conformal array, except in simple geometries. There are good reasons why almost all operational phased arrays are planar.

In some conformal geometries, equal element-to-element spacing is not practical. Because of the nonplanar surface the element polarization can vary from one point on the array to another and with the beam pointing direction. The aperture illumination cannot be separated into two orthogonal patterns, as it can in a rectangular array. The boresight of a difference pattern might vary with angle. The calculation of mutual coupling is more difficult with a nonplanar surface. The issue is not whether a conformal array can be built, but whether some other solution is better.

If one wanted to have a cylindrical antenna, one way to achieve it would be to use four planar arrays arranged in a square and cover the structure with a cylindrical radome—and not let anyone look inside. If the change in beamwidth and gain with scan angle experienced by planar arrays were of concern, adjacent faces of a four-face phased array might be used cooperatively to maintain the beam relatively unchanged with scan. As the beam from one planar array is scanned off broadside, some of the transmitter power can be applied to an adjacent face and diverted to scan in the same direction as the original face.[186] Thus each face might work in conjunction with its two adjacent faces to maintain the beam shape almost independent of scan angle.

Thinned, or Unequally Spaced, Arrays[187,188] A normal phased array antenna has its elements spaced about a half-wavelength apart for good performance. When the elements are, on average, spaced much greater than half-wavelength the array is said to be thinned, or unequally spaced. (This assumes that a wide angular coverage is required; otherwise it would be known as a limited-scan array.) The beamwidth is determined by the electrical size (in wavelengths) of the array but its gain and sidelobe levels are determined by the number of elements that remain. A thinned array will have about the same beamwidth as a filled array, but its gain will be reduced in proportion to the number of elements

removed. Its peak and average sidelobes will increase. [The simple expression for antenna gain, $G = \pi^2/\theta_a\theta_b$ of Eq. (9.5b), doesn't apply to thinned arrays.] Many methods have been tried to determine element spacings that will result in acceptable antenna patterns. Two of the more successful will be described briefly.

Dynamic Programming One method is to have a computer calculate, for a fixed number of elements, the antenna patterns for all possible locations of the elements within the array and determine which is best. This method of total enumeration, is impractical because of the large number of combinations that are possible. A more practical approach is *dynamic programming,* an optimization method that can produce an equivalent result to total enumeration under certain conditions. Its advantage is that it is much less computer intensive. Dynamic programming determines the optimum solution to a multistage problem by optimizing each stage of the problem on the basis of the input to that stage. It is a good method for finding the spacings of a thinned array when the number of elements is not too large.[189]

Density Taper The other method, which is applicable to large linear or large planar arrays, is to employ a *density taper.*[190] Consider a uniform grid of possible element locations with equal spacing of one-half wavelength. The desired amplitude illumination for a conventional filled array is used as the model for determining the *density* of equal-amplitude elements. That is, the density of equal-amplitude elements is made to approximate the desired aperture illumination. The choice of whether or not to include an element in a possible location may be made statistically or deterministically. In one design, a one-degree beamwidth circular array which would have 7800 elements if completely filled, had 3773 elements when a density taper was employed based on a 30-dB Taylor amplitude illumination.[187] This represents a thinning of 52 percent, where the degree of thinning is defined as the ratio of the number of elements removed from a filled array divided by the original number of elements. Density taper was used in designing the receiving aperture of the AN/FPS-85 and the Cobra Dane (AN/FPS-108) space-surveillance phased array radars.

System Degradation Thinning of a phased array will produce serious undesirable characteristics for many radar applications when the degree of thinning is too high. The gain is significantly reduced and there will be high peak and average sidelobes.

A conventional filled phased array will have almost all of its radiated energy within its main beam. Only a few percent of the radiated energy will appear in the sidelobes. With a highly thinned array, however, the reverse is true. Too much energy is wasted in the sidelobes. An array with 90 percent thinning might have about 90 percent of its energy in the sidelobes. If clutter is a problem, as it is in high-prf pulse doppler radars, the high sidelobes throughout space can result in high levels of clutter entering via the sidelobes.

Thinning may look attractive at first glance because it seems to allow a narrow antenna beamwidth with a reduced number of elements, but one does not usually get something for nothing. It should be attempted only with one's eyes wide open to the consequences.

9.16 SYSTEMS ASPECTS OF PHASED ARRAY RADARS

Attractive Attributes of Phased Array Radar The electronically steered phased array antenna is of interest since it can provide capabilities not readily available with other types of antennas. Its advantages are summarized below.

Interialess, rapid beam-steering. The beam from an array can be scanned, or switched from one position to another, in a time determined by the switching speed of the phase shifters. A diode phase shifter, for example, allows the beam to be switched in several microseconds or less. Ferrite phase shifters provide switching speeds that are slightly longer.

Multiple, independent beams. A single array aperture can generate independent simultaneous beams on receive, as described for the digital beam-forming phased array discussed in Sec. 9.9. On the other hand, multiple simultaneous beams on transmit are difficult to obtain, which is why a broad transmitting beam sometimes is used in conjunction with a number of contiguous narrow receive beams. For almost simultaneous tracking of many targets, a simpler method is to rapidly switch a single transmitting beam through a sequence of positions by means of a time-sequenced burst of pulses, with each pulse steered to a different direction. Rapidly acting phase shifters are needed, as well as an application that does not require a short minimum range. Since the targets are in track, their directions are known. On reception the receive beam is switched at the proper time to the direction from which the echo is expected so as to update a target already in track.

Potential for large peak and/or average power. Each element of an array can have its own individual transmitter with the outputs combined in "space" to obtain a large total power. (The power per element will be limited by the need for each individual transmitter or T/R module to fit within the space available between adjacent elements.) The active-aperture radar, Sec. 9.9, is an example. In addition to being able to achieve a large radiated power, an array with a transmitter at each element avoids the loss that can occur when the power from a single high-power transmitter has to be divided and distributed to each radiating element.

Control of the aperture illumination. Since the aperture illumination is determined by the currents at a large number of individual radiating elements across the array, a particular antenna radiation pattern is much easier to obtain with an array than with other antennas. This is important when shaped beams or very low sidelobes are desired. Separate monopulse sum and difference patterns, each with its own optimum characteristics, can also be obtained with arrays.

Adaptive processing. Adaptive arrays are designed to automatically adjust the aperture illumination to place nulls in the antenna pattern in the direction of external noise sources and/or clutter echoes. Full array adaptivity, however, in which each element of a large array is part of the adaptivity process, has been too expensive in the past to implement. The sidelobe canceler is an example of a practical adaptive system that requires the use of only a few auxiliary low-gain antennas. When

sidelobe canceling is employed in a phased array, several of the array's elements can be used as the auxiliary antennas.

Lower radar cross section. Because of its flat surface, the phased array can have a lower radar cross section than conventional reflector antennas, when illuminated by a radar with a frequency lower than the radar frequency. The flat face of a phased array can produce a large specular reflection, but the array can be tilted so that its specular scattering is directed to an angle where it is less likely to be detected. The effect of the tilt on beam steering can be compensated in the commands to the individual phase shifters. On the other hand, the radar cross section of a planar array might not be low when illuminated by a radar at a frequency higher than that for which it was designed.

Flush aperture shape. The flat surface of an array permits it to be flush mounted and to be hardened to resist the effects of blast.

Multiple functions. The agile beam-steering offered by a phased array allows a single array radar to be time-shared (sequenced) among more than one radar function.

Electronic beam stabilization. The ability to steer the beam electronically allows stabilization of the beam-pointing direction when the radar is on a ship or aircraft that is subject to roll, pitch, and/or yaw. This avoids the need for heavy mechanical stabilization machinery, but it also requires that the array be able to steer the beam over wider angles than when it is mechanically stabilized.

One other advantage sometimes claimed for a phased array is that it degrades gracefully when failures occur in the system. Since there can be many elements in the array (several thousand to several tens of thousands, or more), the effect of the failure of a few individual elements is small. It has been said[191] that for an active-aperture phased array "typically, 5 percent or more [T/R] module failures can be tolerated while maintaining acceptable performance as a multimode radar." There are several reservations that need to be mentioned, since graceful degradation is not guaranteed. First, there can be failure modes in a phased array radar that can affect a large number or all of the elements, or even be catastrophic. Second, no matter how "graceful" the failure of an array might be, sooner or later there will come a time when failures finally have to be replaced. Third, if the buyer of the radar (especially if the radar is for the government) is told by the radar company's marketing department that the radar can operate satisfactorily when a significant fraction of its elements fail, it is likely that at some time during the development of the radar—when serious overruns in money or time occur—the margin that allows for graceful degradation might be quietly removed. In spite of difficulties, graceful degradation should be designed into a phased array radar and the radar systems engineer should try to make sure it is not removed.

Limitations of Phased Arrays As with most things in life, the desirable benefits of the phased array do not come without their price—and the price is sometimes measured in more than just dollars.

Complexity The phased array radar is much more complex than a radar with a reflector antenna. In addition to being made up of many thousands of individual elements, there

must be means for insuring that the phase and amplitude at each element are what they were designed to be; and, if not, there needs to be means to readjust them to their correct value. If the phased array is to perform the functions of multiple radars, there must be more equipment behind the aperture than if only a single radar function were being performed. The antenna aperture of a phased array radar is much like the "tip of an ice berg." There is a lot more than what is normally visible. The complexity of the array also increases the problems associated with its *maintainability,* achieving high *reliability,* and assuring that its *availability* is such that it will be able to operate when needed.

Software Intensive Everything that the phased array does is commanded by a computer. The cost of the computer software to control the beam steering of the array and the various radar functions can be a significant portion of the total radar system cost, especially if the radar must perform the multiple functions of search, track, and weapon control.

Cost The cost of phased arrays was discussed in Sec. 9.14, and nothing more need be said here other than the high cost of phased array radars has limited their use to applications where the customer has been willing to pay the higher costs in order to obtain the special attributes of an array radar. For this reason, the phased array that scans in two angular coordinates has seldom been used for other than military applications.

System Limitations An advantage of a phased array is that it can be time shared to perform multiple functions. Some of the functions performed by an array, however, might take more time than is available. Three radar tasks that usually require more time than usual to accomplish properly are doppler processing, target acquisition, and long-range surveillance.

Doppler processing (as in MTI or pulse doppler radar) is used to detect moving targets in heavy clutter. As has been seen in Chap. 3, the longer the dwell time, the better can moving targets be separated from clutter. When a target is detected by the surveillance waveform of the array and is then designated for tracking, the tracking beam must be accurately directed to the direction of the target so that the beam can rapidly acquire the target without having to search for it. (A weapon control radar using mechanical trackers, on the other hand, usually can take the time—a few seconds—to search a limited angular region to find and acquire the target to be tracked. The phased array that has to perform multiple functions generally doesn't have this luxury.) Long-range air-surveillance requires the radar beam to remain in a fixed direction until the potential echoes from all ranges can return to the radar. These and other radar tasks, such as some forms of noncooperative target recognition and burnthrough against ECM jamming, can require long dwell times that could overload the scheduling of the array and cause it to omit or delay tasks of lower priority.

More than Just Firepower One of the reasons the phased array has been used for military air-defense applications is that it has been said to provide increased *firepower.* Firepower has not always been a well-defined term, but it has been defined in Webster's Ninth New Collegiate Dictionary as "the capacity to deliver effective fire on a target." In addition to firepower, a balanced air-defense system must avoid *leakage* (the penetration of

the defense by an attacker when the kill probability is too low), *saturation* (which means that the attack is so large and occurs within such a short time that the defense becomes overwhelmed and cannot engage all targets), and *exhaustion* (when the defense runs out of missiles before it runs out of attackers). The phased array radar addresses only one of these three, which is saturation.

9.17 OTHER ANTENNA TOPICS

This section considers some miscellaneous antenna topics that did not seem to fit in other sections of the chapter. They are discussed in no particular order of importance.

Mirror-Scan Antenna, or Inverse Cassegrain[192] The radiated beam of the antenna configuration shown in Fig. 9.53 can be rapidly scanned over a wide angle by mechanical movement of a light weight planar mirror called a twist reflector. This has been known by many names, including mirror-scan antenna, mirror-track antenna, polarization-twist Cassegrain, flat-plate Cassegrain, parabolic reflector with planar auxiliary mirror, and inverse Cassegrain. The parabolic reflector shown on the left in Fig. 9.53 is made up of parallel wires spaced less than a half-wavelength apart. (The wires are usually supported by a low-loss dielectric material.) For purposes of discussion, assume they are oriented vertically. The thin parallel vertical wires of the parabolic reflector make it sensitive to vertical incident polarization (when the E field is vertical). The parabola will completely reflect linear vertical polarization and be transparent to linear horizontal polarization. If the energy radiated by the feed in the center of the figure is vertically polarized (E field parallel to the vertical wires of the parabolic reflector), it will be completely reflected and directed towards a planar reflector (a mirror) called the *twist reflector.* The twist reflector has the property that it imparts a 90° rotation of the plane of polarization to the energy reflected from it. The polarization of the energy reflected from the twist reflector will then be horizontal and will pass through the parabolic reflector with negligible attenuation. The

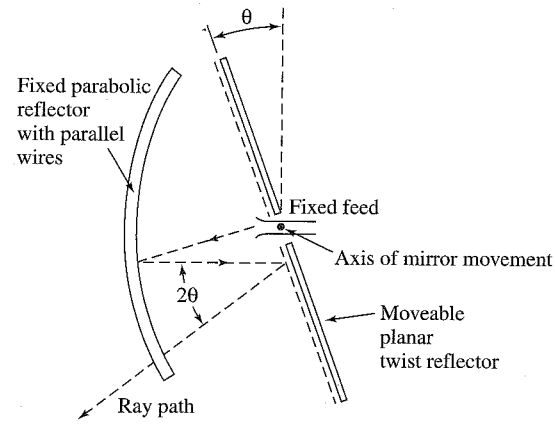

Figure 9.53 Geometry of the polarization-twist mirror-scan antenna, using a polarization sensitive parabolic reflector and a planar polarization-rotating twist-reflector. Rapid scanning of the beam in azimuth and elevation is accomplished by mechanical movement of the lightweight planar twist-reflector.

radiated beam is steered in angle by mechanically rotating the low inertia twist reflector. When the twist reflector is rotated by an angle θ, the radiated beam is rotated through an angle 2θ. The beam can be rapidly scanned over an angle of $\pm$ 90° without the need for microwave rotary joints.

One method of making a twist reflector is to orient a grating of thin wires 45° to the incident polarization and placed a quarter-wavelength in front of the planar reflecting surface. This type of construction is limited to a bandwidth of about 10 percent. Much broader bandwidth is possible with other constructions. A meanderline polarizer backed by a reflector surface, for example, can achieve an octave bandwidth.[193] A mirror-scan antenna with a twist reflector using a number of log-periodic layered structures demonstrated operation over a frequency range from 2 to 12 GHz.[194]

The mirror-scan antenna has been widely used by many countries, especially the former Soviet Union, for land-based, shipborne, and airborne radar applications.

Beam Steering of a Reflector Antenna by Movement of the Feed The beam of a parabolic reflector antenna can be scanned by laterally displacing the feed from the focus of the antenna. Generally the beam can only be scanned a few beamwidths off axis before the antenna pattern degrades significantly.[195,196] The antenna gain decreases and the sidelobes increase; and in radar applications it is often the increase in sidelobe level that determines how far the beam can be scanned rather than the decrease in gain. The larger the f/D ratio (f = focal length and D = antenna diameter) the greater in angle the beam can be scanned, but it is still quite limited.

A *spherical reflector* can produce a slightly larger scan angle when positioning the feed off the focal point, but spherical reflectors have aberrations that cause high sidelobes. The Arecibo antenna in Puerto Rico used for radar and radio astronomy employs a large spherical reflector 1000 ft in diameter. It has a specially designed feed that corrects for aberrations so that the UHF beam can be steered about 20° off axis.

A *parabolic torus* is a reflector antenna that is generated by rotating the parabolic section of Fig. 9.7 over an arc of a circle whose center is on the axis of the parabola.[197,198] Thus the vertical profile of the parabolic torus is a parabola and its horizontal profile (the plane in which the beam is scanned) is a circle of radius r. The radius r of the circular contour of the torus is made large enough so that the portion of the antenna surface illuminated by the feed does not appreciably differ from a true parabola. In other words, even though the horizontal contour of the torus is circular, the portion of the aperture illuminated by the feed approximates a parabolic shape, which is why the antenna generates satisfactory radiation patterns. Only a portion of the reflector surface is illuminated at any beam position. The main use of a parabolic torus is to rapidly scan a beam in a single plane by either mechanically moving a single feed along a circle whose radius is $r/2$, or by switching among many fixed feeds located on the circle of radius $r/2$. The latter method of scanning was used with the original antenna for the Ballistic Missile Early Warning System (BMEWS) radar, a high-power UHF radar for the detection of intercontinental ballistic missiles at ranges over 2000 nmi. Its beam was mechanically scanned 120° in azimuth in two seconds. The BMEWS antenna was 165 ft high by 400 ft wide, and although it is a large antenna, its cost was relatively low since it was a fixed structure and only the feeds were switched by an organ-pipe scanner.[199] The BMEWS parabolic torus

antennas have been replaced by a phased array based on the technology of the Pave Paws radar.

The parabolic torus also was used in the past for naval height-finder radars, such as the AN/SPS-30, which rapidly scanned a horizontal fan beam in the vertical plane to extract an aircraft target's elevation angle.

The torus reflector antenna also has been used to generate two spaced antenna beams separated in azimuth, in addition to the main antenna beam, for the AN/SPQ-9B shipboard radar which uses a single mechanically rotating reflector, Fig. 9.54. The purpose of the two additional azimuth beams is to allow confirmation looks on a target after detection by the main beam so as to more rapidly establish a track on a target. After a single pass by the target, this allows the air-defense system to begin to establish a track on the target.

It has been reported[200] that a torus-like reflector with an elliptical contour rather than a circular one (but with a parabolic contour in the orthogonal plane) can have wide-angle scanning with good performance and yet be much smaller than the conventional parabolic torus discussed in the above. With a modified contour in the plane of scan, this approach has also been demonstrated to scan the beam using an offset-fed reflector to avoid aperture blockage.[201]

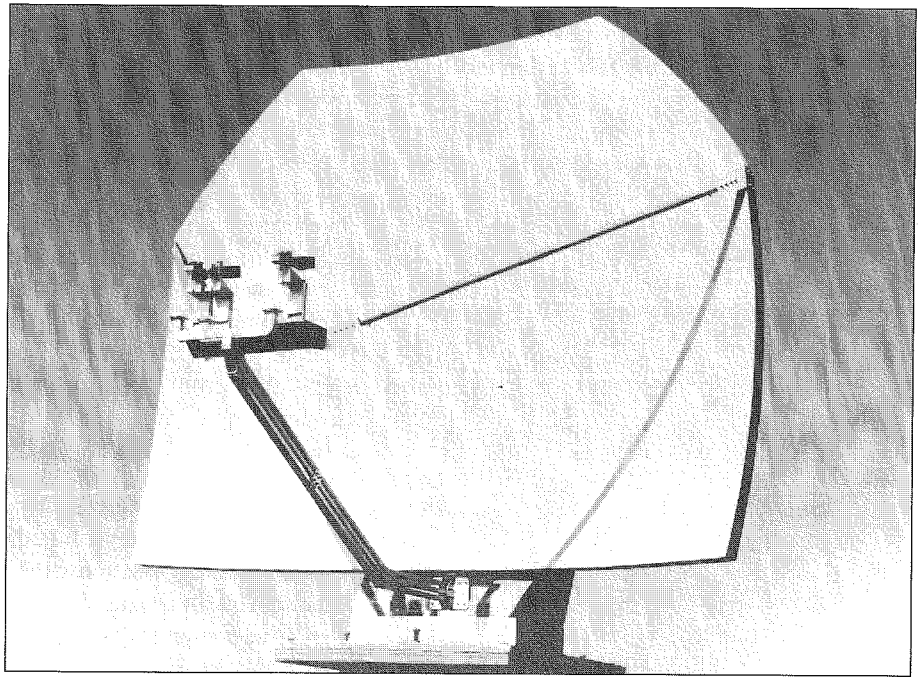

Figure 9.54 Parabolic torus reflector used with the AN/SPQ-9B shipboard radar to obtain three beams separated in azimuth.
(Provided by L. Leibowitz and B. Cantrell of the Naval Research Laboratory Radar Division.)

Lens Antennas[202] Microwave lenses may be constructed from dielectric materials, artificial dielectrics, or metal plates (waveguide media) to cause a focusing action similar to that of an optical lens. Dielectric lenses (the microwave analogy of the optical lens) are generally heavy and difficult to obtain with uniform properties. Lenses constructed from artificial dielectrics[203] can be made lighter but are usually poor conductors of heat so that it might be difficult to dissipate the heat generated in such materials when they are used for high-power radar transmitting antennas.

The metal-plate waveguide lens is constructed from side-by-side parallel-plate waveguides.[204] The phase velocity in a parallel-plate waveguide is greater than that in free space so that its index of refraction (and its dielectric constant) is less than unity, which is why they can be used to make lenses. They were used in early monopulse tracking radars to avoid aperture blockage caused by the large feed systems needed with reflector antennas.

The Luneburg lens[205] differs from optical lenses and other microwave lenses in that it is spherical and its index of refraction η is not uniform, but varies with distance from the center of the sphere as

$$\eta = \left[2 - (r/r_0)^2\right]^{1/2} \qquad [9.70]$$

where r is the radial distance and r_0 is the radius of the lens. It has the property that a plane wave incident on the sphere is brought to a focus on the surface at the diametrically opposite side. Likewise, a transmitting point source on the surface of the sphere emerges as a plane wave on passing through the lens. The beam of a Luneburg lens can be steered by moving the feed along the surface of the lens. With multiple feeds, it can form multiple simultaneous beams which was why it was seriously considered as the antenna for the Nike Zeus ballistic missile defense system, an early intercontinental ballistic missile defense system concept conceived in the late 1950s by Bell Telephone Laboratories for the U.S. Army (but never reached deployment).

The Fresnel zone-plate lens is an interesting form of lens that is simple, of small thickness, light weight, low loss, and low cost, especially for use at millimeter waves.[206] It has not had significant microwave radar application, however.

The lens antenna generally is less efficient than a reflector since unwanted reflections occur from both the front and rear surfaces of the lens. It is not as easy to support mechanically as is a reflector. Dielectric lenses have problems in dissipating heat when radiating high power. The lens antenna has interesting attributes, but it is not often used for radar application.

Radomes[207–209] Mechanical engineers can design a ground-based or shipborne antenna to be structurally strong enough to operate in high winds, icing, and other adverse weather conditions. It is often much cheaper and better, however, to enclose the antenna in an electromagnetically transparent protective shield called a *radome*. An antenna enclosed by a radome can be lighter and have a smaller drive motor than an antenna exposed to the elements.

Radomes for ground-based radars are often in the shape of a sphere (for example, a three-quarters sphere). The sphere is a good mechanical structure and offers aerodynamic advantages in high winds. Precipitation particles blow around a sphere rather than

impinge upon its surface, so that snow or other frozen particles are not readily deposited. Antennas mounted on aircraft must be housed within a radome that does not interfere with the aerodynamics of flight, be strong enough to be a part of the aircraft's structure, as well as not distort the antenna pattern.

A radome with good electromagnetic properties should be of low loss, have an adequate bandwidth, not raise the sidelobe level significantly, provide a low VSWR, a low antenna noise temperature, and not cause the boresight (pointing direction) to shift. In highly accurate tracking radars, the radome must also not increase the rate of change of the shift in the boresight.

There are two types of radomes that have been used for ground-based and shipboard radars: the rigid self-supporting radome and the air-supported radome.

Rigid Radomes An example of a rigid radome is the *space frame,* an example of which is shown in Fig. 9.55. This type of radome consists of a three-dimensional lattice of primary load-bearing structural members enclosed with thin dielectric panels (0.02–0.04 inch thick). The panels can be made of teflon-coated fiberglass and can be very thin, even for large radomes, since they do not carry the main loads or stresses. This type of construction whereby a spherical structure is constructed from flat panels of simple geometric shapes is sometimes called a *geodesic dome.* The supporting framework can be of steel, aluminum, or plastic. Metal structures are superior in electrical performance compared to plastic or fiberglass since they can be made smaller because of their increased strength. Smaller thickness means less aperture blocking. Metal space frames are generally cheaper

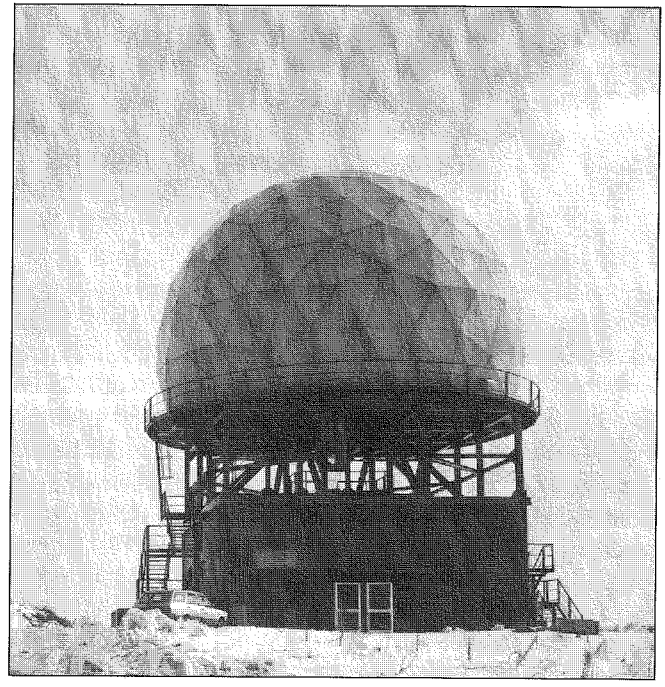

Figure 9.55 Rigid space-frame radome for the Argos-10 air-surveillance radar. (Courtesy Alfonso Farina and Alenia Marconi Systems.)

and easier to fabricate, transport, and assemble, and can be used for larger diameter configurations.

Aluminum structural members are typically used for the space frame. They are larger than steel of equivalent strength, but they are lightweight, noncorrosive, and require no maintenance. It is important that the plastic panels be able to repel water (hydrophobic) rather than absorb water. A hydrophobic material will cause the water on the radome surface to form into beads rather than coat the surface in a sheet or a film. Water in the form of beads usually has dimensions small compared to the radar wavelength and do not cause as much of an effect as a water film.[210] In some radomes, the exterior surface is coated with a white radar-transparent paint, such as Hypalon, to reduce the interior temperature rise caused by solar radiation. A material known as Tedlar has also been used as a surfacing material.

A metal space-frame radome might be made up of individual triangular panels with a relatively uniform pattern. Instead of panels of uniform shape, there can be a quasi-random selection of different panel sizes and shapes to minimize the periodicity of the structure and avoid the generation of spurious sidelobes obtained with a periodic structure. The randomization of the space frame also makes it less sensitive to polarization. A metal space-frame radome might typically have a transmission loss of 0.5 dB and cause the antenna sidelobes to increase an average of 1 dB at the −25 dB level. The boresite might be shifted less than 0.1 mrad and the antenna noise temperature might increase less than 5 K. Space-frame radomes can be larger than 150 ft in diameter, and they can be used at any microwave radar frequency. Typically they can be designed for wind speeds of 150 mph, but they have also been designed to withstand winds as high as 300 mph.

Rigid radomes also have been made of fiberglass-reinforced solid plastic laminates and as a rigid shell sandwich, but these are usually of smaller size than the space frame. Solid laminate radomes can be up to 35 ft in diameter and operate at frequencies up to 3 GHz. Panels are sometimes arranged in an "orange peel" geometry. Large-diameter sandwich radomes, which can be as large as 80 ft, are usually constructed with an A-type sandwich (described later), but are often narrowband.[207] Some *L*-band sandwich radomes for long-range FAA enroute ARSR radars have been said to have transmission efficiencies of 98 percent (less than 0.1 dB).[211]

Weather Effects on Rigid Radomes An important advantage of the rigid radome is its ability to withstand the rigors of severe climate. Rime ice, the prevalent type of icing in the Arctic region, has little or no effect on most radomes. Although it tends to collect on many types of structures and can obtain large thickness, both theory and experiment show a lack of rime-ice formation on a spherical radome.[212] The trajectories of water droplets in the air stream flowing around a large spherical radome do not impinge upon the surface. Droplets of freezing rain, on the other hand, are large and almost 100 percent of freezing rain can collect on the radome's surface. Dry snow does not stick to cold surfaces and is generally not a problem. Wet snow can stick to the radome and affect its transmission properties. Removal of snow by thermal means is expensive; but on the smaller radomes snow can be removed mechanically by tying a rope at the top of the radome and having someone walk the rope around the radome to knock off the snow.

Liquid water can collect on a radome as a film due to condensation or rainfall if the surface is non-hydrophobic. The films can be very thin and still cause attenuations of

several dB or more depending on the frequency and the amount of water. Effenberger et al.[213] state that at *X* band a water film can result in 8 dB of added transmission loss. If the water is in the form of droplets instead of a film, the added transmission loss is reduced to 1 dB. These losses compare to a loss of a dry air-supported radome of 0.1 dB and a dry metal space frame of 0.7 dB. Thus it is important that materials used for a radome not absorb water and not allow water to form a film on its surface. Radomes should be checked periodically to insure that their hydrophobic properties do not weaken with time.

Air-Supported Radomes The first large radomes for ground-based radar antennas that appeared shortly after World War II were constructed of a strong, flexible rubberized airtight material supported by air pressure from within. Since the radome material is relatively thin and uniform, it approximates the electrically thin shell that provides very low loss (less than 0.1 dB) and very small boresight error. The air-supported radome is constructed of gore-shaped fabric sections with the gores or seams in the vertical direction. Reliable operation depends on the use of uninterruptable power supplies and redundant blower systems. Teflon fiberglass is a commonly used material.[210] Air-supported radomes can be folded into a small package which makes them suitable for transportable radars requiring mobility and quick assembly and disassembly times. At a prepared site, a 50-ft air-supported radome can be installed in about one or two hours.[214] They are also of interest when wideband operation is important.

The life of an air-supported radome is limited by exposure to ultraviolet light, surface erosion, and the constant flexing of the material in the wind. The life can be increased by the use of better materials such as neoprene-coated nylon and teflon-coated fiberglass. In high winds the material can be damaged by flying debris. The rotation of the antenna might have to be stopped to prevent the fabric from being blown against the antenna and torn. Nevertheless, these structures are designed to withstand winds of 100 mph, and in special applications it has been extended to 200 mph.[215] Maintaining the internal pressure in high winds can sometimes be difficult. Frequent and costly maintenance is another problem. The air-supported radome has superior electrical properties to the rigid spaceframe radome, but the latter is much more rugged.

Aircraft Radomes[208,216] The shape of the radome used in the nose of a military fighter/attack aircraft is determined primarily by aerodynamic requirements rather than by electromagnetics. It is often an ogive or some other similar conical shape. Because of the aerodynamic shape of the nose radome, the angle of incidence of the beam on the surface of the radome depends on the scan angle and might be from 0 to 80°, or more. Also, the incident polarization can vary with angle of scan. This is unlike the situation with spherical shaped ground-based radomes where the incidence angle and polarization are relatively independent of the scan angle. Thus there can be distortions in the antenna pattern, spurious sidelobes, and angle errors that depend on the angle of scan. Airborne radomes, especially those used at supersonic speeds, can be subjected to mechanical stress and aerodynamic heating so severe that the electromagnetic requirements of a radome made of dielectric materials might have to be sacrificed in order to obtain sufficient mechanical strength to survive. Rain impinging on an unprotected radome in flight can cause

structural damage within minutes due to erosion at high subsonic speeds. Rain erosion is reduced by coating the radome surface with a shock-absorbing rubber-like material such as neoprene or polyurethane elastomer. A lightning strike can puncture a hole in the radome wall and severely damage the radar equipment inside. The damaging effects of lightning are reduced by placing conductors on the external surface of the radome to divert the lightning to these conductors rather than puncture the radome wall. If a large number of conductors is necessary to insure that lightning is diverted, the performance of the radar might be affected. Other factors in radome design are avoidance of static charge build-up and damage due to bird strike or the impact of hail. The radome must, in addition, withstand high temperatures and not be too heavy. It has been said[216] "Few, if any, other components [of an airborne radar system] have such a variety of conflicting requirements as does a radome."

Radome Wall Construction The following are some wall constructions that have been used in radomes:

Thin wall. The wall is electrically thin compared to the radar wavelength. If the wall physical thickness is d, with a dielectric constant ϵ, and a wavelength λ, then a thin wall radome is characterized by $d < 0.05\lambda/\sqrt{\epsilon}$. A thin wall radome has good electrical properties, but it can be weak structurally.

Half wavelength. This is a solid dielectric surface whose electrical thickness is approximately a half-wavelength. Theoretically, the halfwave-thick surface is nonreflecting and has no loss other than ohmic losses of the material. It is of limited bandwidth, as well as limited in the range of incidence angles over which the electromagnetic energy can be transmitted with minimal reflection. There can be multiple half-wave surfaces.

A-sandwich. A three-layer wall consisting of two thin relatively high-dielectric-constant skins separated by a low-dielectric-constant core whose thickness is approximately one-quarter wavelength. The skins are glass reinforced plastic laminates and are thin compared to a wavelength. The core might be a honeycomb or a foam.

B-sandwich. The inverse of the A-sandwich with quarter-wavelength skins having a dielectric constant lower than that of the core.

C-sandwich. Two back-to-back A-sandwiches. It is used when the ordinary A-sandwich does not provide sufficient strength.

Multilayer. A general term for more layers than that of the C-sandwich.

Metallic Radomes A thin metal sheet with periodically spaced openings (such as slots) has a bandpass characteristic and can be used for radomes. The metallic structure overcomes the mechanical limitations of radomes made of dielectric materials, yet has good electrical properties.[217] It also is better able to distribute frictionally induced heating and better able to withstand the stresses caused by rain, hail, dust, and lightning. This type of radome is a *frequency selective surface* that reduces interference because of its bandpass characteristic. It also reduces the nose-on radar cross section of the aircraft when viewed by radar systems not within its own passband.[218] The penalty for its use, however, is

narrow bandwidth. A frequency selective surface can be more sophisticated and have better properties than a thin metallic sheet with simple periodic slots.[219]

Rotodomes In some cases the radome is made to rotate in synchronism with the antenna. It is then called a *rotodome.* An example is the AWACS AN/APY-1 antenna, Fig. 3.45b, where the antenna and radome are designed together so that the antenna can maintain the very low sidelobes required of a high-prf pulse doppler radar. A rotodome is also used with the ASDE-3, see Fig. 1.9, the Airport Surface Detection Equipment found at the top of the control tower of major airports for monitoring taxiing aircraft and ground traffic at airports.

Adaptive Antennas[220–224] An adaptive antenna, usually an array, is one that senses the received signals incident across its aperture and adjusts the phase and amplitude of the aperture illumination to maximize the signal-to-external-noise ratio or signal-to-clutter ratio. Adaptive arrays usually require some prior knowledge of the desired signal and the nature of the noise or clutter to be rejected. When one speaks of a *fully adaptive array* it means one where each element of the array is part of the adaptive process. There have been many investigations of the theory and algorithms to perform adaptive array processing, but the difficulty and cost of implementing fully adaptive processing at each element of a large array antenna has been prohibitive. Until large fully adaptive arrays become more practical, they will be mainly of academic interest. There are, however, two important radar applications where adaptive array technology has proven to be practical and important. These occur when only a relatively few adaptive elements are needed. One such application is the *sidelobe canceler;* the other is the AEW radar that employs *space-time adaptive processing.*

Sidelobe Cancellation[225] This adaptively places nulls in the antenna radiation pattern in the direction of a limited number of noise jammers so as to reject the noise before it enters the receiver. A small number of omnidirectional (or wide beamwidth) auxiliary antenna elements are placed on or in the near vicinity of the main radar antenna. Typically there might be from 3 to 6 auxiliary elements used for the sidelobe canceler. The main radar antenna can be a reflector or a phased array. In theory, one auxiliary element (one degree of freedom) can create one adaptive null; but, in practice, especially when multipath propagation occurs, two auxiliary elements might be needed in some instances to place a suitable null in the direction of one noise source. The sidelobe canceler has been a successful application of adaptive antennas and has been applied operationally to a number of radar systems.

Space-Time Adaptive Processing (STAP) Military airborne MTI radars, or Airborne Early Warning (AEW) radars, must be able to cancel ground clutter echoes which have a non-zero doppler velocity with respect to the moving radar, along with hostile jamming that enters the radar via the antenna sidelobes. According to J. Ward[226] "Space-time adaptive processing (STAP) refers to multidimensional adaptive filtering algorithms that simultaneously combine the signals from the elements of an array antenna and the multiple pulses of a coherent radar waveform, to suppress interference and provide target

detection." Fred Staudaher,[227] of the Naval Research Laboratory, described the differences between spatial processing, temporal processing, and space-time processing as follows: "Spatial adaptive array processing combines an array of signals received at the same instant of time that are sampled at the different spatial locations corresponding to the antenna elements. Temporal adaptive array processing combines an array of signals received at the same spatial location (e.g., the output of a reflector antenna) that are sampled at different instances of time, such as several periods for an adaptive MTI. Space-time adaptive array processing combines a two-dimensional array of signals sampled at different instances of time and at different spatial locations."

STAP and other forms of antenna adaptive processing are more subjects in circuit design and algorithm development than antennas.

The Quest for Superresolution The ability of a radar to resolve two targets in angle depends on their relative radar cross section, signal-to-noise ratio, antenna beamwidth, the phase difference between the two signals, and the criterion used to establish resolution. It has been generally accepted that two equal targets can be resolved in angle when they are separated by eight-tenths of a beamwidth, provided the signal-to-noise ratio is large enough for good detection. Resolution can be better than this with high signal-to-noise ratios and a criterion which acknowledges that there can be a phase difference between the two signals. Every now and then, however, there have been different proposals for obtaining better angular resolution with radar systems—all without true success thus far!

A technique that has had impressive claims made for it is known as *spectral estimation* or *superresolution*.[228] It is also known by some of the many algorithms that are used, such as the maximum entropy method, autoregression, Burg algorithm, and others. These angular resolution methods apply for noncoherent sources, such as independent noise radiators (jammers or radio stars). Superresolution methods are basically the same as adaptive antennas which place sharp nulls in the direction of noise sources. Superresolution and adaptive antennas use the same algorithms and the same hardware, and the plots of their outputs are the same except that one is plotted upside down with respect to the other. That is, the nulls of the adaptive antenna become the narrow spikes of superresolution when inverted.

Superresolution may resolve closely spaced noise-like sources, but it does not reliably resolve the echoes from multiple targets illuminated by the same radar. The echoes from targets illuminated by the same radar have a phase relationship among each other and are thus coherent. Superresolution, or spectral estimation, algorithms employ nonlinear mathematical operations. When multiple echo signals from the same radar are subject to nonlinear processing, they can produce spurious signals that do not allow good resolution capabilities. Thus superresolution does not provide improved angular resolution with radar echo signals. This was first stated in the radar literature by A. W. Rihaczek.[229]

Other "Superresolution" Concepts In the traditional antenna literature, one can often find discussed the concept of a "superdirective" array antenna (formerly called supergain).[230] This is defined as an array antenna with a directivity higher than that obtained when the same antenna has a uniform aperture illumination. (Its antenna illumination efficiency is said to significantly exceed 100 percent.[231]) Many reasons have been offered why such an antenna is not practical (narrow bandwidth, high Q, large aperture currents, high loss, and

extremely precise tolerances), but supergain antennas require aperture illuminations that must change amplitude (spatially) across the aperture faster than can be expected of a signal operating at the given RF frequency. Superdirectivity appears to result from the simple algebraic models of an antenna pattern rather than as a solution to Maxwell's equations applied to a real radar antenna.

In the 1960s the *multiplicative array* was the "superresolution" technique that caused excitement, for a while. In a multiplicative array the outputs of the individual radiating elements were combined in a nonlinear manner rather than linearly. The nonlinear manipulation of the aperture illumination results in an apparently narrower antenna pattern. For example, the pattern of an N-element array can be expressed by a polynomial of degree N. If the output of one half of the array is multiplied by the output from the other half, the resulting expression is a polynomial of order $(N^2/4)$, which when plotted appears as a much narrower pattern of an array with $N^2/4$ elements rather than N. This narrower pattern looks exciting as a means for obtaining improved resolution by simple multiplicative processing of the array output. When two closely spaced targets are examined, however, with such multiplicative processing the resolution is not that of a larger array and, to make matters worse, there will be spurious signals generated because of the nonlinear mathematical operation. (The nonlinear operation of squaring or cubing the antenna pattern also will make it narrower and appear to provide better resolution than a conventional antenna, but when multiple targets are present, the resulting pattern is not the superposition of the individual patterns, but much worse.)

There have also been attempts to achieve improved resolution by what was called "data restoration," which smoothed the received aperture illumination and extrapolated it beyond the physical confines of the antenna. This also did not produce the significant improvement in resolution that was desired.

Thus one should not expect to obtain significantly better angular resolution with an antenna by some nonlinear form of antenna processing. There seems to be no magic radar resolution algorithm. The only method that has worked in the past for obtaining improved resolution when the electrical size of the aperture cannot be increased is to increase the signal-to-noise ratio and recognize in the resolution procedure that the echoes signals can be of different phase.

Microelectromechanical Switches in Phased Arrays[232,233] A microelectromechanical switch, or MEMS, is a small, low-inertia fast-acting switch activated by an electrostatic field. The switching mechanism may be in the form of a cantilever, rotary, or membrane configuration. In one example, the upper contact is a 0.3-μm aluminum membrane suspended across polymer posts. This suspended membrane is 4 μm above a substrate surface with the bottom contact of 0.7-μm gold or aluminum metal layer. On top of this metal layer is a thin dielectric layer, typically 0.1 μm (1000 Å) of silicon nitride. It is not a metallic contact switch, but switches by providing a change in capacitive impedance. The dielectric on the bottom part of the switch makes contact with the metallic portion of the suspended membrane, which eliminates the problem of striction that would occur if two metallic layers came into contact.

MEMS can have very wide bandwidth and can be made to operate with signals from a few MHz to 40 GHz. Measured insertion loss is less than 0.2 dB per switch. The switch

can activate in 2 to 5 μs and it can handle RF power up to 10 watts. The pull-in voltage is from 10 to 30 volts. Since a MEMS is activated by a d-c electrostatic field, no d-c current is required and power consumption is small. The energy required to activate a switch is on the order of 10 nJ.

The MEMS can be used in the same way that diode switches are used in the description of the digital phase shifter, shown in Fig. 9.17, to switch in and out fixed length of lines to obtain various phase shifts. In this type of *X*-band phase shifter the loss in a four-bit phase shifter is from 1.2 to 2 dB. Its size is approximately 6 mm by 9 mm. These phase shifters can be fabricated on silicon wafers. Hundreds of phase shifters can be built on a single 8-in. wafer, which makes them inherently low cost.

It has been said[234] that the MEMS for electronically scanned phased array radars has the potential to reduce the cost, weight, and power consumption for such systems when the array size exceeds 10,000 elements.

REFERENCES

1. Kraus, J. D. *Antennas,* 2nd ed. New York: McGraw-Hill, 1988, Sec. 10–12.
2. Probert-Jones, J. R. "The Radar Equation in Meteorology." *Quart. J. Roy. Meteor. Soc.* 88 (1962), pp. 485–495.
3. Stutzman, W. L. "Estimating Directivity and Gain of Antennas." *IEEE Antennas and Propagation Magazine* 40 (August 1998), pp. 7–11.
4. Evans, G. E. *Antenna Measurement Techniques,* Artech House, Boston, MA, 1990, p. 115.
5. Cutler, C. C., A. P. King, and W. E. Kock. "Microwave Antenna Measurements." *Proc. IRE* 35 (December 1947), pp. 1462–1471.
6. Sherman, J. W. "Aperture-Antenna Analysis." *Radar Handbook,* 1st ed., M. Skolnik (Ed.). New York: McGraw-Hill, 1970, Chap. 9.
7. Mints, M. Ya., Ye. D. Prilepskiy, and V. M. Zaslonko. "Optimization of the Radiation Power Concentration Factor of an Antenna with a Circular Aperture and a Maximally Flat Radiation Pattern." *Soviet J. of Communications Technology and Electronics* 34 (May 1989), pp. 33–39.
8. Silver, S. *Microwave Antenna Theory and Design,* vol. 12 of the M. I. T. Radiation Laboratory Series. New York: McGraw-Hill, 1949, Chap. 6.
9. Silver, S. Ref. 8, Sec. 6.5.
10. Sherman, J. W. Ref. 6, Sec. 9.2
11. Bodnar, D. G. "Materials and Design Data." *Antenna Engineering Handbook,* 3rd ed., R. C. Johnson (Ed.). New York: McGraw-Hill, 1993, Chap. 46, Sec. 46–5.
12. Jasik, H. "Fundamentals of Antennas." *Antenna Engineering Handbook,* 3rd ed., R. C. Johnson (Ed.), New York: McGraw-Hill, 1993, Chap. 2, Sec. 2.7.

13. Johnson, R. C. *Designer Notes for Microwave Antennas.* Boston: Artech House, 1991, Sec. A.12.

14. Cutler, C. C. "Parabolic Antenna Design for Microwaves." *Proc. IRE* 35 (November 1947), pp. 1284–1294.

15. Sciambi, A. F. "The Effect of the Aperture Illumination on the Circular Aperture Antenna Pattern Characateristics." *Microwave J.* 8 (August 1965), pp. 79–84.

16. Olver, A. D., P. J. B. Clarricoats, A. A. Kishk, and L. Shafai. *Microwave Horns and Feeds.* New York: IEEE Press, 1994.

17. Ruze, J. "Feed Support Blockage Loss in Parabolic Antennas." *Microwave J.* 11 (December 1968), pp. 76–80.

18. Kildal, P-S, E. Olson, and J. A. Aas. "Losses, Sidelobes, and Cross Polarization Caused by Feed-Support Struts in Reflector Antennas: Design Curves." *IEEE Trans.* AP-36 (February 1988), pp. 182–190.

19. Rudge, A. W., and N. A. Adatia. "Offset-Parabolic-Reflector Antennas: A Review." *Proc. IEEE* 66 (December 1978), pp. 1592–1618.

20. Cook, J. H., Jr. "Earth Station Antennas." *Antenna Engineering Handbook,* 3rd ed., R. C. Johnson (Ed.), New York: McGraw-Hill, 1993, Chap. 36, pp. 36-8 to 36-10.

21. Terada, M. A., and W. L. Stutzman. "Design of Offset-Parabolic-Reflector Antennas for Low Cross-Pol and Low Sidelobes." *IEEE Antennas and Propagation Magazine* 35, no. 6 (December 1993), pp. 436–449.

22. Terada, M. A., and W. L. Stutzman. "Computer-aided Design of Reflector Antennas." *Microwave J.* 38 (August 1995), pp. 64–73.

23. Weiss, H. G. "The Haystack Microwave Research Facility." *IEEE Spectrum* 2 (February 1965), pp. 50–59.

24. Hannan, P. W. "Microwave Antennas Derived from the Cassegain Telescope." *IRE Trans.* AP-9 (March 1961), pp. 140–153.

25. Josefsson, L. G. "A Broad-Band Twist Reflector." *IEEE Trans.* AP-19 (July 1971), pp. 552–554.

26. Lewis, B. L., and J. P. Shelton. "Mirror Scan Antenna Technology." *Record of the IEEE 1980 International Radar Conf.,* Arlington, VA, pp. 279–283. IEEE Publication 80CH1493-6 AES.

27. Dwight, H. B. *Tables of Integrals and Other Mathematical Data.* New York: Macmillan, 1947, Equation No. 420.3.

28. Bickmore, R. W. "A Note on the Effective Aperture of Electronically Scanned Arrays." *IRE Trans.* AP-6 (April 1958), pp. 194–196.

29. Elliott, R.S. "The Theory of Antenna Arrays." *Microwave Scanning Antennas,* R. C. Hansen, (Ed.). New York: Academic, 1966, vol. II, Chap. 1.

30. Koul, S. K., and B. Bhat. *Microwave and Millimeter Wave Phase Shifters, Vol. II, Semiconductor and Delay Line Phase Shifters.* Boston: Artech House, 1991.

31. Garver, R. V. *Microwave Diode Control Devices.* Boston: Artech House, 1976.

32. Tang, R., and R. W. Burns. "Phased Arrays." *Antenna Engineering Handbook,* 3rd ed., R. C. Johnson (Ed.). New York: McGraw-Hill, 1993, Chap. 20, pp. 20-36 to 20-44.

33. White, J. F. *Microwave Semiconductor Engineering.* New Jersey: Van Nostrand, 1982.

34. Temme, D. H. "Diode and Ferrite Phaser Technology." *Phased Array Antennas,* A. A. Oliner and G. H. Knittel (Eds.). Boston: Artech House, 1972, pp. 212–218.

35. Koul, S. K., and B. Bhat. Ref. 30, Chap. 11.

36. Andricos, C., I. J. Bahl, and E. L. Griffin. "C-Band 6-Bit Monolithic Phase Shifter." *IEEE Trans.* MTT-33 (December 1985), pp. 1591–1596.

37. Koul, S. K., and B. Bhat. Ref. 30, Chap. 12.

38. Shenoy, R. P. "Phased Array Antennas." *Advanced Radar Techniques and Systems,* G. Galati (Ed.). Peter Peregrinus, 1993, Chap. 10, Sec. 10.27.

39. Stark, L. "Microwave Theory of Phased Array Antennas—A Review." *Proc. IEEE* 62 (December 1974), pp. 1661–1701.

40. Koul, S. K., and B. Bhat. *Microwave and Millimeter Wave Phase Shifters, Vol. I, Dielectric and Ferrite Phase Shifters.* Boston: Artech House, 1991.

41. Rodrique, G. P. "A Generation of Microwave Ferrite Devices." *Proc. IEEE* 76 (February 1988), pp.121–137.

42. Stark, L., R. W. Burns, and W. P. Clark. "Phase Shifters for Phased Arrays," *Radar Handbook,* 1st ed., M. Skolnik (Ed.), New York: McGraw-Hill, 1970, Chap. 12.

43. Whicker, L. R. (Ed.). *Ferrite Control Devices, Vol. 2, Ferrite Phasers and Ferrite MIC Components.* Boston: Artech House, 1974.

44. Wicker, L. R., and R. R. Jones. "A Digital Current Controlled Latching Ferrite Phase Shifter." *IEEE 1965 International Convention Record,* pt. V, pp. 217–223.

45. Cattgasrin, G., et al. "A Digital Ferrite Phase-Shifter for High Power S-Band Operation." *Rivista Tecnica, Selenia* 8, no. 2 (1982), pp. 29–34.

46. Hord, W. E. "Microwave and Millimeter-Wave Ferrite Phase Shifters." *Microwave J.* 1989 State of the Art Reference, pp. 81–93.

47. Ince, W. J., and E. Stern. "Nonreciprocal Remanence Phase Shifters in Rectangular Waveguide." *IEEE Trans.* MTT-15 (February 1967), pp. 87–95.

48. Koul, S. K., and B. Bhat. Ref. 40, Sec. 4.8.

49. Junding, W., et al. "Analysis of Twin Ferrite Toroidal Phase Shifter in Grooved Waveguide." *IEEE Trans.* MTT-42 (April 1994), pp. 616–621.

50. DiBartolo, J., W. J. Ince, and D. H. Temme. "A Solid State 'Flux Drive' Control Circuit for Latching-Ferrite-Phaser Applications." *Microwave J.* 15 (September 1972), pp. 59–64.

51. Koul, S. K., and B. Bhat. Ref. 40, Sec. 5.6.

52. Fox, G. A., S. E. Miller, and M. T. Weiss. "Behavior and Application of Ferrites in the Microwave Region." *Bell System Tech. J.* 34 (January 1955), pp. 5–103.

53. Fox, A. G. "An Adjustable Wave-Guide Phase Changer." *Proc. IRE* 35 (September 1947), pp. 1489–1498.

54. Yansheng, X., and J. Zhengchang. "Dual-Mode Latching Ferrite Devices, Part I." *Microwave J.* 29 (May 1986), pp. 277–280.

55. Whicker, L. R., and C. W. Young, Jr. "The Evolution of Ferrite Control Components." *Microwave J.* 21 (November 1978), pp. 33–37.

56. Ince, W. J. "Recent Advances in Diode and Ferrite Phaser Technology for Phased-Array Radars, Part II." *Microwave J.* 15 (October 1972), pp. 31–36.

57. Yansheng, X., and J. Zhengchang. "Dual-Mode Latching Ferrite Devices, Part II." *Microwave J.* 29 (May 1986), pp. 282–286.

58. Monaghan, S. R., and M. C. Mohr. "Polarization Insensitive Phase Shifter for Use in Phased-Array Antennas." *Microwave J.* 12 (December 1969), pp. 75–80.

59. Hord, W. E. "Design Considerations for Rotary-Field Ferrite Phase Shifters." *Microwave J.* 31 (November 1988), pp. 105–115.

60. Boyd, C. R., Jr. "Progress in Ferrite Phase Shifters," Microwave Applications Group brochure, Santa Maria, CA (no date).

61. Varadan, V. K. "A Novel Microwave Planar Phase Shifter." *Microwave J.* 38 (April 1995), pp. 244–254.

62. Ajioka, J. S. "Frequency-Scan Antennas." *Antenna Engineering Handbook,* R. C. Johnson (Ed.), New York: McGraw-Hill, 1993, Chap. 19.

63. Hammer, I. W. "Frequency-Scanned Arrays." *Radar Handbook,* 1st ed., M. Skolnik (Ed.). New York: McGraw-Hill, 1970, Chap. 13.

64. Begovich, N. A. "Frequency Scanning." *Microwave Scanning Antennas, Vol. III,* R. C. Hansen (Ed.). New York: Academic, 1966, Chap. 2.

65. Johansson, F. S., L. G. Josefsson, and T. Lorentzon." A Novel Frequency-Scanned Reflector Antenna." *IEEE Trans.* AP-37 (August 1989), pp. 984–989.

66. Johansson, F. S. "Frequency-Scanned Gratings Consisting of Photo-Etched Arrays." *IEEE Trans.* AP-37 (August 1989), p. 996–1002.

67. Croney, J. "Doubly Dispersive Frequency Scanning Antenna." *Microwave J.* 6 (July 1963), pp. 76–80.

68. Tang, R. "Practical Aspects of Phased Array Design." *Antenna Handbook,* Y. T. Lo and S. W. Lee (Ed.). New York: Van Nostrand Reinhold, 1988, Chap. 18, pp. 18-6 to 18-11.

69. Hansen, R. C. *Phased Array Antennas.* New York: John Wiley, 1998, Chap. 5.

70. Hansen, R. C. Ref. 69, Sec. 8.2.

71. Stark, L. "Comparison of Array Element Types." *Phased Array Antennas, Proc. 1970 Phased Array Antenna Symp.* Dedham, MA: Artech House, 1972, pp. 51–67.

72. Tang, R., and R. W. Burns. "Phased Arrays." *Antenna Engineering Handbook,* 3rd ed., R. C. Johnson (Ed.). New York: McGraw-Hill, 1993, Chap. 20.

73. Edward, B., and D. Rees. "A Broadband Printed Dipole with Integrated Balun." *Microwave J.* 35 (May 1987), pp. 339ff.

74. Mailloux, R. J. *Phased Array Antenna Handbook.* Boston: Artech House, 1994.

75. Richard, W. F. "Microstrip Antennas." *Antenna Handbook,* Y. T. Lo and S. W. Lee (Eds.). New York: Van Nostrand Reinhold, 1988, Chap. 10.

76. Lewis, L. R. "Phased Array Elements—Part 2." In *Practical Phased Array Antenna Systems,* E. Brookner (Ed.). Boston: Artech House, 1991, Lecture 5.

77. Cheston, T. C., and J. Frank. "Phased Array Radar Antennas." *Radar Handbook,* 2nd ed., M. Skolnik (Ed.). New York: McGraw-Hill, 1990, Chap. 7, pp. 7.31–7.32.

78. Mailloux, R. J. Ref. 74, Chap. 6.

79. Hansen, R. C. Ref. 69, Chap. 7.

80. Hannan, P. W. "The Element-gain Paradox for a Phased-Array Antenna." *IEEE Trans.* AP-12 (July 1964), pp. 423–433.

81. Pozar, D. M., and D. H. Schaubert. "Scan Blindness in Infinite Arrays of Printed Dipoles." *IEEE Trans.* AP-32 (June 1984), pp. 602–610.

82. Byron, E. V., and J. Frank. "'Lost Beams' from a Dielectric Covered Phased-Array Aperture." *IEEE Trans.* AP-16 (July 1968), pp. 494–499.

83. King, D. D., and H. J. Peters. "Element Interaction in Steerable Arrays." *Microwave J.* 6 (February 1963), pp. 73–77.

84. Mailloux, R. J. Ref. 78, p. 314.

85. Kinsel, J., B. J. Edward, and D. E. Rees. "V-Band Space-Based Phased Arrays." *Microwave J.* 30 (January 1987), pp. 89–102.

86. Mailloux, R. J. "Phased Array Architecture." *Proc. IEEE* 80 (Jaunary 1992), pp. 163–172. See also Mailloux, Ref. 74, Sec. 5.3.1.

87. Patton, W. T. "Array Feeds." In *Practical Phased-Array Antenna Systems,* E. Brookner (Ed.). Boston: Artech House, 1991, Lecture 6.

88. Hansen. R. J. Ref. 69, Secs. 2.3.4 and 2.3.5.

89. Smith, M. S., and Y. C. Guo. "A Comparison of Methods for Randomizing Phase Quantization Errors in Phased Arrays." *IEEE Trans.* AP-31 (November 1983), pp. 821–828.

90. Cheston, T. C., and J. Frank. Ref. 77, Sec. 7.8.

91. Cheston, T. C., and J. Frank. Ref. 77, pp. 7.53–7.55.

92. Patton, W. T. "Compact, Constrained Feed Phased Array for the AN/SPY-1." In *Practical Phased-Array Antenna Systems,* E. Brookner (Ed.). Boston: Artech House, 1991, Lecture 8.

93. Sharp, E. D. "A Triangular Arrangement of Planar-Array Elements that Reduces the Number Needed." *IRE Trans.* AP-9 (March 1961), pp. 126–129.

94. Cheng, D. H. S. "Characteristics of Triangular Lattice Arrays." *Proc. IEEE* 56 (November 1968), pp. 1811–1817.

95. Nelson, E. A. "Quantization Sidelobes of a Phased Array with a Triangular Element Arrangement." *IEEE Trans.* AP-17 (May 1969), pp. 363–365.

96. Agrawal, A. K., and E. L. Holzman. "Beamformer Architectures for Active Phased-Array Radar Antennas." *IEEE Trans.* AP-47 (March 1999), pp. 432–442.

97. Holzman, E. L., A. K. Agrawal, and J. G. Ferrante. "Active Phased Array Design-for High Clutter Improvement Factor." *1996 IEEE International Symposium on Phased Array Systems and Technology,* October 15–18, 1996, IEEE Catalog Number 96TH8175, pp. 44–47.

98. Reed, J. E. "The AN/FPS-85 Radar System." *Proc. IEEE* 57 (March 1969), pp. 324–335.

99. Grimes, M. D., J. M. Major, and T. J. Warnagiris. "Peak Power Tailoring and Phase Nulling of the AN/FPS-85 Radar." *SPIE* 2154, *Intense Microwave Pulses II,* pp. 241–246, 1994.

100. Brookner, E. *Aspects of Modern Radar.* Boston: Artech House, 1988, Sec. 2.2.1.2, p. 198, and pp. 279–281.

101. Sarcione, M., et al. "The Design, Development and Testing of the THAAD (Theater High Altitide Area Defense) Solid State Phased Array (formerly Ground Based Radar)." *1996 IEEE International Symp. on Phased Array Systems and Technology,* October 15–18, 1996, IEEE Catalog Number 96TH8175, pp. 260–265.

102. Dryer, et al. "EL/M 2080 ATBM Early Warning and Fire Control Radar System." *1996 IEEE International Symp. on Phased Array Systems and Technology,* October 15–18, 1996, IEEE Catalog Number 96TH8175, pp. 11–16.

103. Malas, J. A. "F-22 Radar Development." *Proc. IEEE 1997 NAECON* 2, pp. 831–839, IEEE Catalog no. CH36015-97.

104. Barton, D. K. "The 1993 Moscow Air Show." *Microwave J.* 37 (May 1994), pp. 24ff.

105. Corey, L. E. "A Survey of Russian Low Cost Phased-Array Technology." *1996 IEEE International Symp. on Phased Array Systems and Technology,* October 15–18, 1996, IEEE Catalog Number 96TH8175, pp. 255–259.

106. Ajioka, J. S., and J. L. McFarland. "Beam-Forming Feeds." Chap. 19, *Antenna Handbook,* Y. T. Lo and S. W. Lee (Ed.). New York: Van Nostrand Reinhold, 1988. See also references 86 to 100, Chap. 8. In *Introduction to Radar Systems,* 2nd ed. M. Skolnik.

107. Shelton, J. W. "Fast Fourier Transform and Butler Matrices." *Proc. IEEE* 56 (March 1968), p. 350.

108. White, W. D. "Pattern Limitations in Multiple-Beam Antennas." *IRE Trans.* AP-10 (July 1962), pp. 430–436.

109. Barton, P. "Digital Beam Forming of Radar." *IEE Proc.* 127, Pt. F., No. 4 (August 1980).

110. Steyskal, H., and J. F. Rose. "Digital Beamforming for Radar Systems." *Microwave J.* 32 (January 1989), pp. 121ff.

111. Steyskal, H. "Digital Beamforming at Rome Laboratory." *Microwave J.* 39 (February 1996), pp. 100ff.

112. Farina, A. *Antenna-Based Signal Processing Techniques for Radar Systems.* Boston: Artech House, 1992, Sec. 2.7.

113. Skolnik, M. "Improvements for Air-Surveillance Radar." *Proc. 1999 IEEE Radar Conf.* April 20–22, 1999, IEEE Catalog Number 99CH36249, pp. 18–21.

114. Steyskal, H., and J. S. Herd. "Mutual Coupling Compensation in Small Array Antennas." *IEEE Trans.* AP-38 (December 1990), pp. 1971–1975.

115. Lewis, B. L., F. F. Kretschmer, and W. W. Shelton. *Aspects of Radar Signal Processing.* Norwood, MA: Artech House, 1986, Chap. 3.

116. Brookner, E., and J. M. Howell, "Adaptive-Adpative Array Processing." *Proc. IEEE* 74 (April 1986), pp. 602–604.

117. Gabriel, W. F. "Using Spectral Estimation Techniques in Adaptive Processing Antenna Systems." *IEEE Trans.* AP-34 (April 1986), pp. 291–300.

118. Mailloux, R. J. "Array Failure Correction with a Digitally Beamformed Array." *IEEE Trans.* AP-44 (December 1996), pp. 1543–1550.

119. Wirth, W. D. "Long Term Integration for a Floodlight Radar." *1995 IEEE International Radar Conf.* Arlington, VA, pp. 698–703.

120. Headrick, J. M. "HF Over-the-Horizon Radar." *Radar Handbook,* M. Skolnik (Ed.). New York: McGraw-Hill, 1990, Chap. 24.

121. Sparks, R. A. "Systems Applications of Mechanically Scanned Array Antennas." *Microwave J.* 31 (June 1988), pp. 26–48.

122. Richardson, P. N., and H. Y. Yee. "Design and Analysis of Slotted Waveguide Antenna Arrays." *Microwave J.* 31 (June 1988), pp. 109ff.

123. Yee, H. Y, and R. C. Voges. "Slot-Antenna Arrays." *Antenna Engineering Handbook.* 3rd ed., R. C. Johnson (Ed.), New York: McGraw-Hill, 1993, Chap. 9.

124. Watson, C. K., and K. Ringer. "Feed Network Design for Airborne Monopulse Slot-Array Antennas." *Microwave J.* 31 (June 1988), pp. 129ff.

125. Kraus, J. D. *Antennas,* 2nd ed., New York: McGraw-Hill, 1988, Sec. 4.6.

126. Butler, J. M., A. R. Moore, and H. D. Griffiths. "Resource Management for a Rotating Multi-Function Radar." *Radar-97, 14-16 October 1997,* IEE Publication No. 449, pp. 568–572.

127. Billam, E. R. "Rotating vs Fixed Active Arrays for Multifunction Radar." *Radar-97, 14-16 October 1997,* IEE Publication No. 449, pp. 573–575.

128. Mailloux, R. J. Ref. 74, Chap. 3, "Pattern Synthesis for Linear and Planar Arrays."

129. Dolph, C. L. "A Current Distribution for Broadside Arrays Which Optimizes the Relationship between Beamwidth and Side Lobe Level." *Proc. IRE* 34 (June 1946), pp. 335–348; also discussion by H. J. Riblet, vol. 35, pp. 489–492.

130. Taylor, T. T. "Design of Line-Source Antennas for Narrow Beamwidth and Low Side Lobes." *IRE Trans.* AP-3 (January 1955), pp. 16–28.

131. Hansen, R. C. "Linear Arrays." *Handbook of Antenna Design,* vol. 2, A. W. Rudge, K. Milne, A. D. Oliver, and P. Knight (Eds.). London: Peter Peregrinus, 1983, Chap. 9.

132. Hansen, R. C. "Measurement Distance Effects on Low Sidelobe Patterns." *IEEE Trans.* AP-32 (June 1984), pp. 591–594.

133. Taylor, T. T. "Design of Circular Apertures for Narrow Beamwidths and Low Sidelobes." *IRE Trans.* AP-8 (January 1960), pp. 17–22.

134. White, W. D. "Desirable Illuminations for Circular Aperture Arrays." Institute for Defense Analyses, Arlington, VA, Research paper P-351, IDA Log No. HQ 67–6476, December 1967.

135. White, W. D. "Circular Aperture Distribution Functions." *IEEE Trans.* AP-25 (September 1977), pp. 714–716.

136. Elliott, R. S. *Antenna Theory and Design.* Englewood Cliffs, NJ: Prentice-Hall, 1981.

137. Bayliss, E. T. "Design of Monopulse Antenna Difference Patterns with Low Sidelobes." *Bell System Tech. J.* 47 (May–June 1968), pp. 623–650.

138. Hansen, R. C. *Phased Array Antennas.* New York: John Wiley, 1998, Sec. 3.7.

139. Lopez, A. R. "Sharp Cutoff Radiation Patterns." *IEEE Trans.* AP-27 (November 1979), pp. 820–824.

140. Ruze, J. "Physical Limitations on Antennas." MIT Research Lab. Electronics Tech, Rept. 248, Oct. 20, 1952; or see p. 255 of the 2nd ed. of this text.

141. Shrader, W. W., and V. Gregers-Hansen. "MTI Radar." *Radar Handbook,* 2nd ed., M. Skolnik (Ed.). New York: McGraw-Hill, 1990, Chap. 15, Fig. 15.64.

142. Ruze, J. "Antenna Tolerance Theory—A Review." *Proc. IEEE* 54 (April 1966), pp. 633–640.

143. Ruze, J. "Physical Limitations on Antennas." MIT Research Lab. Electronics Tech. Rept. 248, Oct. 30, 1952.

144. Skolnik. M. I. "Nonuniform Arrays." *Antenna Theory,* Pt I, R. E. Collin and F. J. Zucker (Eds.). New York: McGraw-Hill, 1969, Chap. 6, Sec. 6.6.

145. Rondinelli, L. A. "Effects of Random Errors on the Performance of Antenna Arrays of Many Elements." *IRE Natl. Conv. Record* 7, pt. 1 (1959), pp. 174–187.

146. Lichter, M. "Beam-Pointing Errors of Long Line Sources." *IRE Trans.* AP-8 (May 1960), pp. 268–275.

147. Hsiao, J. K. "Design of Error Tolerance of a Phased Array." *Electronic Letters* 21, no. 19 (September 12, 1985), pp. 834–836.

148. Hsiao, J. K. "Array Sidelobes, Error Tolerance, Gain, and Beamwidth." Naval Research Laboratory, Washington, D.C., Report 8841, September 28, 1984.

149. Cheston, T. C., and J. Frank. "Phased Array Radar Antennas." Chap. 7, *Radar Handbook,* 2nd ed., M. I. Skolnik (Ed.), New York: McGraw-Hill, 1990, p. 7.41.

150. Cheston, T. C., and J. Frank. Ref. 149, Sec. 7.6.

151. Miller, C. J. "Minimizing the Effects of Phase Quantization in an Electronically Scanned Array." *Proc. of Symp. on Electrically Scanned Array Techniques and Applications,* Rome Air Development Center Technical Documentary Report RADC-TDR-64–225, vol. 1, pp. 17–38, July, 1964.

152. Evans, G. E., and H. E. Schrank. "Low-Sidelobe Radar Antennas." *Microwave J.* 26 (July 1983), pp. 109–117.

153. Schrank, H. E. "Low Sidelobe Phased Array Antennas." *IEEE APS Newsletter* (April 1983), pp. 5–9.

154. White, W. D. "Desirable Illuminations for Circular Aperture Antennas, Research Paper P-351." Institute for Defense Analyses, Arlington, VA, December 1967.

155. Ludwig, A. C. "Low Sidelobe Aperture Distribution for Blocked and Unblocked Circular Apertures." *IEEE Trans.* AP-30 (September 1982), pp. 933–946.

156. Taylor, T. T. "Design of Circular Apertures for Narrow Beamwidth and Low Sidelobes." *IRE Trans.* AP-8 (January 1960), pp. 17–22.

157. Green, T. J. "The Influence of Masts on Ship-Borne Radar Performance." *Radar-77, IEE (London) Conference Publication* no. 155 (October 1977), pp. 405–408.

158. Mangulis, V. "Effective Sidelobe Levels Due to Scatterers." *IEEE Trans.* AES-15 (May 1979), pp. 325–333.

159. Mangulis, V. "Antenna Sidelobes in the Presence of Flat Reflectors." *IEEE Trans.* AES-30 (October 1994), pp. 1122–1125.

160. Scorer, M. "The Calculaton of Radome Induced Sidelobes." *Radar-77,* IEE (London) Conference Publication No. 155 (October 1977), pp. 414–418.

161. Ricardi, L. J. "Radiation Properties of the Binomial Array." *Microwave J.* 15 (December 1972), p. 20.

162. Krall, A. D., D. G. Jablonski, and J. Coughlin. "Radiation Properties of a 'Gaussian' Antenna." *Microwave J.* 27 (May 1984), pp. 283 & 288.

163. Patton, W. T. "Low-Sidelobe Antennas for Tactical Phased-Array Radars." *RCA Engineer* 27 (Sept./Oct 1982), pp. 31–36.

164. Maine, E. E., Jr., and J. M. Willey. The Fixed Array Surveillance Radar, private communication.

165. Schrank, H. E. "Low Sidelobe Reflector Antennas." *IEEE APS Newsletter,* (April 1985), pp. 5–16.

166. Scudder, R. M. "Advanced Antenna Design Reduces Electronic Countermeasures Threat." *RCA Engineer* 23 (Feb./Mar. 1978), pp. 61–65.

167. Williams, N., P. Varnish, and D. J. Browning. "Reduced Cost Low Sidelobe Reflector Antenna Systems." *IEE (London) International Conf. Radar-82* (October 1982), pp. 351–354.

168. Fante, R. L., P. R. Franchi, N. R. Kerweis, and L. F. Dennett. "A Parabolic Cylinder Antenna with Very Low Sidelobes." *IEEE Trans.* AP-28 (January 1980).

169. Evans, G. E. *Antenna Measurement Techniques.* Boston: Artech House, 1990.

170. Hacker, P. S., and H. E. Schrank. "Range Distance Requirements for Measuring Low and Ultralow Sidelobe Antenna Patterns." *IEEE Trans.* AP-30 (September 1982), pp. 956–966.

171. Tang, R., and R. Brown. "Cost Reduction Techniques for Phased Arrays." *Microwave J.* 30 (January 1987), pp. 139–146.

172. Skolnik, M. "The Radar Antenna—Circa 1995." *J. Franklin Inst.* 332B, no. 5 (May 1995), pp. 503–519.

173. Cheston, T. C., and J. Frank. "Phased Array Radar Antennas." Chap. 7, *Radar Handbook,* M. Skolnik (ed.) New York: McGraw-Hill, 1990, Chap. 7, Sec. 7.7.

174. Mailloux, R. J. Ref. 74, Sec. 8.3.

175. Smolders, A. B. "Design and Construction of a Broadband Wide-Scan-Angle Phased-Array Antenna with 4096 Radiating Elements." *1996 IEEE International Symp. on Phased Array Systems and Technology,* Boston, MA, October 15–18, 1996, pp. 87–92.

176. Baugh, R. A. *Computer Control of Modern Radars.* published by RCA Corp., (now Lockheed Martin) Aegis Department, Moorestown, NJ, 1973.

177. Huizing, A. G., and A. A. F. Bloemen. "An Efficient Scheduling Algorithm for a Multifunction Radar." *1996 IEEE International Symp. on Phased Array Systems and Technology,* Boston, MA, October 15–18, 1996, pp. 359–364.

178. Billam, E. R. "The Problem of Time in Phased Array Radar." *Radar-97,* October 14–16, 1997, IEE Publication No. 449, pp. 563–567.

179. Bony, Gilbert. "Electrically Controlled Dielectric Panel Lens," United States Patent No. 3,708,796, Jan. 2, 1973.

180. Skolnik, M. I. "The Radar Antenna—Circa 1995." *J. Franklin Institute,* 332B, No. 5 (1995), pp. 503–519.

181. Chekroun, C., et al. "RADANT. New Method of Electronic Scanning." *Microwave J.* 24 (February 1981), pp. 45–53.

182. Rao, J. B. L., G. V. Trunk, and D. P. Patel. "Two Low-Cost Phased Arrays." *1996 IEEE International Symp. on Phased Array Systems and Technology,* Boston, MA, October 15–18, 1996, pp. 119–124.

183. Colin, Jean-Marie. "Phased Array Radars in France. Present & Future." *1996 IEEE International Symp. on Phased Array Systems and Technology,* Boston, MA, October 15–18, 1996, pp. 458–462.

184. Rao, J. B. L., D. P. Patel, and V. Krichevsky. "Voltage-Controlled Ferrolelectric Lens Phased Arrays." *IEEE Trans.* AP-47 (March 1999), pp. 458–468.

185. Mailloux, R. J. "Conformal and Low-Profile Arrays." *Antenna Engineering Handbook,* 3rd ed., R. C. Johnson (Ed.). New York: McGraw-Hill, Chap. 21, 1993.

186. Hsiao, J. K. "Approximation of a Conformal Array with Multiple, Simultaneously Excited Planar Arrays," Naval Research Laboratory, Washington, D. C., Report 7442, July 28, 1972.

187. Skolnik, M. I. "Nonuniform Arrays." *Antenna Theory,* pt. I, R. E. Collin and F. J. Zucker (Eds.). New York: McGraw-Hill, 1969, Chap. 6.

188. Mailloux, R. J. *Phased Array Antenna Handbook.* Boston: Artech House, 1994, Sec. 2.4.

189. Skolnik, M. I., G. Nemhauser, and J. W. Sherman. "Dynamic Programming Applied to Unequally Spaced Arrays." *IEEE Trans.* AP-12 (January 1964), pp. 35–43.

190. Skolnik, M. I., J. W. Sherman, and F. C. Ogg. "Statistically Designed Density-Tapered Arrays." *IEEE Trans.* AP-12 (July 1964), pp. 408–417.

191. Hall, W. P., Jr., and R. D. Nordmeyer. "Active-Element, Phased Array Radar: Affordable Performance for the 1990s." *IEEE National Telesystems Conf. Proc.,* Atlanta, GA, pp. 193–197, March 26 and 27, 1991.

192. Cross, D. C., D. D. Howard, and J. W. Titus. "Mirror-Antenna Radar Concept." *Microwave J.* 29 (May 1986), pp. 323–335.

193. Orleansky, E., C. Samson, and M. Havkin. "A Broadband Meanderline Twistreflector for the Inverse Cassegrain Antenna." *Microwave J.* 30 (October 1987), pp. 185–192.

194. Lewis, B. L., and J. P. Shelton. "Mirror Scan Antenna Technology." *1980 IEEE International Radar Conf.,* Washington, D.C., pp. 279–283, April 1980.

195. Ruze, J. "Lateral Feed Displacement of a Paraboloid." *IEEE Trans.* AP-13 (September 1965), pp. 660–665.

196. Imbriale, W. A., P. G. Ingerson, and W. C. Wong. "Large Lateral Feed Displacement in a Parabolic Reflector." *IEEE Trans.* AP-22 (November 1974), pp. 742–745.

197. Kelleher, K. S., and H. H. Hibbs. "A New Microwave Reflector." Naval Research Laboratory, Washington, D.C., Report 4141, 1953.

198. Kelleher, K. S., and G. Hyde. "Reflector Antennas." *Antenna Engineering Handbook,* 3rd ed., R. C. Johnson (Ed.). New York: McGraw-Hill, 1993, Chap. 17, pp. 17-46 to 17.52.

199. Kelleher, K. S. "Electromechanical Scanning Antennas." *Antenna Engineering Handbook.* 3rd ed., R. C. Johnson (Ed.). New York: McGraw-Hill, 1993, Chap. 18, pp. 18-23 to 18-24.

200. Rappaport, C. M., and W. P. Craig. "High Aperture Efficiency Symmetric Reflector Antennas with up to 60° Field of View." *IEEE Trans.* AP-39 (March 1991), pp. 336–344.

201. Craig, W. P., C. M. Rappaport, and J. S. Mason. "A High Aperture Efficiency, Wide-Angle Scanning Offset Reflector Antenna." *IEEE Trans.* AP-41 (November 1993), pp. 1481–1490.

202. Bodnar, D. G. "Lens Antennas." *Antenna Engineering Handbook,* 3rd ed., R. C. Johnson (Ed.). New York: McGraw-Hill, 1993, Chap. 16.

203. Harvey, A. F. "Optical Techniques at Microwave Frequencies." *IEE Proc.* 106, pt. B (March 1959), pp. 141–157. Contains an extensive bibliography.

204. Kock, W. E. "Metal Lens Antennas." *Proc. IRE* 34 (November 1946), pp. 828–836.

205. Luneburg, R. K. *Mathematical Theory of Optics.* Berkeley: University of California, 1964. (Originally mimeographed lecture notes, Brown University Graduate School, Providence, R.I., 1944.)

206. Wiltse, J. C., and J. E. Garrett. "The Fresnel Zone Plate Antenna." *Microwave J.* 34 (January 1991), pp. 101–114.

207. Huddleston, G. K., and H. L. Bassett. "Radomes." *Antenna Engineering Handbook,* 3rd ed., R. C. Johnson (Ed.), New York: McGraw-Hill, 1993, Chap. 44.

208. Walton, J. D., Jr. *Radome Engineering Handbook.* New York: Marcel Dekker, 1970.

209. Schrank, H. E., G. E. Evans, and D. Davis. "Reflector Antennas." *Radar Handbook,* 2nd ed., M. Skolnik (Ed.). New York: McGraw-Hill, 1990, Chap. 6. Sec. 6.9.

210. Electronic Space Systems Corporation (Essco) Web site, 1998.

211. Hughes, D. "New FAA Radomes to Have 98% Transmission Efficiency." *Aviation Week & Space Technology* (January 10, 1994), pp. 66–67.

212. Vitale, J. A. "Large Radomes." *Microwave Scanning Antennas,* Vol. 1." R. C. Hansen (Ed.). New York: Academic, 1964, Chap. 5.

213. Effenberger, J. A., R. R. Strickland, and E. B. Joy. "The Effect of Rain on a Radome's Performance." *Microwave J.* 29 (May 1986), pp. 261–274.

214. Punnett, M. S. "Developments in Ground Mounted Air Supported Radomes." *IEEE 1977 Mechanical Engineering in Radar Symposium,* Nov. 8–10, 1977, Arlington, VA, pp. 40–45, IEEE Publication 77CH1250-0 AES.

215. Advertising brochure "Engineered Fabric Structures," from Birdair Structures Division, North Bennington, Vermont (no date).

216. Conti, D. A. "Special Problems Associated with Aircraft radomes." *IEE Proc.* 128, Pt. F, no. 7 (December 1981), pp. 412–418.

217. Pelton, E. L., and B. A. Munk. "A Streamlined Metallic Radome." *IEEE Trans.* AP-22 (November 1974), pp. 799–803.

218. Knott, E. F., J. F. Shaeffer, and M. T. Tuley. *Radar Cross Section,* 2nd ed. Boston: Artech House, 1993, Sec. 10.4.

219. Mittra, R., C. H. Chan, and T. Cwik. "Techniques for Analyzing Frequency Selective Surfaces—A Review." *Proc. IEEE* 76 (December 1988), pp. 1593–1615.

220. Farina, A. *Antenna-Based Signal Processing Techniques for Radar Systems.* Boston: Artech House, 1992.

221. Nitzberg, R. *Adaptive Signal Processing for Radar.* Boston: Artech House, 1992.

222. Widrow, B., and S. D. Stearns. *Adaptive Signal Processing.* Englewood Cliffs, NJ: Prentice-Hall, 1985.

223. Gabriel, W. F. "Adaptive Arrays—An Introduction." *Proc. IEEE* 64 (February 1976), pp. 239–272.

224. Gabrial, W.F. "Adaptive Processing Array Systems." *Proc. IEEE* 80 (January 1992) pp. 1521–162.

225. Howells, P. W. "Explorations in Fixed and Adaptive Resolution at GE and SURC." *IEEE Trans.* AP-24 (September 1976), pp. 575–584.

226. Ward, J. "Space-Time Processing for Airborne Radar." MIT Lincoln Laboratory Technical Report 1015, December 13, 1994.

227. Staudaher, F. M. "Airborne MTI." *Radar Handbook,* M. Skolnik (Ed.). New York: McGraw-Hill, 1990, Chap. 16, Sec. 16.8.

228. Gabriel, W. F. "Spectral Analysis and Adaptive Array Superresolution Techniques." *Proc. IEEE* 68 (June 1980), pp. 654–666.

229. Rihaczek, A. W. "The Maximum Entropy of Radar Resolution." *IEEE Trans.* AES-17 (January 1981), p. 144.

230. Hansen, R. C. *Phased Array Antennas.* New York: John Wiley, 1998, Chap. 9.

231. *IEEE Standard Dictionary of Electrical and Electronics Terms.* New York: IEEE, 1988.

232. Pugh, M. L., et al. "Electromechanically Scanned Arrays Using Micro Electro Mechancical Swith (MEMS) Technology." *Proc. 5th International Conf. on Radar Systems,* Brest, France, May, 1999, Subassemblies Section.

233. Smith, J. K., F. W. Hopwood, and K. A. Leahy, "MEM Switch Technology in Radar." *Record of the IEEE 2000 International Radar Conference*, Alexandria, VA, pp. 193–198.

234. Norvell, B. R., et al. "Micro Electro Mechanical Switch (MEMS) Technology Applied to Electrically Scanned Arrays (ESA)." *Proc. International Radar Symp. (IRS 98),* Munich Germany, September 15–17, 1998, vol. II, German Institute of Navigation.

PROBLEMS

9.1 (a) Derive the expression for the field-intensity pattern for a uniformly illuminated line-source aperture of dimension D. (b) Make a rough sketch of its radiation (power) pattern (with the ordinate in dB). (c) If the antenna dimension is 60 wavelengths, what is the width between the first nulls that define the main beam? (d) What is its half-power beamwidth?

9.2 The pattern of problem 9.1 also is the pattern from either of the two principal planes of a uniformly illuminated square aperture. Derive the field-intensity pattern in the diagonal plane of the square aperture, where the aperture illumination is triangular. (The triangular illumination is also known as a *gabled illumination.* It can be expressed as $A(z) = 1 - \frac{2}{D_g}|z|$, where $|z| \leq D_g/2$, and D_g is the diagonal of the square aperture.)

9.3 Determine and roughly sketch the field-intensity pattern for an antenna with the following aperture illumination pattern:

$$A(z) = -1 \text{ for } -D/2 < z < 0$$

$$A(z) = 0 \text{ for } z = 0$$

$$A(z) = +1 \text{ for } 0 < z < +D/2$$

where D = aperture dimension. What is the peak sidelobe level? (This is the difference pattern that would be obtained from an antenna whose sum pattern is of the form $(\sin x)/x$ obtained with a uniform aperture as in problem 9.1.)

9.4 Calculate and sketch the field-intensity pattern produced by an aperture illumination of a line source of dimension D given by $A(z) = \cos(\pi z/D)$. What is its null width (width between the two nulls defining the main beam), and what is the level of the first sidelobe?

9.5 In what manner is the field-intensity pattern $E(\phi)$ of an antenna, Eq. (9.10), and its aperture illumination $A(z)$ related to the time waveform $s(t)$ and the spectrum $S(f)$? Identify the analogous pairs of parameters between these two relationships?

9.6 Efficiency is generally defined as the ratio of the output power to the input power. The "aperture efficiency" of a reflector antenna, Eq. (9.9), is not defined in this manner and the term aperture "efficiency" can therefore be misleading. Discuss the effect of the aperture efficiency on radar performance and why it should not be interpreted as an indicator of a power loss.

9.7 Why does a parabolic surface make a good reflector antenna?

9.8 When might each of the following parabolic reflector antennas be used: (a) paraboloid, (b) section of a paraboloid, (c) parabolic cylinder, (d) parabolic torus, (e) offset-fed reflector, (f) Cassegrain, and (g) mirror-scan antenna? When might (h) a spherical reflector or (i) a lens antenna be used?

9.9 *Background.* In a Cassegrain antenna, Fig. 9.11, the feed is located at (or near) the apex of the primary paraboloid reflector. The radiation from the feed is reflected by a secondary reflector in front of the primary reflector. The radiation is returned to the primary reflector where it is reradiated in the forward direction. Blockage of the radiated energy occurs because of the obstruction by the secondary reflector and by the interception of energy by the feed. If the secondary reflector is made smaller so as to reduce its blockage, the feed has to be made larger so as to illuminate without spillover the smaller secondary reflector. Similarly, if the feed is made smaller to avoid blockage, the secondary reflector has to be made larger in order to intercept the wide-angle energy from the feed. If the secondary reflector and the feed are both circular with a diameter of S and d, respectively, the total blockage is due to their combined area $(\pi/4)(S^2 + d^2)$. *Problem:* What should the relationship be between the diameter S of the feed and the diameter d of the secondary reflector in order to minimize the total blockage in a Cassegrain antenna? (You may assume that the beamwidth of the feed is λ/d radians.)

9.10 List the five basic methods available for obtaining a phase shift, and give an example of a phase shifter based on each.

9.11 When might ferrite phase-shifters be used in an electronically steered phased array antenna, and when might diode phase-shifters be used?

9.12 (a) If the minimum range of radar is to be no greater than 1.2 nmi, what should be the maximum switching time of a phase shifter so that the array is ready to receive after it has transmitted? (Assume that the pulse duration is small and can be neglected.) (b) Select a type of ferrite phase shifter that can probably meet this requirement. (c) What limitation might occur with your selection? (d) If the minimum allowable range were increased to

12 nmi, how might your answer for (b) and (c) change? (e) What type of ferrite phase shifter can be used when the radar operates with dual orthogonal linear polarizations? (f) What type of ferrite phase shifter might be used in a reflectarray?

9.13 (a) Derive the array factor for a uniformly spaced linear array of N isotropic elements. [Suggest you start with Eq. (9.22); but instead of a summation of sinewaves, it will be easier to use the exponential relation such as $1 + e^{j\phi} + e^{j2\phi} + e^{j3\phi} \cdots$ where $\phi = 2\pi(d/\lambda) \sin \theta$, as in Eq. (9.22). You also will have to recall or rederive the expression for the sum of a geometric series that you learned in high school.] (b) At what angles will grating lobes appear (over a range of $\pm 90°$) when the element spacing is four wavelengths? (c) Compare, in words, the pattern produced by the linear array of equal amplitude elements to the pattern produced by a continuous line source with uniform illumination (as in problem 9.1) and the same aperture size.

9.14 When the beam of a phased array antenna is electronically steered to an angle θ_0 from broadside, show that its beamwidth varies inversely as $\cos \theta_0$.

9.15 (a) Show that grating lobes will not appear in a steered phased array if the element spacing is less than one-half wavelength. (b) What should the element spacing be when $\theta_0 = 0$ if there can be grating lobes at $\pm 30°$, but not at smaller angles?

9.16 (a) What wrap-up factor is required in a frequency-scan array to scan the beam over an angle of $\pm 50°$ using no more than a total tunable (relative) bandwidth of 5 percent? (Assume a TEM transmission line where the velocity of propagation is the velocity of light.) (b) If there are 80 elements in the frequency scan array with an element spacing of 10 cm and a wrap-up factor the same as computed for part (a), what is the time required for a signal to fill the array aperture? (c) What bandwidth does this correspond to?

9.17 Consider the series-fed linear array of Fig. 9.16b. How far will the beam deviate from the broadside direction when the frequency is changed by 20 percent from the design frequency? (Assume the transmission feed-line propagates in the TEM mode so that the velocity in the line is c, the velocity of light.)

9.18 A frequency-scan array has an element spacing $d = 5$ cm, aperture dimension $D = 3$ m, and a feed system with a wrap-up factor = 16. As the beam is frequency scanned past the target, the echo will be frequency modulated with a bandwidth Δf_B [Eq. (9.42)]. (a) If a frequency $f = 1.05\, f_0$ points the beam to 30°, what is the spectral width of the echo signal due to the linear FM modulation induced on the echo? (b) If pulse compression processing is used on receive to take advantage of the frequency modulation of the echo signal, what will be the compressed pulse width?

9.19 Why do you think problems might occur when attempting to apply the theory of the infinite array to a finite size array?

9.20 Compare the corporate-fed (passive) phased array, the active-aperture phased array, and the space-fed phased array with respect to loss, transmitter efficiency (Sec. 10.3), relative prime power required for the transmitter, and any other factors of concern.

9.21 The Dolph-Chebyshev antenna illumination produces an antenna pattern with a narrow beamwidth and all sidelobes equal. It would appear to be a good antenna pattern except

that it is not practical. What is it about the Dolph-Chebyshev illumination that makes it unrealizable, especially with large gain?

9.22 What approximate reduction in gain [Eq. (9.51)] results when an antenna pattern is rectangular from 0 to 3° and is shaped to have a cosecant-squared variation of gain over the angular region from $\theta_0 = 3°$ to $\theta_m = 25°$?

9.23 For a fixed-size reflector antenna with an rms surface error ϵ: (a) Show that the wavelength that results in maximum antenna directivity is $\lambda_m = 4\pi\epsilon$. [This is Eq. (9.53.)] (b) How does this relate to the usual "rule of thumb" for reflector antenna tolerances which states that the rms error ϵ should be less than $\lambda/32$, where λ = wavelength? (c) Determine the loss of gain at the wavelength λ_m compared to the gain of a perfect (no error) antenna. (d) What is the maximum gain that is achievable for $D/\epsilon = 1000$ and $D/\epsilon = 10{,}000$? (Assume the aperture efficiency is 1.) (e) In your opinion, how high an antenna gain might be achieved with a practical radar antenna (and explain your answer)?

9.24 If a one-dB reduction in antenna gain is allowed due to errors in a 100-element linear array, what is the phase error (in degrees), the amplitude error (in dB), and the fraction of missing elements that can be tolerated when each one of these three factors is the only one contributing to the gain reduction? (That is, determine the phase error with the amplitude error zero and no missing elements, and so on.)

9.25 *Background.* A periodic error in an antenna will produce multiple equally spaced beams (or sidelobes) in sin θ space similar to the formation of grating lobes in an array antenna, except that these periodic error sidelobes are much smaller in gain. *Problem.* An antenna is suspected of having a periodic error since there are prominent sidelobes in its radiation pattern at angles of ± 37.3 and $\pm 53.9°$. If there is a periodic error, there will be other closer-in sidelobes; but in this problem we assume that these closer-in lobes are masked by the normal antenna sidelobe radiation. Based on the observed sidelobes whose directions are given above, what is the period (spacing) of this periodic error?

9.26 (a) With a uniformly illuminated planar array of 1000 isotropic elements, what should be the rms value of the phase error (in degrees) and the rms value of the amplitude error (in dB) to make the average error-sidelobes equal to -50 dB? (Assume that the contribution from the phase error equals that from the amplitude error.) (b) Repeat for an array antenna with 10,000 elements.

9.27 What determines the number of bits to be used in a digitally switched phased shifter?

9.28 According to G. Evans [Ref. 169, p. 115] the accuracy with which the antenna gain can be measured is commonly $\pm$ 0.5 dB. What is the maximum rms phase error in a reflector antenna that results in a loss of antenna gain of 0.5 dB?

9.29 (a) In a phased array with a square aperture of 100 by 100 elements, with half-wave spacing between elements, what is the rms angle error (in degrees) when the rms value of the normalized error current is $\sigma = 0.4$? (b) What fraction of a beamwidth would this be if the aperture illumination were uniform?

9.30 (a) What are the characteristics of an aperture illumination that can achieve ultralow sidelobes? (b) When might ultralow sidelobes be needed? (c) What antenna characteristics

have to be sacrificed for ultralow sidelobes? (As a start, see Table 9.1) (d) What factors ultimately limit the sidelobe levels that can be achieved in practice?

9.31 When might a radar systems engineer decide not to use an ultralow sidelobe antenna?

9.32 Why is a phased array antenna more suitable than a reflector antenna as an ultralow sidelobe antenna?

9.33 Compare the advantages and disadvantages for shipboard air defense of a traditional four-faced phased array radar and a system consisting of two trainable phased array radars and one 2D rotating air-surveillance radar with 360° azimuth coverage.

9.34 (a) What are the advantages and limitations of operating a ground-based air-surveillance radar under a radome? (b) Compare the air-inflated radome and the rigid geodesic radome for this application.

9.35 What types of antennas might be used for the detection and tracking of hostile ballistic missiles? (This is a question not just about antennas, but also about how radar systems might be applied for ballistic missile defense. There is no simple unique answer to this question, and there has not been general agreement as to the best approach.)

9.36 Why are phased array radars for air surveillance generally cheaper at the lower radar frequencies than at the higher frequencies?

9.37 For the application of air defense, compare the advantages and disadvantages of a single multifunction phased array that operates in one frequency band with a system having a separate air-surveillance radar and a separate phased array weapon control (tracking) radar, each operating in different bands.

9.38 A phased array has a beamwidth of 2° when pointed to broadside. If it is required to scan to an angle of 60° from broadside, what is the maximum signal bandwidth in MHz that a radar can have that operates at a center frequency of 3.3 GHz?

9.39 What does one have to do to obtain an electronically steered phased array with a large instantaneous signal bandwidth?

9.40 *Background.* It has sometimes been suggested (usually by non-radar administrators) that increasing the frequency of an air-defense phased array radar will result in a smaller size antenna for the same beamwidth (which is true), and thus provide a smaller radar system (which might not be true). If a smaller system were to result it can be made more mobile if a ground based system or, if a ship-based system, it can be employed on smaller ships. A smaller radar, however, does not result when the frequency is increased and all other requirements remain the same. *Problem.* What is wrong with reasoning that concludes that a smaller radar system will result if the array antenna is reduced in size by operating at a higher frequency? [To illustrate your answer, you can, if you wish, assume an S-band multifunction phased array radar (3.5 GHz) having a 12 by 12 foot aperture and 10 kW of average power. If the radar is increased to 35 GHz, the aperture is reduced in size to 1.2 by 1.2 foot.]

9.41 The typical *L*-band 2D air-surveillance radar usually has its maximum elevation coverage extending to about 20 to 40°, depending on the particular radar. If it is required to extend coverage of the radar to higher elevation angles, there are reasons why it might be better

to employ a separate antenna at a different frequency to fill the surveillance hole above the radar. (a) What are some reasons why a separate radar might be used rather than attempt to increase the elevation coverage of the 2D antenna? (b) If the elevation hole extends from 30° elevation angle to the zenith at 90°, what type of scanning patterns might be used? (There can be more than one choice of scanning pattern.) (c) What frequency band might be used for this hole-filler (and explain the reason for your selection)? (d) What type of antenna might be used for the hole-filler radar?